Lymphostromal Interactions In The Development And Function Of Thymic Epithelial Cells

By

NATALIE AMY ROBERTS

A thesis submitted to the
University of Birmingham

For the Degree of
DOCTOR OF PHILOSOPHY

Department of Anatomy
Institute of Biomedical Research
University of Birmingham
B15 2TT
United Kingdom

October 2010

ABSTRACT

The thymus is a primary lymphoid organ that supports the production, differentiation and selection of self-tolerant T cells from immature precursors of extrathymic origin. T cell development is a dynamic process involving the movement of thymocytes through specialised regions of the thymus, each directing distinct developmental stages. The formation of these microenvironments is crucial for providing the ordered and continuous signalling required to drive the non-cell autonomous process of T cell development. The development of thymocytes and thymic epithelial cells (TEC) are interdependent processes involving reciprocal signalling termed “thymic crosstalk”.

Using novel *in vitro* and *in vivo* experimental techniques we elucidated novel processes in the regulation of thymic epithelial cell development. We corroborated the importance of thymic crosstalk by revealing a new role for innate like γδ T cells in influencing medullary thymic epithelial cell development. Furthermore, this study argues against a specific time frame for the occurrence of thymic crosstalk by demonstrating that adult thymic epithelium retains its receptivity to lymphostromal signalling. In addition, we have recognised the importance of intrathymic niches in regulating early T cell progenitor development.

Collectively these data have provided an insight into the development of the thymic epithelium and thus have important implications in relation to developing rejuvenation strategies for the atrophied thymus and following ablative therapy.

ACKNOWLEDGEMENTS

I would firstly like to thank my supervisor Professor Graham Anderson for providing me with such a fruitful project and for all his help, advice and support that has guided me through the four years of this PhD. I would also like to thank Graham for all the encouragement and what must have been fabulous letters of recommendation, that have lead to me pursuing my academic career in the USA! I would also like to acknowledge the scientific guidance and opportunities provided by my second supervisor, Professor Eric Jenkinson.

A huge thank you to all the members of both the Anderson and Lane labs, past and present, for all their help and knowledge, and importantly for making my time here enjoyable. A special thank you must go to Will Jenkinson, Andrea White and Simona Rossi for showing me the ropes when I first arrived and for the hours spent teaching me how to do kidney capsule grafting. Also a big thanks to Saba Shakib, Stephanie Glanville, Moni Saini and Fabrina Gaspal for advice and patience in spite of my endless questioning!

Special thanks must go to Sonia Parnell for the PCR experiments, Mahmood Khan for being 'king of the cryostat' and finally Guillaume Desanti and Dave Withers for some of the experimental work reproduced here. I would also like to acknowledge everyone in the IBR for all the help, favours, advice and friendship during my time at Birmingham.

I would not be here today if it was not for the support of my parents especially my mum, ever since my first day at school she has encouraged, inspired and made me believe that I can achieve anything. I would also like to thank my boyfriend Chris Church for supporting me through the rollercoaster that has been the last four years whilst completing his own PhD – I couldn't have done this without you.

Thank-you everyone!!

CONTENTS

LIST OF FIGURES

Figure **Following page**

LIST OF TABLES

Table **Page**

LIST OF ABBREVIATIONS

Ag	Antigen
Aire	autoimmune regulator
AP-1	activator protein 1
APC	Antigen Presenting Cell
APECED	autoimmune polyendocrinopathy-candidiasis-ectodermal dystrophy
Bcl	B cell lymphoma
BCR	B cell Receptor
BM	Bone Marrow
BMSU	Biomedical Services Unit
BrdU	Bromodeoxyuridine (5-bromo-2-deoxyuridine)
bTECp	bipotent thymic epithelial cell progenitor
C	Constant domain
C	Cortex
Ca^{2+}	Calcium
Ccl	CC chemokine ligand
Ccr	CC chemokine receptor
CD	Cluster determination
cDNA	Complementary Deoxyribonucleic acid
CD3ε*tg*	Cluster determination 3 epsilon transgenic
CDR	complimentarity determining regions
Cld	claudin
CLIP	Class II associated invariant chain peptide
CLP	Common lymphoid progenitor
CO_2	Corbon Dioxide
cTEC	cortical thymic epithelial cell
DAG	diacylglycerol
DC	Dendritic Cell
DETC	Dendritic Epidermal T cell
dGuo	2-deoxyguanisine
DMEM	Dulbecco's Modified Eagle's Medium
DNA	Deoxyribonucleic acid
DN	Double Negative
dNTPs	Deoxynucleotide Triphosphates
DP	Doupbe positive
dT	deoxy-thymidine
E	Embryonic day
EpCam	Epithelial cell adhesion molecule 1
ER	Endoplasmic reticulum
ETP	Early T lineage progenitors
F1	Filial 1
FACS	Fluorescence activated cell sorting
FcR	Fc Receptor (Binds fragment, crystallisable region of antibodies)
FCS	Fetal Calf Serum
FL	Fetal Liver
Flt3	fms-related tyrosine kinase 3 (CD135)

FoxN1	Forkhead box protein N1
FoxP3	Forkhead box protein 3
FTOC	Fetal thymus organ culture
GATA3	GATA-binding protein 3
Gcm2	glial cells missing 2
γc	common cytokine γ-chain
GPCR	G protein coupled receptor
h	Hour
HSA	Heat stable antigen (CD24)
HSC	Haematopoietic Stem Cell
IFN	Interferon
Ig	Immunoglobulin
Ii	Invariant peptide
IL	Interleukin
ISP	Immature single positive
ITAM	immunoreceptor-based tyrosine activation motif
J	Joining domain
K	Keratin
KAR	Killer activating receptor
KIR	Killing Inhibitor Receptor
KLF	Kruppel-like factor
KREMEN1	kringle containing transmembrane protein 1
LAT	linker for activation of T cells
LBP	Lipopolysaccharide-binding protein
LEF	lymphoid enhancer factor
Lin	Lineage
LPS	Lipopolysaccharides
L-selectin	Lymphocyte selectin (CD62L)
LT	Lymphotoxin
LTβR	Lymphotoxin beta receptor
LTi	Lymphoid tissue inducer cell
M	medulla
MAC	Membrane attack complex
MALT	Mucosa-associated lymphoid tissue
MAP	mitogen-activated protein
Mg^{2+}	Magnesium
MHC	Major Histocompatibility Complex
min	minutes
MPP	Multipotent progenitors
mTEC	medullary thymic epithelial cell
NB	New Born
NFAT	nuclear factor for the activation of T cells
NK-κB	Nuclear factor- κB
NK	Natural killer Cell
ns	not significant
OPG	osteoprotegerin
P-selectin	Platelet selectin (CD62P)
PAMPs	Pathogen-associated molecular patterns

PBS	Phosphate Buffered Saline
PCR	Polymerase Chain Reaction
pgp	phagocytic glycoprotein
PIR	paired immunoglobulin receptor
PKC	protein kinase C
PLC	Phospholypase C
PRRs	Pattern recognition receptors
P-selectin	Platelet selectin
PSGL	P-selectin glycoprotein ligand
pTα	preTCRα
PTK	Protein tyrosine kinases
PTX	Pertussis Toxin
Rag	Recombinase activating genes
Rank	receptor activator of NF-κB
Rankl	receptor activator of NF-κB ligand
RF10-H	RPMI-1640 Hepes
Rorγ	retinoic acid-related orphan receptor gamma
rpm	Revolutions per minute
RTOC	reaggregate thymus organ culture
RT-PCR	Reverse Transcription - Polymerase Chain Reaction
RUNX3	runt-related transcription factor 3
Sca1	Stem cell antigen 1
SCID	Severe Combine Immune Deficiency
SCZ	subcapsular zone
SH	src homology domain
Skint1	Selection and upkeep of intraepithelial T cells 1
SLC	Secondary lymphoid tissue chemoattractant
SLP	SH2 domain containing leukocyte protein of 76kDa
SP	single positive
S1P	sphingosine-1-phosphate
$S1P_1$	sphingosine-1-phosphate receptor-1
TAP	Transporter associated with Antigen Processing
TCF-1	T cell factor-1
TCR	T cell Receptor
$TCR\delta^{-/-}$	T cell Receptor delta knockout
TdT	Terminal deoxynucleotide transferase
TEC	Thymic epithelial cell
TGF	Transforming growth factor
Th1	Type 1 helper T cell
Th2	Type 2 helper T cell
Th-POK	T-helper-inducing POZ/Kruppel like factor
TLR	toll-like receptors
TN	Triple Negative
TNF	Tumor necrosis factor
TNFR	Tumor necrosis factor receptor
TOX	thymus high-mobility group (HMG) box protein
TRA	Tissue Restricted self antigen
TRAF6	tumour necrosis factor receptor associated factor 6

T reg	Regulatory T cell
TSA	Tissue specific antigens
TSSP	thymus specific serine protease
UEA-1	Ulex europaeus agglutinin 1
V	Variable domain
VCAM	vascular cell adhesion molecule
wks	weeks
WNT	Wingless and Int
WT	Wild Type
w/v	weight to volume ratio
ZAP-70	ζ associated protein-70

CHAPTER 1 GENERAL INTRODUCTION

1.1 Overview Of The Immune System

1.1.1 The Role For The Immune System

The expression *immunity* is derived from the Latin word *immunitas*, which referred to the protection from legal prosecution offered to Roman senators during their tenures in office. Immunity traditionally meant protection from disease and, more specifically, infectious disease. The complex and organised network of cells and molecules responsible for immunity constitute the immune system, and their collective and coordinated response to the introduction of invading pathogenic microorganisms is the immune response (Delves and Roitt, 2000a). The immune system has evolved under enormous selective pressure imposed by pathogens and is consequently capable of detecting and eradicating foreign pathogens by discriminating between self and non-self (Medzhitov and Janeway, 1997; Takeda et al., 2003). A series of systems are presented to an invading organism that can be broadly divided into two fundamentally different types of response that function together, to eliminate infectious agents and provide an effective system; the evolutionarily ancient, innate immune system and the more recently evolved adaptive immune system (Basset et al., 2003; Delves and Roitt, 2000a).

1.1.2 The Innate Immune Response

Innate or 'natural' immunity is a relatively basic, non-specific, rapid response that constitutes the first line of defence against infection. It is essentially comprised of mechanical, molecular and cellular elements (Akira, 2009; Basset et al., 2003). The characteristics of the innate immune response include a lack of immunological memory, non-specific killing of pathogens by phagacytosis, leukocyte recruitment to sites of infection and initiation of inflammation (Akira, 2009). In addition, innate immune responses remain unchanged regardless of frequent antigen encounters (Delves and Roitt, 2000a).

The mechanical component of the innate system is the physical barrier provided by the epidermis and the more delicate mucosa, preventing the penetration of microbes. This extra-epithelial barrier possesses chemical and cellular defences including the secretion of enzymes (e.g. lysozyme and pepsin), mucus and motility, natural antibody production and secretion of anti-microbial peptides. Collectively these factors make it difficult for pathogens to attach to the skin epithelia and colonise the surface (Basset et al., 2003; Delves and Roitt, 2000a). These anti-microbial defence mechanisms are differentially employed from one surface to another and have different roles in the capture, removal and eradication of pathogens. Should a pathogen overcome this physical barrier a further barrage of defence mechanisms will be activated.

After engagement of a microbe with the epithelial surface the molecular components of innate immunity are activated resulting in the production of chemokines, cytokines, prostoglandins and leucotrines by the epithelium, indicating cell injury (Basset et al., 2003). The innate system recognises pathogens and distinguishes them from self by recognising highly conserved structures that are essential for the survival or pathogenicity of the micro-organism, referred to as pathogen-associated molecular patterns (PAMPs) (Medzhitov and Janeway, 2000; Medzhitov and Janeway, 1997). PAMPs include lipopolysaccharides (LPS), lipoproteins, peptidoglycan, lipoarabinomannan and oligosaccharides. The germ line encoded receptors that recognise PAMPs are another component of the molecular element of innate immunity and are known as pattern recognition receptors (PRRs) (Medzhitov and Janeway, 1997). PRRs can be classified into two groups, soluble and cell surface bound. Soluble PRRs include the collectins, the complement cascade, pentraxins, and lipopolysaccharide-binding protein (LBP). Membrane bound receptors are found on cellular components of the innate system, most importantly on dendritic cells (DC), B cells and macrophages. They include toll-like receptors (TLR), scavenger receptors, complement receptors and formyl-peptide receptors (Basset et al., 2003; Medzhitov

and Janeway, 2000). Once PRRs identify PAMPs, the effector cells are stimulated to perform their effector functions immediately (Medzhitov and Janeway, 2000).

The signals induced by PAMP – PRR engagement can be grouped into three categories; i) inflammatory mediators, such as tumor necrosis factor (TNF)-α, interleukin (IL)-6 and various chemokines, ii) T cell costimulators, for example CD80 and CD86, and iii) inducers of effector function, including transforming growth factor (TGF)-β and interferon (IFN)-γ (Medzhitov and Janeway, 1997). Chemokines and cytokines induced in the immediate phase of the host response are important for the maturation of DCs and are consequently a link between the innate and adaptive response (Basset et al., 2003). In addition, pro-inflammatory cytokines such as TNF-α and IL-6 upregulate the acute phase response leading to the activation of complement. The complement system is an enzymatic-amplifying cascade triggered primarily by complement proteins binding to numerous components of microbial cell walls. The active components produced by this cascade result in attraction and activation of phagocytic cells, production of inflammatory mediators, opsonisation of bacteria for clearance by macrophages and formation of the Membrane Attack Complex (MAC), a pore forming apparatus that induces cell death by creating a permeable bacterial cell wall (Carroll, 2004).

The secretion of chemokines is vital for the recruitment of the cellular components of the innate immune system (Basset et al., 2003). Consequently the invading pathogen interacts with components of the innate immune system such as DCs and macrophages. Resident macrophages are the first phagocytes to enter into action, followed by polymorphonuclear neutrophils, if necessary (Basset et al., 2003). Through their PRRs, invading organisms are recognised and subsequently internalised, ultimately leading to death and removal of the microbe (Basset et al., 2003). IL-12 secretion by macrophages leads to the activation of natural killer (NK) cells that can recognise their targets through both Fc receptors specific for IgG (FcγR) and killer activating

receptors (KAR). They kill via antibody-dependent cellular cytotoxicity when their FcγR is engaged. However, NK cells can kill directly through activation of their KAR unless a simultaneous signal is received through Killing Inhibitory Receptors (KIRs) that recognise Major Histocompatiblity Complex class I (MHC I), present in normal circumstances on all nucleated cells (Delves and Roitt, 2000a; Yokoyama et al., 2004).

1.1.3 The Adaptive Immune Response

Adaptive or 'acquired' immunity is a highly sophisticated, slowly developing, targeted system found in vertebrates. It provides the ability to combat infectious micro-organisms specifically and more rapidly upon subsequent challenge, due to the production of immunological memory. The type of effector response generated is dependent on the innate system and can be largely categorised into humoral and cellular immunity (Medzhitov and Janeway, 2000; Medzhitov and Janeway, 1997). Eradication of microbes present in the blood or extracellular fluid is the responsibility of humoral immunity, through the generation of antibodies by B cells, and is usually initiated within the spleen. Cellular immunity is involved in the elimination of microbes found inside cells, is mediated primarily by cytotoxic T cells and is generated in local lymph nodes (Akira, 2009; Delves and Roitt, 2000b). However, most pathogens enter the body after ingestion or inhalation and are consequently encountered at mucosal surfaces, the response therefore tends to begin within mucosa-associated lymphoid tissue (MALT). In response to infection, clonal expansion of lymphocytes is absolutely necessary for the generation of an efficient immune response. However, to produce sufficient numbers of clones that differentiate into effector cells can take up to five days, which is sufficient for most pathogens to cause damage to the host (Delves and Roitt, 2000b; Medzhitov and Janeway, 2000). The two major types of lymphocytes that perform adaptive immunity are T and B cells. They express unique T cell receptors (TCRs) and B cell receptors (BCRs) that

recognise a huge variety of different antigens. TCRs and BCRs belong to the immunoglobulin (Ig) gene superfamily and are generated by somatic DNA recombination during T and B cell differentiation; hence each lymphocyte possesses a structurally unique receptor (Hedrick et al., 1984). When an infectious agent invades the host, T and B cells with the corresponding receptors are selected for clonal expansion and simultaneous differentiation into effector or memory cells (Akira, 2009; Medzhitov and Janeway, 2000).

The potent adaptive immune response requires initial instruction and regulation by DCs, professional antigen presenting cells (APCs) with the ability to induce primary immune responses (Banchereau et al., 2000; Guermonprez et al., 2002). DC progenitors derive from bone marrow, which develop into tissue resident immature cells with high endocytic and phagocytic capacity. Following tissue damage, danger signals (e.g. PAMPs) or recognition of local inflammatory mediators, induce immature DCs or 'antigen (Ag) capturing cells' to enter a maturational programme, transforming them into efficient antigen presenting cells and powerful T cell activators that subsequently migrate to the lymphoid organs (Guermonprez et al., 2002; Lane and Brocker, 1999). B cells are effectors of the adaptive immune system through their production of antibody and activation factors. In addition they function as APCs primarily in secondary lymphoid organs, enabling the required cognate T-B interactions to elicit a T cell dependent humoral response to occur (Bryant and Ploegh, 2004). DCs and macrophages link the two branches of the immune system to efficiently combat pathogen invasion (Banchereau et al., 2000; Harding et al., 2003). These phagocytic APCs are suitably located in peripheral tissues, poised to interact with pathogenic invaders (Harding et al., 2003)

1.1.4 Antigen Processing And Presentation To T cells

For the adaptive immune system, antigen processing and presentation plays a fundamental role in the induction of specific immune responses (Harding et al., 2003).

Pathogenic peptides are presented on MHC class I and class II molecules for T cell recognition and subsequent activation. MHC class I and II biogenesis are strictly compartmentalised processes. Class I molecules are constitutively expressed on nearly all cell types, however, class II molecules are only expressed constitutively on a subset of cells of immune lineage (Yewdell and Haeryfar, 2005). There is a third class of MHC, which is primarily known to encode the complement component genes essential for complement activation pathways. This region also encodes heat shock proteins, tumor necrosis factors (TNF) and lymphotoxins (Yung Yu et al., 2000). In addition 'non-classical' MHC molecules for example CD1, a class I-like molecule, may present lipids and glycolipids to certain γδT cells (Born et al., 1999; Chien and Konigshofer, 2007). CD1d has been identified as the restricting element for invariant Vα14 (mouse) Vα24 (human) NKT cells (Watts, 2004).

1.1.4.1 Major Histocompatibility Complex class II

Exogenous antigens, those that have been ingested, inhaled or injected, are loaded on to MHC class II molecules through an endocytic pathway. MHC class II antigen processing and presentation is largely restricted to three main professional APCs, namely B cells, macrophages and DCs (Harding et al., 2003). In addition, they can be found on epithelial cells of the thymus. MHC class II molecules are synthesised within the endoplasmic reticulum (ER), where three αβ MHC class II dimers associate to a trimer of invariant peptide (Ii) chains. Ii functions as both a targeting subunit and a guardian of the peptide binding site. The nonamers subsequently enter the endocytic pathway where they encounter and fuse with acidic protease- and protein-rich vesicles, thus within a single compartment both antigen processing and peptide loading occurs (Guermonprez et al., 2002; Watts, 2004). The different types of APCs are equipped with similar and distinct intracellular acidic proteases, known as cathepsins. This leads to the progressive degradation of Ii, leaving the class II associated invariant chain peptide (CLIP) fragment in the

MHC class II peptide binding groove (Bryant et al., 2002; Honey and Rudensky, 2003). CLIP removal and loading of peptide on to new MHC class II requires the peptide exchange catalyst HLA-DM (or H-2M in mice), a MHC class II homolog, whose function is to stabilise and/or induce a MHC class II conformation that facilitates the peptide selection process. The newly synthesised peptide-MHC complex is subsequently transported to the cell surface (Bryant and Ploegh, 2004; Guermonprez et al., 2002; Watts, 2004).

1.1.4.2 Major Histocompatibility Complex class I

Antigens generated within a cell 'endogenous antigens' are loaded onto MHC class I molecules in the endoplasmic reticulum. However, antigen processing and MHC peptide assembly are segregated events (Watts, 2004). MHC class I is a trimeric complex composed of a polymorphic heavy chain, an invariant light chain (β_2-microglobulin) and the bound peptide (Flutter and Gao, 2004). Newly synthesised ubiquitinated proteins are constitutively degraded within proteosomes and the ensuing peptides, generally 8-12 amino acids long, transferred to the ER in an ATP dependent fashion, by a specialised dimer Transporter associated with Antigen Processing (TAP) (Flutter and Gao, 2004). MHC class I molecules complexed with the loading complex, composed of ER resident chaperones such as calreticulin and tapasin, binds to TAP, in a tapasin dependent manner, resulting in peptide loading. The resulting peptide MHC complex is rapidly transferred to the plasma membrane. MHC class I molecules do not traffic to the Golgi body and subsequently the cell membrane, without the provision of peptides by TAP, instead they are degraded in the ER (Knittler et al., 1999). Furthermore internalised antigens may be presented on MHC class I, a phenomenon known as 'cross presentation' (Guermonprez et al., 2002; Lane and Brocker, 1999).

1.1.5 T Lymphocytes

T cells are derived from haematopoietic precursors that seed and develop within the thymus. Several different subsets of T cells exist, each with a distinct function, which can be broadly divided into two main conserved lineages of T cells distinguished by their TCR chain composition, either an αβ or a γδ protein heterodimer. Due to their earlier discovery, the development, selection, and peripheral localisation of newly differentiated αβ T cells are understood in considerable detail. Conversely, these processes are less well characterised for the γδ T cell subset (Xiong and Raulet, 2007). γδ and αβ T cells arise from a common progenitor cell in the thymus, however the molecular events leading to lineage decision of developing CD4 CD8 double negative (DN) thymocytes to differentiate into γδ versus αβ T cells have not been fully resolved (Komori et al., 2006; Medzhitov and Janeway, 2000; Xiong and Raulet, 2007).

1.1.4.1 αβ T Cells

The αβ TCR repertoire is composed of clonally variable αβ heterodimers in association with the invariant components of the CD3 complex. αβ T cells recognise antigens as peptide fragments in the context of Class I or Class II MHC, express the co receptors CD8 or CD4, and mediate cytotoxic reactions or perform B cell help respectively. Both types of αβ T cells draw upon the same pool of α and β gene segments during the production of their antigen receptors. The functional TCR receptor of the αβ T cell population is shaped by positive and negative selection events that occur during intrathymic maturation (Allison and Havran, 1991).

CD4 T cells are predominantly cytokine-secreting helper cells that can be further divided into four major types, dependent upon early signals received in concert with antigen. i) Type 1 (Th1) helper T cells secrete lymphotoxin α (LTα), IL-2 and IFN-γ, facilitating cell-mediated immunity to intracellular microorganisms, for instance macrophage activation and T cell

mediated cytotoxicity. ii) Type 2 (Th2) helper T cells produce IL-4, 5, 9, 10, 13 and 25 and help B cells generate antibodies, thus primarily mediating immunity to extracellular parasites including helminths (Delves and Roitt, 2000b; Mosmann et al., 1986). iii) The more recently recognised Th17 cells play a critical role in microbial protection, particularly against extracellular bacteria and fungi. Th17 cells express low levels of GATA-3 and T-bet; RORγt has been identified as their master regulator. They produce IL-17a, IL-17f, IL-21 and IL-22 (Weaver et al., 2006; Zhu and Paul, 2008). iv) T regulatory cells (Treg) of which two different subsets can be differentiated by their distinct suppressive mechanisms. Naturally occurring Tregs (nTreg) exert their suppressive effects via cell contact by membrane-bound molecules and inducible Treg (iTreg) use contact independent mechanisms for their suppressive capacity. nTreg express $CD4^+$ and $CD25^+$, develop within the thymus through a process involving the recognition of self peptides in MHC molecules on thymic epithelial cells (TECs) (Lin et al., 2007). Phenotypically iTreg resemble nTreg and they both have a critical role in the maintenance of self tolerance. Induction of iTreg occurs through the stimulation of activated naïve CD4 T cells with TGF-β. Several mechanisms are involved in Treg suppressive function; the molecular basis of suppressive function often involves their production of cytokines including TGF-β, IL-10 and IL-35 (Shevach, 2006; Zhu and Paul, 2008).

CD8 T cells are mainly cytotoxic killer cells and are primarily involved in the elimination of virally infected cells via one of two mechanisms. They have the ability to insert perforins into the target-cell membrane, creating pores through which granzymes are passed through, leading to activation of the caspase mediated apoptotic cascade and thus apoptosis. Alternatively, through Fas ligation on the target cell they are able to induce apoptosis also through caspase activation (Delves and Roitt, 2000b). In addition to direct killing of infected cells, CD8 cytotoxic T cells produce several cytokines such as, TNF-α, lymphotoxin and IFN-γ, which reinforce

antiviral resistance by rendering adjacent cells resilient to infection (Delves and Roitt, 2000b). CD8 T cells recognise MHC class I through interactions with multiple residues located at the edge of the peptide binding groove, enabling the exertion of this direct antipathogen activity (Ajitkumar et al., 1988).

1.1.4.2 γδ T cells

γδ T cells constitute only a small proportion of the circulating lymphocyte population, and are found in high abundance on mucosal and epithelial surfaces (Allison and Havran, 1991; Ferrero et al., 2001; Komori et al., 2006). Different γδ subsets are characterised by the expression of specific Vγ and Vδ gene segment combinations. An intriguing correlation between individual γδ T cell subsets and the particular epithelial layers of tissues they tend to reside in, for instance, the skin, gastrointestinal tract, and reproductive tract, has been drawn (Haas et al., 1993; Hayday, 2000). The underlying process presumably evolved to produce functionally distinct sets of γδ T cells in an organised fashion (Ferrero et al., 2001; Xiong and Raulet, 2007). Some subsets of γδ T cells develop largely or exclusively prenatally, requiring peripheral stimulation for subsequent expansion and each γδ subset is restricted to a distinct wave of differentiation; it is thought that only fetal Haemopoeitic Stem Cells (HSCs) have the capability to differentiate into $V\gamma5^+$ T cells and that they specifically require a fetal thymic microenvironment (Ikuta et al., 1990).

The earliest γδ T cell emigrants express an invariant Vγ5Vδ1 TCR and are designated dendritic epidermal T cells (DETCs). They migrate to the skin and physically interact with keratinocytes through dendritic processes (Boyden et al., 2008; Komori et al., 2006). Studies suggest, crucial to the maintenance of the DETC population, is the presence of a γδ TCR that can recognise an antigen expressed in skin (Komori et al., 2006). A recently identified gene cluster

has been implicated in influencing the development and function of DETCs. *Skint1* (selection and upkeep of intraepithelial T cells 1) represents a prototype member of this rapidly evolving gene family, whose expression is restricted to the thymus and skin, more specifically, in thymic epithelial cells and keratinocytes. These proteins are unusual among immunologlobulin superfamily members due to their multiple transmembrane domains (Boyden et al., 2008). *Skint1* is thought to be required for positive selection of $V\gamma5^+$ T cells in the embryonic thymus and normal numbers in the skin. It is expressed at E15 and continuing into adulthood. *Skint1* expression in keratinocytes advocates a role in epidermis, possibly in the selective localisation and maintenance of DETCs in skin (Boyden et al., 2008).

The relative absence of γδ T cells from lymph nodes and T cell areas of the spleen, anatomical structures where a great diversity of antigens are presented, suggests these cells do not routinely rely on professional APCs for antigen recognition (Hayday, 2000). Instead they may recognise antigens directly in tissues, which do not require large TCR diversity; in support of this γδ T cells assigned to each epithelial surface have extremely limited diversity. This provokes the "first line of defence" hypothesis, which proposes that in contrast to αβ T cells, which respond to a diversity of microbial antigens, γδ T cells respond to unique stress-induced self antigens that are markers of cell infection or transformation, rather than foreign antigens (Boyden et al., 2008; Hayday, 2000). γδ T cells perform a number of functions depending upon the location and the type of stress occurring. Once activated, γδ T cells regulate epithelial homeostasis, modulate inflammation, lyse transformed cells and increase the efficiency of wound healing (Komori et al., 2006).

Relatively little is known about the mechanisms and checkpoints involved in γδ T cell development however, what is known demonstrates that these cells are an exceptional cell type possibly resembling a more innate like cell than the αβ T cell lineage. Consequently the

subsequent information provided will focus on the more conventional T cell subset, the αβ T cells unless otherwise stated.

1.1.6 Structure And Function Of The αβ T Cell Receptor

One essential interaction of an immune response is between the T cell receptor (TCR) and peptide-MHC complexes. The TCR delivers signals that are crucial at distinct stages of T cell development within the thymus, as well as for the differentiation and activation of mature T cells into effector and memory cells (Call and Wucherpfennig, 2005). The TCR exhibits homology with immunoglobulins however, it recognises proteolytically processed short peptide antigens in association with either MHC class I or class II molecules on the surface of an APC (Hedrick et al., 1984; Weiss and Littman, 1994). The TCR is exclusively produced as a transmembrane molecule consisting of either an αβ or a γδ disulphide linked glycoprotein heterodimer (Figure 1.1) (Blumberg et al., 1990). The TCRδ chain is more closely related to TCRα, whereas the TCRγ chain has greater sequence homology to TCRβ (Call and Wucherpfennig, 2005).

Each α, β, γ, and δ chain contains a variable (V) and a constant (C) domain, which are spliced together during development in the thymus, giving rise to a TCR complex of single specificity. The V domain is composed of three different segments the variable (V), joining (J), and diversity (D). However in contrast to the β and δ chains, the α and γ chains, do not contain a D region (Delves and Roitt, 2000a). The V domain contains three sections of hypervariability known as complimentarity-determining regions (CDRs), which recognise peptide-MHC complexes (Davis et al., 1998; Garcia et al., 1999). The immunologlobulin-like fold of the TCR positions the three CDRs from each chain in close proximity to each other, creating the binding furrow that contacts antigen (Goldrath and Bevan, 1999).

Figure 1.1 Structure Of The T Cell Receptor And CD3 Signalling Complex

The T cell receptor is disulphide linked glycoprotein heterodimer composed of an α and β chain. Each chain is comprised of a variable (V) region and a constant (C) region. The V domains contain three sections of hypervariability known as complimentarity-determining regions (CDRs), which recognise peptide-MHC complexes. The immunologlobulin-like fold of the TCR positions the three CDRs from each chain in close proximity to each other, creating the peptide-MHC binding site. The CD3 complex is comprised of six nonvariant proteins, CD3γ, CD3δ, and two molecules of CD3ε, together with a disulfide linked ζ chain, which exists primarily as a disulphide-linked homodimer. Each CD3 subunit contains cytoplasmic domains with conserved immunoreceptor tyrosine based activation motifs (ITAMs).

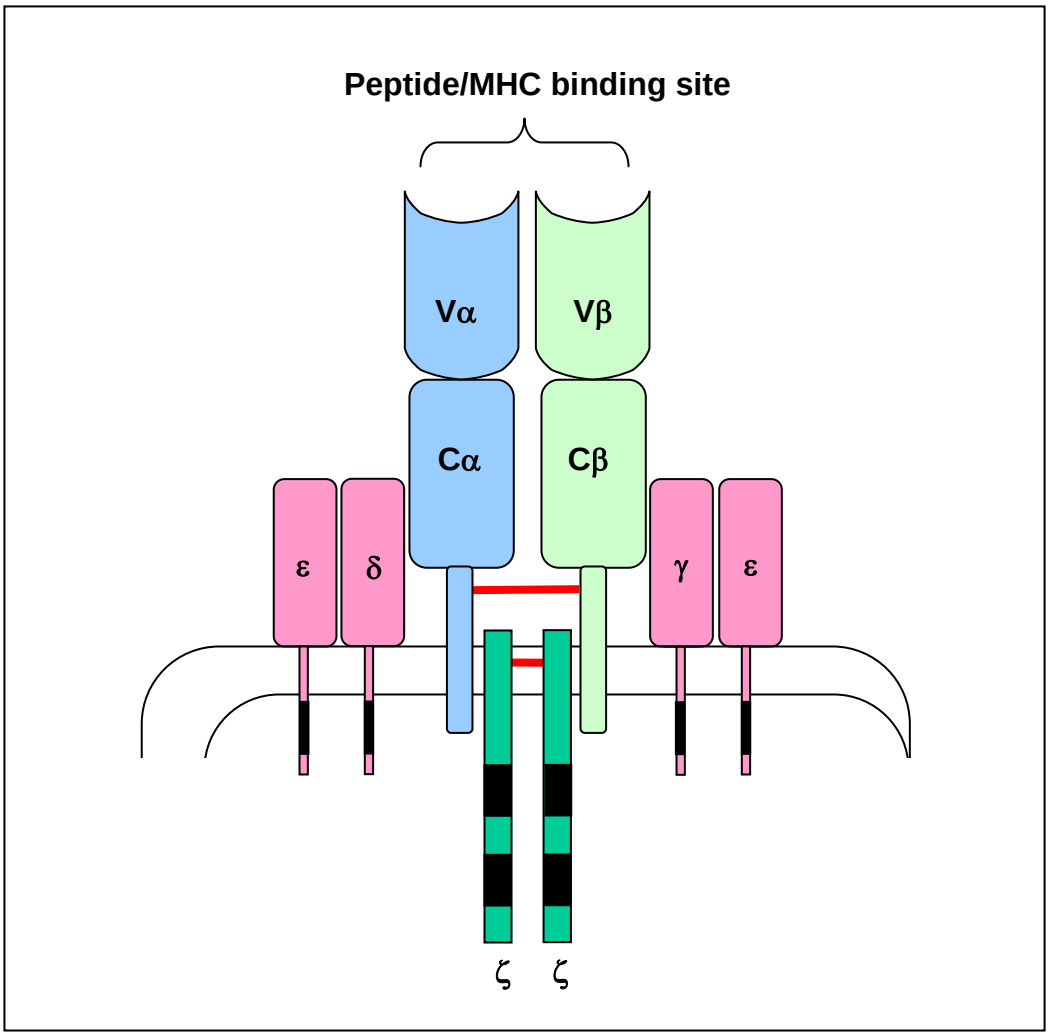

Key

- CD3 complex
- TCRα chain
- TCRβ chain
- ITAM
- disulphide bond

These gene segments are recombined and joined together through a complex and highly regulated, site-specific genomic process known as V(D)J recombination (Alt et al., 1992; Krangel, 2009). Successive rounds of recombination of the original and the second allele ensue if the first recombination fails to produce a successful TCR. This combinatorial rearrangement generates a huge diversity in the nascent TCR repertoire, which is increased further through both a lack of precision during rearrangement and the addition of non-template encoded 'N' nucleotides at the joining sites by the enzyme terminal deoxynucleotide transferase (TdT) (Fugmann et al., 2000). The dimeric protein encoded by recombinase activating genes RAG-1 and RAG-2 regulates V(D)J recombination. These genes are expressed in developing lymphocytes when undergoing antigen receptor assembly.

Intracellular signalling cascades are initiated upon TCR engagement and the concomitant binding of the coreceptors CD4 and CD8 to invariant regions of MHC class II and MHC class I respectively (Rudd, 1990; Weiss and Littman, 1994). This leads to T cell proliferation, cytokine production and acquisition of complex effector functions. Normal development, homeostasis and function of T cells is reliant on the integration of these signals (Wilkinson et al., 2005). However, the ligand binding αβ or γδ TCR chains do not posses any intrinsic cell signalling ability due to their short cytoplasmic domains (Kane et al., 2000). Rather the noncovalently associated CD3 complex of molecules accomplishes this. The CD3 complex is comprised of six nonvariant proteins, CD3γ, CD3δ, and two molecules of CD3ε, together with a disulfide linked ζ chain homodimer or in a minority of complexes a disulfide linked ζ chain η chain (a splice variant of ζ) heterodimer (Figure 1.1) (Blumberg et al., 1990; Delves and Roitt, 2000a). These molecules are integral TCR components not only for signal transduction, but they are also required for receptor assembly and cell surface expression (Ashwell and Klusner, 1990; Samelson, 2002). Their cytosolic components contain a critical and unique region, the ITAM

(immunoreceptor-based tyrosine activation motif), which contains the consensus sequence YxxI/L $x_{(6-8)}$ YxxI/L (Cambier, 1995; Reth, 1989). Each of the CD3 chains contains one ITAM motif while each ζ chain contains three, consequently the TCR can contain a total of ten ITAMs (Samelson, 2002; Wange and Samelson, 1996). These motifs are necessary and sufficient for TCR mediated activation, upon which the tyrosine residues within the ITAMs become phosphorylated (Samelson, 2002; Wange and Samelson, 1996).

Two families of cytoplasmic protein tyrosine kinases (PTK) have been implicated in TCR signalling; Lck and Fyn are members of the Src family, while ZAP-70 and syk comprise the second family. The Src family members primarily mediate ITAM phosphorylation, of which Lck is the best characterised. Lck is complexed with the cytoplasmic domains of either of CD4 or CD8, at high stoichiometry, thus is brought into the proximity of the cytoplasmic domains of the TCRζ and CD3 chains (Veillette et al., 1989; Wange and Samelson, 1996; Weiss and Littman, 1994). ITAM phosphorylation leads to the recruitment and binding of ZAP (ζ associated protein)-70, a 70 kd PTK exclusively expressed in T and NK cells, to the membrane receptor complex via its src-homology (SH) 2 domains. ZAP-70 is phosphorylated and activated by the already functional Lck. Syk is central to BCR function however, it is possibly involved in the function of certain γδ T cell subsets (Cheng et al., 1995).

The activated PTKs consequently phosphorylate and thus activate a large number of protein substrates including phospholypase Cγ1 (PLCγ1), and the adaptor proteins LAT (linker for activation of T cells) and SLP-76 (SH2 domain containing leukocyte protein of 76kDa) (Bubeck Wardenburg et al., 1996; Raab et al., 1997). PLCγ1 hydrolyses phophatidylinositol (4,5)-bisphosphate [PtdIns(4,5)P_2], generating both diacylglycerol (DAG) and inositol (1,4,5)-trisphosphate [Ins(1,4,5)P_3], responsible for the activation of the serine/threonine protein kinase C (PKC) family and the release of intracellular calcium (Ca^{2+}) respectively. Increases in

intracellular Ca^{2+} levels activates the serine/threonine phosphatase calcineurin leading to the dephosphorylation and activation of the transcription factor NFAT (nuclear factor for the activation of T cells) allowing its nuclear translocation and activation of IL-2 transcription (Rao et al., 1997; van Leeuwen and Samelson, 1999; Wilkinson et al., 2005). In addition, downstream events of LAT and SLP-76 bring about cytoskeletal rearrangement via Vav-dependent activation of Rac, which is essential for the formation of the immunological synapse (Ardouin et al., 2003). Furthermore this leads to the activation of the MAP (mitogen-activated protein) kinase-dependent transcription factors nuclear factor-κB (NF-κB) and activator protein 1 (AP-1) (Godfrey et al., 2009; Kane et al., 2000; Wilkinson et al., 2005). The interpretation of the signal transduced by the TCR may differ depending on the developmental stage of the responding cell or the cellular context of antigen recognition (Weiss and Littman, 1994)

In addition to the antigen receptor, other molecules contribute to T cell activation. These include molecules functioning as coreceptors (CD4, CD8), components operating to increase the avidity of the interaction with antigen or the antigen-presenting cell (LFA-1), or those that induce separate signal transduction events that influence the cellular response (CD28, CD40) (Weiss and Littman, 1994). In the absence of theses signals, lymphocytes fail to respond effectively and instead TCR engagement leads to either the induction of apoptosis or a state of anergy (Sharpe and Freeman, 2002).

1.2 T cell Development

1.2.1 Structure And Function Of The Thymus

The thymus is an encapsulated primary lymphoid organ situated within the mediastinum that consists of numerous lobules separated by mesenchymal trabeculae (Miller, 2002; Rodewald, 2008). It is essential for homeostatic maintenance of the peripheral immune system.

Despite this it is most prominent during early life, subsequently undergoing profound age-associated atrophy, ultimately regressing to thin shreds of fibrofatty tissue (Anderson et al., 2000a; Lynch et al., 2009). The thymus can be found in all vertebrates and its emergence in evolution parallels the appearance of V(D)J recombination (Boehm, 2008).

The stromal cell content of the thymus creates an organised three-dimensional cellular network composed of DCs, macrophages, endothelial cells, fibroblasts and thymic epithelial cells (TECs) (Alves et al., 2009). This provides highly specialised microenvironments to support and direct the production, differentiation and selection of self-tolerant T cells. It is anatomically divided into the outer cortex and the inner medulla that contain distinct types of TECs (Anderson et al., 2006; Boyd et al., 1993; Takahama, 2006). Numerous processes constitute the thymic development of T cells, involving the dynamic relocation of developing lymphocytes into, within and out of the multiple environments of the thymus (Takahama, 2006). T cell precursor maturation is not a thymocyte autonomous process. Consequently, interactions with the thymic microenvironment and the delivery of multiple essential signals are required throughout T cell development (Anderson et al., 2006). However, prior to intra-thymic T cell development, haematopoietic precursors must first colonise the thymus.

1.2.2 Colonisation Of The Thymus By Thymocyte Progenitors

Long-term self-renewing potential is not a property of intrathymic progenitors (Petrie, 2003). Consequently, the recruitment of mulitpotent progenitors that circulate in the blood is required to continuously colonise the thymic microenvironment in order to efficiently generate T cells (Anderson et al., 2006; Petrie, 2003). These immature T cell precursors are of extrathymic origin and are derived from different haematopoietic sites depending on the developmental stage (Anderson et al., 2006). The first wave of haematopoiesis is observed in the yolk sac, it then transiently moves to within the aorta-gonad-mesonephros region at 7-9 days post conception

(Bellantuono, 2004; Kikuchi and Kondo, 2006). The next wave begins in the fetal liver from 12 days after coitus to birth, and is therefore the predominant site of haemopoiesis throughout fetal life (Bellantuono, 2004; Kieusseian et al., 2006). HSC activity is subsequently identified in the bone marrow as early as 17.5 days post conception and is sustained throughout adult life (Kikuchi and Kondo, 2006). Seeding of the thymus with lymphoid progenitor cells occurs as early as embryonic day 11.5 (E11.5) in mice, the eighth week of gestation in humans, and is mediated by at least two different pathways: the vasculature-independent pathway, and the vasculature-dependent pathway (Hollander et al., 2006; Jotereau et al., 1987; Liu et al., 2006; Takahama, 2006).

During the early stages of embryonic development, thymus colonisation occurs prior to vascularisation. Consequently, precursors have to enter the early thymus rudiment by exiting nearby vessels, travelling through the perithymic mesenchyme, and migrating directly across an epithelial basement membrane (Anderson and Jenkinson, 2001; Anderson et al., 2006; Takahama, 2006). On the contrary, throughout the late stage of embryogenesis and postnatally, precursors enter the thymus directly by migrating from blood vessels at the corticomedullary junction (Anderson et al., 2006; Takahama, 2006). Despite this difference, in the fetal and adult setting, precursor recruitment to the thymus is likely to involve a chemotactic mechanism (Anderson et al., 2006).

Vasculature independent colonisation of the fetal thymus is thought to be regulated by chemotactic attraction of lymphoid progenitor cells, potentially via the roles of two chemokines, CC-chemokine ligand 21 (Ccl21) and its G protein-coupled receptor Ccr7, plus Ccl25 (thymus expressed chemokine (TECK)) and Ccr9. Both of these chemokines have been demonstrated to play a role in guiding the migration of precursors to the thymus during the first wave of fetal thymus colonisation by their absence leading to a reduction in thymus cellularity (Jenkinson et

al., 2007; Meurens et al., 2007; Takahama, 2006; Wurbel et al., 2001). Interestingly, a selective loss of the first wave of T cell development that generates epidermal $V\gamma3^+$ γδ T cells is observed in mice deficient for both Ccr7 and Ccr9 (Liu et al., 2006). Ccr9 is the only physiologic receptor for Ccl25 and is mainly expressed by thymocytes and intraepithelial (IEL) and lamina propria lymphocytes of the small intestine. Ccl25, is expressed by the parathyroid primordium from E11 onwards and is detectable in both cortical and medullary regions of the postnatal thymus (Liu et al., 2006; Meurens et al., 2007; Wurbel et al., 2001). As well as Ccl25, Cxcl12 (Stromal derived factor-1 (SDF-1)), and Ccl21 (secondary lymphoid tissue chemotractant (SLC)) are expressed in the alymphoid thymic anlage present at E12 of gestation (Wurbel et al., 2001). However, Cxcl12/Cxcr4 signalling is not required for recruitment of progenitors to the fetal thymus (Jenkinson et al., 2007).

In the postnatal thymus, following vascularisation at around E16, lymphoid progenitor cells that have just entered the thymic parenchyma are found mainly at the cortico-medullary junction, due to their entry via extravasation through post capillary venules in this area (Liu et al., 2006). Many aspects of this process remain poorly understood and the role of chemokines in postnatal thymus seeding is unclear (Guidos, 2006). However, it has been reported that seeding of the adult thymus is regulated by the adhesive interaction between platelet (P)-selectin (CD62P), a carbohydrate binding protein, expressed by thymic endothelium and P-selectin glycoprotein ligand 1 (PSGL1) expressed on circulating lymphoid progenitor cells. This interaction slows T cell progenitors, allowing them to respond to local chemokine gradients and to engage the endothelial adhesion molecules vascular cell adhesion molecule 1 (VCAM-1) and intercellular adhesion molecule 1 (ICAM-1), via integrins leading to cessation on the thymic endothelium (Gossens et al., 2009; Scimone et al., 2006; Takahama, 2006). Interestingly, thymus seeding is not a continuous event, but a periodic and gated event that occurs in waves, with a

periodicity of approximately 15 days. The intermittent opening of microvascular gates regulates this cyclical process, allowing thymus specific progenitors to occupy the limited number of available intrathymic niches (Ceredig and Rolink, 2002; Donskoy et al., 2003; Foss et al., 2001). It is thought that the concentration of P-selectin may contribute to this process as its expression is regulated in concert with the availability of intrathymic niches (Ladi et al., 2006). Once T cell progenitors enter the thymus they subsequently undergo a tightly regulated process of T cell development.

1.2.3 Early Intra-Thymic T cell Development

The first thymocyte progenitors to enter the thymus are described as double negative thymocytes (DN) due to their lack of expression of the coreceptors CD4 and CD8. The early phase in T cell development is consequently called the DN stage and includes four phenotypically and genetically distinct stages occurring over a 2-week period. This is the most proliferative stage of T cell development, as each precursor entering the thymus gives rise to around 1 million daughter cells (Lind et al., 2001). The four stages are designated, DN1- DN4, and are defined by their differential expression of CD117 (c-kit), CD44 (phagocytic glycoprotein 1) and CD25 (IL-2 receptor α) (Figure 1.2) (Ciofani and Zuniga-Pflucker, 2007; Godfrey et al., 1993; Porritt et al., 2004). DN cells comprise about 3% of the total thymocytes numbers (Goldrath and Bevan, 1999). They are mostly surface CD3/TCR negative, but are in the process of rearranging their TCR genes. Progression through the DN substages is regulated by an interplay between Notch1 and interleukin-7 (IL-7) that leads to the progressive loss in multi-lineage potential. Consequently, the early thymocytes begin to acquire a characteristic T cell phenotype. This process also includes the concomitant migration of the progenitors across the cortex in the direction of the capsule, differentiating as they move through various cortical depths (Figure 1.3) (Godfrey and Zlotnik, 1993; Guidos, 2006; Lind et al., 2001; Petrie, 2003).

Figure 1.2 Stages Of Intrathymic T Cell Development

Stages of T cell development in the thymus as defined by phenotypic changes in the surface expression of cell markers including the coreceptors CD4 and CD8. Thymocytes differentiate from double negative ($CD4^-CD8^-$ (DN)) to double positive ($CD4^+CD8^+$ (DP)) and finally to single positive (SP). The brach-point for γδT cell development from the DN3 stage is indicated and the sequential development of specific γ chains outlined. Key developmental checkpoints are marked by blue bars, and blue arrows depict the occurrence of TCR gene rearrangements and the requirement for Notch signalling.

Adapted from Hayday *et al* 2007.

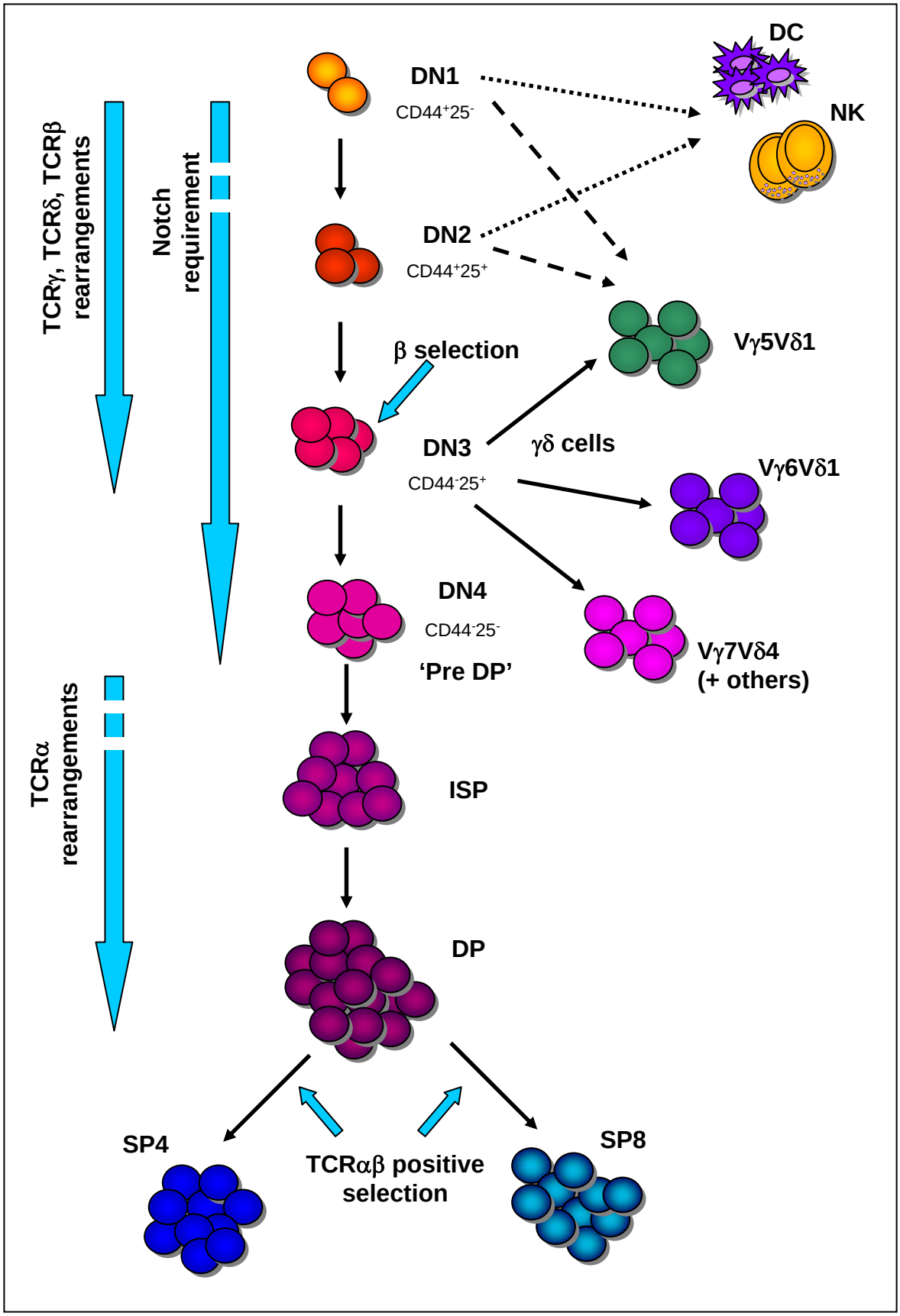
DC
NK
DN1
CD44+25-
DN2
CD44+25+
TCRγ, TCRδ, TCRβ rearrangements
Notch requirement
β selection
Vγ5Vδ1
DN3
CD44-25+
γδ cells
Vγ6Vδ1
DN4
CD44-25-
'Pre DP'
Vγ7Vδ4
(+ others)
TCRα rearrangements
ISP
DP
SP4
TCRαβ positive selection
SP8

Figure 1.3 Migration Of T Cells During Development

Early thymocyte progenitors (ETP) enter the thymus through blood vessels at the corticomedullary junction, due to their lack of expression of CD4 and CD8 they are known as double negative (DN) cells. The differentiation through the different DN subsets (DN1-DN4) occurs during the concomitant migration of the progenitors across the cortex in the direction of the capsule. DN4 thymocytes within the subcapsular region begin to differentiate into DP thymocytes with the upregulation of the coreceptor proteins, most often CD8 first followed by CD4. In addition their polarity of migration is reversed and they begin their journey back through the cortex in the direction of the medulla. As the DP cells further mature to become single positive (SP) CD4 or CD8 cells they cross the corticomedullary junction into the medulla. Once maturation and differentiation of the SP cells in complete, mature $CD8^+$ and $CD4^+$ T cells are exported from the thymus. BV, Blood Vessel. This directed migration through the different thymic microenvironments enables the developing thymocytes to receive essential signals from specialised stromal cells.

Arrows indicate direction of migration. DN, double negative, DP, double positive, SP4, single positive CD4 T cell, SP8, single positive CD8 T cell, cMES, cortical mesenchyme, cTEC, cortical thymic epithelial cell, mTEC, medullary epithelial cell, DC, dendritic cell.

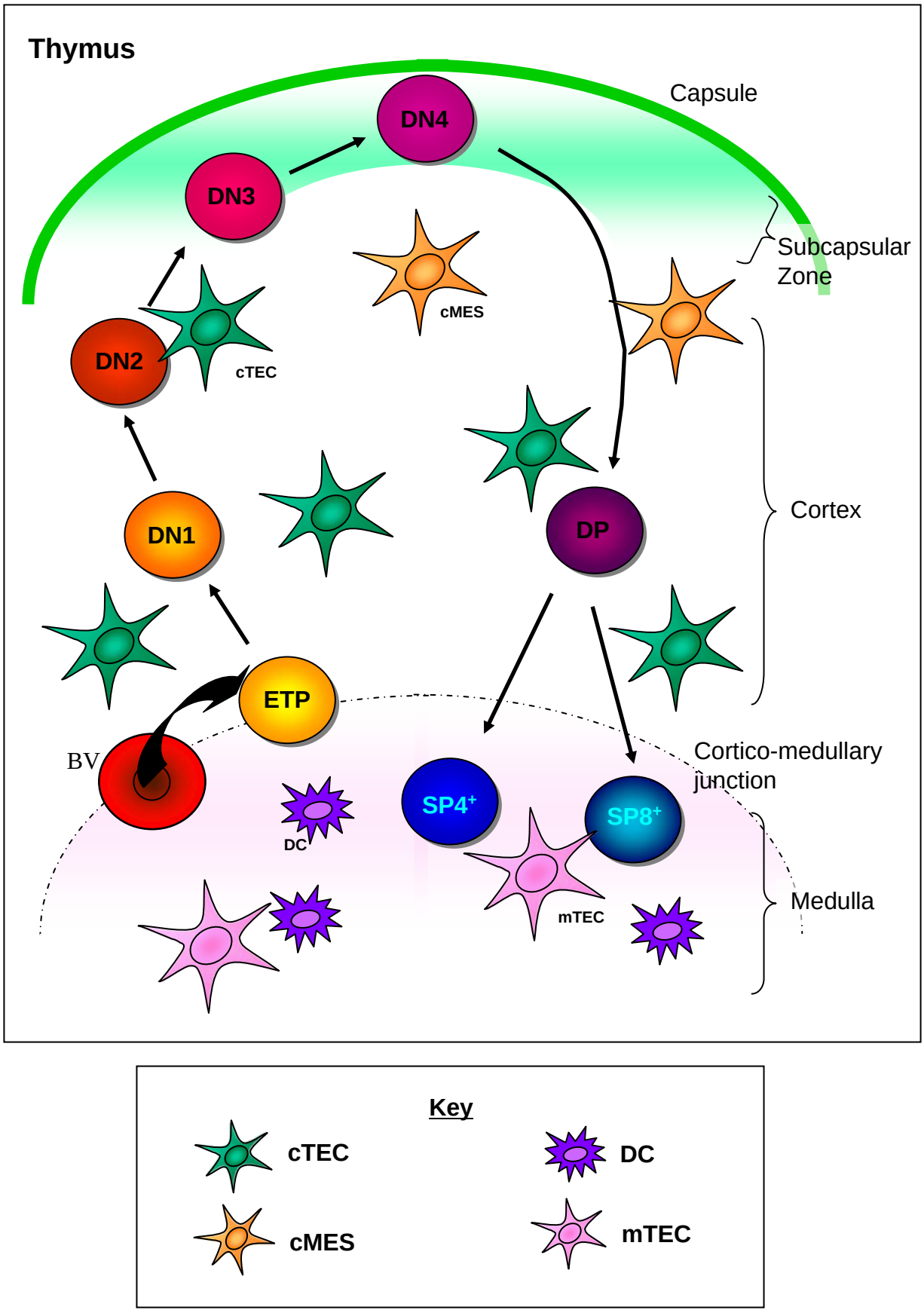
Thymus
Capsule
DN4
DN3
Subcapsular Zone
cMES
DN2
cTEC
Cortex
DN1
DP
ETP
BV
Cortico-medullary junction
DC
SP4+
SP8+
mTEC
Medulla
Key
cTEC
DC
cMES
mTEC

The signals that mediate this thymocyte trafficking are yet to be fully elucidated. Adhesion molecules linked to the actin cytoskeleton, primarily integrins mediate this movement. However, there is increasing evidence to suggest an important role for the expression of positional signals that polarise cell movement, such as chemokines and their receptors during this process (Petrie, 2003; Takahama, 2006). Chemokines are a super family of chemotactic cytokines that stimulate cell migration via G-protein-coupled seven-transmembrane receptors (Rossi and Zlotnik, 2000). In particular, Cxcl12 and its receptor Cxcr4 has been identified as essential for the proper localisation of $CD4^-$ $CD8^-$ double negative thymocytes (DN cells) in the cortex and their migration outwards (Plotkin et al., 2003).

Interestingly, while polarised migration of the developing lymphoid cells between distinct stromal environments is required during postnatal T cell development, in the fetal thymus, compartmentalisation of the fetal organ occurs simultaneously with lymphoid differentiation (Lind et al., 2001). Therefore, it is important to note that the requirement for chemokine receptor mediated migration of thymocytes is likely to differ in the fetal thymus, due to the absence of vasculature and structure during progenitor colonisation.

The first stage, defined as $CD117^+CD25^-CD44^{hi}$ (DN1), contains a heterogeneous population of cells, the majority of which are not T cell progenitors, as T lineage commitment is a protracted process, not uniformly achieved until the DN3 stage (Allman et al., 2003; Ciofani and Zuniga-Pflucker, 2007; Porritt et al., 2004). The early T lineage progenitors (ETPs) within the DN1 population are phenotypically analogous to bone marrow multipotent cells, lineage marker negative with high expression of Sca-1 and c-Kit ('LSK' cells), however they are efficient T cell precursors (Balciunaite et al., 2005). The DN1 population includes cells with multilineage potential, however the precise lineage potential of these cells is controversial. It is thought they are able to differentiate into T and B-lymphocytes, DC and NK cells but not

myeloid cells (Allman et al., 2003; Lind et al., 2001). Furthermore, this classification of DN1 cells is highly simplified and heterogeneity has been identified within this stage as defined by the further expression of haemato-lymphoid lineage markers such as CD24 (heat stable antigen (HSA)) (Porritt et al., 2004) and fms-related tyrosine kinase 3 (Flt3(CD135)) (Sambandam et al., 2005). These various DN1 progenitor subsets all home to the thymus but have different proliferative capacities and lineage potentials, therefore the observed heterogeneity is probably not due to the presence of multilineage progenitors (Kawamoto et al., 1998). These cells enter the thymus at the cortico-medulary junction (CMJ) and can be predominantly found here. Interestingly in addition to Cxcr4, Ccr7 the receptor for Ccl19 and Ccl21 has been partially implicated in the outward migration of DN thymocytes, as DN2 thymocytes are partially arrested at the corticomedullary junction in the absence of Ccr7 (Misslitz et al., 2004).

The DN2 stage ($CD25^{+}$ $CD44^{hi}$ $CD117^{+}$) represents a predominant T lineage specified population that retains a limited NK and DC lineage potential (Ciofani et al., 2006; Shen et al., 2003). These cells are primarily found within the mid-cortical region of the thymus. Recombination-activating gene (Rag)-1 and Rag-2 mediated TCR rearrangements of the TCRδ, TCRγ and TCRβ loci are initially detected during the DN2 phase continuing to the DN3 stage where fully rearranged (V-DJ and VJ) loci are present (Ciofani and Zuniga-Pflucker, 2007; Godfrey et al., 1994; Livak et al., 1999). Notch 1 signalling is essential for TCRβ gene rearrangement consequently it is likely to coincide with T cell lineage commitment (Schmitt et al., 2004). In addition, IL-7 regulates TCRγ gene rearrangement by controlling locus accessibility and thus is essential for γδ T cell development (Laky et al., 2003; Zamisch et al., 2005).

$CD117^{-}$ $CD44^{-}$ $CD25^{+}$ (DN3) cells appear to be fully T lineage committed and are concentrated in the outermost region of the thymus adjacent to the capsule, the subcapsular zone

(SCZ). Ccl25 and its receptor Ccr9 are thought to be important for the localisation of these cells to the SCZ (Benz et al., 2004). The two T cell lineages αβ and γδ diverge at or prior to this stage (Starr et al., 2003). For cells that proceed along the αβ TCR pathway, the functional TCRβ chain associates with a transiently expressed invariant pre-TCRα (pTα) chain and the CD3 complex of molecules to form the pre-TCR (Ciofani and Zuniga-Pflucker, 2007; Hayes et al., 2003). The pTα functions as a surrogate for TCRα before the rearrangement of the TCRα locus however, it differs from TCRα in that it is encoded by an non-rearranging locus, has a single extracellular Ig-domain and a larger cytoplasmic domain (Germain, 2002). The pre-TCR complex is required to mediate β selection, which signals the successful completion of TCRβ chain gene rearrangement. Pre-TCR expression is approximately 50-100 fold lower than that of TCR on mature cells, nonetheless this step represents the first of three critical checkpoints for T cell maturation; failure to assemble the pre-TCR results in apoptosis (von Boehmer et al., 1999). The pre-TCR is thought to signal cell-autonomously in a ligand independent manner through self-oligomerisation (Ciofani and Zuniga-Pflucker, 2007; Yamasaki et al., 2006). It provides survival signals and results in proliferation, differentiation and cessation of TCRβ rearrangement preventing expression of a rearranged receptor by the second allele, a process known as allelic exclusion (Alt et al., 1992; Baldwin et al., 2005; Levelt et al., 1995). The occurrence of β-selection can be identified by the marked increase in CD27 and CD28 expression as well as the induction of IL-7Rα which is thought to be responsible for providing the survival and proliferation signals (Taghon et al., 2006; Teague et al., 2010; Williams et al., 2005). In addition β-selection initiates TCRα rearrangement, and development of positive and negative selection "competence" factors (Michie and Zuniga-Pflucker, 2002). Only the cells that have successful in-frame β rearrangements are selected for further differentiation beyond the DN3 stage (Godfrey and Zlotnik, 1993; Takahama, 2006).

The cells that emerge from β-selection, the DN4 ($CD117^-$ $CD25^-$ $CD44^-$) population undergo 6-8 cell divisions and represent an early $CD4^+CD8^+$ double positive (DP) population (pre-DP) (Germain, 2002; Prockop and Petrie, 2000; Schmitt et al., 2004). DN4 cells reside within the subcapsular region of the thymus. It is at this stage where they begin to differentiate into DP thymocytes with the upregulation of the coreceptor proteins, most often CD8 first followed by CD4 (Germain, 2002). Vα/Jα joins can be detected at low levels at the DN4 stage, however, full-scale α locus rearrangement does not occur until the cell becomes a quiescent DP cell (Starr et al., 2003). The progression from DN cells to DP cells occurs through the transitory subset of thymocytes known as immature single positives (ISP), defined as either $CD4^+$ $CD8^-$ $CD3^-$ or $CD4^-$ $CD8^+$ $CD3^-$ (Hugo et al., 1990; Tatsumi et al., 1990). Such ISP cells represent a rapidly cycling intermediate precursor for $CD4^+$ $CD8^+$ cells. Transition to the DP stage is accompanied by attenuation of Notch receptor activity and expression (Huang et al., 2003). A role for chemokines in the migration from the subcapsular region until positive selection of DP thymocytes within the cortex is yet to be fully defined.

1.2.4 Pre – TCR Development

During the DP stage of thymocyte differentiation, the *Rag* genes are expressed once again, and the cells undergo TCRα chain rearrangement. Multiple V/J recombination events occur on the same allele at the α locus, enabled by its configuration, and each event results in the excision of the prior recombined DNA. In addition recombination events begin at the 5' end of the J locus and proceed to the 3' end, enabling multiple different productive rearrangements to be tested per cell (Petrie et al., 1993). However, due to the 3-4 day lifespan of DP thymocytes this process is finite. DP lifespan is regulated by the expression of several factors, including the steroid transcription factor Rorγ (retinoic acid-related orphan receptor γ) and its thymus specific isoform Rorγt as well as the transcription factors in the *wnt* signalling pathway, T cell factor

(TCF)-1 and lymphoid enhancer factor (LEF)-1 which control expression of the anti-apoptotic factor, Bcl-X_L. Without the activity of these factors Bcl-X_L is not expressed, and as a result DP thymocytes die by neglect before having the opportunity to undergo positive selection (Ioannidis et al., 2001; Starr et al., 2003; Sun et al., 2000).

Once successful rearrangement of the α locus has occurred the thymocytes lose the expression of the pre-TCR and the successfully rearranged α chain pairs with the existing TCRβ chain and is expressed at low levels on the cell surface. This exchange process occurs efficiently due to the TCRβ chain having a higher affinity for the TCRα than for the pTα (Baldwin et al., 2005; Goldrath and Bevan, 1999). DP αβ TCR expressing immature cells constitute 90% of the thymic lymphoid compartment. At this stage the polarity of migration of the DP thymocytes is reversed and they begin their journey back through the cortex in the direction of the medulla. Thus DP cells are resident within the cortex and are the first population to successfully express a functional heterodimeric TCR at the cell surface (Starr et al., 2003).

TCR assembly itself is not sufficient to trigger the further differentiation of the DP thymocytes. A process termed positive selection is responsible for the maturation events concerned and ensures stable expression of the selected TCR (Hamrouni et al., 2007; Starr et al., 2003). Positive selection represents the second checkpoint of αβ T cell development. It involves the screening of the newly expressed functional TCRs for their ability to bind self MHC expressed on cortical epithelium with sufficiently low affinity. It results in *Rag* gene downregulation, thus termination of Vα to Jα rearrangements, long-term survival, migration to the medulla and maturation. Conversely, when this interaction occurs with too high affinity the DP cell is eliminated in a process termed negative selection (Bommhardt et al., 2004; Hamrouni et al., 2007). This is important because of the stochastic generation of diversity in the T cell repertoire, creating potentially autoaggressive T cells (Cabarrocas et al., 2006). Elimination of

these self-reactive cells from the repertoire, by negative selection is necessary to avoid the potentially pathological state of autoimmunity (Anderson et al., 2002; Cabarrocas et al., 2006). In the absence of MHC recognition DP thymocytes will undergo apoptotic death because of receptor neglect (Goldrath and Bevan, 1999). Less than 5% of DP thymocytes with αβ TCRs that recognise self MHC are selected to mature into single positive (SP) T cells and this low-affinity recognition determines commitment to either the CD4 or CD8 lineage. It is generally thought that relatively rare, low affinity self-peptides promote positive selection (Merkenschlager et al., 1997; Starr et al., 2003). With remarkable consistency, DP thymocytes that receive signals through MHC class II restricted TCRs differentiate into $CD4^+$ T cells, and those that receive signals through MHC class I restricted TCRs differentiate into $CD8^+$ T cells (Singer et al., 2008). DP thymocytes are unique among T-lineage cells as they are bipotential cells that express both CD4 and CD8 coreceptors. CD4 and CD8 coreceptors are transmembrane proteins with extracellular domains that augment TCR engagement of peptide MHC complexes and intracellular domains that enhance TCR signal transduction through association with the protein tyrosine kinase Lck (Singer et al., 2008). By binding the MHC presenting the ligand, CD4 and CD8 bring intracellular Lck into physical proximity with the cytosolic domains of the engaged TCR and initiate signalling (Discussed in detail in section 1.1.6). By expressing both coreceptor molecules, all potentially useful TCRs can generate positive selection signals and rescue DP thymocytes from cell death (Singer et al., 2008).

The initiation of positive selection is critically dependent upon interactions with MHC molecules expressed on thymic epithelial cells. As thymocyte development is arrested at the DP stage in the absence of both MHC class I and class II expression (Crump et al., 1993; Lucas and Germain, 1996). However, the requirement for MHC molecules is restricted to the initial phase of positive selection as terminal stages of positive selection and early postselection events occur

in an MHC independent manner (Hare et al., 1999a). During positive selection, a variety of phenotypic changes occur, including the up-regulation of the αβ TCR complex and transient expression of the early activation/selection markers CD69 and CD5 (Azzam et al., 1998; Hare et al., 1998; Merkenschlager et al., 1997). In addition, positive selection signalling causes the up-regulation of Ccr7 expression and as mTECs predominantly produce the ligands, Ccl19 and Ccl21, signalling through Ccr7 has been identified as essential for the rapid and directed migration to the thymic medulla (McCaughtry et al., 2007; Ueno et al., 2004; Witt et al., 2005). Positive selection enriches for 'useful' T cells that are potentially reactive to foreign antigens but are self tolerant through MHC restriction (Takahama, 2006).

1.2.5 CD4/CD8 Lineage Choice

The concomitant down-modulation of both CD4 and CD8 after TCR signalling occurs irrespective of the MHC class involved, creating a $CD4^{lo}CD8^{lo}TCR^{int}$ transitional population (Lucas and Germain, 1996). This is followed by an intermediate $CD4^{+}CD8^{lo}$ population, better defined by their $Cd4^{+}Cd8^{-}$ transcriptional phenotype, due to the termination of *Cd8* gene transcription during positive selection (Brugnera et al., 2000).

The underlying molecular and cellular mechanisms regulating CD4/CD8 lineage decisions remain unclear. However, the most recent model "the kinetic signalling model" proposes that CD4/CD8 lineage choice is determined by TCR-signal duration and that cytokines of the common cytokine γ chain (γc) family serve as 'sensors' that detect the duration of the TCR signal (Singer et al., 2008). This model makes it apparent that positive selection and lineage choice are sequential, not simultaneous events. TCR mediated positive selection leads to the termination of *Cd8* gene transcription, converting signalled DP thymocytes into an intermediate $CD4^{+}CD8^{lo}$ population that remains lineage-uncommitted, with the ability to differentiate into either $CD4^{+}$ or $CD8^{+}$ T cells, depending on whether TCR signalling persists or ceases

respectively. The persistence or cessation of TCR signalling inversely regulates signalling that is induced by IL-7 and other γc cytokines, creating a sensor of TCR duration (Brugnera et al., 2000; Singer and Bosselut, 2004).

'Coreceptor reversal' is the collective name for molecular events involved in the termination of CD4 gene transcription and the reinitiation of CD8 gene transcription in $CD4^+CD8^-$ intermediate thymocytes committed to the CD8 lineage (Brugnera et al., 2000). It depends on signalling by IL-7 and possibly other γc cytokines which are important for the survival of the CD8 committed $Cd4^+Cd8^-$ intermediate thymocytes as they are no longer receiving TCR signals. Furthermore these cytokines have been shown to enhance CD4 silencing and promote the reinitiation of CD8 gene transcription (Yu et al., 2003).

1.2.5.1 Transcription Factors In Lineage Choice

The identification of transcription and nuclear factors involved in the regulation of *Cd4* and *Cd8* gene transcription has improved the understanding of CD4/CD8 lineage choice. Some factors are involved in cromatin remodelling, such as Ikaros, whereas others directly regulate transcription of downstream effector genes (Singer et al., 2008; Urban and Winandy, 2004). These include Th-POK (T-helper-inducing POZ/Kruppel like factor), and RUNX3 (runt-related transcription factor 3), together with TOX (thymus high-mobility group (HMG) box protein) and GATA3 (GATA-binding protein 3) (Singer et al., 2008).

Th-POK is a zink finger protein that appears to be both necessary and sufficient for CD4 lineage choice and it is thought to be a master regulator of CD4 lineage choice and CD4 T cell differentiation (He et al., 2005; Kappes and He, 2006). It is initially expressed at the $CD4^+CD8^{lo}$ intermediate stage where the level is too low to limit the bipotentiality of this population and is upregulated after persistent TCR signalling (He et al., 2005).

1.2.6 Post-Selection Maturation And Export To The Periphery

Positively selected DP thymocytes are stimulated to differentiate into SP $CD4^+CD8^-$ or $CD8^+CD4^-$ thymocytes and relocate to the medulla where they spend approximately 12 days before being exported to the periphery (Egerton et al., 1990; Takahama, 2006). During their residency within the medulla, the newly generated SP thymocytes undergo sequential maturational changes commonly identified by the expression profiles of the adhesion molecule CD62 ligand ((CD62L) lymphocyte (L)-selectin) and CD69. This process of SP thymocyte maturation results in receptor tuning and final functional development to become mature naïve T cells (Bendelac et al., 1992; McCaughtry et al., 2007). Newly generated SP thymocytes are $CD62L^{lo}CD69^{hi}$ semi mature and functionally incompetent and further maturation produces functional SP thymocytes that are $CD62L^{hi}CD69^{lo}$ (Takahama, 2006). Additional markers used to identify the maturation of SP thymocytes include the progressive down-regulation of CD24 and the up-regulation of Qa-2, H-2K, and CD45RB (Jin et al., 2008; Takahama, 2006).

In addition, during medullary residency the nascent thymocyte population undergoes further deletion of potentially self-reactive thymocytes that escaped negative selection in the cortex. This occurs through exposure to tissue specific antigens (TSA) and is particularly important for establishing central tolerance. This negative selection process is a vital step supported by medullary thymic epithelial cells (mTEC); more specifically an autoimmune regulator (Aire) expressing subset is fundamental for this regulation (see section 1.3.2.3 for more detailed discussion of the role of mTECs in central tolerance). Within a few days, SP thymocytes up-regulate the transcription factor Kruppel-like factor (KLF) 2 and KLF2 target genes, including the G protein-coupled receptor, sphingosine-1-phosphate (S1P) receptor-1 ($S1P_1$), and CD62L (Zachariah and Cyster, 2010).

1.2.6.1 Thymic Egress

Systemic immune surveillance ultimately requires the release of newly derived T cells from the thymus and into the peripheral circulation (Petrie, 2003). Thymic egress is a highly ordered process where only the oldest and most mature cells exit (McCaughtry et al., 2007). However, it is poorly understood and a route by which egress occurs has only recently been identified. Although cells have been identified crossing blood vessels at the corticomedullary junction, these studies were nonquantitative (Raviola and Karnovsky, 1972; Toro and Olah, 1967). It was assumed that cells ready for export would change their integrin status and/or adhesion ligand requirements, or change their responsiveness to positional cues (Petrie, 2003). As a result chemokine signals were implicated in the thymic egress process, however these signals typically come from stable stromal cells for example, Ccl19 on endothelial cells. Therefore, chemokines cannot be the only signals implicated in this process, as they would only be able to guide migration to their source, after which additional signals would be required. Ccl19 is highly enriched on medullary endothelial venules and has consequently been implicated in mediating thymocyte export by guiding the positioning of mature thymocytes near the vessels through which they exit (Dong et al., 2009). Additionally thymic egress is tightly regulated by a chemoattractant lipid receptor, the $S1P_1$ (Dong et al., 2009). CD69 regulates $S1P_1$ function in peripheral T cells; however within the thymus, where it is expressed on semimature SP thymocytes, it is responsible for regulating the timing of thymocytes egress, delaying it by several hours to ensure complete selection and maturation (Shiow et al., 2006; Zachariah and Cyster, 2010). The receptor S1P exists at high concentrations in blood however, plasma S1P alone appears to be insufficient to promote normal egress (Pappu et al., 2007). S1P is also present at a low concentration in the thymus due to the action of the enzyme S1P lyase, and it has been recognised that the major S1P source, necessary for thymic egress, is radioresistent

suggesting a local stromal cell type as the supply (Pappu et al., 2007; Schwab et al., 2005; Zachariah and Cyster, 2010). Pericytes closely ensheath blood vessels and interestingly it has been shown that thymic pericytes contribute to the S1P required for thymocytes egress (Foster et al., 2008; Krueger and Bechmann, 2010; Muller et al., 2008; Zachariah and Cyster, 2010). Postcapillary venules at the corticomedullary junction are thin walled, with only a single layer of ensheathing pericytes, it has been established that T cells emigrate via blood vessels at the corticomedullary junction, so maybe these venules are specialised to support thymocyte egress (Muller et al., 2008; Zachariah and Cyster, 2010).

T cells undergo phenotypic and functional changes even after leaving the thymus. Recent thymic emigrants slightly reduce CD3 and CD24 expression while increasing Qa2, IL7Ra, CD62L and CD28 expression to mature naïve T cell levels, by about two weeks after thymic emigration (Boursalian et al., 2004; Jenkins et al., 2010).

1.3 The Thymic Stroma

As T cell development is a non-cell autonomous process, the thymic microenvironment provides an essential location that fosters the growth, differentiation and selection of the nascent T cell population. This unique role of the thymus is intimately linked to the specialised functions of thymic stromal cells and the thymus architecture. Consequently failure to build or maintain a proper thymus structure can lead to immunodeficiency or autoimmunity. The thymic stroma consists of all non-haematopoietic components of the thymus that are functionally defined as, the elements that constitute the thymus structure. Regardless of their origin and lineage, these cells provide a matrix on which thymocytes develop (Anderson and Jenkinson, 2001; Petrie and Zuniga-Pflucker, 2007). The unique functions of the thymus reside mainly in the thymic epithelium, which forms the major component of the stroma. The stroma is divided into two main regions on histological grounds, the cortex and medulla, which contain several

ultrastucturally and phenotypically distinct kinds of thymic epithelial cells (TEC). TECs play crucial roles at multiple stages of T cell development, and provide an array of signals to developing thymocytes that include soluble factors for survival and expansion (e.g IL-7, SCF), and Notch ligands for commitment and differentiation (Anderson et al., 2009; Rodewald, 2008; Shakib et al., 2009; Takahama, 2006). In addition, TECs also provide peptide-MHC ligands for selection. Cortical TECs (cTEC) impose self-MHC restriction on immature thymocytes via positive selection and medullary TECs (mTEC) facilitate the elimination of autoreactive thymocytes via negative selection.

Thymus development not only involves differentiation of T cell precursors into mature T cells, as discussed previously, but also modifications in the TEC compartment that supports this process. Thus gaining a better understanding of the development of cTEC and mTEC including the stages and mechanisms involved will also improve the understanding of intrathymic T cell production.

1.3.1 Thymus Organogenesis

An essential prerequisite for the generation of a functionally competent T cell pool is the creation of a mature thymic epithelial microenvironment (Jenkinson et al., 2003). In analogy to organ development in general, thymus organogenesis has been divided into steps; positioning, determining specifically where the organ rudiment will develop, budding and outgrowth of the thymus anlage from the third pouch, detachment of the primitive thymus from its endodermal basis, and patterning, differentiation and migration of the thymus towards its final anatomical location (Blackburn and Manley, 2004; Manley, 2000; Rodewald, 2008).

Thymus organogenesis is a highly complex and dynamic process involving reciprocal tissue interactions between epithelial cells derived from the endoderm of the anterior foregut, and neural crest derived mesenchyme to form the thymic rudiment (Boehm, 2008). Segmentation

of the posterior pharynx constitutes the gateway to thymus formation as the primordium emerges from the ventral aspect of the third pharyngeal pouch endoderm resulting in the specification of epithelial cells to a thymic cell fate (Hollander et al., 2006; Manley and Blackburn, 2003). The first signs of the budding and outgrowth of the epithelial rudiment are morphologically detectable by embryonic day 10-11 (E10-11). Early organogenesis of the thymus is closely coupled to that of the parathyroid gland, as they are formed from a common primordium (Anderson et al., 2006; Hollander et al., 2006). However, they are already partitioned as identified by gene expression studies indicating the appearance of FoxN1 (Forkhead box protein N1) and glial cells missing 2 (Gcm2), essential transcription factors for thymus and parathyroid development respectively (Gunther et al., 2000; Nehls et al., 1996; Nehls et al., 1994). Once formed, the thymus epithelial primordium evaginates and extends into the underlying tissue of the pharyngeal arch. Budding and outgrowth coincides with onset of the expression of the *FoxN1* gene, which is first detected at E11.5. At about E12.5, the thymic primordium has separated from the endodermal surface of the foregut and begins to migrate towards the anterior chest cavity. This provides a structure that attracts lymphocyte precursors of haematopoietic origin, which begin to colonise the anlagen (Blackburn and Manley, 2004; Rodewald, 2008).

At around E12.5, coinciding with haematopoietic colonisation and prior to vascularisation, the immature thymus undergoes further patterning and differentiation (Rodewald, 2008). This phase initiates the first signs of morphological medulla-cortex separation and is the major developmental checkpoint with respect to the functional epithelial anlage. The discrete cortical and medullary areas contain increasingly defined subsets of epithelial cells (Anderson and Jenkinson, 2001; Hollander et al., 2006). This bifurcation is associated with changes in keratin (K) expression patterns in the epithelium and can occur in the absence of lymphocytes (Boehm, 2008; Jenkinson et al., 2005). Throughout ontogeny, and in the adult

thymus, TEC subsets express different members of the keratin family (Rodewald, 2008). How immature thymic epithelial cells are triggered to generate defined cortical and medullary microenvironments capable of supporting lymphocyte precursor differentiation and functional maturation into a self-tolerant diverse repertoire of T cells, is unclear (Boehm, 2008; Hollander et al., 2006; Jenkinson et al., 2003).

In addition to endodermal epithelium, another important stromal cell type that influences thymocyte development and plays a critical role in regulating thymus primordium formation, is neural crest derived mesenchymal cells of neuroectoderm origin (Anderson et al., 2006; Hollander et al., 2006). Neural crest cells are a developmentally plastic population that migrate from the dorsal side of the neural tube. At E13, perithymic mesenchyme migrates towards the epithelial rudiment and establishes a condensing mesenchymal capsule that interacts with immature thymocytes in addition to immature epithelial cells (Jenkinson et al., 2003). Such cells contribute to the thymic capsule, and septae, as well as connective tissue and pericytes associated with blood vessels penetrating the thymic lodes (Anderson and Jenkinson, 2001; Hollander et al., 2006; Zachariah and Cyster, 2010). Thymic mesenchyme also promotes epithelial development and proliferation, and might also influence TEC differentiation, by providing undefined inductive signals essential for thymus morphogenesis before E12.5. Additionally neural crest cells may guide the migration of the thymic primordium towards the anterior chest cavity (Blackburn and Manley, 2004; Jenkinson et al., 2003).

1.3.2 Composition Of The Thymic Stroma

The thymic stroma is an extremely heterogeneous population comprised of many cell types with specialised functions. A simple, nevertheless useful classification of stroma lacking the pan-hematopoietic marker CD45 is based on expression of keratins (K); mature thymic epithelial cells can be characterised by their differential expression of K5 and K8. Medullary

epithelial cells (mTEC) are largely $K5^{+}K8^{-}$ whereas cortical epithelial cells (cTEC) are predominantly $K5^{-}K8^{+}$ (Anderson et al., 2006; Rodewald, 2008). In addition, the cortex and medulla differ in their anatomical location, cellular morphology and their functional properties (Alves et al., 2009). Interestingly, epithelial cells are primarily $K5^{+}K8^{+}$ double positive, early in thymocyte development, possibly representing a bipotent cell precursor, which proliferates and differentiates into mature single positive epithelial cells (Anderson et al., 2006). A subset of epithelial cells simultaneously express K5 and K8 in the adult thymus and these are normally located at the corticomedullary junction (Anderson and Jenkinson, 2001).

Keratin negative cells are generally considered as mesenchymal cells and include fibroblasts, nonfibroblastic mesenchymal cells, capsule- and septae-forming connective tissue cells and endothelial cells forming the typical thymus vasculature (Rodewald, 2008). Additionally, non-epithelial components include extracellular matrix proteins (such as ER-TR7 and perlecan), podoplanin and bone marrow derived dendritic cells and macrophages, which are $CD45^{+}$ haematopoietic cells that also form an integral element of the thymic stroma (Ladi et al., 2006).

1.3.2.1 Bipotent Thymic Epithelial Progenitors

During early thymus organogenesis the murine thymic primordium is a relatively simple structure, comprising of a core of undifferentiated epithelial cells surrounded by a capsule of neural crest derived mesenchyme (Rossi et al., 2006). While recent evidence shows that cortical and medullary epithelial lineages share a common endodermal embryonic origin, the phenotype and possible persistence of a progenitor population in the thymus at later stages of development remains incompletely understood (Rossi et al., 2007a); even though it was speculated early on that cTEC and mTEC shared a common bipotent progenitor (bTECp) (Ritter and Boyd, 1993; Ropke et al., 1995). Later, ectopic transplantation of isolated E12 thymus lobes indicated that the

cells within this thymic primordium have substantial potential for growth, and the capacity to generate a correct thymus structure with cortical and medullary architecture, demonstrating that the progenitor activity required to establish a complete thymus environment can be found within the isolated rudiment at this stage (Bennett et al., 2002; Rossi et al., 2006). It is now widely accepted that both cortical and medullary epithelial lineages arise from a common progenitor population (Bleul et al., 2006; Rossi et al., 2007a).

Two studies simultaneously reported the existence of bTECp. A clonal analysis of individual TEC from early embryonic thymus demonstrated the presence of a dominant common epithelial precursor population (Rossi et al., 2006). Additionally, random reactivation of *FoxN1* in individual TEC enabled the important observation that the progenitor population persists in the postnatal thymus (Bleul et al., 2006). It has been shown that progenitor activity resides within a rare thymic epithelial cell that co-expresses markers that segregate later into cortical and medullary epithelium, namely Keratin 5 (medulla) and Keratin 8 (cortex) (Bennett et al., 2002; Gill et al., 2002; Klug et al., 1998). It was originally thought that bipotent potential was a feature of the MTS24 positive subset of $K8^{+}K5^{+}$ thymic epithelial cells (Bennett et al., 2002; Gill et al., 2002; Klug et al., 2002). The MTS24 antibody has recently been shown to bind to Plet-1 (Depreter et al., 2008). However, subsequent studies illustrated that both $MTS24^{+}$ and $MTS24^{-}$ populations, in the context of the pan epithelial markers, epithelial cell adhesion molecule (EpCam1) and pancytokeratin, were able to generate a functional thymus comprised of both cortical and medullary areas (Rossi et al., 2007a). Although EpCam is a pan epithelial marker, different levels of expression, high or low, represent a differentiated medullary and cortical phenotype respectively (Rossi et al., 2007a). The differentiation of the bTECp to cortical and medullary lineages is dependent on the transcription factor FoxN1 (Ciofani and Zuniga-Pflucker, 2007; Shakib et al., 2009). In the absence of *FoxN1* expression the development of early bTECp

appears to be reversibly arrested, as restoration of FoxN1 expression can induce normal differentiation (Bleul et al., 2006).

bTECp have only been identified on the basis of their functional properties to date, and despite evidence for their persistence beyond the embryonic period, the identification of appropriate phenotypic markers is required for the further elucidation of TEC biology (Anderson et al., 2009; Bleul et al., 2006). The identification of bTECp provides a clear starting point from which to study the development of the distinct lineages (Shakib et al., 2009).

1.3.2.2 Development And Function Of Cortical Epithelium

The cortex is characterised by a meshwork of reticular epithelial cells that can be identified by the expression of specific cell markers including MTS44, Keratin 8 and Ly51 (Gray et al., 2006). However, typically cTECs are phenotypically identified as $EpCam1^{+}Ly51^{+}$. The recent identification of a novel proteasomal subunit, β5t, and the integral membrane protein, CD205 (DEC205), along with maturation markers such as MHC class II and CD40, have facilitated the identification of their developmental pathway (Figure 1.4) (Gray et al., 2006; Jiang et al., 1995; Murata et al., 2007). β5t is a novel catalytic subunit of the 20S proteasome, expressed exclusively in cTECs. Proteasomes are responsible for generating peptides presented by the class I MHC molecules, which in this context are responsible for the positive selection of developing thymocytes. Thus, β5t has a key role in generating MHC class I-restricted $CD8^{+}$ T cells during thymic selection (Murata et al., 2007). It is thought that in contrast to constitutive proteosomes, which produce high affinity ligands, thymoproteosomes such as β5t produce low affinity MHC I ligands in cTECs, thereby supporting positive selection rather than activation or negative selection (Murata et al., 2007).

A small but detectable $EpCam^{+}$ $CD205^{+}$, expressing β5t cTEC subset first appears in ontogeny at E12 (Shakib et al., 2009). However, this population is absent from $FoxN1^{nu/nu}$

Figure 1.4 A Model Of mTEC And cTEC Development From A Bipotent Progenitor

The left is the developmental pathway for medullary thymic epithelial cells, right is the cortical epithelial developmental pathway both originating from an endoderm derived bipotent thymic epithelial cell. Epithelial cells are acknowledged by their universal expression of EpCam. Medullary epithelial cells are identified by their expression patterns of UEA-1 and AIRE which alter at different stages. Cortical epithelial cells are identified by their expression of CD205, β5t and cathepsin-L. Mature epithelial cells are recognised as a low proliferative population; Circular arrows represent proliferation. In red shows signalling pathways important at the stages indicated. Also indicated is the requirement for FoxN1 expression.

mTEC, medullary thymic epithelial cells. cTEC, cortical thymic epithelial cells. Imm, immature, Mat, mature. bTECp, bipotent cortical and medullary progenitor.

Modified from Shakib *et al* 2009 and Nishikawa, *et al* 2010 .

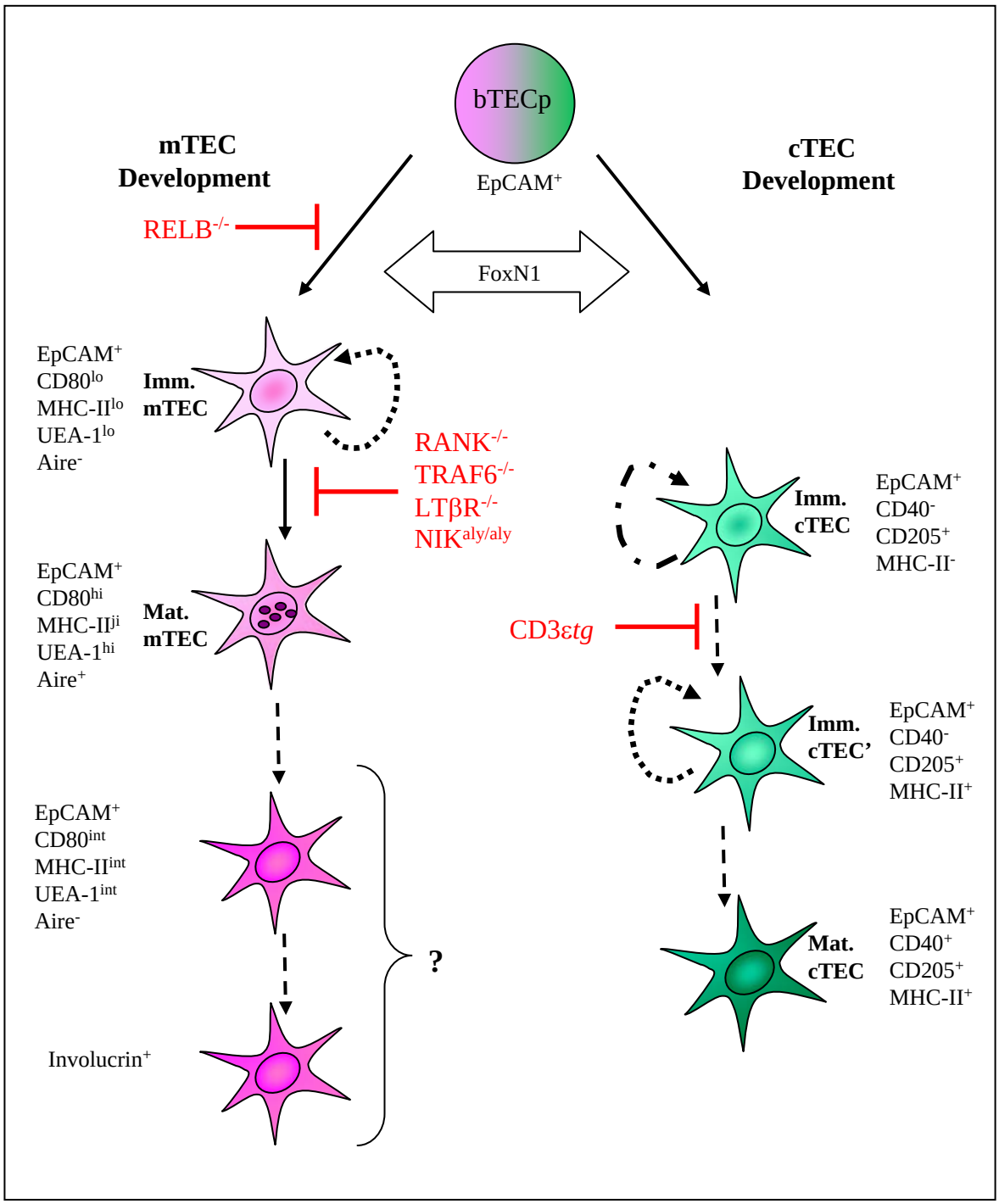
bTECp
EpCAM+
mTEC Development
cTEC Development
RELB-/-
FoxN1
EpCAM+ CD80lo MHC-IIlo UEA-1lo Aire-
Imm. mTEC
RANK-/-
TRAF6-/-
LTβR-/-
NIKaly/aly
EpCAM+ CD80hi MHC-IIji UEA-1hi Aire+
Mat. mTEC
EpCAM+ CD80int MHC-IIint UEA-1int Aire-
Involucrin+
?
Imm. cTEC
EpCAM+ CD40- CD205+ MHC-II-
CD3εtg
Imm. cTEC'
EpCAM+ CD40- CD205+ MHC-II+
Mat. cTEC
EpCAM+ CD40+ CD205+ MHC-II+

thymic epithelium suggesting the acquisition of these markers and thus cTEC lineage choice, is a FoxN1 dependent process (Shakib et al., 2009). $CD205^+$ cTECs initially emerge as $CD40^-$ MHC class II^-, the expression of MHC class II occurs before CD40 expression, which is gradually obtained by E14-E15 of gestation (Shakib et al., 2009). In addition, this subset concomitantly increases expression of cTEC-associated genes such as Cathepsin-L and β5t with maturation (Shakib et al., 2009). A recent study has also highlighted the role of thymus-specific serine protease (TSSP), which is exclusively expressed in the endosomal compartment of cTECs, in the positive selection of a subset of $CD4^+$ T cells (Gommeaux et al., 2009). TSSP is thought to be involved in the processing of self-peptides for MHC class II presentation at the cTEC surface and likely constitutes the first serine protease to play a role in the intrathymic presentation of self-peptides in the context of MHC class II (Gommeaux et al., 2009).

Another parameter used to identify different developmental stages of cTEC development is proliferation, as TECs are known to undergo phases during maturation, rapidly dividing during early stages and slowing as they progress (Gray et al., 2006; Jenkinson et al., 2003). In addition, the recently described differential expression of the cTEC expressed Notch ligand Delta-like 4, in combination with other markers described above, may help further highlight the stages of cTEC development and increase the understanding of their regulation (Anderson et al., 2009; Fiorini et al., 2008). Interestingly, three dimensional reconstruction of thymus histology demonstrates that the cortex occupies three times more volume than the medulla, however the medulla is more densely packed with keratin whereas cTECs appear ‘stretched’ (Fontenot et al., 2005; Nasreen et al., 2003). Thus the adult cortex is established by relatively few cTEC extending long processes, whereas the medulla harbours greater numbers of more compact epithelial cells (Gray et al., 2006).

Relatively little is known about the regulation of cTEC development. However, abnormal cTEC architecture has been identified in mice lacking KREMEN1 (kringle containing transmembrane protein 1), a negative regulator of Wnt signalling. In addition, cTEC have been shown to express a range of Wnt molecules, including Wnt4 and Wnt10b (Osada et al., 2006; Pongracz et al., 2003). Taken together these findings are consistent with a role for the Wnt signalling pathway in the formation of the cortical microenvironment (Anderson et al., 2007). In addition, it is known that the initial stages of cTEC development, involving the upregulation of CD205 expression alone, can occur independently of thymocyte crosstalk, however, the presence of DN1 to DN3 thymocytes is necessary and sufficient for their further maturation to MHC class II^+ $CD40^+$ $CD205^+$ (Shakib et al., 2009).

Of functional significance cortical epithelial cells express both MHC I and II molecules and they have been identified as efficient and unique mediators of positive selection (Anderson et al., 1994). Regulation of thymic selection by cTEC and the accessory molecules involved are poorly defined. However, a potential candidate is CD83 as its absence appears to affect $CD4^+$ T cell positive selection (Fujimoto et al., 2002). Due to the specific expression of CD205, Cathepsin L, TSSP and β5t, cTECs posses distinct antigen processing and presentation capacities that influence their unique ability to support positive selection (Anderson et al., 2007).

A role for cTECs in the induction of central tolerance, through their ability to support negative selection of potentially autoreactive thymocytes remained controversial until recently (Goldman et al., 2005). McCaughtry *et al* demonstrated unequivocally that the clonal deletion of thymocytes can occur in the cortex and that it does not require the involvement of the medulla (McCaughtry et al., 2008). Additionally, it was shown that elimination of autoreactive T cells by apoptosis could occur in the absence of cortex-medulla migration, which is consistent with

previous thoughts (Kurobe et al., 2006). However, this mechanism requires induction via a rare $CD11c^+$ cortical DC population (McCaughtry et al., 2008).

1.3.2.3 Development And Function Of Medullary Epithelium

Medullary thymic epithelial cells are heterogeneous with regard to their phenotype (Derbinski et al., 2005). Markers such as MTS10 and Ulex europaeus agglutinin 1 (UEA-1), in addition to their globular morphology and expression of an array of co-stimulatory markers implicated in T cell activation such as, CD40 and CD80 (B7.1), distinguish them from cTECs (Dunn et al., 1997; Nelson et al., 1993). Furthermore, they express varying levels of MHC class II, CD80 and UEA-1, the increase of which is presumed to denote their progressive maturation (Figure 1.4) (Derbinski et al., 2005).

The first TECs with a medullary phenotype ($MTS10^+$), form single cell-derived islets that are apparent at E13 colocalising with clusters of $K5^+K8^+$ TECs (Gray et al., 2005; Rodewald et al., 2001). It has been proposed that mTEC development may be associated with the development of thymic post capillary venules (Anderson et al., 2000b). In support of this, it is thought that the expression of tight junction proteins claudin-3 (Cld3) and Cld4 signifies an mTEC progenitor population, located selectively in the TECs lining the apical layer of the stratified thymic anlage (Hamazaki et al., 2007). The thymus medulla, characteristically identified as $EpCam^+Ly51^-$, can be subdivided into immature $CD80^{lo}$ and mature $CD80^{hi}$ populations (Derbinski et al., 2005; Rodewald et al., 2001; Rossi et al., 2007b). Early in development mTECs are $CD80^{lo}$ with $CD80^{hi}$ first appearing around E16 (Rossi et al., 2007b). Interestingly it has been shown that $CD80^+$ mTECs associate with the putative transcription factor autoimmune regulator (Aire) (Rossi et al., 2007b).

Abnormal mTEC development and organisation are often associated with autoimmunity (Anderson et al., 2007). This is due to the specialised function of mTECs in the negative

selection of the nascent T cell repertoire and thus their contribution to T cell tolerance that is largely attributable to their expression of Aire (Rossi et al., 2007a). The importance of Aire was established when its absence resulted in the human autoimmune condition autoimmune polyendocrinopathy-candidiasis-ectodermal dystrophy (APECED), characterised by the presence of autoimmune antibodies specific for multiple self-antigens. Consistently, mice with Aire deficiency show comparable signs of autoimmunity with multi-organ lymphocytic infiltration and the presence of autoantibodies (Peterson et al., 2008).

Aire is responsible for the expression of a plethora of tissue-restricted self-antigens (TRAs), defined as genes expressed in fewer than 5 of 45 tissues (Kyewski and Klein, 2006). TRAs within the thymus consequently represent essentially all parenchymal organs. This is important as the extent of central self-tolerance is specified by the diversity of self-antigens accessible to the nascent repertoire. Thus promiscuous gene expression widens the scope of central tolerance and consequently emulates the peripheral self, pre-empting the peripheral encounter of potentially dangerous T cells with TRAs. This remarkable mechanism means that medullary thymocytes can be screened for reactivity to self-antigens that they might encounter in the periphery without ever leaving the thymus and causing autoimmune pathology (Ladi et al., 2006). Of relevance, any particular set of TRAs are only expressed by a small subset of mTECs, thus apparently TRAs are not homogenously distributed in the medulla but are restricted to local areas. The extensive time developing SP thymocytes reside within the medulla and their high motility, probably facilitates the extensive sampling of the mTEC environment required to ensure proper TRA experience is achieved to ensure efficient negative selection (Ladi et al., 2006).

Interestingly, a recent study claims that Aire expression in the perinatal period is both necessary and sufficient to induce self-tolerance, as this pool of tolerised T cells are able to

control newly emerging autoreactive T cells. As a result Aire mediated tolerance in the adult is largely dispensable (Guerau-de-Arellano et al., 2009). So, establishing a competent tolerising thymic microenvironment is especially important during initial thymus development.

It has been shown that, postmitotic Aire^{+} CD80^{hi} MHC class II^{hi} mTECs derive from a cycling Aire^{-} CD80^{lo} MHC class II^{lo} progenitor population, indicating that Aire is expressed in a more mature mTEC population (Gray et al., 2007). Consistent with this, Aire^{+} mTECs are negative for p63, a regulator of epithelial cell proximal differentiation (Dooley et al., 2008). However, recent advances have identified a biphasic Aire expression pattern during embryonic development (Nishikawa et al., 2010). Furthermore, Nishikawa *et al* demonstrated that Aire^{+} CD80^{hi} MHC class II^{hi} mTECs end their differentiation program by down-regulating CD80 and MHC class II. Thus identifying Aire^{-} CD80^{int} as an important maturation step occurring before terminal differentiation (Nishikawa et al., 2010). It is understood that mTEC differentiation culminates in the appearance of involucrin, a terminal differentiation marker, often found associated with Hassall's corpuscle-like structures in the medulla (Figure 1.4) (Anderson et al., 2009; Yano et al., 2008).

Furthermore, it has been observed that numbers of involucrin expressing mTECs were reduced in Aire deficient mouse thymus, suggesting a role for Aire in the control of the mTEC differentiation program. Thereby Aire organises the global mTEC integrity that enables TRA expression from terminally differentiated mTECs in the thymic microenvironment (Yano et al., 2008). In addition, mTEC maturation is associated with the expression of a broader set of TRA (Ladi et al., 2006). Moreover, it is believed that mTECs also contribute to self-antigen expression by being phagocytosed by professional APCs, known as cross-presentation (Koble and Kyewski, 2009; Nishikawa et al., 2010). So, when mTECs are expressing their most extensive TRA repertoire, Aire induces their death through stimulation of the apoptotic pathway.

Consequently they are phagocytosed enabling further expression of a broad range of TRAs by APCs, such as DCs, within the medulla.

The elucidation of these stages and checkpoints in the development of mTECs provides an opportunity to identify the molecular regulators involved. Several molecular mediators have now been identified, most of which tend to utilise the NF-κB signalling pathway (Naquet et al., 1999). LTβR signalling clearly influences the full maturation of the medulla, including the development of the appropriate architecture since LTβR deficient mice display an autoimmune phenotype (Boehm, 2008; Boehm et al., 2003). Interestingly, defects in LTβR signals have a more detrimental affect on mTEC architecture than those exhibited by mice deficient for both of the known LTβR ligands, LIGHT and lymphotoxin (Boehm et al., 2003). In keeping with this, it was shown that lymphotoxin does not appear to be involved in the induction of $Aire^+$ mTEC development, contrasting previous thoughts (Chin et al., 2003). Another study demonstrated the onset of organ-specific autoimmunity in tumour necrosis factor receptor (TNFR) associated factor 6 (TRAF6) deficient mice, which lacked $Aire^+$ mTECs (Akiyama et al., 2005). Importantly LTβR signalling does not involve TRAF6 (Derbinski and Kyewski, 2005). Instead signalling through the tumour necrosis factor receptor, receptor activator of NF-κB (Rank) on mTEC utilises TRAF6 and is directly responsible for $Aire^+$ mTEC differentiation (Rossi et al., 2007b). Moreover, Rank ligand (Rankl) is expressed on intrathymic $CD4^+CD3^-$ lymphoid tissue inducer (LTi) population that have now been identified as a key population involved in this mTEC differentiation programme (Boehm, 2008; Gray et al., 2007; Rodewald, 2008; Rossi et al., 2007b; Yano et al., 2008). TRAF6 is also involved in the regulation of CD40 signalling (Derbinski and Kyewski, 2005). Thus, subsequent studies revealed the involvement of CD40 in cooporation with Rank in mTEC development during neonatal stages (Akiyama et al., 2008; Yano et al., 2008). The participation of CD40 is further demonstrated by the associatation of an

absence of CD40 expression with a reduction in Aire^{+} mTECs numbers (White et al., 2008b). Interestingly, Rankl can also be provided by SP thymocytes, which also express CD40L, in the adult thymus (Hikosaka et al., 2008). The recognition of these molecular mediators has highlighted the importance of thymic crosstalk where lymphocyte derived signals play a vital role in the development of TECs and vice versa.

1.4 General Aims of Study

As discussed in this chapter, the T cell developmental pathway including important checkpoints are relatively well understood. However, the stages and mechanisms involved in the developmental progression of the thymic epithelium and the establishment and regulation of the various thymic microenvironments are yet to be fully elucidated. Hence, the aims and objectives of this thesis are as follows;

- To further investigate and characterise the cellular and molecular mechanisms involved in mTEC development downstream of immature mTEC progenitors.
- To study the establishment of thymic microenvironments with particular regard to the timing of thymic crosstalk and the requirement for thymic crosstalk to occur within a developmentally restricted time frame.
- To examine the developmental potential and intrathymic niche requirements of a single cohort of lymphoid progenitors.

CHAPTER 2: MATERIALS AND METHODS

2:1 Mice

The mice used in this study (see table 5:1 for details) were bred and maintained in the Biomedical Services Unit (BMSU), University of Birmingham, under specific pathogen-free (SPF) conditions and in accordance with Home Office Regulations. Mice were obtained from either a commercial supplier, as a kind gift from research groups or from in-house stock at the BMSU. Timed matings were achieved by placing a male mouse into a cage with two or three female mice overnight. Successful matings were identified by the presence of a vaginal plug (VP), the day of which was designated as day zero of gestation (E0). This makes it possible to obtain fetal material of specified developmental stages. The gestation of mice is usually between 18-21 days. Details of all wild type and genetically modified mouse strains used in this study are outlined in Table 2.1.

Strain	MHC	CD45 Isotype	Phenotype	Source
BALB/c	H-2^{d}	CD45.2	Wild type	BMSU
C57BL/6J	H-2^{b}	CD45.2	Wild type	BMSU
*Rag*2$^{-/-}$γc$^{-/-}$ (BALB/c)	H-2^{d}	CD45.2	Deficient for *Rag2* and common gamma chain cytokine receptor resulting in T, B and NK cell development blocked	Marcus Manz Bellinzona Switzerland
CD3 epsilon transgenic (CD3ε*tg*26)	H-2^{b}	CD45.2	Over express human CD3ε gene, T cell development consequently blocked at CD4^{-} CD8^{-}CD25^{-}CD44^{+} (DN1) stage. (Wang et al., 1995)	The Jackson Laboratory
Balb/c nude (nu/nu)	H-2^{d}	CD45.2	Deficiency in the FoxN1 gene results in abnormal thymic epithelial cell development. Thymus rudiment is not populated by lymphoid precursors and consequently nude mice do not have T cells.	BMSU
C57BL/6J nude (nu/nu)	H-2^{b}	CD45.2	Deficiency in the FoxN1 gene results in abnormal thymic epithelial cell development. Thymus rudiment is not populated by lymphoid precursors, consequently nude mice do not have T cells.	BMSU
TCRδ$^{-/-}$ (C57Bl6)	H-2^{b}	CD45.2	Deficient for the T cell receptor delta gene, resulting in a block in γδ T cell development.	BMSU
Ccr7$^{-/-}$	H-2^{b}	CD45.2	A lack of CC chemokine receptor 7, leads to impaired thymocyte migration into the medulla and thymocyte exit from the thymus.	Antal Rott, University of Birmingham, UK
FVB/N Jax	H-2^{q}	CD45.2	Wild type	Adrian Hayday, Kings College London, UK
FVB/N Tac	H-2^{q}	CD45.2	A naturally occurring single point mutation introduces a premature stop codon into the *Skint1* gene causing a reduction in the number of peripheral Vγ5 T cells.	Adrian Hayday, Kings College London, UK
Rorγ$^{-/-}$ (C57Bl6)	H-2^{b}	CD45.2	Deficiency in retinoic acid-related orphan receptor gamma gene leads to an absence of lymphoid tissue inducer cells.	BMSU
Rank$^{-/-}$ (C57Bl6)	H-2^{b}	CD45.2	Absence of Rank leads to impaired medullary thymic epithelial development, consequently an autoimmune phenotype is observed.	BMSU
CD3ε*tg*26$^{-/-}$*Rorγ*$^{-/-}$ (C57Bl6)	H-2^{b}	CD45.2	Over expression of human CD3ε gene and deficiency in retinoic acid-related orphan receptor gamma gene leads to an absence of lymphoid tissue inducer cells and mature T cells	BMSU
Rankl$^{-/-}$ (C57Bl6)	H-2^{b}	CD45.2	Absence of Rank ligand abrogates Rank signalling therefore leading to impaired medullary thymic epithelial development.	Yousuke Takahama, University of Tokushima, Japan
Plt	H-2^{b}	CD45.2	A spontaneous mutation resulting in the removal of one of the three CCL21 genes, leaving expression in peripheral lymphatic endothelium and the CCL19 gene.	Yousuke Takahama, University of Tokushima, Japan

Table 2.1 Wild Type and Genetically modified Strains Used In This Study

2.2 Medium and Culture Reagents

2.2.1 Medium

The isolation of tissues and short term handling of cells was completed in RPMI-1640 Hepes (RF10-H) supplemented with 10% heat inactivated fetal calf serum (FCS) (preparation detailed in Table 2.2). The long term culture of cells and tissues was carried out in Dulbecco's Modified Eagle's Medium (DMEM) supplemented with 10% FCS and other additives as indicated in Table 2.3 and 2.4. Aliquots of media were prepared in advance and stored at $4^{o}C$.

2.2.2 Additives

To deplete lymphoid cells including dendritic cells from fetal thymic organ cultures, whilst allowing the stromal elements to continue to survive, 2-deoxyguanosine (2-dGuo, Sigma) was added to the culture media (Jenkinson et al., 1982; Jenkinson et al., 2008). Stock solutions of 9mM 2-dGuo were stored at -20°C prior to addition to the culture medium, the effective final concentration was 1.35mM.

To prepare stromal cell suspensions, 2.5% stock of trypsin in Hank's balanced salt solution (HBSS, Sigma) was diluted 10-fold in 0.02% EDTA in Ca^{2+} and Mg^{2+} free phosphate buffered saline (PBS), to give a working concentration of 0.25% trypsin.

To test the role of Rank in the maturation of medullary thymic epithelial cells (mTEC), the culture media was supplemented with 10μg/ml recombinant anti-Rank antibody (R&D systems). Appropriately sized aliquots of 100μg/ml stock solutions were stored at $-20^{o}C$ to prevent repetitive freeze thawing.

Investigation of the role of chemokine signalling in the medullary localisation of T cells required the addition of Pertussis Toxin (PTX) (Sigma) to the culture media. Pertussis toxin works by blocking the GTP binding proteins G_0 and G_i. 250μg/ml PTX in DMEM was used. A stock solution of 50mg/ml was stored at $4^{o}C$.

Medium and Additives	Volume	Final Concentration	Source
RPMI-1640 + 20mM Hepes with L-Glutamine without bicarbonate	20ml	-	Sigma, Poole, UK
200mM L-Glutamine	200µl	2mM	Sigma, Poole, UK
5000 IU/ml Penicillin and Streptomycin	400µl	100 IU/ml	Sigma, Poole, UK
Heat-inactivated Fetal Calf Serum (FCS)	2ml	10%	Sigma, Poole, UK

Table 2.2 RF10-H Constituents

Medium and Additives	Volume	Final Concentration	Source
Dulbecco's Medium with 3.7g/l bicarbonate and without glutamine	20ml	-	Sigma, Poole, UK
100x non-essential amino acids (for constituent details see Table 5:4)	200µl	-	Sigma, Poole, UK
1M Hepes	200µl	10mM	Sigma, Poole, UK
$5x10^3$ M2 Mercaptoethanol	200µl	-	Sigma, Poole, UK
200mM L-Glutamine	400µl	4mM	Sigma, Poole, UK
5000 IU/ml Penicillin and Streptomycin	400µl	100 IU/ml	Sigma, Poole, UK
Heat-inactivated FCS	2ml	10%	Sigma, Poole, UK

Table 2.3 DMEM Constituents

Constituent	Concentration (mg/ml)
L-Alanine	8.9
L-Asparagine	15.0
L-Aspartic acid	13.0
Glycine	7.5
L-Glutamic acid	14.2
L-Proline	11.5
L-Serine	10.5

Table 2.4 100x Non-Essential Amino Acids Constituants

2.3 Organ Culture Systems

2.3.1 Fetal Thymus Organ Culture (FTOC)

Fetal thymus organ culture (FTOC) is an established system that supports a complete programme of T cell development *in vitro*, whilst maintaining the integrity of the three-dimensional architecture of the thymic stroma (Jenkinson and Anderson, 1994). This technique

promotes efficient interactions between developing T cells and stromal cells, thus emulating the specialised microenvironment that is typical of a mature thymus *in vivo* (figure 2.1).

Dissection and culture preparation were completed within a laminar flow hood (Holton, Brøndy, Denmark) to ensure a sterile environment. From embryonic mice at the appropriate stage of gestation (typically E15), thymic lobes were removed. For thymus organ culture, 0.8μm sterile nucleopore filters (Millipore) were placed on top of a sterile antiwrap sponge support (approximately $1cm^2$ in size) (Medipost Ltd) within 90mm single vent sterile petri dishes (Sterilin) containing 4mls DMEM. The nucleopore filters maintain the organ cultures at the liquid-air interface, enabling optimal exchange with the medium and gas phase, vital for optimal growth (Jenkinson and Anderson, 1994). Two sponges and filters were set up per dish. Using a finely drawn mouth-controlled glass pipette, a maximum of 6 lobes cultured on each filter. Three petri dishes were placed within each sterile humidified chamber. The cultures were purged with 10% CO_2 in air for approximately 10 minutes, to maintain the desired pH of the media (pH 7.2-7.4) and afterwards transferred into a 37^oC incubator for approximately 7 days.

When required, 2-dGuo was added to the DMEM to give a final concentration of 1.35mM. For optimal lymphoid and dendritic cell depletions by 2-dGuo, fetal lobes were cultured for 5-7 days.

2:4 Mouse Tissue Isolation

According to home office regulations, all adult mice, when required for this study, were culled by cervical dislocation. For embryonic work, the timed pregnant mice were culled and the uterus was removed whole. The embryos in their amniotic sacs were subsequently removed from the uterus and washed in in PBS. Placentas and sacs were then removed and the embryos washed in 1:1 PBS:RF10-H. From both embryonic and adult mice, Thymic lobes were dissected from the thoracic tree (encompassing the heart, lungs, thymus and trachea) and placed in RF10-H and

kept on ice until further manipulation was required. Other required tissues were also isolated placed in RF10-H and kept on ice until further manipulation was required.

2.5 Isolation of Cell Types

To study development and phenotype of thymic stromal cells, methods for enrichment of specific thymic epithelial cells was employed. Two approaches for this are highlighted below and include high-speed cell sorting and immunomagnetic bead separation.

2.5.1 Isolation of Thymocytes

To obtain cell suspensions of thymocytes for flow cytometry, adult or embryonic (fresh or cultured) thymic lobes were gently teased apart in RF10-H medium with fine forceps to release the cells. Cells were counted using a haemocytometer.

2.5.2 Isolation of Splenocytes

Cell suspensions from fetal or adult spleens were obtained by gentle teasing apart, in RF10-H, with fine forceps. The resulting adult splenocyte suspensions were subjected to red cell lysis by incubation with Red Blood Cell Lysis Buffer (Sigma, Poole, UK) for 10 minutes at 4^{o}C; the reaction was subsequently neutralised by an equal volume of RF10-H. The cell number was calculated using a haemocytometer.

2.5.3 Isolation of Haematopoietic Precursors

E15 fetal liver cell suspensions were obtained by gentle mechanical disaggregation using a P1000 Gilson Pipette. The resulting cell suspensions were counted using a haemocytometer and the cell number was subsequently calculated.

2.5.4 Isolation of Thymic Stromal Cells

Stromal cell suspensions were obtained from either E15 thymus lobes cultured for between 5 and 7 days in the presence of 2-dGuo or freshly isolated E17 thymus. The thymic lobes were subsequently transferred into 1.5 ml eppendorfs and washed three times in Ca^{2+} Mg^{2+} free PBS, to remove traces of serum that could potentially inactivate trypsin. The washed lobes were then suspended in 600µl 0.25% trypsin diluted in 0.2% EDTA, and incubated at 37°C for 10-15 minutes (the precise incubation time is dependent on the embryonic stage and the culture interval). Subsequent disaggregation of the lobes was facilitated by gentle mechanical force, until a stromal cell suspension was formed. In order to quench the trypsin activity an equal volume of RF10-H was added followed by centrifugation (1000rpm, 10mins, 4^{o}C). The pellet was resuspended in 1ml RF10-H and the cell number subsequently calculated using a haemocytometer.

2.5.6 Preparation of Cells for High Speed Sorting

High speed sorting of cellular populations was performed using a MoFlo high-speed cell sorter (Dako Cytomations). This utilises the identical fluorescent antibody labelling used for flow cytometry (described in section 5.4). The antibody volume was altered according to the number of cells to be stained, following approximately 2 x 10^6 cells per 100µl of antibody. Once labelled the cells were suspended in RF10-H, volume dependent on cell number, and transferred to polypropylene FACS tubes (Becton Dickinson). Using single colour control samples of approximately 100,000 cells, suspended in 200µl RF10-H the MoFlo high-speed cell sorter was compensated. Experimental samples of no less than 1 x 10^6 cells/ml in RF10-H, were first filtered to remove any adherent cell clumps through a 30µm mesh-membrane filter unit (Miltenyi Biotech) before a small volume was passed through to enable the required gating to be set on the desired populations. The cells were then sorted into either polypropylene FACS tubes

containing 500µl RF10-H or 1.5ml eppendorfs containing 200µl RF10-H, depending on the size of the sorted population. The cell number was calculated using a haemocytometer. A small volume of the sorted sample was kept inorder to determine the purity. Sorted cells were either used for reaggregate organ culture experiments (detailed in section 3.2.3), intravenous injection or snap-frozen for cDNA extraction (as described in section 3.2.6.2).

If the sorted cell suspension was intended for intravenous injection after the cell number was established the population was resuspended in sterile PBS (Sigma) at a minimum concentration of $1.4x10^5$ cells/200µl.

If the intention was for cDNA isolation the population was centrifuged (1000rpm, 4°C, 5 mins), the supernatant removed and the dry pellet snap frozen in liquid nitrogen and stored at -80°C until required.

2.6 Immunolabelling And Flow Cytometry

2.6.1 Antibodies and Immunoconjugates

All primary antibodies and the dilutions used for flow cytometry are listed in table 2.5. Outlined in table 2.7 are all secondary antibodies and the dilutions used when the primary was not conjugated to a fluorochrome. Antibodies were titrated to optimise working concentrations prior to use.

2.6.2 Immunolabeling of cell suspensions for flow cytometric analysis

As described in section 5.3, cell suspensions were prepared and counted. Cell aliquots (generally ≤1 x 10^6 cells) were transferred to 1.5ml eppendorf tubes and after the addition of 500µl PBS (sigma), centrifuged at 1400rpm, 4 min, 4°C to form a pellet. The supernatant was removed and the cell pellet resuspended in 50µl ($2x10^6$ cells per 100µl of antibody) of the appropriate antibody mix (diluted in PBS). To treat the samples identically, if an antibody was

not required, the pellet was resuspended in PBS. In addition, appropriate staining controls were prepared. A negative control sample was also prepared to set the negative peak of florescence, where primary antibodies were not directly conjugated to a flourochrome this sample only included the secondary antibody to control for non-specific binding of the antibody.

After incubation (30 minutes, 4^{o}C), the samples were washed with 500µl PBS and centrifuged (1400rpm, 4 minutes, 4^{o}C) to form a pellet. The supernatant was removed and if required, the secondary antibody was applied as described for the primary. The process was repeated for tertiary antibodies, if required.

Once the immunolabelling was complete, the cells were washed as described earlier, the pellet resuspended in 200µl PBS and the cell suspension transferred to 12.5ml polystyrene FACS tubes (Becton Dickinson) and stored in the dark at 4^{o}C until analysis. If the samples could not be analysed the same day the cells were fixed in 200µl of 1% paraformaldehyde (PFA) (16% PFA (Taab, Reading, UK) diluted in PBS) and stored in the dark at 4^{o}C until ready to analyse (Refer to section 2.6.6).

Specificity (Clone)	Host/ Isotype	Stock Solution	Working Dilution	Suppliers
CD4 PeCy7 (GK1.5)	Rat IgG2a κ	0.2mg/ml	1:500	eBioscience
CD8 FITC (53-6.7)	Rat IgG2a κ	0.5mg/ml	1:200	eBioscience
CD3ε PE (145-2C11)	Hamster IgG1, k	0.2mg/ml	1:100	BD Pharmingen
CD19 APC (1D3)	Rat IgG2a κ	0.2mg/ml	1:400	BD Pharmingen
CD8β (H35-17.2) APC	Rat IgG2b κ	0.2mg/ml	1:200	eBioscience
TCRβ PE (H57 597)	Armenian Hamster IgG	0.2 mg/ml	1:100	eBioscience
FoxP3 FITC (FJK-16s)	Rat IgG2a κ	0.2mg/ml	1:50	BD Pharmingen
LIN biotin (refer to table 2.11)	-	-	1:200	BD Pharmingen
TRANCE (Rankl) biotin (IK22/5)	Rat IgG2a κ	0.5mg.ml	1:100	eBioscience
Human anti CCL19 Fc Fusion Protein (ELC, CKb11)	Human IgG	0.1mg/ml	1:100	eBioscience
Ccr10 (6E10)	Rat IgG	-		Millennium Pharmaceuticals, Cambridge, MA
CD45RB biotin	Rat IgG2a κ	0.5mg/ml	1:200	eBioscience
CD45RB PE	Rat IgG2b κ	0.2 mg/ml	1:100	eBioscience
Anti-mouse Vγ3 FITC (536)	Syrian Hamster IgG1 κ	0.5mg/ml	1:50	BD Pharmingen
CD45 PECy7 (30-F11)	Rat IgG2a κ	0.2mg/ml	1:1500	eBioscience
Ly51 / BP1 PE (6C3)	Rat IgG1 κ	0.2 mg/ml	1:500	eBioscience
Purified anti-mouse EpCAM-1 (G8.8) conjugated to Alexa 647 by A.White, University of Birmingham	Rat	-	1:150	Andrew Farr, University of Washington, USA
Purified anti-mouse AIRE conjugated to Alexa 488 by A.White, University of Birmingham	rat IgG monoclonal	-	1:150	Hamish Scott, Walter and Eliza Hall Institute, Melbourne, Australia
CD44 / Pgp-1 PECy7 (IM7)	Rat IgG2b κ	0.2 mg/ml	1:400	eBioscience
CD25 APC (PC61.5)	Rag IgG1 λ	0.2mg/ml	1:400	eBioscience
CD25 Alexa Flour 488 (PC61.5)	Rag IgG1 λ	0.5 mg/ml		eBioscience
CD45.1 biotin (A20)	Mouse IgG2a κ	0.5mg/ml	1:100	eBioscience
CD45.1 FITC (A20)	Mouse IgG2a	0.5mg/ml	1:200	eBioscience
Pan γδ TCR PE (GL3)		0.2mg/ml	1:200	Biolegend
Pan γδ TCR biotin (GL3)	Armenian Hamster IgG	0.5 mg/ml	1:100	eBioscience
CD117 / cKit APC (2B8)	Rat IgG2b κ	0.2 mg/ml	-	eBioscience
CD11c PE (N418)	Hamster IgG	0.5mg/ml	1:300	eBiosciences
B220 PE texas red (RA3-6B2)		0.5mg/ml	1:200	BD Pharmingen
OX40L biotin (RM134L)	Rat IgG2b	0.5mg/ml	1:50	eBioscience
IL-7Rα Alex Flour 647 (A7R34)	Rat IgG2a	0.5mg/ml	1:50	eBiosciences
BrdU (B44)	Mouse IgG_1, κ	-	1:50	BD Pharmingen

Table 2.5 Primary Antibodies used in flow cytometry

Specificity (Clone)	Host/ Isotype
TER-119/Erythroid cells (Ly-76)	Rat IgG_{2b}, κ
CD11b (Mac-1) (M1/70)	Rat IgG_{2b}, κ
Ly-6G and Ly6C (Gr-1) (RB6-8C5)	Rat IgG_{2b}, κ
CD45R/ B220 (RA3-6B2)	Rat IgG_{2b}, κ
CD3ε (145-2C11)	Armenian Hamster IgG1, κ

Table 2.6 Constituents of the Mouse Linage Panel

Specificity (Clone)	Host/ Isotype	Stock Solution	Working Dilution	Suppliers
Streptavidin PE-Cy7	-	0.2mg/ml	1:400	eBioscience
Streptavidin PE			1:1200	eBioscience
Anti human IgG Biotin			1:100	eBioscience
Anti-Rat PE	Goat IgG	0.5mg/ml	1:400	Southern Biotec

Table 2.7 Secondary Antibodies used in flow cytometry

2.6.3 Intracellular Staining for Flow Cytometric Analysis – FoxP3

For the intracellular staining of FoxP3, the cells were surface stained as described in section 2.6.2 after which they were washed in PBS and the surface stain fixed and the cells permeabilised by incubation (30minutes, 4°C) with Fixation/Permeabilisation buffer (paraformaldehyde and saponin) (eBioscience). A PBS wash followed and further permeabilisation by two washes with permeabilisation buffer (0.1% saponin, 0.009% sodium azide) (eBioscience). A rat serum block was completed and the cells were subsequently incubated (4°C, 30 minutes) with the anti-FoxP3 antibody. After which the cells were washed twice with permeabilisation buffer and the pellet resuspended in 250μl PBS and stored in the dark at 4°C until ready to analyse (refer to section 2.6.6). Refer to tables 2.5 and 2.7 for the antibodies and their dilutions used for flow cytometric analysis.

2.6.4 Intracellular Staining for Flow Cytometric Analysis – Aire

For the intracellular staining of autoimmune regulator (Aire), the cells were first surface stained as described in section 2.6.2. After which they were washed in PBS and the surface stain fixed by incubation (30-60 minutes, 4°C) with 200μl Intracellular (IC) fixation buffer (4%

Paraformaldehyde) (eBiosciences). Two washes with permeabilisation buffer (Diluted 1:10 in dH_2O) (0.1% saponin, 0.009% sodium azide) (eBioscience) followed, after which the Aire antibody diluted in permeabilisation buffer was applied to the cell pellet and incubated for 30 minutes at 4°C. The cells were subsequently washed twice with permeabilisation buffer before being resuspended in 200µl PBS and stored in the dark at 4°C until ready to analyse (refer to section 2.6.6). Refer to tables 2.5 and 2.7 for the antibodies and their dilutions used for flow cytometric analysis.

2.6.5 Intracellular Staining for Flow Cytometric Analysis – BrdU

For the intracellular staining of Bromodeoxyuridine (5-bromo-2-deoxyuridine, BrdU), the cells were first surface stained as described in section 2.6.2. After which they were washed in PBS, the surface stain fixed and the cells permeabilised by incubation (30-60 minutes, 4°C) with 500µl Cytofix/Cytoperm buffer (Paraformaldehyde and Saponin) (BD Pharmingen). One wash with Perm/Wash buffer (Diluted 1:10 in dH_2O) (saponin, FCS) (BD Pharmingen) followed and treatment with Cytoperm Plus Buffer (100µl) (BD Pharmingen) to permeabilise the cells. The cells were washed (Perm/Wash buffer) and a second treatment with Cytofix/Cytoperm buffer completed. Subsequently the cells were treated with 100µl DNase (300µg/ml) (30 mins, 37°C) to expose the BrdU epitopes, after which the BrdU antibody (50µl) diluted in Perm/Wash buffer was applied to cell pellet and incubated for 30 minutes at 4°C. Afterwards the cells were washed twice with Perm/Wash buffer before being resuspended in 200µl PBS and stored in the dark at 4°C until ready to analyse (refer to section 2.6.6). Refer to tables 2.5 and 2.7 for the antibodies and their dilutions used for flow cytometric analysis.

2.6.6 Flow Cytometric Analysis

Flow cytometric analysis was performed using a Becton Dickinson LSR flow cytometer and Cellquest Pro software. Subsequent analysis was carried out using FloJo software. Prior to acquisition of experimental samples, control samples were run to set up the machine. The negative control enabled the negative peaks to be set for populations not expressing the tested antibodies. The remaining single colour controls were used to set the positive peaks for populations expressing the tested antibodies, adjust the compensation levels required between the various fluorochrome detection channels and enable the appropriate gating to be set.

Adequate event numbers were collected for each sample, for example, control samples were run until compensation was completed. The number of events recorded was dependent on both cell numbers prior to immunolabelling and the frequency of the cell population of interest. However, where possible at least 50,000 events were recorded per experimental sample, within the forward and side scatter gates set to exclude non-viable cells.

2.7 Immunohistology Techniques.

2.7.1 Freezing, Sectioning and Fixation of Tissues

To produce sections of embryonic and adult tissues of interest, the organs were dissected, and cleaned up by removal of adjoining fat and tissue. The tissues, if small, were subsequently embedded in a small amount of OCT compound (Tissue Tek, Sakura, Japan) placed onto aluminium foil. Tissues were frozen in liquid nitrogen and stored at –80^{o}C until required for sectioning.

The frozen tissues, were mounted onto a microtome chuck, in OCT compound (Tissue Tek) at a defined orientation and loaded onto the microtome. Sections of 5μm thickness were cut using a cryostat (Bright, Huntingdon, UK) and mounted onto 4 spot Vectabond coated multispot glass slides (Vector Laboratories, Burlingame, USA). All slides were dried at room temperature

for a minimum of half an hour in front of a desktop fan. The slides were subsequently fixed in acetone (Sigma, Poole, UK) (4^{o}C, 20 minutes), air dried for 10 minutes, packaged into grip-seal polythene bags before storage at –20^{o}C until required.

2.7.2 Immunolabelling of Frozen Tissue Sections.

For immunolabelling, the sections were removed from storage at –20^{o}C and dried at room temperature for approximately 30 minutes. The sections were then re-hydrated in PBS (Sigma), for 10-15 minutes. The sections were stained with fluorochrome-conjugated anti-mouse antibodies diluted in PBS containing 1% bovine serum albumin (BSA). Incubations with primary antibodies ranged between 40-60 minutes and 30-40 minutes for subsequent steps after a 10 minute wash in PBS. The slides were incubated in a dark humid chamber. For details of the primary antibodies used in this study refer to table 2.8 and the details of secondary and tertiary antibodies are detailed in table 2.9. After the final antibody had been applied the slides were washed in fresh PBS and stained with DAPI (4',6-diamidino-2-phenylindole) (molecular probes). DAPI is a strong nuclear stain, thus enables visualisation of the whole tissue section. Subsequent PBS washes and the application of small drops of DABCO (Invitrogen/Sigma), in glycerol at pH7 to each spot, preserves the fluorochromes and prepares the sections for mounting of the coverslip. The slides are then sealed with clear nail varnish and stored in the dark at -20^{o}C until analysis.

2.7.3 Confocal Analysis

Confocal images were acquired using a Zeiss LSM510 laser scanning confocal head with a Zeiss Axiovert 100M microscope (Carl Zeiss, Oberkochen, Germany). Digital images were recorded in four separate channels, each were scanned individually with no overlap in the detection of emissions from the respective fluorochromes. FITC or Alexa 488 conjugated

antibodies were excited with a 488nm argon laser, TRITC and Alexa 555 and 594 conjugated antibodies were excited with a 561nm helium laser, Alexa 647 conjugated antibodies were excited with the 633nm helium laser and DAPI was excited with the 405nm diode laser after which its emission maximum is approximately 461 nm. Confocal micrographs were stored as digital arrays of 2048x2048 pixels with 8 bit sensitivity. Tile scans were stored as arrays of 1024x1024 pixels with 8 bit sensitivity and Z stacks were stored as arrays of 1024x1024 pixels with 7 bit sensitivity.

Specificity (Clone)	Host/ Isotype	Stock Solution	Working Dilution	Suppliers
Anti-mouse Keratin 5 purified	Rabbit IgG	-	1:2000	Covance
Anti-mouse Keratin 8 biotin (Ks8.7)	Mouse igG1	-	1:10	Progene
Purified anti-mouse EpCAM-1 (G8.8) conjugated to Alexa 647 by A.White, University of Birmingham	Rat	-	1:150	Andy Farr, University of Washington, USA
Purified anti-mouse CD4 (GK 1.5) conjugated to Alexa 647 by D.Withers, University of Birmingham.	Rat IgG1	1mg/ml	1:100	eBioscience
Anti-mouse CD8β biotin (CT-CD8b)	Rat IgG2a κ	0.5mg/ml	1:200	eBioscience
Anti-mouse CD25 FITC (7D4)	Rat IgM	0.2 mg/ml	1:150	BD Pharmingen
Anti-mouse CD40 biotin (3/23)	Rat IgG2a		1:50	BD Pharmingen
Anti-mouse CD205 (DEC205) FITC (NLDC145)	Rat IgG2a	0.2 mg/ml	1:50	AbCAM
Anti-mouse FoxP3 FITC (FJK-16s)	Rat IgG2a κ	0.2mg/ml	1:200	BD Pharmingen
Anti-mouse Vγ3 FITC (536)	Syrian Hamster IgG1 κ	0.5mg/ml	1:50	BD Pharmingen
Anti-mouseVγ2 FITC (UC3-10A6)	Armenian Hamster IgG1 κ	0.5mg/ml	1:50	BD Pharmingen
Nkp46 biotin (NCR1)	Goat IgG	0.1 mg/ml	1:50	R & D Systems
Anti-mouse CD11b (Mac-1) biotin (M1/70)	Rat IgG2b κ	0.5 mg/ml		eBiosciences
CD11c FITC (N418)	Armenian Hamster IgG	0.5 mg/ml	1:300	eBioscience
CD45.1 biotin (A20)	Mouse IgG2a κ	0.5 mg/ml		eBioscience
CD45.1 FITC (A20)	Mouse IgG2a κ	0.5 mg/ml		eBioscience
B220 biotin (RA3-6B2)	Rat IgG2a	0.2mg/ml	1:200	BD Pharmingen
Anti-mouse IgM Rhodamine Red-X-AffiniPure	Donkey IgM	-	1:300	-
CD3ε FITC (145-2c11)	Hamster IgG1 k	0.5mg/ml	1:300	BD pharmingen
VCAM FITC (429)	Rat IgG2a κ	0.5mg/ml	1:50	BD Pharmingen
AIRE	Rabbit	-	1:400	Santa Cruz
AIRE	Goat		1:200	Santa Cruz
gp38 supernatant (8.1.1)	Hamster	-	1:2	Andrew Farr, University of Washington, Seattle
CCL21 (polyclonal)	Goat	0.5mg/ml	1:100	R&D Systems
ER-TR7 supernatant	Rat	-	1:2	W. van Ewijk, Leiden University, Netherlands

Table 2.8 Primary Antibodies Used For Immunohistochemisty

Specificity (Clone)	Host/ Isotype	Stock Solution	Working Dilution	Suppliers
Streptavidin Alexa Fluor 555 conjugate	-	1mg/ml	1:1000	eBioscience
Anti-FITC (polyclonal)	Rabbit	1mg/ml	1:200	BD Pharmingen
Anti-Rabbit FITC	Goat		1:200	Southern Biotec
Anti-rabbit Alexa Flour 488 (H+L) (polyclonal)	Goat	1mg/ml	1:300	Molecular Probes
Anti-Rabbit Alexa Flour 647 (polyclonal)	Goat		1:400	Molecular Probes

Table 2.9 Secondary And Tertiary Antibodies Used For Immunohistochemisty

CHAPTER 3: A NOVEL ROLE FOR γδT CELLS IN MEDULLARY THYMIC EPITHELIAL CELL DEVELOPMENT

3.1 Introduction

Genes assembled through random somatic DNA rearrangement encode the antigen specific receptors of T cells. As a result of this stochastic generation of diversity, potentially autoaggressive T cells are able to develop (Cabarrocas et al., 2006). Elimination of self-reactive T cells from the repertoire, either by removal or silencing is necessary to avoid the potentially pathological state of autoimmunity (Anderson et al., 2002). Several "central" and "peripheral" mechanisms are involved in the imposition, regulation and maintenance of self-tolerance (Cabarrocas et al., 2006).

Central tolerance is accomplished within the thymus where the development and selection of the nascent T cell repertoire strongly biases against self-reactivity. However, the extent of central self-tolerance is specified by the diversity of self-antigens accessible to the nascent repertoire within the thymus. Medullary thymic epithelial cells (mTECs) and more specifically a specialised subset of mTECs that express the transcription factor Aire (Autoimmune Regulator) are involved in this process. Aire promotes the ectopic expression and presentation of peripheral tissue antigens and thus provides a plethora of tissue-restricted antigens (TRAs) for the nascent T cell repertoire to be selected against (DeVoss et al., 2006; Guerau-de-Arellano et al., 2009). In support of this Aire deficiency results in a multi-organ autoimmune disease in both humans and mice, thus underlining the importance of $Aire^{+}$ mTECs in maintaining self-tolerance (Anderson et al., 2002; Derbinski et al., 2005).

There has long been an impression that the initial period of the immune systems development is particularly important for the establishment of tolerance to self. Early studies suggested that the challenge of self/nonself discrimination could be explained by time considerations as it was shown that antigens exposed to the immune system during fetal or early neonatal stages were assigned as self, thereby inducing long term tolerance (Brent, 1997;

Guerau-de-Arellano et al., 2009; Owen, 1945). In addition, it was suggested that immature lymphocytes had a heightened sensitivity to tolerance induction (Lederberg, 1959). More recently a compelling study has illustrated that Aire expression during the perinatal period is both necessary and sufficient to induce long-lasting tolerance and avoid autoimmunity (Guerau-de-Arellano et al., 2009).

Despite their key role and the recent identification of a bipotent epithelial progenitor the developmental pathways and mechanisms regulating development of $Aire^+$ mTECs from the progenitor population remain incomplete (Rossi et al., 2006). It is understood that the interaction between the tumour necrosis factor receptor, receptor activator of NF-κB (Rank) expressed by mTEC, and Rank ligand (Rankl) provided by haematopoietic cells, is crucial for the differentiation of the thymic medulla. Importantly redundancy in the source of Rankl during thymic epithelial development has been observed (Hikosaka et al., 2008; Rossi et al., 2007b). During postnatal and adult life CD4 SP T cells can provide Rankl (Hikosaka et al., 2008). During fetal thymus development, an intrathymic $CD4^+CD3^-$ lymphoid tissue inducer (LTi) population primarily provides Rankl (Rossi et al., 2007b). However, when embryonic mTEC development has been investigated within mice that lack LTi cells, retinoic acid related orphan receptor-γ knockout ($Ror\gamma^{-/-}$) mice, numbers of $Aire^+$ mTECs are dramatically reduced, but they are not completely absent (Figure 3.1) (Eberl et al., 2004; White et al., 2008b). This suggests further redundancy in the Rankl providing cell or that a potentially novel ligand is involved in this process.

In view of this, the aims and objectives of this chapter were to identify additional haematopoietic elements that play a role in initial formation of the thymic medulla in particular in the development of the first cohort of $Aire^+$ mTEC.

Figure 3.1 A Current Model of Aire$^+$ mTEC Development

Rankl – Rank interactions between haematopoietic cells and mTEC progenitors provide the necessary stimulus for medullary epithelial development and the development of Aire$^+$ mTECs After removal of the two known sources of Rankl LTi and CD4 SP thymocytes an Aire$^+$ mature mTEC population remains, suggesting an additional Rankl$^+$ cell type may be involved (3.1A).

Frozen section from E16 WT and *Rorγ*$^{-/-}$ thymus were stained for Keratin 5 and Aire (3.1B). Solid line denotes the corticomedullary junction. C, cortex, M, medulla. Arrow indicates Aire$^+$ mTEC in *Rorγ*$^{-/-}$ thymus.

Absolute cell numbers of Aire$^+$ mTECs were calculated by FACS analysis (3.1C). The Mann Whitney nonparametric two tailed statistical test was completed, *P = 0.0108. Data is representative of at least two distinct experiments.

A

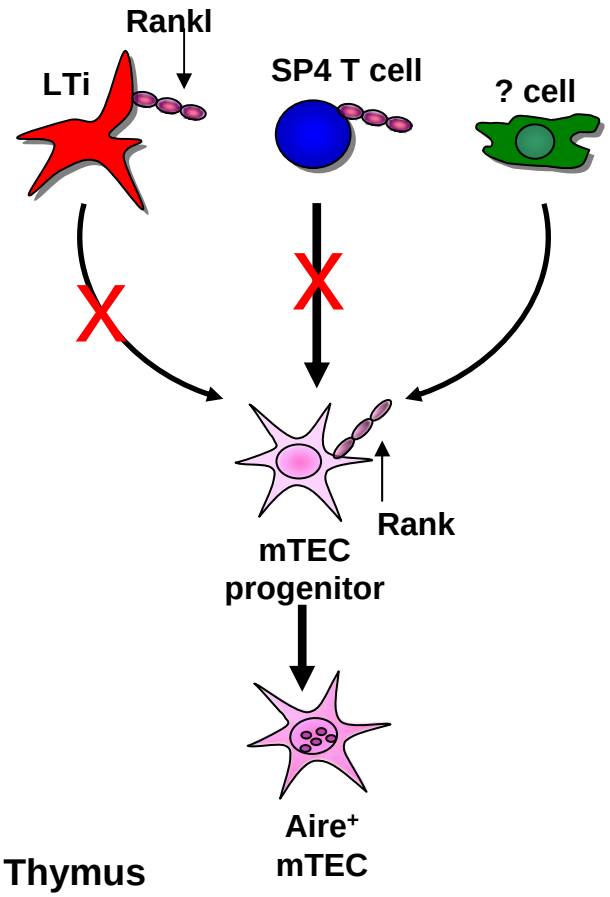
Rankl
LTi
SP4 T cell
? cell
Rank
mTEC
progenitor
Aire+
mTEC

B

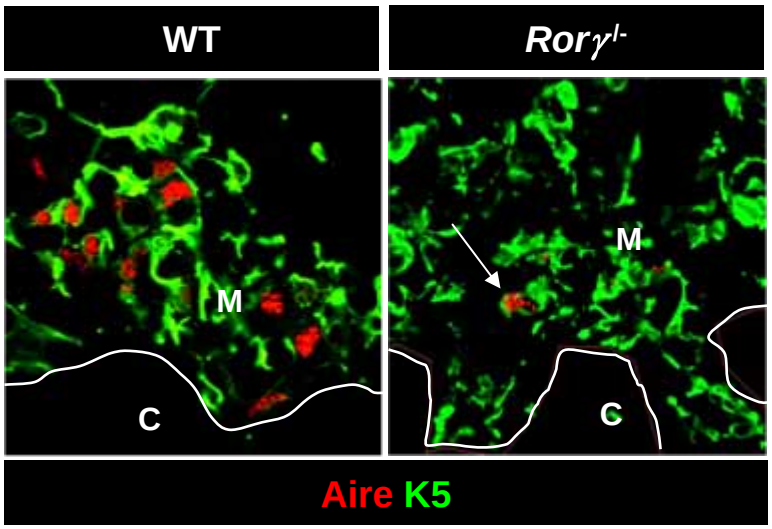
E16 Thymus
WT
Rorγ-/-
M
C
M
C
Aire K5

C

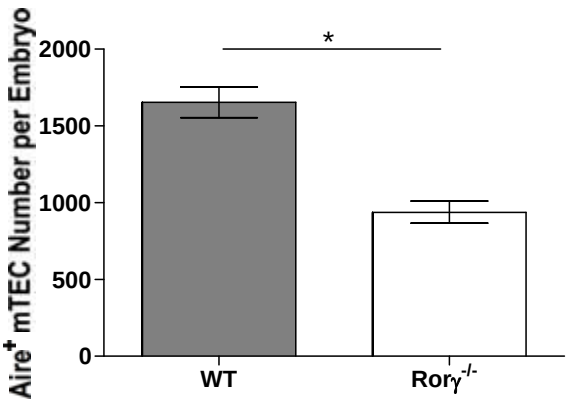
Aire+ mTEC Number per Embryo
2000
1500
1000
500
0
*
WT
Rorγ-/-

3.2 Specialised Materials And Methods

3.2.1 Confocal Analysis For Vγ5$^+$ T Cell Quantitation

Numerical quantitation of confocal images enables a visual observation of a single image to be corroborated by determining the extent of the occurrence within multiple replicates and multiple depths, throughout the tissue of interest. Staining a minimum of 5 E17 thymus sections from three separate thymuses enabled the quantitation of Vγ5$^+$ thymocytes within the cortex and medulla. Each section was separated by 50μm as one 5μm section was collected in every 10 5μm sections. The staining was completed as described in section 2.8.2. Each section was imaged using a Zeiss LSM510 laser scanning confocal head with a Zeiss Axiovert 100M microscope (Carl Zeiss, Oberkochen, Germany). Using Zeiss LSM 510 software, tile scans were taken by defining the centre of the section and the number of tiles in both the x and y direction using the stage and focus control panel to include the entire section (Figure 3.2A). Tile scans were stored as arrays of 1024x1024 pixels with 8 bit sensitivity. Before each image was recorded the tile scan rotation was calibrated. Each image was analysed with Zeiss LSM Image Browser, where the medullary areas (EpCam$^+$ CD8$^-$) were identified and highlighted using the overlay function (see Figure 3.2B). By only viewing the Vγ5$^+$ thymocytes within the separate areas (Figure 3.2C) individual Vγ5$^+$ thymocytes were highlighted as they were counted (Figure 3.2D). This was repeated for both the cortex and medulla. The numbers were recorded in an excel file and the number within the medulla expressed as a percentage of the total number recorded for each individual image.

Figure 3.2 Confocal Tile Scan Analysis For Quantitation

An example tile scan of WT E17 thymus stained for Vγ5, CD8 and EpCam is shown (3.2A). To determine the medullary areas the Vγ5 and CD8 channels are turned off and an overlay is drawn around the medullary areas (3.2B). The channel is then changed to look at the $V\gamma5^+$ thymocytes (3.2C). The $V\gamma5^+$ thymocytes residing within the medulla are counted and highlighted by yellow circles (3.2D), the counts are recorded within an excel file. This is repeated for the $V\gamma5^+$ thymocytes residing in the cortex, a different colour for the circles is used to distinguish them.

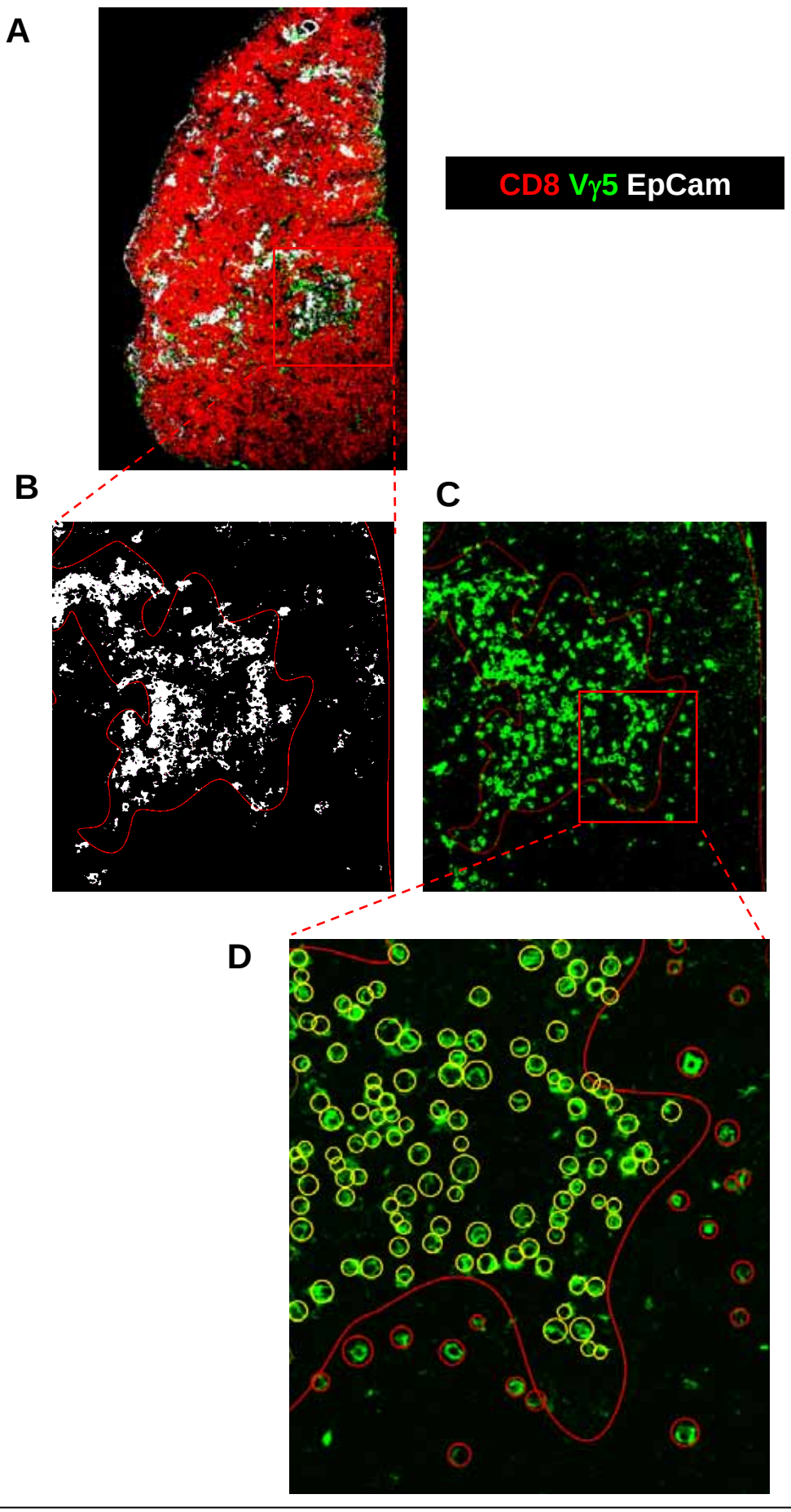
A
CD8 Vγ5 EpCam
B
C
D

3.2.2 Organ Culture Systems

3.2.2.1 Induction Of Aire$^+$ mTEC Development By Anti -RANK Stimulation Of dGuo FTOC

Day 15 embryonic lobes were placed in fetal thymus organ culture (FTOC) with 2-dguo to eliminate lymphoid cells as described in section 2.3.1. After 7 days in culture the 6 2-dguo treated FTOC lobes on a nucleopore filter were transferred to a centre-well organ culture dish (BD Labware) containing 200μl of DMEM, either supplemented with 10μg/ml anti-Rank (R&D systems) or not. The outer well contained 1.5ml of sterile water, to increase the humidity in the dish and prevent the small volume of media from dehydrating. After 4 days, lobes were removed from culture, disaggregated and analysed by flow cytometry or PCR.

3.2.2.2 Investigation Of Chemokine Signalling In Thymocyte Migration By Addition Of Pertussis Toxin To FTOC

Using a finely drawn mouth-controlled glass pipette, 2 embryonic day 15 (E15) thymic lobes from an individual embryo were placed onto 0.8μm sterile nucleopore filters (Millipore) within the centre well of a centre-well organ culture dish (BD Labware) containing 200μl of DMEM supplemented with either 250μg/ml PTX (1:200 dilution of the stock), or 1:200 PBS as a control. The outer well contained 1.5ml of sterile water, to increase the humidity in the dish and prevent the small volume of media from dehydrating. Ten organ culture dishes were placed within each sterile humidified chamber, purged with 10% CO_2 in air for approximately 10 minutes, to maintain the desired pH of the media (pH 7.2-7.4) and afterwards transferred into a 37^{o}C incubator for between 2 and 5 days.

3.2.2.3 Investigation Of Vγ5$^+$ Thymocyte And mTEC Interactions With Reaggregate Thymus Organ Culture (RTOC)

The formation of reaggregate thymus organ cultures (RTOCs) enables the investigation of thymic epithelial cell development within a 3D setting (Hare et al., 1999b; White et al., 2008a). This allows investigation of the potential of specific cell types to provide maturation signals to immature thymic stroma. CD3$^+$ Vγ5$^+$ thymocytes were isolated by MoFlo cell sorting from E15 FTOCs cultured for 6-7 days (for full method see section 2.3). The stromal cells were prepared from 5-7 day dGuo treated FTOCs using the technique described within section 2.5.4. The resulting single cell suspension was then subjected to a CD45 depletion (detailed in section 3.2.8) to remove any contaminating haematopoietic cells such as macrophages from the preparation. The numbers of thymocytes and stromal cells were counted using a haemocytometer and mixed at an approximate ratio of 5:1 stroma: haematopoietic cells of interest. RTOCs were produced with approximately 1 x 10^6 cells in total. The stromal cells and haematopoietic cells were mixed together and centrifuged at 1000rpm for 10 minutes at 4^{o}C. The supernatant was then carefully removed using a P200 pipette, leaving a concentrated cell suspension of approximately 2-3μl in volume, which was subsequently vortexed. Using a finely drawn glass pipette the cell suspension was taken up as a result of capillary action and via mouth-control and with the use of a microscope, layered in a dropwise manner onto the centre of a 0.8μm sterile Whattman filter (Whattman), to create a three-dimensional structure. The filters were placed on top of a 1cm^2 sterile anti-wrap sponge support and cultured in an identical manner to FTOCs (described within section 2.3.1). Only one RTOC was placed on one filter and only one filter and sponge were cultured within a 90mm Petri dish containing 4mls DMEM (Hare et al., 1999b; White et al., 2008a).

3.2.3 Isolation Of Vγ5$^+$ DETC From Ear Skin Epidermal Sheets

3.2.3.1 Preparation Of Epidermal Sheets

Ears were removed from ~3 week old mice and collected in Ca^{2+} Mg^{2+} free PBS, split into dorsal and ventral sides and placed epidermal side up, onto a Ca^{2+} Mg^{2+} free PBS solution containing 20mM EDTA to separate the epidermis from the dermis (Bergstresser and Juarez, 1984). Following incubation for 2 h at 37^{o}C the sheets were peeled from the ear and washed in PBS with Ca^{2+} Mg^{2+}. PBS was removed and the epidermal sheets fixed in cold acetone for 20 min at -20^{o}C. Acetone was removed and the sheets washed twice with PBS. Sheets were incubated in a blocking solution, 2% (w/v) BSA in PBS (≥300μl), for 1 h at 37^{o}C. Primary antibodies were added directly into the blocking solution and incubated for either 90 min at 37^{o}C or overnight at 4^{o}C. Following incubation the antibody solution was removed and the epidermal sheet washed 4 times in PBS. If a secondary antibody was required they were added in a 1% (w/v) BSA in PBS solution and incubated for either 90 min at 37^{o}C or overnight at 4^{o}C. After washing in PBS four times the epidermal sheets were dried onto silane-coated slides and mounted with Vectashield (VectorLabs) and the slides sealed with clear nail varnish to prevent water damage whilst analysing. The sheets were analysed as described in section 2.7.3.

3.2.3.2 Preparation Of Epidermal Cell Suspensions

In order to isolate Vγ5$^+$ dendritic epidermal T cells (DETC) from the skin, adult mice not in active hair growth (either 3-3.5 or 8-9 wks of age) were sacrificed. The skin was soaked with 95% ethanol and the hair removed using surgical prep blades (Owens & Minor) (Havran et al., 1991; Sullivan et al., 1985). The skin was isolated and spread dermal side up on a Petri dish lid to allow the subcutaneous fatty tissue to be scraped away using curved forceps. The skin was cut into strips of approximately 1cm in width using a prep blade and the strips placed dermal side

down in Trypsin-GNK (see table 3.1 for details) for 2 hours at 37^{o}C. The epidermis was then removed from the dermis using forceps; holding one piece of skin with one set of forceps, after removing any excess fluid by blotting the skin on sterile gauze, a second pair of forceps were used to scrape the epidermis from the dermis. The epidermis was subsequently transferred into a 50ml tube containing 9ml of Trypsin-GNK, 1ml 10 x DNAse buffer (constituents detailed in table 3.2), 50μl DNAse (constituents detailed in table 3.3) and incubated for 15mins at 37^{o}C whilst shaking. 10ml of media A (see table 3.4 for details) was added to each tube and remove stratum corneum, hairs and large debris by filtering cells through nitex nylon mesh (90 micron). The resulting cell suspension was collected in 50ml polypropylene tubes filled with Media A and centrifuged (10min, 1000rpm, 4^{o}C). Dead cells and keratinocyte depletion was completed by centrifuging the crude epidermal cell suspension over a Histopaque 1083 density gradient. Up to 40 million crude cells were resuspended in 4ml of Media A in a 15ml polypropylene tube. Underlay 4ml Histopaque (Sigma), centrifuge (20 min, 1600rpm, 22^{o}C, no break) and harvest the interface and wash twice with Media A.

The resulting cell suspension was stained in preparation for MoFlo cell sorting of the V$\gamma5^{+}$ T cell population (see section 2.5.6 for detailed protocol). Single colour staining controls were prepared to enable compensation of the MoFlo cell sorter. The CD45^{+} V$\gamma5^{+}$ CD3ε^{+} T cell population was sorted into 1.5ml eppendorf containing 300μl RF10-H, a small volume of the sorted population was analysed to determine the purity of the population, and populations of less than 95% purity were discarded. The total cell number was calculated and the resulting population used for RTOCs (section 3.2.3).

Amount	Components
2.94g	NaCl
0.14g	KCl
0.34g	Glucose
1g	Trypsin (Sigma T-1005)
pH 7.6	pH with $NaHCO_3$
340ml	total volume in dH_2O

Table 3.1 Constituents of Trypsin-GNK

Amount	Components
21.21g	Tris Base
0.5g	$MgCl_2$
0.073g	$CaCl_2$
100ml	Total volume in dH_2O
pH 7.5	pH

Table 3.2 Constituents of 10 x DNAse buffer

Amount	Components
1ml	10 x DNAse buffer
4 ml	sterile H_2O
5 ml	glycerol

Table 3.3 Reconstitution of 10 million Dornase units of DNAse

Amount	Components
100ml	MEM (Gibco)
10ml	FCS
1ml	10 x Pen/Strep
50µl	DNAse

Table 3.4 Media A Constituents

3.2.4 Preparation And Isolation Of Splenic LTi For RTOC

Splenic LTi were isolated from WT fetal spleen organ cultures by MoFlo cell sorting (section 2.5.6). WT E15 fetal spleens were found and isolated from the outer edge of the embryonic stomach. They were cultured as whole organs in a similar way to fetal thymus (section 2.3.1 for details), 100ng/ml interleukin-7 (IL-7; PeproTech EC, London, UK) was added to the culture medium (Kim et al., 2008). After 6-7 days of culture (10% CO_2, 37^{o}C) the fetal spleens were removed from the filter into cold RF10-H medium. Approximately 20 spleens at a time were gently teased apart using fine forceps and the resulting single cell suspension counted and stained for CD3ε FITC and CD4 PE (see section 2.6 for full staining protocol). Single colour staining controls were also prepared. $CD4^{+}CD3\varepsilon^{-}$ LTi were subsequently sorted into 1.5ml eppendorf containing 300µl RF10-H. A small volume of the sorted population was analysed to determine the purity, any purity less than 95% was discarded. The total cell number was calculated and the resulting population used for RTOCs (section 3.2.3).

3.2.5 Preparation And Isolation Of $V\gamma5^{+}$ Thymocytes For RTOC

Fetal $V\gamma5^{+}$ thymocytes were isolated from WT fetal thymus organ cultures (section 2.3.1 for detailed protocol) by MoFlo cell sorting (section 2.5.6). Approximately 20 6-7 day FTOC at a time were teased and counted, and stained with anti CD3ε PE and anti Vγ5 FITC (see section 2.6 for full staining protocol). Single colour staining controls were also prepared. $V\gamma5^{+}CD3\varepsilon^{+}$ thymocytes were sorted into a 1.5ml eppendorf containing 300µl RF10-H. As before, preparations of a post-sort purity less than 95% were discarded. The total cell number was calculated and the resulting population used for RTOCs (section 3.2.3).

3.2.6 Preparation Of Samples For Gene Expression Analysis

3.2.6.1 Snap Freezing Of Cell Populations

Cell populations obtained following MoFlo sorting or immunomagnetic bead separations were transferred into 1.5ml RNase-free eppendorf tubes (Camlab) and centrifuged at 1000rpm for 10 minutes. Supernatants were removed to leave a dry pellet. Closed eppendorfs were immersed in liquid nitrogen before storage at -80°C until further use.

3.2.6.2 RNA Extraction And cDNA Synthesis

cDNA was extracted from MoFlo sorted cells or cells obtained after immunomagnetic separation, using a μMACS^{TM} one-step mRNA Isolation and reverse transcription kit (Miltenyi Biotech). The whole procedure was carried out in a laminar flow cabinet. Lysis/binding and wash buffers were allowed to equilibrate to room temperature prior to carrying out the protocol. The isolated cell pellet was resuspended in lysis/binding buffer (1ml ≤ $1x10^7$ cells) and vigorously vortexed (3-5 minutes) to ensure total cell lysis. For cells obtained from immunomagnetic bead separation, cells were separated from the beads by resuspending the rosettes in lysis/binding buffer and using a 21-gauge needle to lyse the cells. The resulting mix was subsequently centrifuged briefly at 13,000 rpm to separate the cells from the beads and the beads discarded. The lysate was applied to the Lysate Clear Column in a centrifuge tube and centrifuged (3 minutes, 13000g). 50μl of oligo deoxy-thymidine (dT) microbeads were gently mixed with the lysate to permit hybridisation of the mRNA. The mixture was subsequently applied to a MACS μ column, previously primed with 100μl Lysis/Binding buffer, which was held within the magnetic field of the thermoMACS^{TM} Separator. The magnetically labelled mRNA remained bound to the column allowing removal of proteins and DNA by the addition of 2 x 200μl of lysis/binding buffer, and the removal of ribosomal RNA and DNA by the addition

of wash buffer (4 x 100µl) to the column. To continue with cDNA synthesis directly, the bound mRNA was not eluted from the column. 2 x 100µl of equilibration/wash buffer was added to the column matrix and allowed to run through. Afterwards, lyophilised enzyme mix was dissolved in 20µl resuspension buffer and applied to the top of the column, followed by 1µl sealing solution, to prevent sample evaporation. The column was incubated on the thermo block at 42^{o}C for 1 hour for reverse transcription to take place. Following the incubation period, 2 x 100µl of equilibration/wash buffer was applied to rinse the column. If the column flow was hindered the tip of the column was gently wiped to remove dried salt accumulation. Finally, a 30 min incubation with 20µl of release solution at 42^{o}C was completed and the synthesised cDNA eluted by the addition of 50µl of cDNA elution buffer, into an eppendorf. The cDNA was stored at –20^{o}C until required. High yields and purity of cDNA were obtained with this procedure.

3.2.6.3 Real Time Quantitative PCR

Real Time quantitative PCR was performed on the RotorGene RG-3000 (Corbett Research) using SYBR green with primers specific for various genes of interest. Details of the primers used in this study are outlined in Table 3.5, if two primer sequences are provided they were both used to verify the result. β-actin was chosen as the housekeeping gene for sample normalisation prior to amplifying the target genes of interest. Primers were made by Sigma-Genosys and primer pairs were designed using the aid of PrimerBank software (http://pga.mgh.harvard.edu/primerbank/index.html) to minimise the possibility of primer dimerisation that could lead to non-specific PCR amplification. The PCR reactions were carried out in triplicates or duplicates in a 15µl reaction volume which contained 7.5µl 2 x qPCR mastermix (Quantace Sensimix) containing heat activated Taq polymerase, dNTPs, $MgCl_2$ and reaction buffer, 0.15µl (0.2µM) of both forward and reverse gene specific primers, 0.3µl Sybr

green, 5.9μl DNAse-free, RNAse-free, PCR-grade water (Sigma), and 1μl cDNA template [5-25ng]. The amplification program comprised of an initial 'hot start' (95°C for 15 minutes), followed by cycling at 95°C for 15 seconds, 60 to 62°C (depending on primer pair) for 20 seconds and 72°C for 5 seconds (39 cycles).

The fluorescent signal produced from the amplicon was acquired at the end of each polymerisation step and at the end of amplification, a dissociation curve was produced (72-99°C, hold 30 seconds on 1st step then 5 seconds on next steps) for each primer set in order to check the specificity of the amplicon. Reaction amplification efficiency and the Ct values were obtained from the Rotor Gene 6.0 software (Corbett Research, Sydney Australia) using standard curves primarily obtained from cDNA from fetal thymic organ cultures (FTOCs). For calculation of the relative expression values for samples normalised to β-actin, the Pfaffl model was employed. The PfaffI model takes gene-dependent differences in the amplification efficiency into account. In addition to the post-amplification melt curve analysis specific amplification of target genes was verified by fractionation of PCR products on a 2.0% agarose gel, where the products were identified by their fragment size (section 3.6.3.4).

Primer	Forward 5' end primer sequence	Reverse 3' end primer sequence	Product size (base pairs)
β-actin NM_007393.2	CGTGAAAAGATGACCCAGATCA	TGGTACGACCAGAGGCATACAG	100
β-actin NM_007393	Sequence not provided Primers designed validated and synthesised QuantiTect Mm_Actb_1_SG PRIMER Assay (Qiagen QT00095242)	Sequence not provided Primers designed validated and synthesised QuantiTectMm_Actb_1_SG PRIMERAssay(QiagenQT00095242)	149
Aire NM_009646	TGCATAGCATCCTGGACGGCTTCC	CCTGGGCTGGAGACGCTCTTTGAG	187
Ccl19 (ELC)	GGGGTGCTAATGATGCGGAA	CCTTAGTGTGGTGAACACAAC	137
NM_011888.2	TGTGTTCACCACACTAAGGG	CCTTTGTTCTTGGCAGAAGACT	105
Ccl21 (SLC) NM_011335.2	GCTGCCTTAAGTACAGCCAGA	CTTCCTCAGGGTTTGCACAT	150
Ccl21a (SLC) NM_011124.4	ATCCCGGCAATCCTGTTCTC	GGGGCTTTGTTTCCCTGGG	129
Ccr7 NM_007719.2	TGTACGAGTCGGTGTGCTTC	GGTAGGTATCCGTCATGGTCTT	162
Ccl28	GTGTGTGGCTTTTCAAACCTCA	TGCATGAACTCACTCTTTCCAG	110
NM_020279	AGAGTGAGTTCATGCAGCATC	CTGCTTCAAAGTACGATTGTGC	117
Ccl27a NM_011336.1	ATGATGGAGGGGCTCTCCCCCGCCAGCAG Not best specific seq taken from Zou *et al* Cellular sig 19(2007)	TTCAGGAGCCGGGCTCAGAAGCAACAG	69
Ccr10 NM_007721	GGACTTTACTCCGGGTACGAT	CAGGGAGACACTGGGTTGGA	114
	AGAGCTCTGTTACAAGGCTGATGTC	CAGGTGGTACTTCCTAGATTCCAGC	255
RankL NM_011613.3	CACACCTCACCATCAATGCTGC	GAAGGGTTGGACACCTGAATGC	394
Skint1 NM_001102662.1	TTCAGATGGTCACAGCAAGC	GAACCAGCGAATCTCCATGT	143
	TTCAGATGGTCACAGCAAGC	TGTACAGGTGCACAGGCTCT	177
Rorγt NCBI GenBank Ref: AJ132394.1	GGA CAG GGAGCCAAGTTCTCAG	CACAGGTGATAACCCCGTAGTGG	106

Table 3.5 Quantitative RT-PCR Primer Sequence

3.6.3.4 Agarose Gel Electrophoresis

A 2% agarose (Sigma) gel, 0.5 × TBE buffer (Sigma), 0.5μg/ml Ethidium bromide (Sigma), was used to confirm the presence of the PCR products. A 15μl aliquot of the reaction mixture containing Reddymix™ (Abgene, UK), was loaded onto the gel and run for approximately 15-20 minutes dependent on the size, at 70V.1μl (1.5μg) 100bp DNA ladder (Invitrogen, Paisley, UK) containing, bromophenol blue was run, to confirm the product size was correct. The gel was visualised with a gene genius phosphor-imager with GeneSnap software (Syngene).

3.2.7 Thymocyte Cell Culture For Rankl Staining

Total thymocytes from embryonic day 16.5 (E16.5) were cultured for 16 hours (37^{o}C, 10% CO_2) without stimulation with PMA and ionomysin. Cell-surface Rankl detection and control staining were examined in indicated subpopulations.

Antibodies: anti-CD3 (2C11), anti-TCRδ (GL3), anti-TCR Vγ2 (UC3-10A6), anti-TCR Vg3 (536), anti-Rankl (IK22/5).

3.2.8 Immunomagnetic Isolation of Cell Types For RT-PCR And RTOCs

For further enrichment and selection of thymic epithelial cells or thymocytes, an immunomagnetic separation technique was employed using Dynalbeads (Dynal, Wirral, UK). The beads were prepared at least 24 hours before use by washing in 500μl RF10 three times to remove sodium azide after which the beads were incubated at 4°C overnight in the presence of the appropriate antibody, diluted to the required concentration in PBS. Details of antibodies used to coat Dynalbeads are outlined in table 3.6. Tissue culture derived CD45 supernatant was coated onto anti-rat Immunoglobulin (Ig)G Dynalbeads, whilst anti-CD205 and anti-CD40 biotin were coated onto streptavidin Dynalbeads and anti-rabbit IgG Dynalbeads were coated with rabbit

anti-FITC followed by anti-Vγ3 FITC or anti-Vγ2 FITC. Following over night incubation, beads were washed three times in RF10 to remove any excess antibody, and then resuspended in 100μl of RF10. Beads were next added to cell suspensions in 200μl of RF10 at an approximate ratio of 10:1. The beads and cells were mixed well within round-bottomed sterile cryogenic vials (Cryovial, Quebec, Canada) to ensure a large surface area for optimal cell to bead interactions and centrifuged (1000rpm, 10 minutes). After gentle resuspension of the pellet the cetrifugation was repeated a second time. The suspension was subsequently checked for 'rosettes', clusters of cells bound to beads, by light microscopy after gentle pippetting. Once positive binding was detected, cells rosetted to beads were isolated from unbound cells using an Eppendorf (1.5ml) Dynal Magnetic Particle Concentrator (Dynal). Supernatant containing the unbound populations was removed and rosettes were washed gently to eliminate any none specifically binding cells.

To obtain cells of defined epithelial populations for RT-PCR, cell suspensions depleted of CD45 were treated with biotin conjugated CD205 and CD40 streptavidin beads as described above. Rather than discarding, the rosettes were resuspended in 300μl PBS and centrifuged at 1400rpm, 5 minutes, 4^{o}C and the supernatant removed. The pellets were snap frozen and stored at –80^{o}C until required for RT-PCR.

Bead type	Coating antibody and dilution	Use
Anti-rat IgG	Anti-mouse CD45 tissue culture supernatant used neat (ATCC)	Depletion of $CD45^+$ haematopoietic cells from organ cultured embryonic thymus lobes.
Streptavidin	Anti-mouse CD205 biotin used 1:20	Selection of $CD205^+$ thymic epithelial cells from freshly dissected embryonic thymus lobes.
Streptavidin	Anti-mouse CD40 biotin used 1:50	Selection of $CD40^+$ thymic epithelial cells from freshly dissected embryonic thymus lobes.
Anti-Rabbit IgG	Rabbit Anti- FITC used 1:50	Selection of $V\gamma3^+$ thymocytes from organ cultured embryonic thymus lobes.
Anti-Rabbit IgG	Anti-mouse Vγ3 FITC used 1:20	Selection of $V\gamma3^+$ thymocytes from organ cultured embryonic thymus lobes.
Anti-Rabbit IgG	Anti-mouse Vγ2 FITC used 1:20	Selection of $V\gamma2^+$ thymocytes from organ cultured embryonic thymus lobes.

Table 3.6 Details Of Antibodies Used To Coat Dynabeads For Immunomagnetic Separation

3.3 Results:

3.3.1 Vγ5$^+$ Thymocytes Associate With Medullary Areas In The Developing Thymus

Previous studies have shown that LTi within the developing fetal thymus and single positive CD4$^+$ (SP4) thymocytes within the adult thymus play a key role in the development of Aire$^+$ mTECs (Hikosaka et al., 2008; Rossi et al., 2007b; White et al., 2008b). However, mice lacking LTi (*Rorγ*$^{-/-}$) examined at a stage before the presence of SP4 thymocytes (~E16-E17) demonstrate a detectable Aire$^+$ population albeit reduced when compared to wild type (WT), implicating the involvement of an additional cell type (Figure 3.1). Reports that CD80^{hi}Aire$^+$ mTECs first emerge around embryonic day 16 (E16) imply that progenitors responsive to known maturation signals are also present at this stage (Rossi et al., 2007b). Therefore, to begin to identify a cell type that could be involved in providing embryonic medullary epithelial progenitors with the capacity to provide a maturation stimulus, E16-17 thymus was analysed.

Embryonic thymus lobes were dissected from E17 WT embryos, prepared for immunohistochemistry (see section 2.8 for a detailed protocol), and frozen sections stained for confocal microscopy analysis. Medullary epithelium was identified by high expression levels of EpCam (a cell surface epithelial marker). Medullary areas were also identified using CD8, owing to thymocytes at this stage of development being predominantly DP (CD4$^+$CD8$^+$) and thus residing within the cortex (Figure 3.3). The γδ T cell lineage is the primary TCR$^+$ lineage present within the early fetal thymus and defined subsets develop in sequential waves, each of a restricted repertoire with defined homing capacity to specific intraepithelial compartments (Havran and Allison, 1988; Houlden et al., 1988). Interestingly, it was previously reported that total γδ thymocytes within the fetal thymus localised to the medulla (Farr et al., 1990). To establish whether the γδ T cell lineage was involved in the development of Aire$^+$ mTECs, two distinct subsets of the γδ T cell lineage known to develop in the fetal thymus

Figure 3.3 Vγ5$^+$ But Not Vγ4$^+$ Thymocytes Show Evidence Of Medullary Accumulation In Fetal Thymus

Frozen tissues sections of thymus dissected from day 17 of gestation (E17) from wild type (WT) mouse embryos were stained for EpCam, CD8 and Vγ5 (3.3A) and EpCam, CD8 and Vγ4 (3.3B). Two representative images of each staining are shown. Note the medullary accumulation of the Vγ5 subset. Scale bar, 50μm. Solid line denotes the corticomedullary junction. C, cortex, M, medulla.

The percentage of Vγ5$^+$ thymocytes was calculated from the number of Vγ5$^+$ thymocytes within each region (3.3C). Counts were taken from tiles scans of at least 5 sections of varying depths through 3 individual thymuses. Each point represents a single image. The median is indicated. The Mann Whitney nonparametric two tailed statistical test was completed, ***$p < 0.0001$

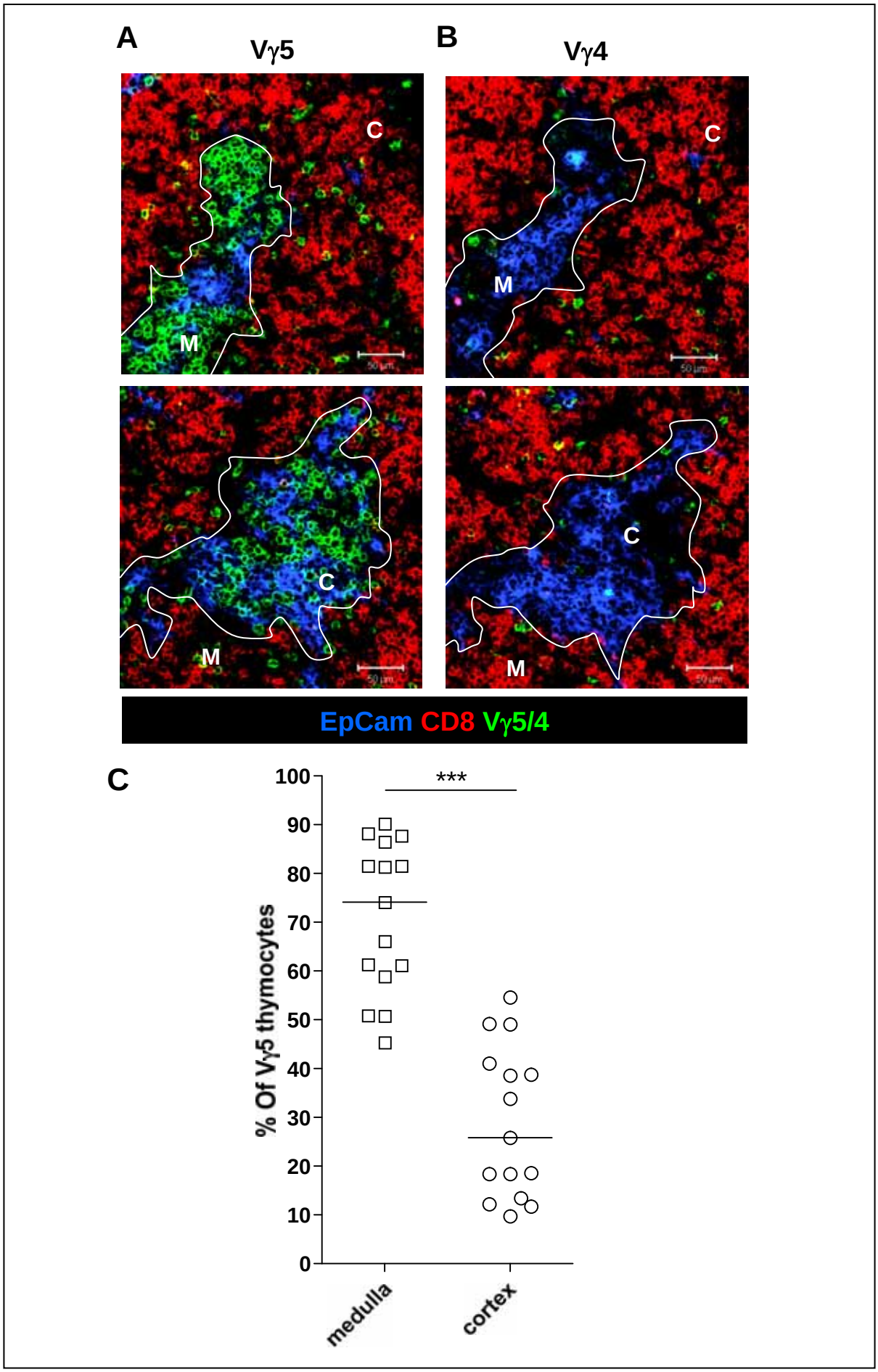
A
Vγ5
B
Vγ4
C
M
EpCam CD8 Vγ5/4
C
***
% Of Vγ5 thymocytes
100
90
80
70
60
50
40
30
20
10
0
medulla
cortex

were analysed, the Vγ5$^+$ thymocytes (Haas et al., 1993) and the Vγ4$^+$ thymocytes (Allison and Havran, 1991; Sperling et al., 1992). Two examples of serial sections are shown, the Vγ5$^+$ thymocyte subset [nomenclature according to Tonegawa and Heilig equivalent to the Vγ3 designation by Garman *et al* (Hayday and Pao, 1998)] appeared to reside within the medulla (Figure 3.3A), in contrast the Vγ4$^+$ thymocyte population did not at this stage (Figure 3.3B), illustrating that Vγ5$^+$ thymocytes could potentially provide signals to the mTEC precursors.

The association between Vγ5$^+$ thymocytes and Aire$^+$ mTECs was further demonstrated by the completion of confocal quantitation (refer to section 3.2.1 for a detailed protocol). This enabled the proportion of Vγ5$^+$ thymocytes residing within the medulla to be compared to the cortex. Tile scans were taken of at least 5 sections from different depths of three thymuses isolated from different mice. The number of Vγ5$^+$ thymocytes was counted within the cortex and the medulla and then plotted as a percentage of the total number of Vγ5$^+$ thymocytes (Figure 3.3C). This result clearly indicates that a significant percentage (~70%) of Vγ5$^+$ thymocytes in an E17 WT thymus localise to the thymic medulla when compared to the cortex (***$p < 0.0001$).

3.3.2 Vγ5 Thymocytes Express Rankl

The tumor necrosis family member Rankl has been shown to play a key role in the development of the thymic medulla (Akiyama et al., 2008; Hamazaki et al., 2007; Rossi et al., 2007b). Therefore, to identify whether the medullary association of Vγ5$^+$ thymocytes was to enable provision of Rankl thus permitting embryonic mTEC maturation, *Rankl* expression was measured by RT-PCR in Vγ5$^+$ thymocytes isolated from E15 WT thymus lobes after 7 days in organ culture and compared to SP4$^+$ thymocytes and DP thymocytes obtained from adult thymus (Figure 3.4A). Analysis showed the greater abundance of *Rankl* transcripts in Vγ5$^+$ thymocytes as compared to DP and SP4 thymocytes, the latter known to be involved in mTEC development

in the adult thymus (Hikosaka et al., 2008). Further confirming a potential role for Vγ5$^+$ thymocytes in the development of a functional medullary microenvironment. In addition, *Rankl* expression in their adult counterpart, Vγ5$^+$ DETC differed by approximately 8 orders of magnitude when compared to Vγ5$^+$ thymocytes (Figure 3.4B). Moreover, LTi expressed approximately 30 fold more *Rankl* than Vγ5$^+$ thymocytes (Figure 3.4C).

Furthermore, flow cytometric analysis confirmed Rankl surface expression on CD3$^+$Vγ5$^+$ thymocytes isolated from E16 WT thymus (Figure 3.4D). Together these data demonstrate that Vγ5$^+$ thymocytes associate with medullary thymic epithelium, posses the correct signalling machinery known to be involved in mTEC development and are therefore capable of driving mTEC maturation.

3.3.3 Vγ5$^+$ Thymocytes Develop Normally In *Rorγ* Deficient Mice

It has been reported that some γδ T cells require an interaction with or the expression of Rorγ in order to develop normally and express a complete collection of γδ-biased genes (Lochner et al., 2008; Silva-Santos et al., 2005). Due to the interest in investigating the development of the thymic medulla in the absence of LTi, it was important to consider whether the development of the Vγ5$^+$ thymocyte subset was affected in Rorγ deficient mice. To test this the presence, maturation status and localisation of Vγ5$^+$ thymocytes within the embryonic thymus of *Rorγ*$^{-/-}$ mice was analysed. Flow cytometric analysis of Vγ5$^+$ thymocytes isolated from E15 WT and *Rorγ*$^{-/-}$ thymus after 5 days in organ culture revealed a similar proportion of Vγ5 thymocytes present in *Rorγ*$^{-/-}$ thymus in comparison to WT (Figure 3.5A). However, when the absolute cell numbers were calculated a significant ($p = 0.049$) reduction was observed in *Rorγ*$^{-/-}$ thymus (Figure 3.5B). To assess the maturation status of γδ thymocytes the modulation of their cell

Figure 3.4 Vγ5 Thymocytes Express Rankl

Quantitative RT-PCR of *Rankl*, normalised to the housekeeping gene *β-actin*, was carried out on purified $V\gamma5^+$ thymocytes from E15 WT 7d FTOC and DP and SP4 thymocytes from adult WT thymus (3.4A), DETC from adult ear skin epidermal sheets (3.4B) and LTi isolated from 7 day fetal spleen organ culture (3.4C), all were isolated by MoFlo sorting. PCRs were carried out in triplicate. Error bars indicate the standard error of the mean. Data is representative of at least two distinct independent sorting experiments.

Freshly isolated WT thymus lobes from E17 mouse embryos were gently teased to obtain a total thymocyte suspension. Thymocytes were cultured for 16 hours (37^oC 10% CO_2) without stimulation. Cell-surface Rankl detection (solid lines) and isotype control staining (shaded lines) were examined on the $CD3^+$ $V\gamma5^+$ population (3.4D). Data is representative of at least three experiments.

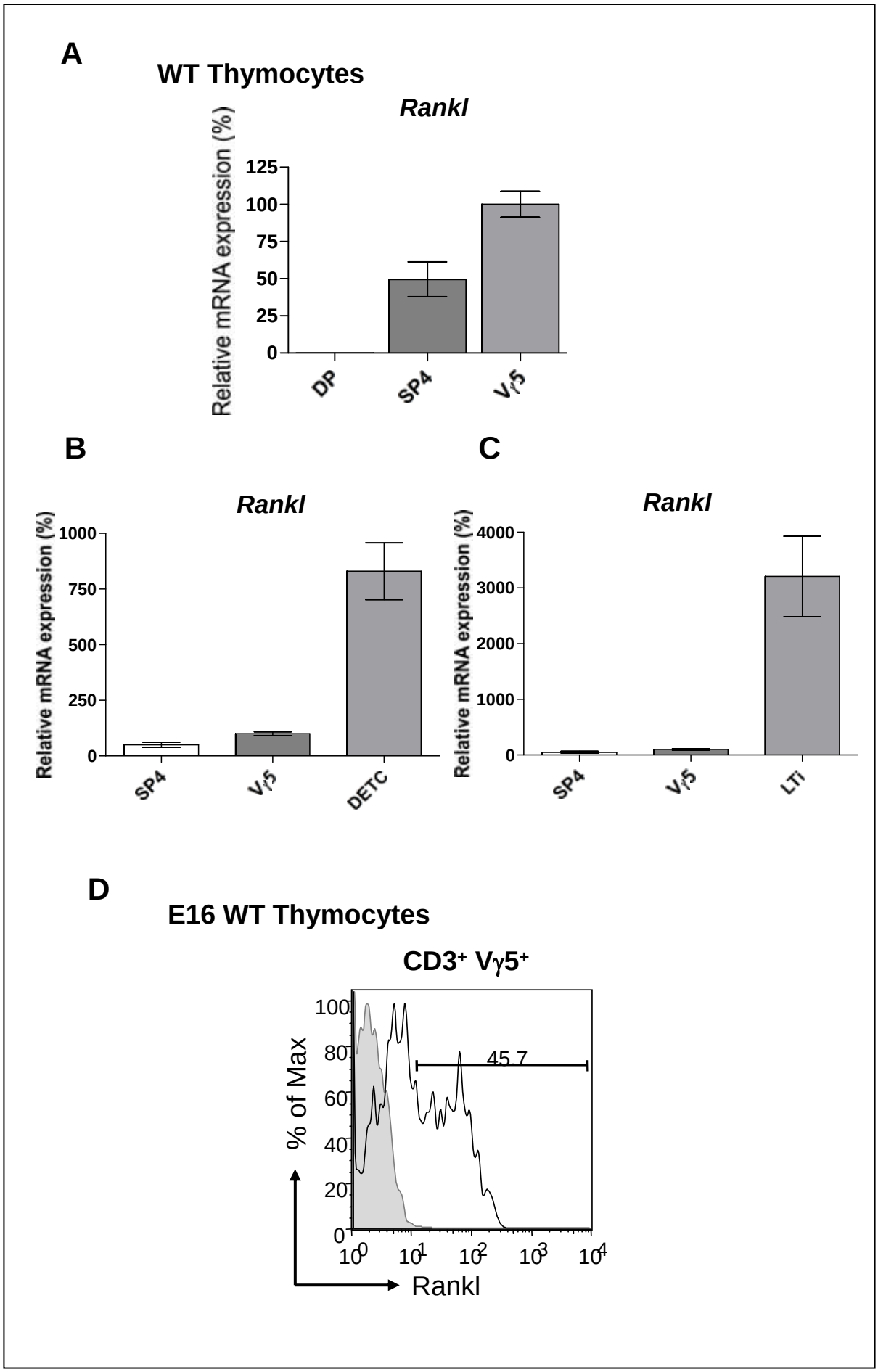
A
WT Thymocytes
Rankl
Relative mRNA expression (%)
125
100
75
50
25
0
DP
SP4
Vγ5
B
Rankl
Relative mRNA expression (%)
1000
750
500
250
0
SP4
Vγ5
DETC
C
Rankl
Relative mRNA expression (%)
4000
3000
2000
1000
0
SP4
Vγ5
LTi
D
E16 WT Thymocytes
CD3+ Vγ5+
% of Max
100
80
60
40
20
0
45.7
10^0
10^1
10^2
10^3
10^4
Rankl

Figure 3.5 Vγ5 Thymocytes Show Evidence Of Normal Development In *Rorγ*$^{-/-}$ Mice

Total thymocyte cell suspensions were obtained by gentle teasing of 5d WT and *Rorγ*$^{-/-}$ E15 FTOCs. Cells were stained for flow cytometric analysis for Vγ5 and CD45RB. The proportion of Vγ5^{+} thymocytes in *Rorγ*$^{-/-}$ compared to WT is shown (3.5A). 3.5B illustrates the comparison of absolute Vγ5^{+} thymocyte number in WT and *Rorγ*$^{-/-}$ thymus. *p = 0.049. Each point represents an individual embryo. The bar indicates the median. Cell-surface CD45RB expression in Vγ5^{+} thymocyte is shown (3.5C). Percentages of cells within gated areas are indicated. The absolute number of immature (CD45RB^{lo}) and mature (CD45RB^{hi}) Vγ5^{+} thymocytes in WT and *Rorγ*$^{-/-}$ thymus, ns = not significant, *p = 0.028 (3.5D). Each point represents an individual embryo and the bar indicates the median.

Confocal analysis of frozen thymus sections from E16 wild type (WT) and *Rorγ*$^{-/-}$ mice were stained for EpCam, Aire and Vγ5 (3.5E). Solid line denotes the corticomedullary junction. C, cortex. M, Medulla. Scale bar, 50μm.

Epidermal sheets were prepared from the skin from adult ears of WT and *Rorγ*$^{-/-}$ mice and stained for Vγ5, note the presence of Vγ5^{+} DETCs in both WT and *Rorγ*$^{-/-}$ epidermis (3.5F). Scale bar, 100μm. Data is representative of at least three experiments.

Quantitative RT-PCR of *Rorγt*, normalised to the housekeeping gene *β-actin*, was carried out on purified Vγ5^{+} thymocytes from E15 WT 7d FTOC and DP thymocytes from adult WT thymus by MoFlo sorting (3.5G). Note the lack of expression in Vγ5^{+} thymocytes. PCRs were carried out in triplicate. Error bars indicate the standard error of the mean. Data is representative of at least two distinct independent sorting experiments.

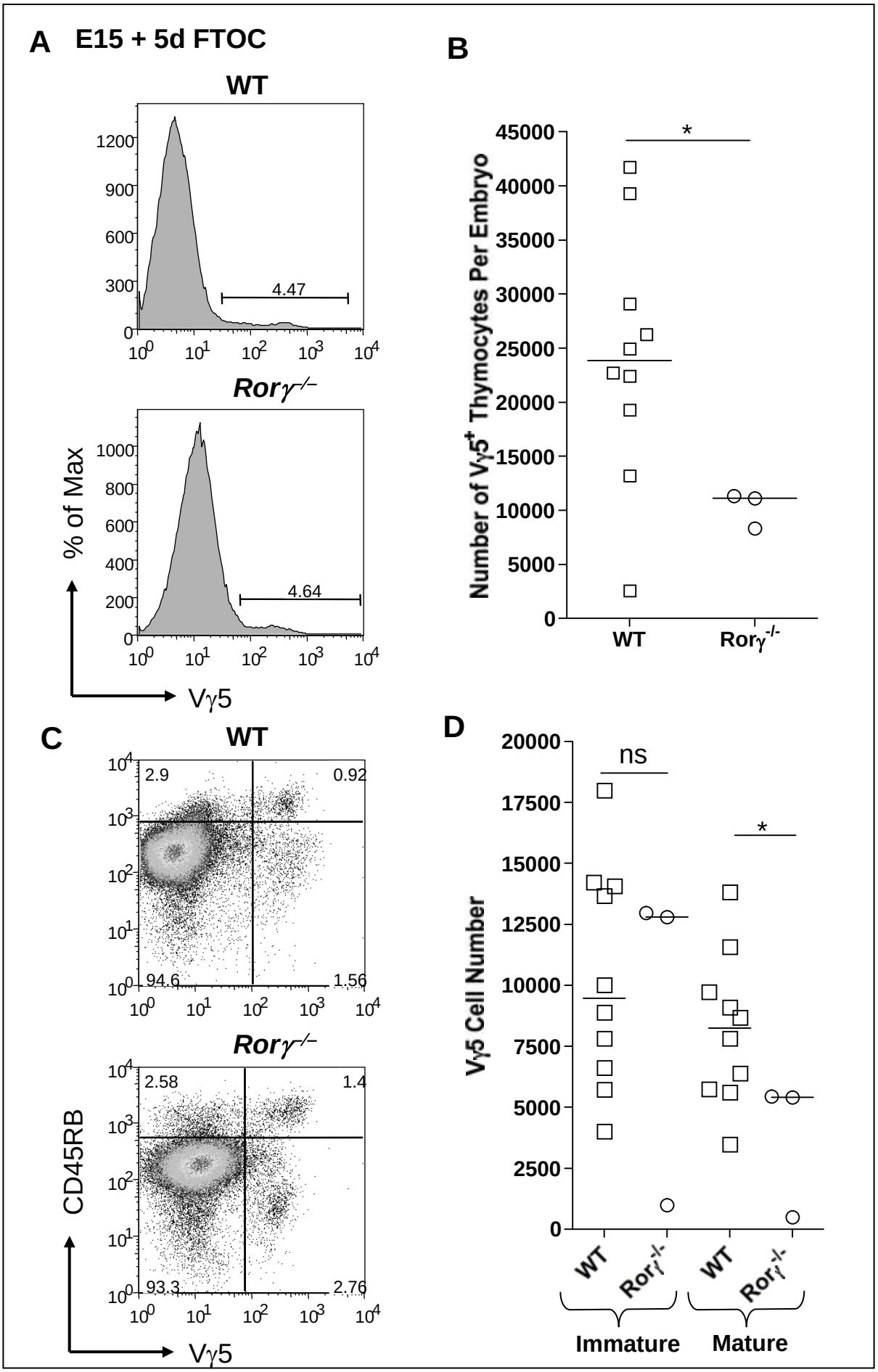
A
E15 + 5d FTOC
WT
4.47
Rorγ-/-
4.64
% of Max
Vγ5
B
Number of Vγ5+ Thymocytes Per Embryo
*
WT
Rorγ-/-
C
WT
2.9
0.92
94.6
1.56
Rorγ-/-
2.58
1.4
93.3
2.76
CD45RB
Vγ5
D
Vγ5 Cell Number
ns
*
WT
Rorγ-/-
WT
Rorγ-/-
Immature
Mature

E E16 Thymus

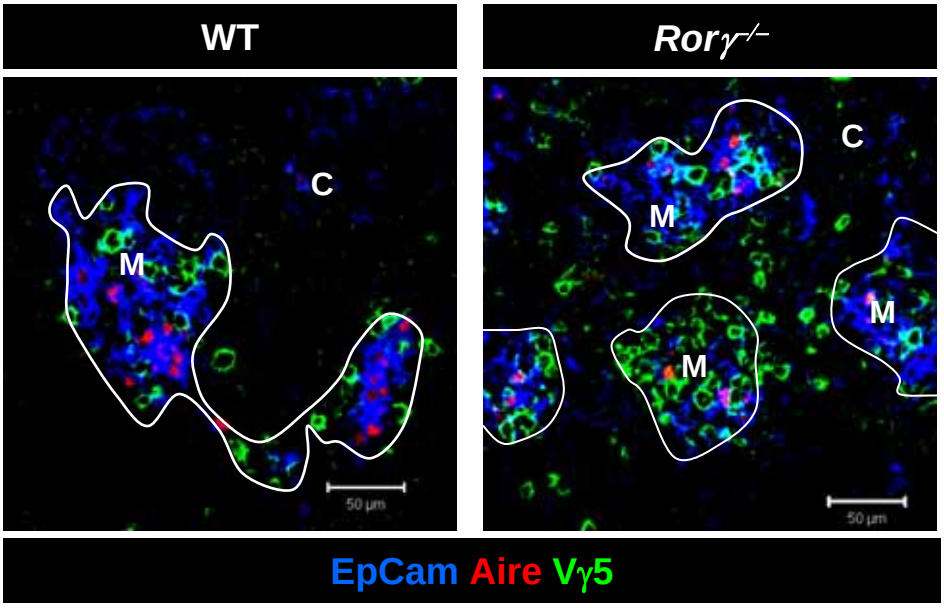

F Adult Epidermal Sheets

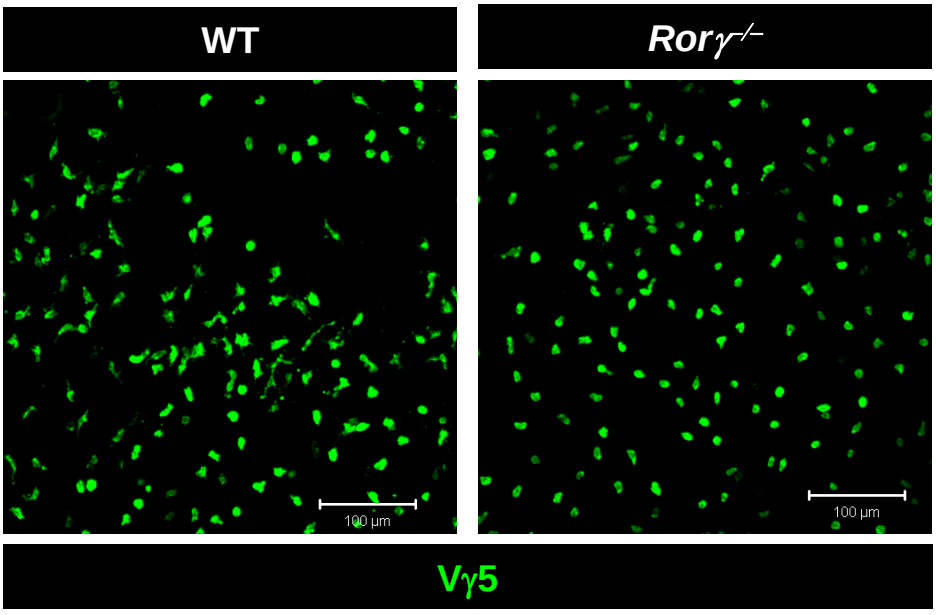

G

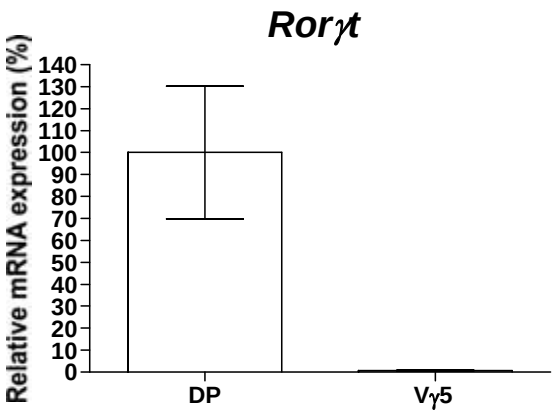

surface marker and chemokine receptor expression can be evaluated (Leclercq et al., 1993; Tatsumi et al., 1993; Xiong and Raulet, 2007). One characteristic indicator of maturation is CD45RB upregulation. Consequently, analysis of CD45RB expression levels on $V\gamma5^+$ thymocytes derived from E15 WT and *Rorγ*$^{-/-}$ thymus after 5 days in organ culture illustrated that *Rorγ*$^{-/-}$ $V\gamma5^+$ thymocytes are able to upregulate CD45RB. However, a 16% increase in the ratio of immature ($CD45RB^{lo}$) to mature ($CD45RB^{hi}$) $V\gamma5^+$ thymocytes was seen in *Rorγ*$^{-/-}$ $V\gamma5^+$ thymocytes as compared to WT (Figure 3.5C). Analysis of the absolute number of $CD45RB^{hi}$ mature $V\gamma5^+$ thymocytes further confirmed a defect in their development as a significant ($p = 0.028$) reduction was observed when compared to WT $V\gamma5^+$ thymocyte maturation (Figure 3.5D). However, a reduction in the number of immature ($CD45RB^{lo}$) $V\gamma5^+$ thymocyte population was observed when compared to WT, but this was not found to be significant ($p = 0.6923$). Nevertheless, $V\gamma5^+$ thymocytes were primarily found associated with the medulla in the *Rorγ*$^{-/-}$ E16 thymus, analogous to their observed medullary location in WT E16 thymus (Figure 3.5E). These data suggests that a significantly reduced percentage of $V\gamma5^+$ thymocytes are able to develop, mature and interact with the thymic medulla in the absence of Rorγ therefore, the defect may be a result of a cell extrinsic mechanism.

Mature $V\gamma5^+$ thymocytes home to the epidermis of the skin where they have a pronounced dendritic morphology and are known accordingly as dendritic epidermal T cells (DETC) (Payer et al., 1991). Consequently, to further evaluate the maturation of $V\gamma5^+$ thymocytes in *Rorγ*$^{-/-}$ mice, their presence within the epidermis and thus their ability to migrate to the epidermis was determined. $V\gamma5^+$ DETC were readily identifiable within the skin epidermis of both adult WT and *Rorγ*$^{-/-}$ mice (Figure 3.5F) suggesting that development of $V\gamma5^+$ thymocytes is sufficiently complete to enable them to home to their peripheral location in the absence of Rorγ. In addition, RT-PCR analysis of *Rorγt* expression showed that $V\gamma5^+$

thymocytes do not express Rorγt (Figure 3.5G), further corroborating the defect observed in their maturation may be due to a cell extrinsic mechanism.

3.3.4 *In Vivo* Functional Data Suggesting A Role For Vγ5$^+$ Thymocytes In mTEC Development

The above data show that Vγ5$^+$ thymocytes reside within the medulla at a time when the medullary epithelium is first developing and that they posses the functional capacity to promote maturation of medullary epithelium. Therefore their functional ability to promote Aire$^+$ mTEC development was tested by assessing whether the presence or absence of γδ T cells (*Tcrδ*$^{-/-}$) had an effect on the number of Aire$^+$ mTECs and was compared to the absence of LTi (*Rorγ*$^{-/-}$), the absence of both LTi and γδ T cells (CD3ε*tgRorγ*$^{-/-}$) and the presence of both LTi and γδ T cells (WT) (Figure 3.6A). Embryonic day 17 (E17) thymuses were removed from background matched, WT, *Tcrδ*$^{-/-}$, *Rorγ*$^{-/-}$ and CD3ε*tgRorγ*$^{-/-}$, enzymatically disaggregated and analysed by flow cyometry. The haematopoietic and cortical epithelial cells were excluded from the analysis by gating on the CD45$^-$Ly51$^-$ population, thus enabling clear analysis of the EpCam$^+$ Aire$^+$ mTEC population. Representative FACS plots from each mouse indicate that WT, *Rorγ*$^{-/-}$ and *Tcrδ*$^{-/-}$ E17 thymuses contain a proportion of Aire$^+$ mTECs (Figure 3.6C, E and F). Interestingly, Aire$^+$ mTECs were completely absent from the E17 CD3ε*tgRorγ*$^{-/-}$ thymus (Figure 3.6D). In addition, the absolute number of Aire$^+$ mTECs revealed the average number of Aire$^+$ mTECs in a WT E17 thymus lobe to be approximately 1700 and within the *Rorγ*$^{-/-}$ and *Tcrδ*$^{-/-}$ E17 thymus to be roughly half this value at ~800 (Figure 3.6B). Statistical analysis of the total cell numbers revealed the reduction in Aire$^+$ mTEC number within the CD3ε*tgRorγ*$^{-/-}$, *Rorγ*$^{-/-}$ and *Tcrδ*$^{-/-}$ E17 thymus compared to WT to be significant. Collectively these data suggest that both γδ T cells and LTi play a role in medullary epithelial cell development as in

Figure 3.6 Aire$^+$ mTEC Are Reduced In The Absence Of Either LTi Or γδT cells

Different mouse strains contain unique combinations of LTi and γδ T cells (3.6A). Absolute cell numbers of Aire$^+$ mTECs within a single E17 thymic lobe from each mouse strain were calculated (3.6B). Each point represents a single lobe from an individual embryo the bar represents the median. The Mann Whitney nonparametric two tailed statistical test was completed, **p = 0.001-0.01, ***p < 0.001.

Thymic stromal cell suspensions from freshly isolated E17 thymus lobes from indicated mouse strains were obtained by enzymatic digestion. Cells were analysed by flow cytometry for expression of CD45, Ly51, EpCam and Aire. Aire expression in CD45$^-$ Ly51$^-$ thymic epithelial cells is shown for each mouse strain (3.6C-F). Percentages of cells within gated areas are indicated. Data is representative of at least three experiments.

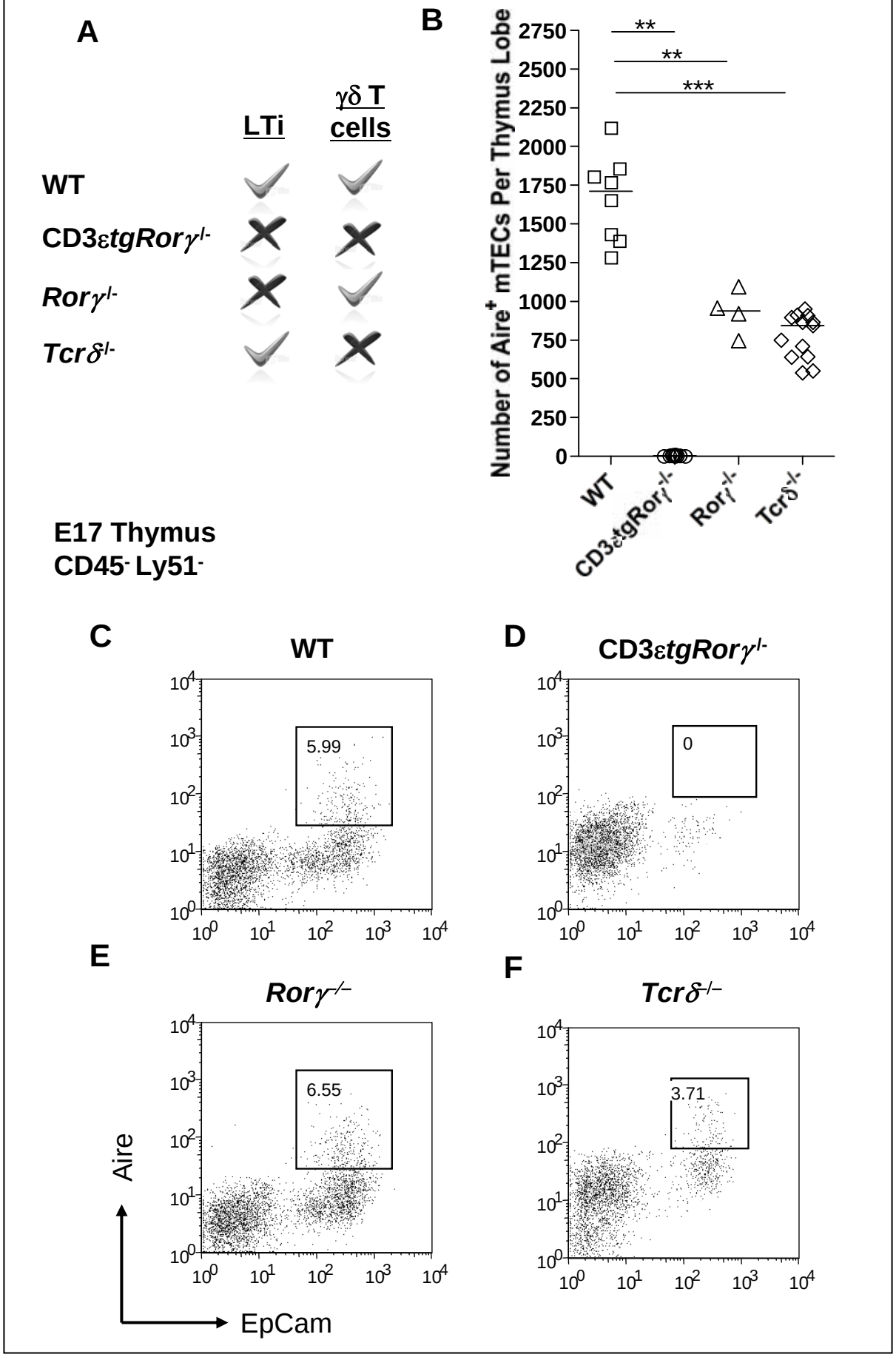
A
LTi
γδ T cells
WT
CD3εtgRorγ-/-
Rorγ-/-
Tcrδ-/-
B
Number of Aire+ mTECs Per Thymus Lobe
2750
2500
2250
2000
1750
1500
1250
1000
750
500
250
0
**
**
***
WT
CD3εtgRorγ-/-
Rorγ-/-
Tcrδ-/-
E17 Thymus
CD45- Ly51-
C
WT
5.99
D
CD3εtgRorγ-/-
0
E
Rorγ-/-
6.55
F
Tcrδ-/-
3.71
Aire
EpCam

their complete absence, Aire$^+$ mTECs are absent. In addition, the presence of either cell type produces comparable numbers of Aire$^+$ mTECs albeit reduced when compared to when both are present. This implies that LTi and γδ thymocytes play redundant roles in the development of Aire$^+$ mTECs.

To confirm a role for the Vγ5$^+$ thymocyte subset in the development of Aire$^+$ mTECs an *in vitro* system, the Reaggregate Thymus Organ Culture (RTOC), was employed. This well established system supports a complete programme of T cell and thymic epithelial cell development *in vitro* allowing the populations of each to be specifically manipulated and the three dimensional (3D) thymic architecture to be recreated allowing efficient interactions between developing T cells and stromal cells (Figure 3.7A) (protocol described in section 3.2.2.1) (White et al., 2008a). G. Turchinovich, Kings College London, carried out the preparation and staining of the DETC from adult skin epidermis.

Using dGuo treated stroma as a starting population, control RTOCs were prepared (Figure 3.7A) either without incorporating a haematopoietic cell population (Figure 3.7B) or introducing purified (>95%) MoFlo sorted LTi isolated from E15 WT spleen organ cultures (Figure 3.7C); LTi are a recognised source of Rankl and are known to be functional within this system (Rossi et al., 2007b). The experimental RTOCs included total Vγ5$^+$ thymocytes isolated by MoFlo cell sorting from 6 day FTOCs (Figure 3.7D) or mature Vγ5$^+$ DETC isolated by MoFlo cell sorting from adult skin epithelium. A ratio of 5:1 of haematopoietic cells to stroma was maintained for each RTOC (Figure 3.7E). The RTOCs were cultured for 7 days (37^{o}C, 10% CO_2) after which they were enzymatically disaggregated and the resulting cell suspension analysed by flow cytometry for expression of CD45, Ly51, EpCam and Aire. Gating on the CD45$^-$ Ly51$^-$ population enabled clear analysis of Aire expression in medullary thymic epithelium (EpCam$^+$) (representative FACS plots are shown Figure 3.7B-E). Figure 3.7C and D

Figure 3.7 Fetal Vγ5$^+$ Thymocytes, But Not Adult Vγ5$^+$ DETC Induce Aire$^+$ mTEC Development

Reaggregate thymic organ cultures (RTOCs) were created by mixing dGuo treated thymic stroma with a haematopoietic cell population of interest at a 5:1 ratio (3.7A). After 7 days culture the RTOCs were enzymatically digested and analysed by flow cytometry for CD45, Ly51, EpCam and Aire. Aire expression within the CD45$^-$ Ly51$^-$ EpCam$^+$ mTEC population is shown for each RTOC (dot plots 3.7B-E). Percentages of cells within gated areas are indicated.

Absolute cell numbers of Aire$^+$ mTECs within each RTOC are depicted in 3.7F. Each point represents a single RTOC. The median is shown. The Mann Whitney nonparametric two tailed statistical test was completed, ns = not significant, *p = 0.0952

Absence of a contaminating CD45$^+$ population in the empty RTOC and persistence of CD45$^+$ haematopoietic cells in the DETC RTOC is shown (3.7G). Data is representative of at least three experiments.

Reaggregate Thymus Organ Culture (RTOC) System

A

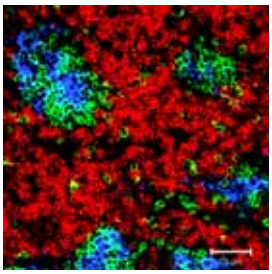

Vγ5⁺ thymocytes

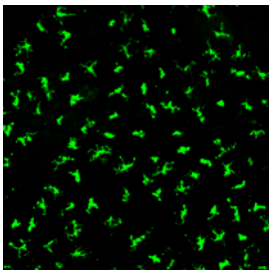

Mature Vγ5⁺ DETC

OR

E15 dGuo
stromal cells

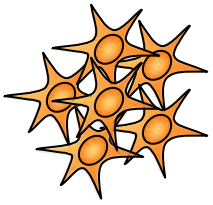

5:1
Stroma : Vγ5⁺ Cells

QuickTime™ and a
TIFF (Uncompressed) decompressor
are needed to see this picture.

Mix and
centrifuge

Reaggregate thymus organ culture

7 days

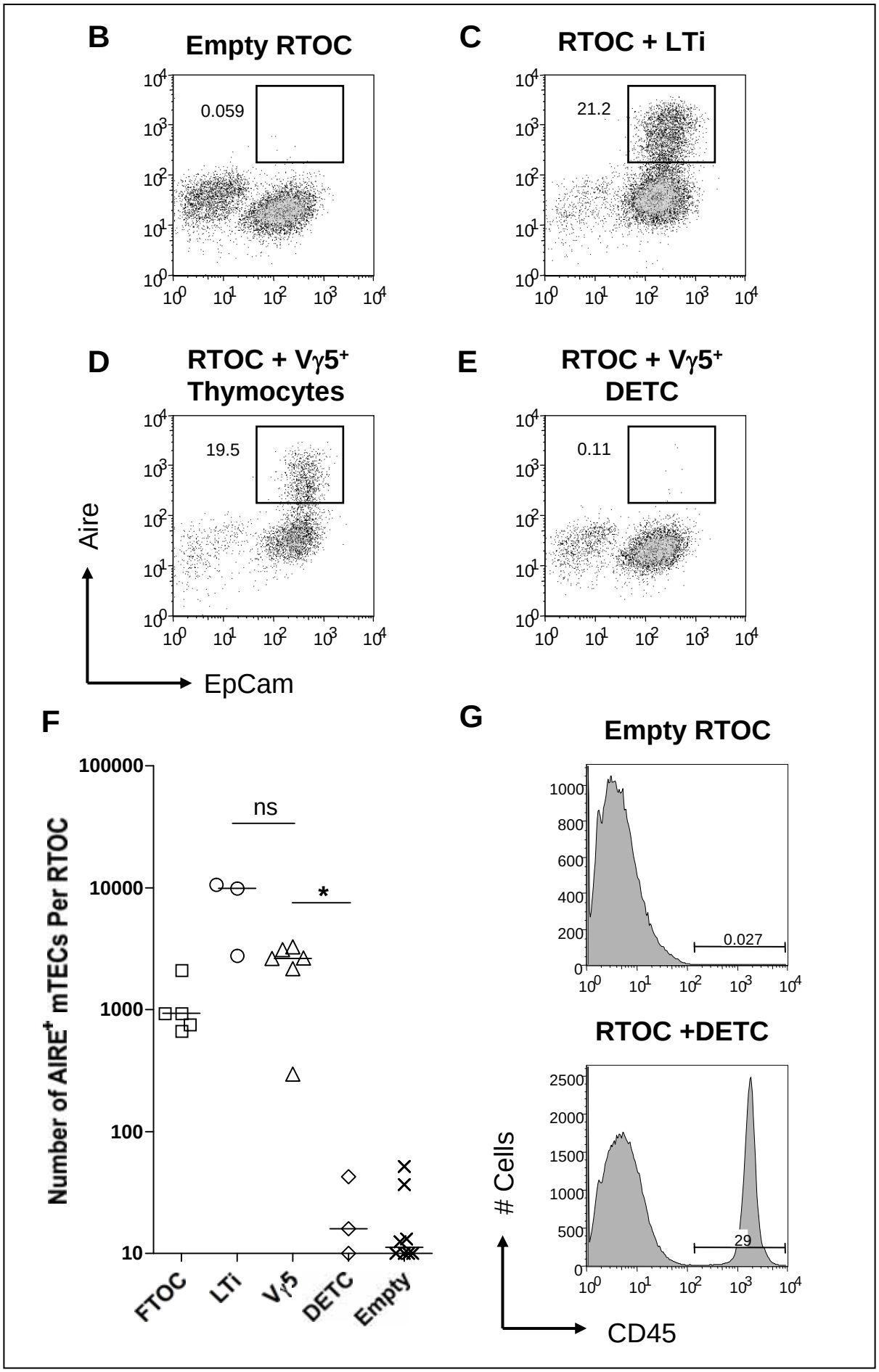
B
Empty RTOC
0.059
C
RTOC + LTi
21.2
D
RTOC + Vγ5+ Thymocytes
19.5
Aire
EpCam
E
RTOC + Vγ5+ DETC
0.11
F
Number of AIRE+ mTECs Per RTOC
100000
10000
1000
100
10
ns
*
FTOC
LTi
Vγ5
DETC
Empty
G
Empty RTOC
0.027
RTOC +DETC
29
Cells
CD45

illustrate that both LTi and Vγ5$^+$ thymocytes stimulate the maturation of a similar proportion of mTEC progenitors as an Aire$^+$ mTEC population (~20%) has developed. Interestingly the DETC do not appear to be able to stimulate development of Aire$^+$ mTECs (Figure 3.7E). The absolute number of Aire expressing mTECs within each RTOC further confirm the observed differences in ability of the haematopoietic cells to induce the development of Aire$^+$ mTECs; each point represents an individual RTOC (Figure 3.7F). Although a slight reduction in the numbers of Aire$^+$ mTEC was observed when Vγ5$^+$ thymocytes were compared with LTi, this was not statistically significant ($p = 0.0952$). A contaminating CD45$^+$ haematopoietic cell population was not present within the empty RTOC (Figure 3.7G) and importantly CD45$^+$ haematopoietic cells persisted in the DETC RTOCs after 7 days in culture (Figure 3.7G). Thus fetal Vγ5$^+$ thymocytes seem to play a role in the maturation of the thymic medulla.

3.3.5 Determining A Role For Chemokines In Vγ5$^+$ T cell Medullary Localisation

Having established that Vγ5$^+$ thymocytes have a functional role in the promotion of mTEC maturation and they reside within the early embryonic thymic medulla, it was important to determine the mechanism involved. As chemokines are known to be key players in directing the migration of developing αβ TCR$^+$ thymocytes through the specialised microenvironments of the established thymus, their role in the regulation of Vγ5$^+$ thymocyte migration and retention in the thymic medulla was investigated (Takahama, 2006). In initial experiments the effects of pertussis toxin were investigated. Pertussis Toxin (PTX) prevents the G (guanine nucleotide-binding) proteins from interacting with G protein-coupled receptors such as chemokine receptors on the cell membrane, thus preventing energy exchange and interfering with intracellular communication (Burns, 1988). E15 WT thymus lobes were organ cultured for 2 days either in the presence or absence of PTX after which frozen sections were prepared and stained for EpCam and Vγ5, confocal analysis allowed the medullary localisation of Vγ5$^+$ thymocytes to be

investigated. Representative pictures of the control (PBS) and PTX treated fetal thymus organ cultures (Figure 3.8A) show the medullary association of $V\gamma5^+$ thymocytes after 2 days with PBS treatment. In contrast, PTX treatment appears to prevent the medullary localisation of $V\gamma5^+$ thymocytes. Four separate experiments, each including 5 E15 WT thymic lobes for each treatment were quantitated. Total $V\gamma5^+$ thymocyte numbers present throughout the thymus were enumerated and the percentage of $V\gamma5^+$ thymocytes within the medulla analysed. A significant reduction in the resident number of $V\gamma5^+$ thymocytes within the medulla of PTX treated FTOC was observed when compared to PBS treated control (Figure3.8B and C). Figure 3.8 is a summary of the four experiments where each point represents the median percentage, however, in Figure 3.8C each point represents the percentage of $V\gamma5^+$ thymocytes from an individual FTOC, showing the variation between organ cultures (Figure 3.8C). Importantly, when numbers of $V\gamma5^+$ thymocytes were analysed by flow cytometry (Figure 3.8D), no significant difference between the presence or absence of PTX was seen, suggesting the decrease in medullary localisation was not due to a decrease in γδ thymocyte numbers.

Given that PTX treatment reduces the number of $V\gamma5^+$ T cells residing within the medulla whilst not having a toxic effect on the $V\gamma5^+$ thymocyte population, the effect of reduced interaction between $V\gamma5^+$ thymocytes with mTECs on their maturation was investigated. E15 WT thymus lobes organ cultured either in the presence or absence of PTX for 2 days were enzymatically disaggregated and stained for CD45, Ly51, EpCam and Aire. FACS analysis of $Aire^+$ medullary epithelium was achieved by gating on the $CD45^-$ $Ly51^-$ population. Representative FACS plots illustrate the proportion of $Aire^+$ $EpCam^+$ mTECs (Figure 3.8E) and suggest that PTX treatment reduces the proportion of mature $Aire^+$ mTECs (~5.5%) to approximately half the proportion observed in control PBS treated FTOCs (~10%). The absolute number of $Aire^+$ mTECs after each treatment was calculated, and established a significant

Figure 3.8 PTX Inhibits Vγ5 Medullary Accumulation In FTOC

E15 WT thymus lobes were organ cultured for 2 days either with or without pertussis toxin (PTX). Frozen sections were prepared, stained for EpCam and Vγ5 and analysed by confocal microscopy. Note the medullary association of $V\gamma5^+$ thymocytes in control thymus and the absence of this after PTX treatment (3.8A). Scale bar, 50μm. C, cortex, M, medulla. Solid line denotes the corticomedullary junction.

The percentage of $V\gamma5^+$ thymocytes within the medulla was calculated from the total number of $V\gamma5^+$ thymocytes within each picture of the entire thymus lobe in each experiment. Four experiments were completed; each point represents the median of each experiment. The Mann Whitney nonparametric two tailed statistical test was completed, ***p = 0.0007 (3.8B). In 3.8C each point represents the percentage from an individual FTOC. The bar indicates the median. Absolute $V\gamma5^+$ cell numbers were calculated (3.8D); no significant difference was observed, ns = not significant.

E15 WT thymus lobes organ cultured for 2 days either with or without PTX were enzymatically disaggregated and analysed by flow cytometry for Ly51, CD45, EpCam and Aire. Aire expression within the $CD45^-$ $Ly51^-$ medullary epithelium is shown in representative FACS plots (3.8E). Percentages of cells within gated areas are indicated. The absolute cell numbers of $Aire^+$ mTECs for each treatment are depicted (3.8F). Each point represents a single FTOC. Median is indicated.

E15 WT thymus lobes organ cultured for 5 days with or without PTX were gently teased and the thymocyte population analysed by flow cytometry for CD45RB and Vγ5. Representative FACS plots are shown (3.8G). Percentages of cells within gated areas are indicated. The absolute cell numbers of mature ($CD45RB^+$) and immature ($CD45RB^{lo}$) $V\gamma5^+$ thymocytes were calculated (3.8H), ***p = 0.0006. Each point represents an individual embryo. Median is illustrated. Data is representative of at least three experiments.

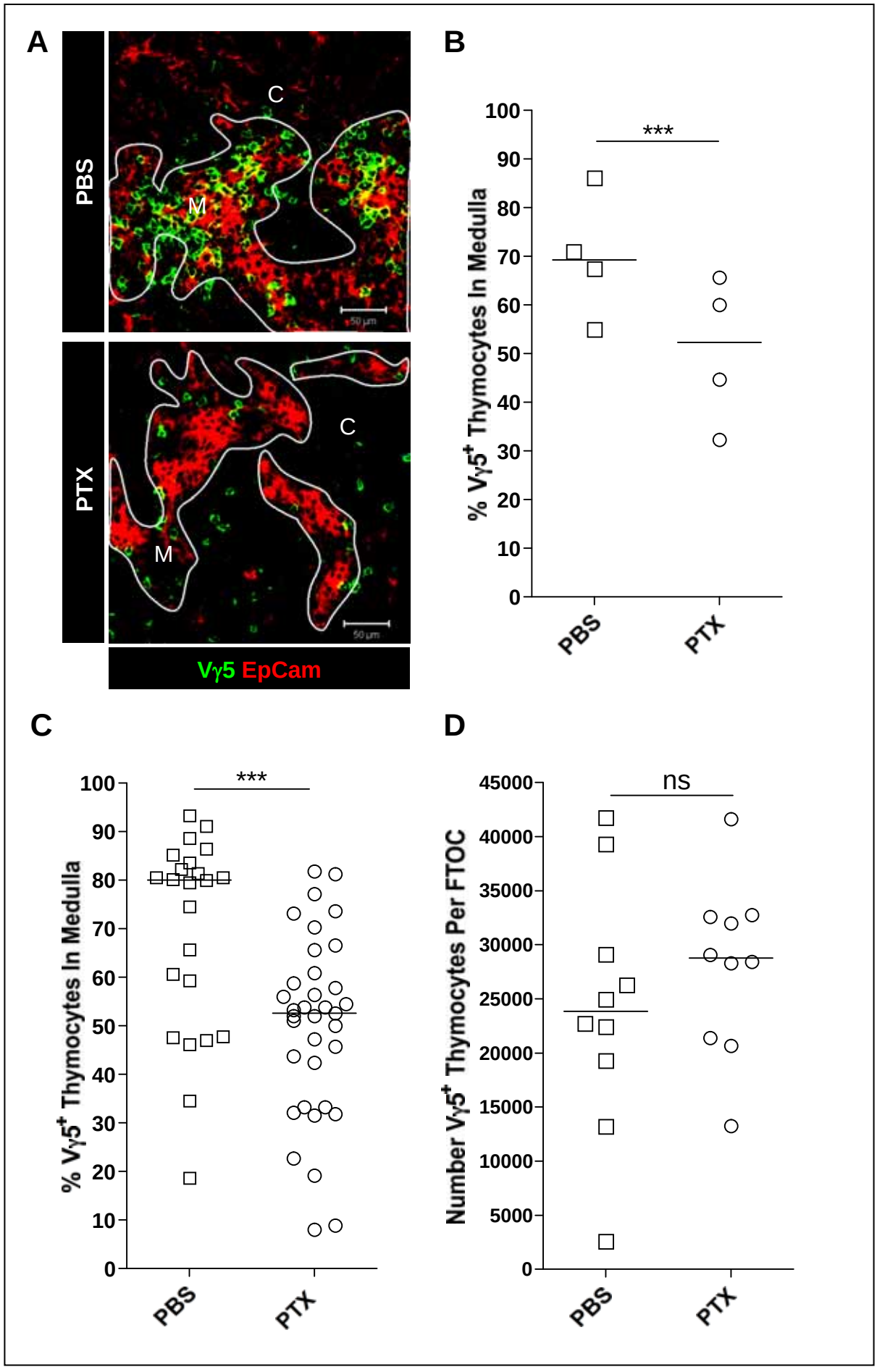
A
PBS
PTX
C
M
C
M
50 µm
50 µm
Vγ5 EpCam
B
% Vγ5+ Thymocytes In Medulla
***
100
90
80
70
60
50
40
30
20
10
0
PBS
PTX
C
% Vγ5+ Thymocytes In Medulla
***
100
90
80
70
60
50
40
30
20
10
0
PBS
PTX
D
Number Vγ5+ Thymocytes Per FTOC
ns
45000
40000
35000
30000
25000
20000
15000
10000
5000
0
PBS
PTX

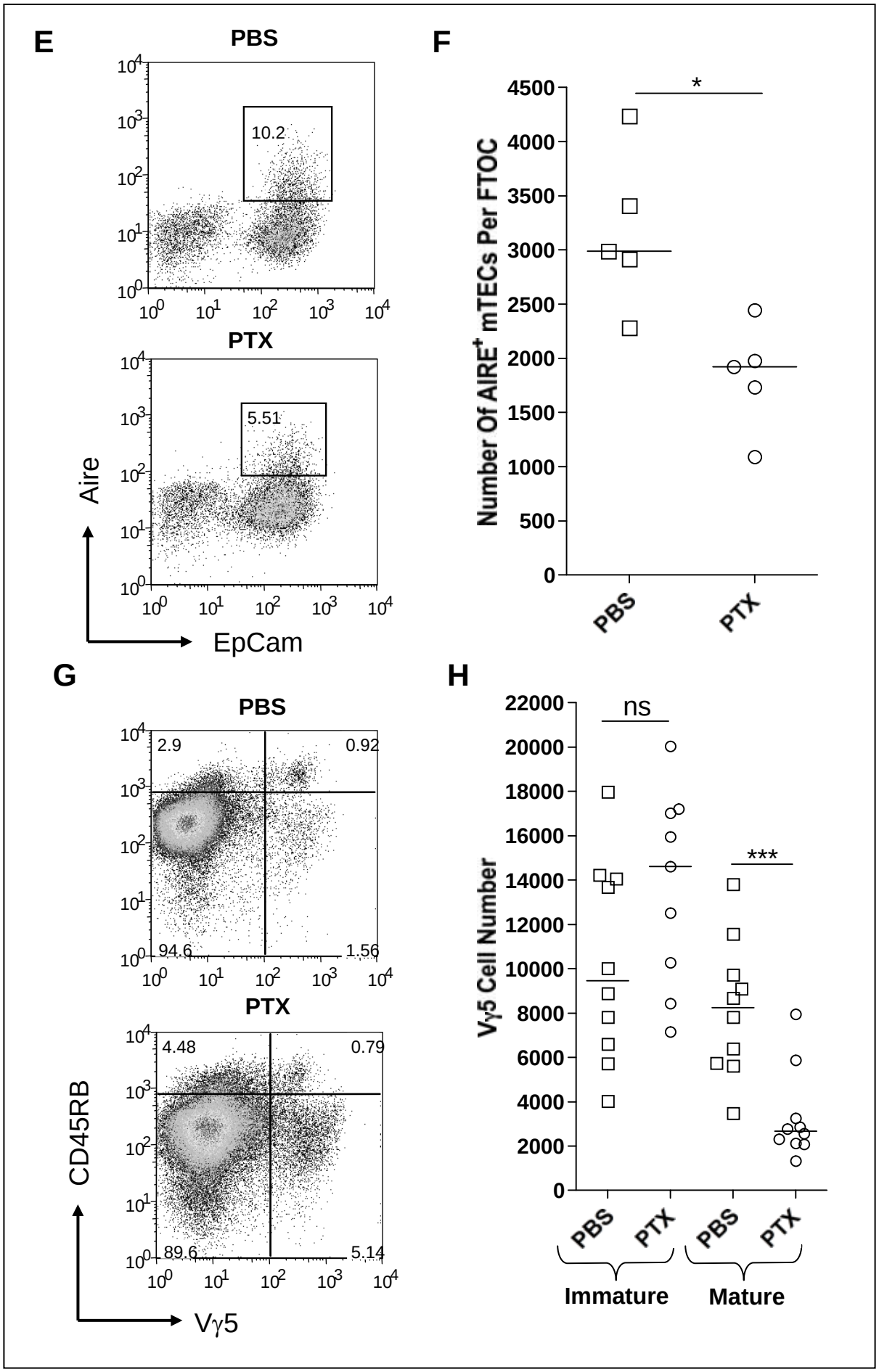
E
PBS
10.2
PTX
5.51
Aire
EpCam
F
Number Of AIRE+ mTECs Per FTOC
4500
4000
3500
3000
2500
2000
1500
1000
500
0
*
PBS
PTX
G
PBS
2.9
0.92
94.6
1.56
PTX
4.48
0.79
89.6
5.14
CD45RB
Vγ5
H
Vγ5 Cell Number
22000
20000
18000
16000
14000
12000
10000
8000
6000
4000
2000
0
ns
***
PBS
PTX
PBS
PTX
Immature
Mature

reduction in Aire$^+$ mTECs after PTX treatment when compared to PBS treatment (Figure 3.8F). Thus these data implicate a role for chemokine signalling in the localisation of Vγ5$^+$ T cells to the thymus medulla enabling them to provide Rankl to immature mTEC precursors permitting their development.

The above data lead to the hypothesis that the reduced medullary residency may also effect the maturation of Vγ5$^+$ thymocytes. Therefore, the CD45RB expression pattern on Vγ5$^+$ thymocytes after culture with or without PTX for 5 days was analysed (Figure 3.8G). Careful examination revealed the ratio of immature to mature Vγ5$^+$ thymocytes increased approximately 3 fold after PTX treatment from, ~2:1 (PBS treatment) to ~6.5:1. In addition, analysis of mature Vγ5$^+$ thymocyte numbers illustrated a significant ($p = 0.0006$) decrease after the addition of PTX (Figure 3.8H). Interestingly, the relative increase in immature Vγ5$^+$ thymocyte numbers was not significant ($p = 0.0621$), suggesting a block in the progression from immature (CD45RB^{lo}) to mature (CD45RB^{hi}). These data suggest that chemokine signalling is involved in both medullary accumulation and the maturation of Vγ5$^+$ thymocytes.

3.3.6 A Role For Ccr10 in γδ T cell - mTEC Association

Having recognised the implication of chemokine signalling in the medullary localisation of the fetal Vγ5$^+$ thymocytes, we sought to investigate which chemokine receptor – chemokine ligand pair might be involved. Previous studies have demonstrated the specific expression of Ccl27, one of the two ligands for Ccr10, in the skin. In addition, it is speculated that γδ precursors specifically upregulated Ccr10 in response to ligand engagement within the fetal thymus and it is understood that mature Vγ5$^+$ T cells specifically home to the skin epidermis, (Homey et al., 2000; Jarmin et al., 2000; Payer et al., 1991; Xiong et al., 2004). Taken together these data suggest Ccr10 may be implicated in the medullary association of Vγ5$^+$ thymocytes.

Therefore, the expression of Ccr10 on the developing Vγ5$^+$ thymocytes and the expression of its ligands Ccl27 and Ccl28 on medullary thymic epithelium was examined (Figure 3.9A-D) (Homey et al., 2000; Wang et al., 2000). Gene expression of *Ccr10* was studied by quantitative real-time PCR on mRNA extracted from Vγ5$^+$ and Vγ4$^+$ thymocyte populations. E15 WT thymus lobes cultured for approximately 7 days were gently teased apart to prepare a total thymocyte suspension and using an immunomagnetic bead separation technique (described in section 3.2.8) the Vγ5$^+$ and Vγ4$^+$ thymocyte populations were isolated. Briefly, anti-rabbit IgG Dynal beads were coated with rabbit anti-FITC antibody and subsequently with either Anti-mouse Vγ3 FITC (BD Pharmingen) or Anti-mouse Vγ2 FITC (BD Pharmingen). Beads were added to the thymocyte suspension and centrifuged; finally the bound cells were isolated using an Eppendorf (1.5ml) Dynal Magnetic Particle Concentrator (Dynal). Analysis showed the presence of *Ccr10* transcripts in both thymocyte populations however, Vγ5$^+$ thymocytes expressed approximately 3 times more than the Vγ4$^+$ thymocyte population (Figure 3.9A). Furthermore, flow cytometric analysis confirmed the surface expression of Ccr10. Thymus lobes from E16 WT mice were teased and the resulting cell suspension stained for CD3, Vγ5 and Ccr10 (Figure 3.9B).

To verify a role for Ccr10 in the medullary localisation of Vγ5$^+$ thymocytes the expression of its ligands (Ccl27 and Ccl28) in medullary thymic epithelium was analysed. Stromal cell suspensions were obtained from fresh E15 thymus lobes and an immunomagnetic Dynal bead separation enriched the stromal cell compartment through depletion of the CD45$^+$ haematopoietic cells. Also using Dynal beads, populations of CD205$^+$ (cTEC) and CD40$^+$ (mTEC) cells were positively selected for. These cells were then processed for mRNA and quantitative RT-PCR was carried out to measure *Ccl27* and *Ccl28* gene expression (Figure 3.9C and D). Relative gene expression was normalised to the housekeeping gene β-actin. These data

Figure 3.9 Does Ccr10 Have A Role In Vγ5$^+$ Medullary Localisation?

Vγ5$^+$ and Vγ4$^+$ thymocytes were isolated from total thymocyte preparations from WT E15 7 day FTOC using immunomagnetic bead separation and processed for mRNA. Quantitative RT-PCR revealed *Ccr10* mRNA expression was ~ 3 times greater in the Vγ5$^+$ thymocytes in comparison to Vγ4$^+$ thymocytes (3.9A). Relative gene expression was normalised to β-actin. PCRs were carried out in triplicate. Error bars indicate the standard error of the mean. Data is representative of at least two distinct independent sorting experiments.

A total thymocyte suspension was obtained from freshly isolated WT E16 thymus. Cell-surface Ccr10 detection (solid lines) and control staining (shaded lines) were examined on the CD3$^+$ Vγ5$^+$ population (3.9B). Data is representative of at least three experiments.

Cortical and medullary epithelial populations were isolated by immunomagnetic Dynal bead enrichment from enzymatically digested WT fresh E15 thymus and processed for mRNA. Quantitative RT-PCR was completed for *Ccl27* and *Ccl28* gene expression (figure 3.9C and D). Relative gene expression was normalised to β-actin. Note *Ccl27* expression in medullary thymic epithelium and an absence of *Ccl28* expression. PCRs were carried out in triplicate. Error bars indicate the standard error of the mean. Data is representative of at least two distinct independent sorting experiments.

WT E15 thymic lobes cultured for 2 days either with or without anti Ccl27 blocking antibody (20μg/ml) were prepared for confocal analysis and frozen sections stained for Vγ5, EpCam and CD8. The proportion of Vγ5$^+$ thymocytes within the medulla revealed a significant increase after blocking antibody treatment compared to none treated control (3.9E). Mann Whitney nonparametric two tailed statistical test was completed, **P = 0.001-0.01. Each point represents an individual FTOC. The bar represents the median.

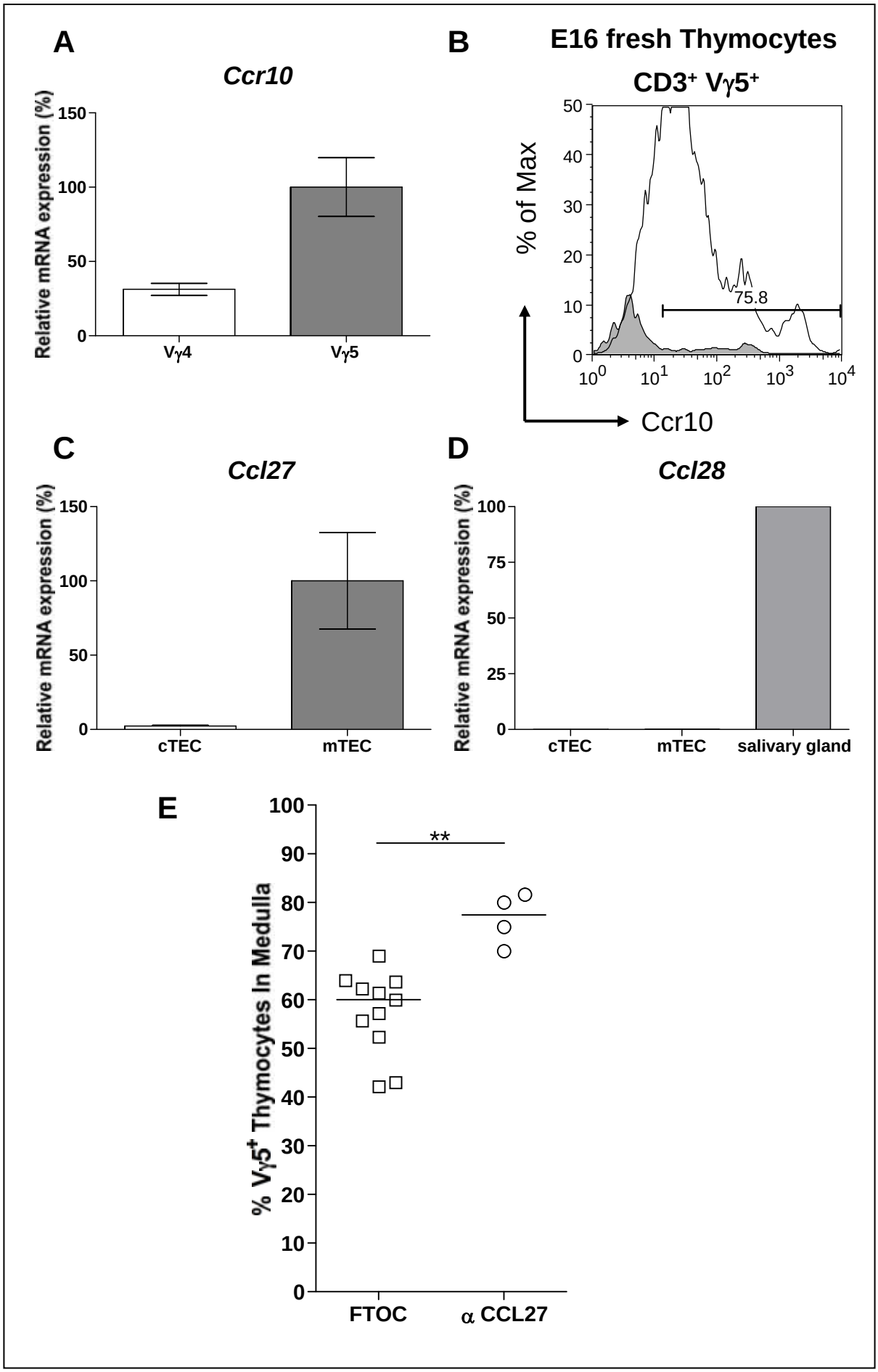
A
Ccr10
Relative mRNA expression (%)
150
100
50
0
Vγ4
Vγ5
B
E16 fresh Thymocytes
CD3+ Vγ5+
% of Max
50
40
30
20
10
0
75.8
10^0
10^1
10^2
10^3
10^4
Ccr10
C
Ccl27
Relative mRNA expression (%)
150
100
50
0
cTEC
mTEC
D
Ccl28
Relative mRNA expression (%)
100
75
50
25
0
cTEC
mTEC
salivary gland
E
% Vγ5+ Thymocytes In Medulla
100
90
80
70
60
50
40
30
20
10
0
**
FTOC
α CCL27

revealed that *Ccl27* was preferentially expressed within the mTEC compartment when compared to cTEC (Figure 3.9C). In contrast, *Ccl28* was not expressed in either the cortical or the medullary thymic epithelium, as shown in comparison to the salivary gland, known to abundantly express Ccl28 (Pan et al., 2000) (Figure 3.9D). Collectively these data suggest that Ccr10 could be involved in Vγ5$^+$ thymocyte migration and association with the medulla.

To gain a better understanding of the role of Ccr10 – Ccl27 signalling in the migration and retention of Vγ5$^+$ thymocytes to the medulla, an assay was performed where this interaction was blocked by the addition of an anti Ccl27 blocking antibody (20μg/ml) to the culture medium of WT E15 thymus lobes for 2 days. The thymic lobes were subsequently prepared for confocal analysis and frozen sections stained for Vγ5, EpCam and CD8. The number of Vγ5$^+$ thymocytes within the medulla was expressed as a percentage of the total number of Vγ5$^+$ thymocytes, which did not reveal a reduction in the number of Vγ5$^+$ T cells residing within the medulla when compared to none treated FTOC control (Figure 3.9E).

3.3.7 Ccr7 Is Involved In The Association Of Vγ5$^+$ Thymocytes With mTECs

A second chemokine – chemokine ligand pair also considered was Ccr7 as it has previously been implicated in the medullary migration and retention of SP αβ thymocytes to the medulla (Ehrlich et al., 2009; Kurobe et al., 2006; Nitta et al., 2009). To determine whether this mechanism was additionally involved during fetal γδ thymocyte development, mRNA was prepared from Vγ5$^+$ and Vγ4$^+$ thymocyte populations enriched by immunomagnetic bead separation (as described in section 3.2.8) from WT E15 7 day FTOCs. *Ccr7* expression was measured via RT-PCR, which revealed that both γδ T cell populations express *Ccr7* when compared to adult DP (CD4$^+$CD8$^+$) thymocytes isolated by MoFlo cell sorting (Figure 3.10A). Importantly flow cytometric analysis illustrated that the mRNA expression of *Ccr7* translated to

Figure 3.10 Does Ccr7 Have A Role In Vγ5$^+$ Medullary Localisation?

mRNA was prepared from Vγ5$^+$ and Vγ4$^+$ thymocyte populations isolated from E15 WT 7 day FTOC by immunomagnetic bead separation. *Ccr7* expression was analysed by quantitative RT-PCR. Note *Ccr7* expression in both Vγ5$^+$ and Vγ4$^+$ thymocytes as compared to DP thymocytes isolated from adult WT thymus (3.10A). Relative gene expression was normalised to β-actin. PCRs were carried out in triplicate. Error bars indicate the standard error of the mean. Data is representative of at least two distinct independent isolation experiments.

Total thymocytes were obtained from freshly isolated WT E16 thymus. Cell-surface Ccr7 detection (solid lines) and control staining (shaded lines) were examined on the CD3$^+$ Vγ5$^+$ population (3.10B). Data is representative of at least three experiments.

Immature (Ly51$^-$EpCam1$^+$CD80$^-$) and mature (Ly51$^-$EpCam1$^+$CD80$^+$) medullary epithelial cell populations were isolated by MoFlo cell sorting stromal cells prepared from enzymatically digested E15 WT 7 day FTOC. The epithelial populations were processed for mRNA and quantitative RT-PCR carried out for *Ccl21* and *Ccl19* gene expression (3.10C and D). Relative gene expression was normalised to β-actin. Note *Ccl21* expression in immature medullary thymic epithelium and the expression of *Ccl19* in both the immature and mature medullary thymic epithelium. PCRs were carried out in triplicate. Error bars indicate the standard error of the mean. Data is representative of at least two distinct independent sorting experiments.

A

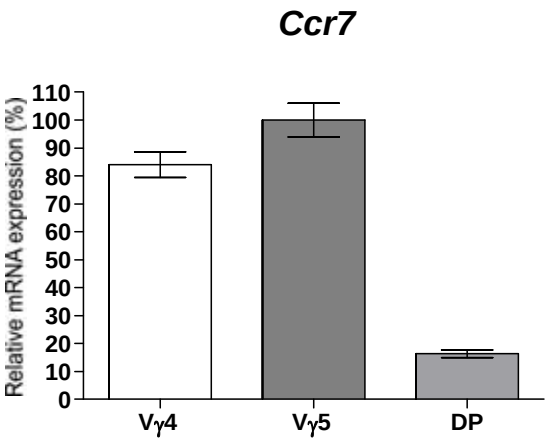

B

E17 Fresh Thymocytes

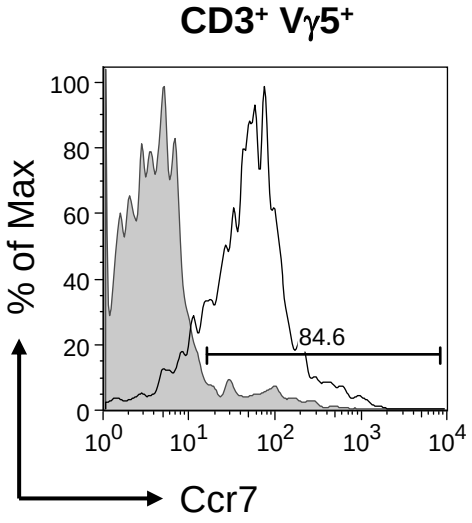

C

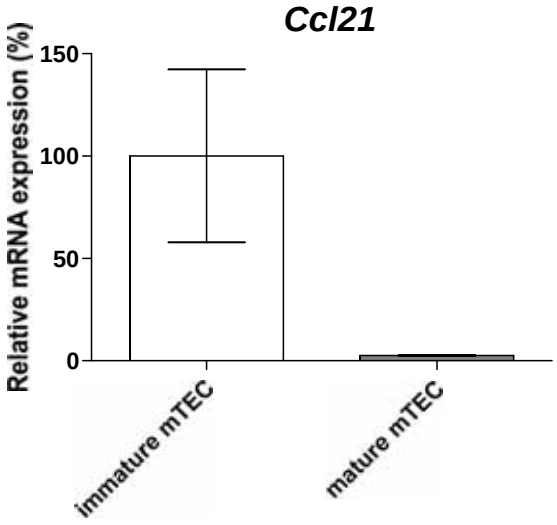

D

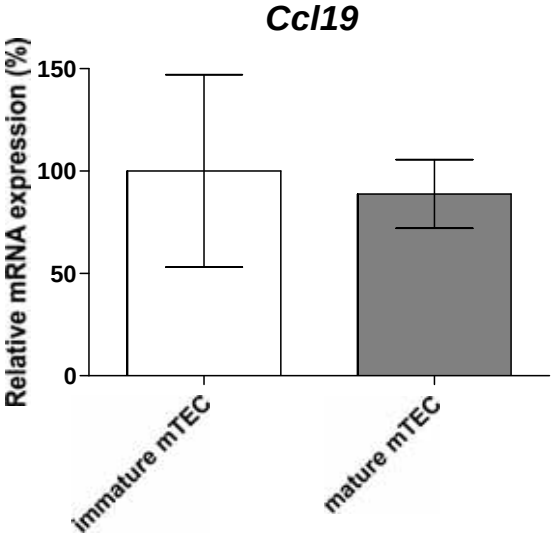

cell surface expression as approximately 85% of the $CD3^+$ $V\gamma5^+$ thymocyte population express Ccr7. Thymocyte suspensions were prepared from freshly isolated WT E17 fetal thymus lobes, stained for CD3, Vγ5 and Ccr7 (Figure 3.10B).

To further corroborate the involvement of Ccr7 in the migration of $V\gamma5^+$ thymocytes to the medulla, and to test the hypothesis that $V\gamma5^+$ thymocytes provide a Rankl mediated maturation signal to mTEC progenitors, *Ccl21* and *Ccl19* expression within immature and mature medullary thymic epithelial compartments was analysed by RT-PCR. To address this directly, purified $Ly51^-EpCam1^+CD80^-$ immature mTECs and $Ly51^-EpCam1^+CD80^+$ mature mTEC populations were isolated from WT E15 7 day FTOCs by MoFlo cell sorting. Interestingly *Ccl21* showed a preferential expression within the immature ($CD80^-$) mTEC population when compared to the mature ($CD80^+$) (Figure 3.10C). In contrast, *Ccl19* expression was detected at comparable levels within both the immature and mature mTEC populations (Figure 3.10D). Together these data suggest that an interaction between Ccr7 and Ccl21 may bring the developing $V\gamma5^+$ thymocytes into contact with immature mTECs where they are able to provide mTECs precursors with Rankl.

To test this the involvement of Ccr7 on the localisation of $V\gamma5^+$ thymocytes to the medulla and the maturation of medullary thymic epithelium, mutant and knockout mice were utilised. *Plt* mice have a spontaneous mutation that has lead to the absence of one out of three Ccl21 genes missing and the second Ccr7 ligand, Ccl19 missing. Only two of the Ccl21 genes are true genes, the third is a pseudogene. The missing gene is the functional gene normally expressed in lymphoid organs, leaving only the expression of Ccl21 in peripheral lymphatic endothelium (Nakano and Gunn, 2001; Vassileva et al., 1999). Therefore, the distribution of $V\gamma5^+$ thymocytes throughout the E17 fetal thymus of Ccr7 knockout (*Ccr7*$^{-/-}$) and *Plt* mice was analysed by confocal quantitation. Confocal images of entire sections were taken of at least 5

sections taken at different depths from three separate thymuses. The numbers of Vγ5$^+$ thymocytes within the medulla or the cortex were expressed as a percentage of the total number of Vγ5$^+$ thymocytes (Figure 3.11B-D). Representative confocal pictures of E17 WT and *Ccr7*$^{-/-}$ thymus illustrate preferential localisation of Vγ5$^+$ thymocytes to the medulla as compared to the cortex in the WT thymus. In contrast the medulla of the E17 *Ccr7*$^{-/-}$ thymus appears to be devoid of Vγ5$^+$ thymocytes (Figure 3.11A), this difference was found to be statistically significant (Figure 3.11B). Accordingly, Vγ5$^+$ thymocytes in *Ccr7*$^{-/-}$ E17 thymus associated preferentially with the cortex to a significant degree, this was also observed in the *Plt* thymus (Figure 3.11C and D). Additionally when the percentage of Vγ5$^+$ thymocytes within the medulla of *Ccr7*$^{-/-}$ and *Plt* thymus were compared to the proportion observed within E17 WT medulla a significant reduction was observed (Figure 3.11E-F). However, when total Vγ5$^+$ thymocyte numbers were analysed a reduction was not observed, suggesting the decrease in medullary localisation is not due to a decrease in γδ thymocyte numbers (Figure 3.11G). Together these data suggest that signalling through Ccr7 may be implicated in the medullary localisation of Vγ5$^+$ thymocytes.

As the absence of Ccr7 appears to reduce the medullary localisation of Vγ5$^+$ thymocytes, it was of interest to establish if this in turn, was effecting medullary epithelial maturation. Consequently, the number of Aire$^+$ mTECs within E17 *Ccr7*$^{-/-}$ thymus was analysed by flow cytometry and compared to WT E17 thymus. Freshly isolated thymus lobes were enzymatically disaggregated, stained for CD45, Ly51, EpCam and Aire and careful analysis did not reveal a difference in the percentage of Aire$^+$ mTECs in WT or *Ccr7*$^{-/-}$ thymus (Figure 3.11H). In addition the absolute cell number of Aire$^+$ mTECs was unexpectedly unaltered compared to WT E17 thymus (Figure 3.11I). Together these data suggest that Aire$^+$ mTEC development does not absolutely depend upon Ccr7 mediated migration of Vγ5$^+$ thymocytes.

Figure 3.11 The Absence Of Ccr7 Or Its Ligands Affects Vγ5$^+$ Medullary Localisation

Frozen tissues sections of E17 thymus from wild type (WT), *Ccr7*$^{-/-}$ and *Plt* mice were stained for EpCam, CD8 and Vγ5 (3.11A). Note medullary accumulation of the Vγ5$^+$ subset in WT thymus and absence of this accumulation in *Ccr7*$^{-/-}$ thymus. Scale bar, 50μm. Solid line denotes the corticomedullary junction. C, cortex, M, medulla.

The percentage of Vγ5$^+$ thymocytes within the cortex and medulla was calculated by counting the number of Vγ5$^+$ thymocytes in tile images. Tile scans were taken of at least 5 sections from varying depths through 3 individual thymuses for WT, *Ccr7*$^{-/-}$, *Plt* E17 thymus. Each point denotes a single image, bars represent median. Mann Whitney nonparametric two tailed statistical test was completed (3.11B-D) ***$p < 0.0001$. The percentage of Vγ5$^+$ thymocytes in the medulla of *Ccr7*$^{-/-}$ and *Plt* E17 thymus was compared to WT (3.11E and F), ***$p < 0.0001$. Total Vγ5$^+$ thymocyte numbers revealed a significant increase in *Ccr7*$^{-/-}$ as compared to WT **$p = 0.0012$ (3.11G).

Freshly isolated E17 thymus from WT and *Ccr7*$^{-/-}$ were enzymatically digested, and analysed by flow cytometry for CD45, Ly51, EpCam and Aire. Aire expression in CD45$^-$ Ly51$^-$ thymic epithelium is shown (3.11H). Percentages of cells within gated areas are indicated. The absolute cell numbers of Aire$^+$ mTECs within each individual thymic lobe from each mouse strain are depicted (3.11I). The bar represents the median. Mann Whitney nonparametric two tailed statistical test was completed ns = not significant. Data is representative of at least three experiments.

Total thymocytes from E17 WT and *Ccr7*$^{-/-}$ thymus were analysed by flow cytometry for CD45RB and Vγ5 (3.11J). The absolute cell numbers of immature (CD45RB^{lo}) and mature (CD45$^+$) Vγ5$^+$ thymocytes were calculated (3.11K). Each point represents a single embryo. The median is shown.

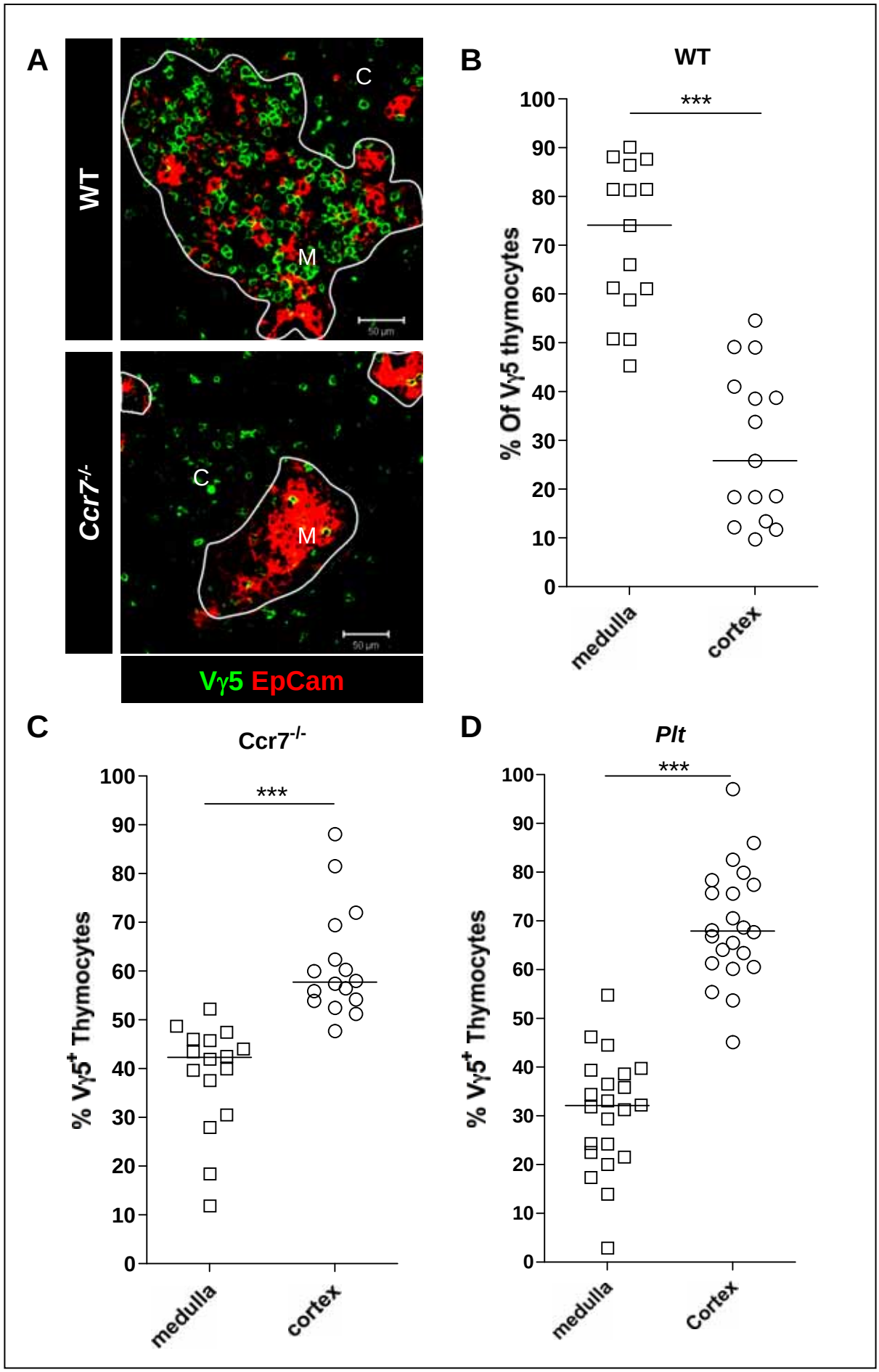
A
WT
Ccr7-/-
C
M
C
M
50 µm
50 µm
Vγ5 EpCam
B
WT
***
% Of Vγ5 thymocytes
100
90
80
70
60
50
40
30
20
10
0
medulla
cortex
C
Ccr7-/-
***
% Vγ5+ Thymocytes
100
90
80
70
60
50
40
30
20
10
0
medulla
cortex
D
Plt
***
% Vγ5+ Thymocytes
100
90
80
70
60
50
40
30
20
10
0
medulla
Cortex

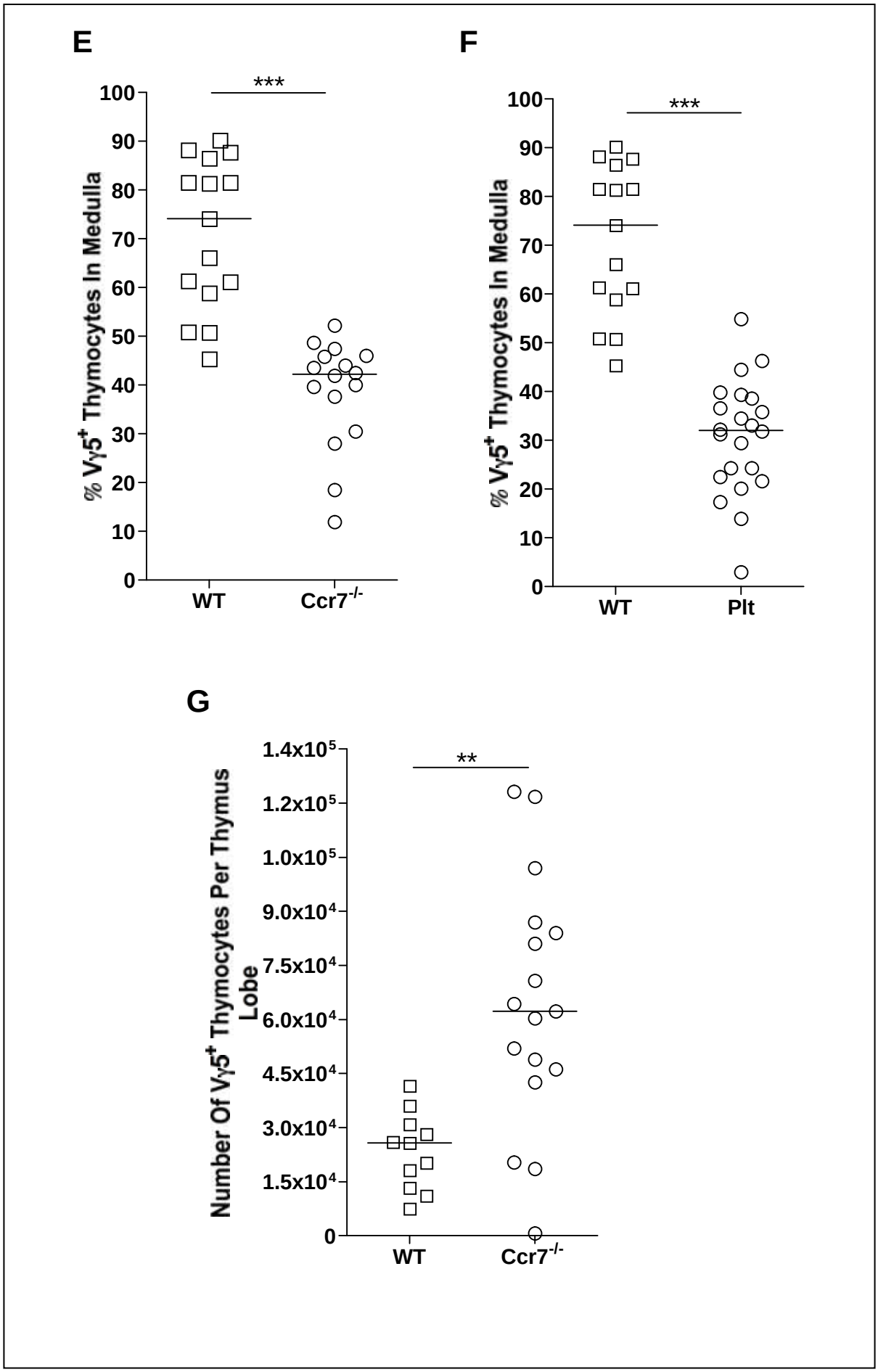
E
***
100
90
80
70
60
50
40
30
20
10
0
% Vγ5+ Thymocytes In Medulla
WT
Ccr7-/-
F
***
100
90
80
70
60
50
40
30
20
10
0
% Vγ5+ Thymocytes In Medulla
WT
Plt
G
**
1.4x10^5
1.2x10^5
1.0x10^5
9.0x10^4
7.5x10^4
6.0x10^4
4.5x10^4
3.0x10^4
1.5x10^4
0
Number Of Vγ5+ Thymocytes Per Thymus Lobe
WT
Ccr7-/-

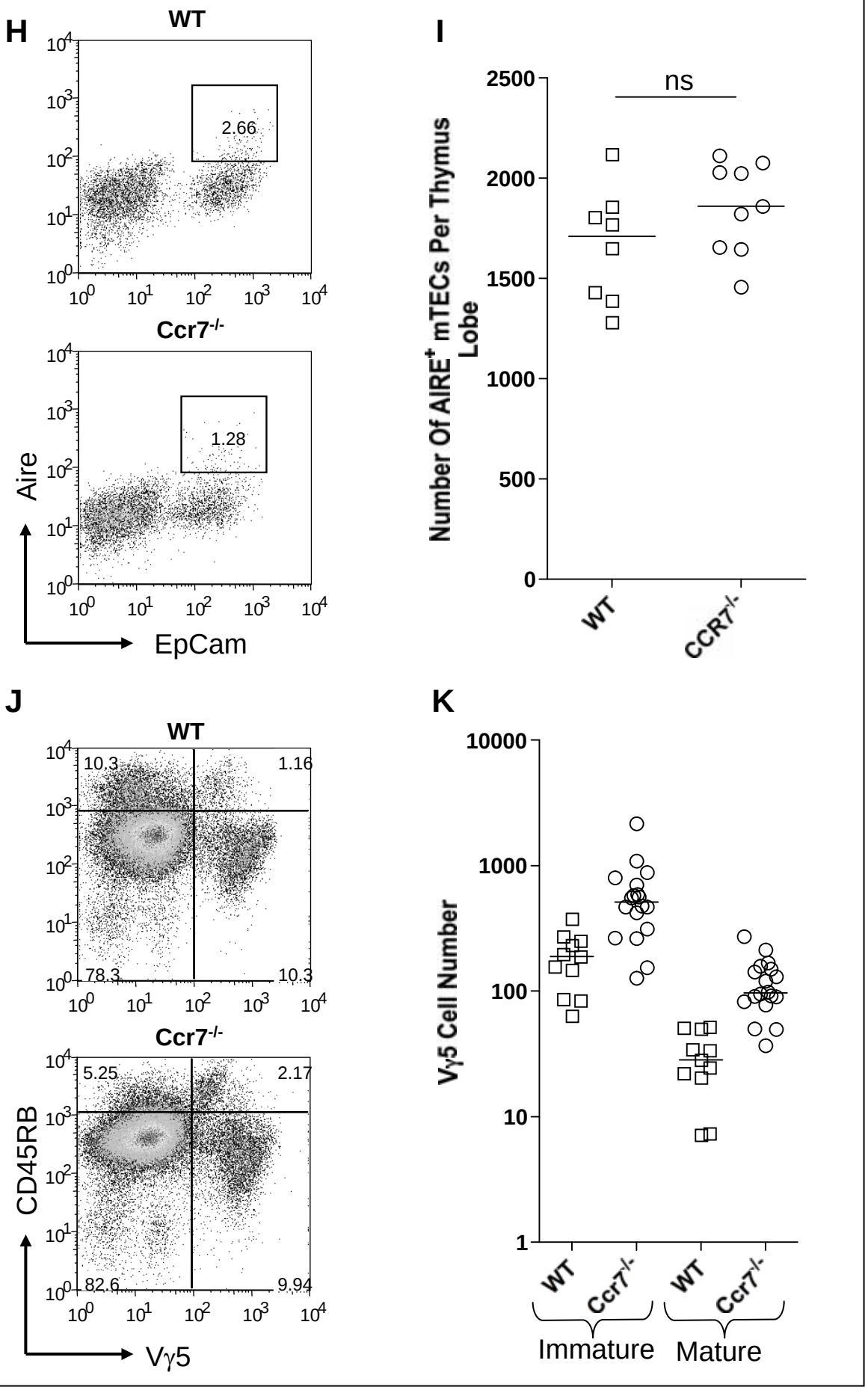
H
WT
2.66
Ccr7-/-
1.28
Aire
EpCam
I
ns
Number Of AIRE+ mTECs Per Thymus Lobe
2500
2000
1500
1000
500
0
WT
CCR7-/-
J
WT
10.3
1.16
78.3
10.3
Ccr7-/-
5.25
2.17
82.6
9.94
CD45RB
Vγ5
K
Vγ5 Cell Number
10000
1000
100
10
1
WT
Ccr7-/-
WT
Ccr7-/-
Immature
Mature

The above data indicated that Vγ5$^+$ thymocyte medullary accumulation was reduced in *Ccr7*$^{-/-}$ thymus in relation to WT thymus. Taken together with a recent report suggesting that SP αβ thymocyte retention, but not entry, into the medulla requires Ccr7 (Ehrlich et al., 2009), may suggest that *Ccr7*$^{-/-}$ immature Vγ5$^+$ thymocytes do not inhabit the medulla for sufficient time to receive the required maturation signals. This prediction was tested by analysing the expression of CD45RB on Vγ5$^+$ thymocytes isolated from E15 WT and *Ccr7*$^{-/-}$ thymus cultured for 5 days with or without PTX. Careful examination revealed a similar trend in Vγ5$^+$ thymocyte maturation between WT and *Ccr7*$^{-/-}$ thymocytes, a greater number of immature (CD45RB^{lo}) thymocytes are observed when compared to mature (CD45RB^{hi}) thymocytes (Figure 3.11K) suggesting that maturation of the Vγ5$^+$ thymocytes in the absence of Ccr7 is normal.

3.3.8 Thymic Crosstalk Occurs Between Vγ5$^+$ Thymocytes And mTEC Progenitors

Two recent reports have suggested that the developing Vγ5$^+$ thymocyte population undergoes a positive selection event similar to that observed for αβ T cell development. Intriguingly, one report suggested that this selection event was carried out by a thymic stromal determinant, and the second report proposed that a prototypic member of a newly identified immunoglobulin superfamily gene cluster *Skint1* (Selection and upkeep of intraepithelial T cells 1) was the selection determinant (Boyden et al., 2008; Lewis et al., 2006). To gain a better understanding, the thymic stromal cell compartment expressing *Skint1* and the mechanism involved in *Skint1* upregulation were investigated. Stromal cell suspensions were prepared from fresh E15 WT thymus by enzymatic disaggregation and subsequent depletion of CD45$^+$ haematopoietic cells via an immunomagnetic separation technique described in section 3.2.8. Also using Dynal beads, populations of CD205$^+$ (cTEC) and CD40$^+$ (mTEC) cells were positively selected. These cells were then processed for mRNA and quantitative RT-PCR for

Skint1 expression. *Skint1* was abundantly expressed in medullary thymic epithelial cells and undetectable in the cortical epithelial cells (Figure 3.12B). Importantly, *Aire* expression was observed in mTEC and not in cTEC as expected (Figure 3.12A). To establish whether immature or mature mTECs expressed *Skint1*, RT-PCR was completed on purified $Ly51^{-}EpCam1^{+}CD80^{-}$ immature mTECs and $Ly51^{-}EpCam1^{+}CD80^{+}$ mature mTEC populations isolated from WT E15 7 day FTOCs by MoFlo cell sorting. *Skint1* transcripts were found exclusively within the mature ($CD80^{+}$) mTEC population (Figure 3.12C).

Given that $V\gamma5^{+}$ thymocytes express Rankl, preferentially interact with immature mTECs and have the functional capacity to drive mTEC maturation, together with the observation that mature mTEC specifically express *Skint1*, lead to the hypothesis that *Skint1* expression was dependent on Rank-Rankl signalling. This was addressed by stimulating E15 WT thymus lobes, depleted of haematopoietic cells by incubation in dGuo, artificially with an anti-Rank agonist antibody, known to induce the development of $Aire^{+}$ mTECs (Figure 3.12D) (Jenkinson et al., 2008; Rossi et al., 2007b). dGuo treated FTOCs without stimulation with anti-Rank agonist antibody were used as controls. Stromal cell suspensions were generated from these by enzymatic disaggregation, which were processed for mRNA and quantitative RT-PCR for *Skint1* and *Aire* expression completed. The pattern of *Skint1* gene expression was the same as that observed for *Aire*, transcripts were identified within the anti-Rank stimulated thymus lobes only (Figure 3.12D and E). Together these data suggest *Skint1* expression may be regulated in a similar manner to *Aire*, involving signalling through the TNF receptor Rank. This supports the idea that reciprocal signalling between the developing $V\gamma5^{+}$ thymocytes and the medullary thymic epithelium is occurring, where both signals are required for the development of each cell type respectively.

Figure 3.12 Does Reciprocal Signalling Occur Between Vγ5$^+$ Thymocytes And mTEC Progenitors?

Quantitative RT-PCR analysis of *Aire* and *Skint1* expression, normalised to the housekeeping gene β-actin, was carried out on cTEC (CD40$^+$CD205$^-$) and mTEC (CD205$^+$CD40$^-$) isolated by immunomagnetic separation from E15 WT thymus lobes cultured for 7 days. Note *Aire* and *Skint1* expression within medullary epithelium specifically (3.12A and B).

Skint1 expression was analysed RT-PCR in Ly51$^-$EpCam1$^+$CD80$^-$ immature mTECs and Ly51$^-$EpCam1$^+$CD80$^+$ mature mTEC populations purified from WT E15 7 day FTOCs by MoFlo cell sorting. *Skint1* transcripts were found exclusively within the mature mTEC population (3.12C).

Quantitative RT-PCR analysis of *Aire* and *Skint1* expression, was carried out on dGuo FTOC (white bars) and dGuo FTOC treated with anti Rank (grey bars) (3.12D and E). Note that *Aire* and *Skint1* expression in anti Rank treated dGuo FTOC.

PCRs were carried out in triplicate. Error bars indicate the standard error of the mean. Data is representative of at least two distinct independent sorting experiments.

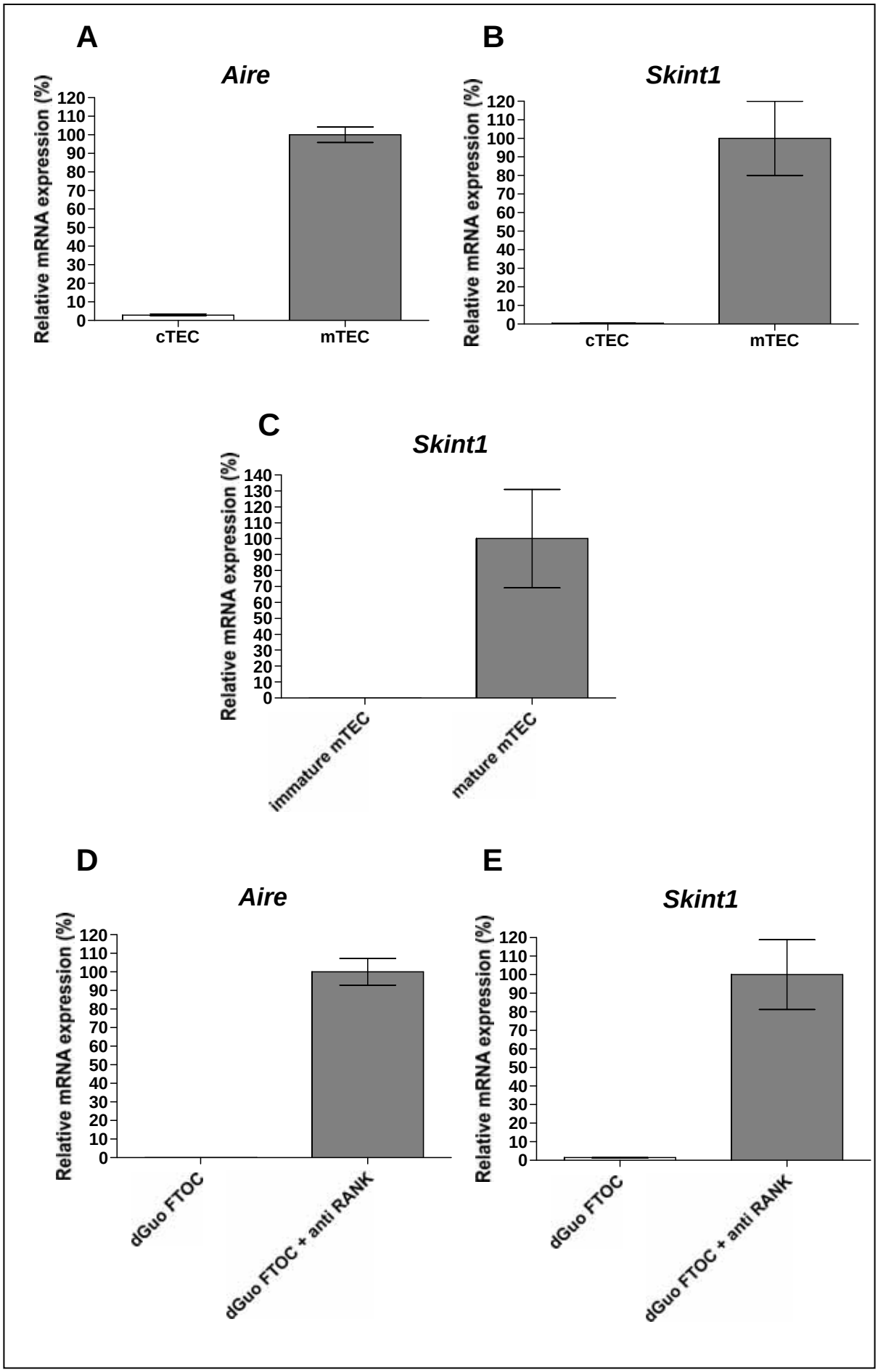
A
Aire
Relative mRNA expression (%)
120
110
100
90
80
70
60
50
40
30
20
10
0
cTEC
mTEC
B
Skint1
Relative mRNA expression (%)
120
110
100
90
80
70
60
50
40
30
20
10
0
cTEC
mTEC
C
Skint1
Relative mRNA expression (%)
140
130
120
110
100
90
80
70
60
50
40
30
20
10
0
immature mTEC
mature mTEC
D
Aire
Relative mRNA expression (%)
120
110
100
90
80
70
60
50
40
30
20
10
0
dGuo FTOC
dGuo FTOC + anti RANK
E
Skint1
Relative mRNA expression (%)
120
110
100
90
80
70
60
50
40
30
20
10
0
dGuo FTOC
dGuo FTOC + anti RANK

3.3.9 Does An Absence Of *Skint1* Affect The Medullary Association Of Vγ5$^+$ Thymocytes?

A naturally occurring *Skint1* deficient mouse strain was identified due to its loss of Vγ5$^+$ DETC. The specific loss of this cell type was identified as being due to a failure in thymic selection; this helped identify *Skint1* as a selection determinant for Vγ5$^+$ thymocytes (Boyden et al., 2008). The *Skint1* deficient mouse is an FVB/N mouse from Taconic Farms (FVB tac); the Taconic Farms colony had 30 generations between the last common ancestor at The Jackson Laboratory (FVB jax (WT)) and within this time had acquired a single point mutation that created a premature stop codon in the *Skint1* gene, resulting in a non functional truncated protein (Boyden et al., 2008).

Whilst the preferential expression of *Skint1* by mature medullary epithelium and the involvement of Rank signaling in regulating *Skint1* expression was established, it motivated investigation into whether a lack of *Skint1* expression effected the medullary localisation of Vγ5$^+$ thymocytes. To investigate this E17 thymus lobes were isolated from *Skint1* deficient "FVB tac" and WT mice and prepared for confocal microscopy. Frozen sections were stained for Vγ5 and EpCam and confocal images of entire sections were taken of at least 5 sections taken at different depths from three separate thymuses. Representative confocal pictures of E17 WT and "FVB tac" thymus illustrate preferential localisation of Vγ5$^+$ thymocytes to the medulla in the WT thymus and the absence of this medullary localisation in the "FVB tac" thymus (Figure 3.13A). Numbers of Vγ5$^+$ thymocytes within the thymus were quantitated and expressed as a percentage of the number of Vγ5$^+$ thymocytes within the medulla or cortex, which revealed the medullary prevalence of Vγ5$^+$ thymocytes in the WT thymus to be statistically significant (Figure 3.13B and C). In contrast, statistically more Vγ5$^+$ thymocytes in "FVB tac" thymus preferentially localised to the cortex (Figure 3.13C) and thus the proportion of Vγ5$^+$ thymocytes within the

Figure 3.13 Absence Of *Skint1* Expression Reduces Vγ5$^+$ thymocyte Medullary Accumulation

Frozen tissues sections prepared from E17 WT, and *Skint1* deficient "FVB tac" mouse thymuses were stained for EpCam and Vγ5 (3.13A). Note the medullary accumulation of the Vγ5$^+$ subset in the WT thymus and the absence of this accumulation in the "FVB tac" thymus. Scale bar, 50μm. Solid line denotes the corticomedullary junction. C, cortex, M, medulla.

The percentage of Vγ5$^+$ thymocytes was calculated from the number of Vγ5$^+$ thymocytes within each region. Counts were taken from whole section images taken of at least 5 sections from varying depths through 3 individual thymuses for WT, and "FVB tac" E17 thymus. Each point denotes a single image. Bars represent the median. Mann Whitney nonparametric two tailed statistical test was completed to compare the percentage of Vγ5$^+$ thymocytes within the cortex to the percentage within the medulla. WT (3.13B) $p = < 0.0001$, "FVB tac" (3.13C) $p = < 0.0001$. The medullary proportions of Vγ5$^+$ thymocytes in "FVB tac" E17 thymus were compared to the proportion of Vγ5$^+$ thymocytes in the medulla of WT E17 thymus (3.13D), $p = < 0.0001$.

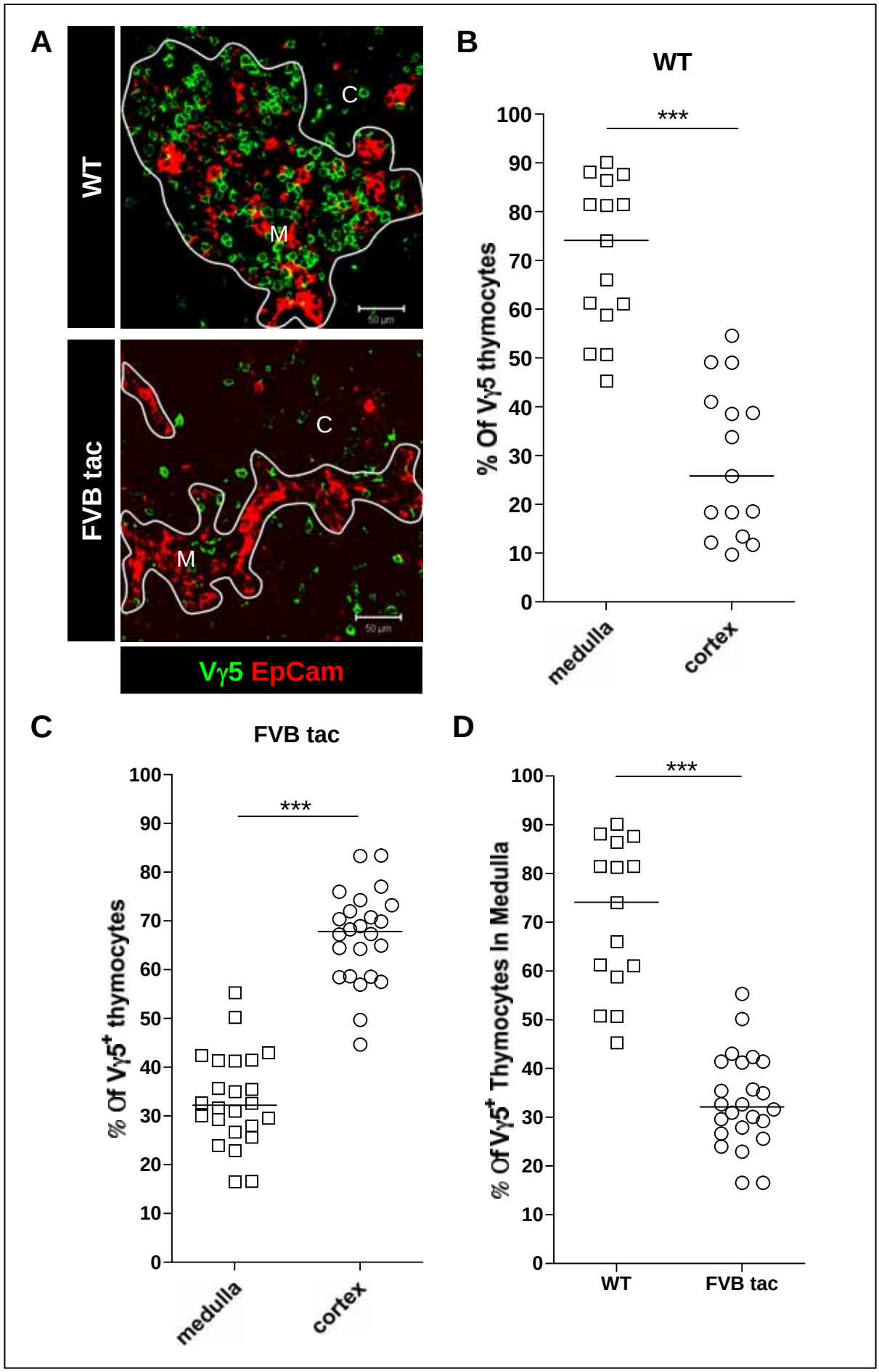
A
WT
C
M
50 µm
FVB tac
C
M
50 µm
Vγ5 EpCam
B
WT
***
% Of Vγ5 thymocytes
100
90
80
70
60
50
40
30
20
10
0
medulla
cortex
C
FVB tac
***
% Of Vγ5+ thymocytes
100
90
80
70
60
50
40
30
20
10
0
medulla
cortex
D
***
% Of Vγ5+ Thymocytes In Medulla
100
90
80
70
60
50
40
30
20
10
0
WT
FVB tac

medulla of the "FVB tac" thymus was significantly reduced when compared WT (Figure 3.13D). Together these data suggest that in the absence of an influence of positive selection, $V\gamma5^+$ thymocytes do not colonise the thymic medulla.

3.3.10 Does An Absence Of Rank Effect The Medullary Localisation Of $V\gamma5^+$ Thymocytes?

Having recognised that the regulation of *Skint1* expression appears to involve Rank signalling the effect of an absence of Rank on *Skint1* expression was examined. In addition the consequence of Rank deficiency on $V\gamma5^+$ thymocyte development and distribution within the thymus was investigated. To identify whether $Rank^{-/-}$ thymic stroma expresses *Skint1*, RT-PCR for *Skint1* was completed on $Rank^{+/-}$ and $Rank^{-/-}$ total thymic stroma isolated from E15 thymus, organ cultured for 7 days, by depletion of the $CD45^+$ haematopoietic cell population (Figure 3.14B). *Aire* expression is completely dependent on Rank signalling, it therefore provided a representative expression profile for that expected for *Skint1* expression if it too required Rank signalling. *Aire* expression was found to be completely absent from the $Rank^{-/-}$ stroma, and in contrast was detectable in $Rank^{+/-}$ littermate control (Figure 3.14A). *Skint1* expression displayed a similar expression profile in comparison to *Aire* however, $Rank^{-/-}$ stroma despite a marked reduction demonstrated a detectable *Skint1* levels, implicating the involvement of an additional mechanism in the regulation of *Skint1* expression (Figure 3.14B).

To determine the effect of a marked reduction in *Skint1* expression on the development of $V\gamma5^+$ thymocytes, the upregulation of a maturation marker CD45RB on $V\gamma5^+$ thymocytes derived from WT and $Rank^{-/-}$ E15 thymus organ cultured for 5 days, was analysed by flow cytometry. Careful examination illustrated that despite a reduced percentage of total $V\gamma5^+$ thymocytes in the $Rank^{-/-}$ thymus a similar percentage upregulated CD45RB when compared to WT, indicated by a 2:1 ratio on average of immature ($CD45RB^{lo}$) to mature ($CD45RB^{hi}$) in both mouse strains

Figure 3.14 Rank Deficiency Effects Medullary Localisation Of Vγ5$^+$ Thymocytes And Their Development

Quantitative RT-PCR of *Aire* and *Skint1*, normalised to the housekeeping gene β-*actin*, was carried out on thymic stromal cells enriched from E15 7 day FTOC of *Rank*$^{+/-}$ and *Rank*$^{-/-}$ thymus (3.14A and B). Note the absence of *Aire* and a marked reduction of *Skint1* expression in *Rank*$^{-/-}$ stroma and high expression levels in *Rank*$^{+/-}$. PCRs were carried out in triplicate. Error bars indicate the standard error of the mean. Data is representative of at least two distinct independent sorting experiments.

Thymocyte suspensions were prepared from 5 day E15 *Rank*$^{+/-}$ and *Rank*$^{-/-}$ FTOC and stained for Vγ5 and CD45RB and analysed by flow cytometry. Percentage of Vγ5$^+$ thymocytes in *Rank*$^{-/-}$ as compared to WT is exhibited (3.14C). Percentages of cells within gated areas are indicated. Cell numbers of immature and mature Vγ5$^+$ thymocytes are illustrated (3.14D) **p = 0.0070, ns = not significant p = 0.2168. Total Vγ5$^+$ thymocyte numbers were calculated in E15 WT and Rank$^{-/-}$ 5 day FTOC (3.14E) p = 0.1608.

Frozen tissues sections prepared from E17 *Rank*$^{+/-}$ and *Rank* $^{-/-}$ mouse thymus were stained for EpCam and Vγ5 (3.14E). Note medullary accumulation of Vγ5$^+$ thymocyte subset in the WT thymus and the absence of this in the *Rank* $^{-/-}$ thymus. Scale bar, 50μm. Solid line denotes the corticomedullary junction. C, cortex, M, medulla.

The percentage of Vγ5$^+$ thymocytes within the cortex and medulla was calculated. Counts were taken from whole section images taken of at least 5 sections from varying depths through 3 individual thymuses for WT and *Rank* $^{-/-}$ E17 thymus. Mann Whitney nonparametric two tailed statistical test revealed a statistical difference between the proportions of Vγ5$^+$ T cells in the cortex and the medulla for each strain *** p = < 0.0001 (3.14G and H). The medullary proportions of Vγ5$^+$ thymocytes in WT and *Rank* $^{-/-}$ E17 thymus were compared (3.14I), p = < 0.0001.

Epidermal sheets were prepared from WT and *Rank* $^{-/-}$ adult ears and stained for Vγ5. Vγ5$^+$ DETCs were identified in the epidermis of both WT and *Rank* $^{-/-}$ mice (3.14J).

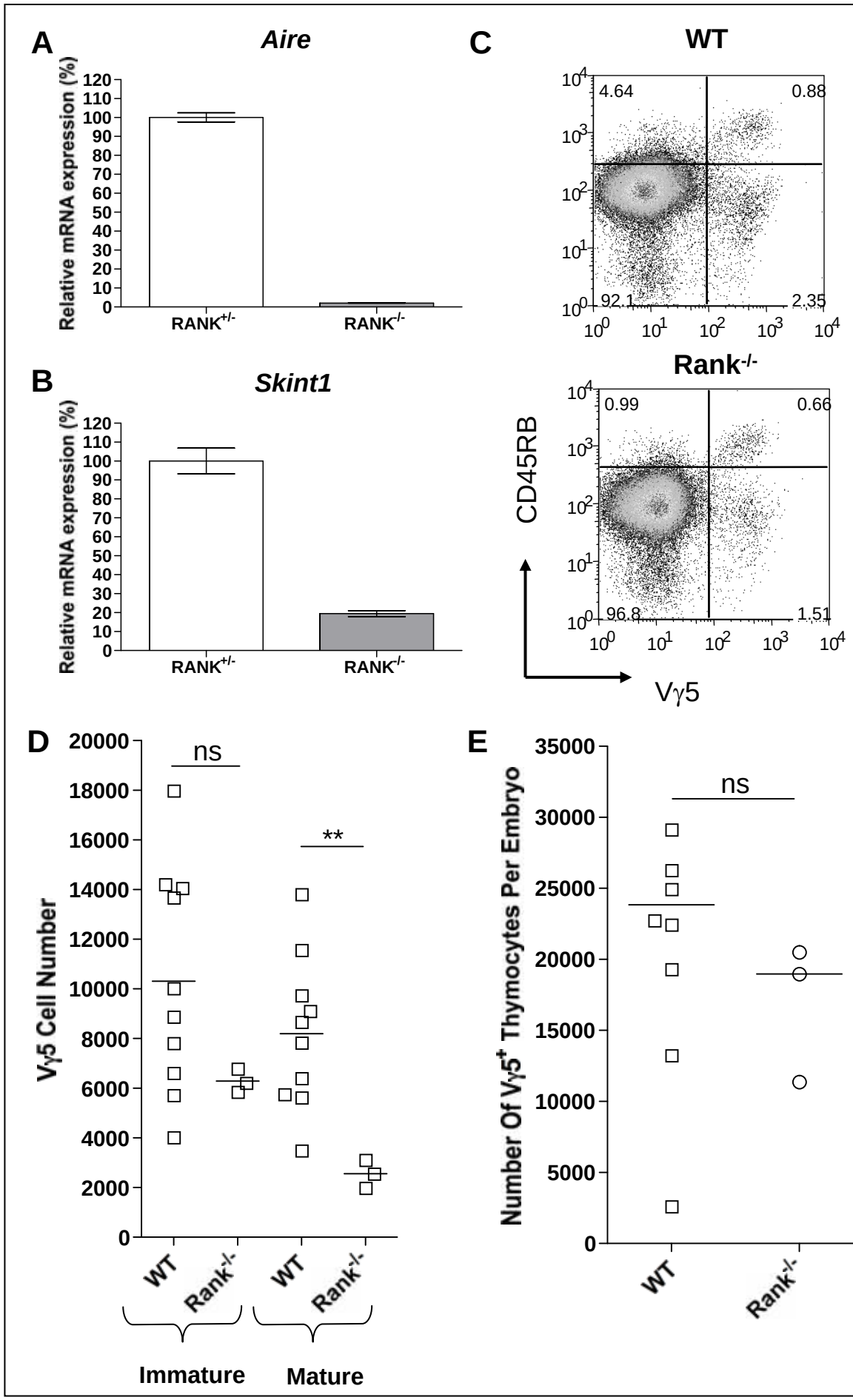
A
Aire
Relative mRNA expression (%)
RANK+/-
RANK-/-
B
Skint1
C
WT
4.64
0.88
92.1
2.35
Rank-/-
0.99
0.66
96.8
1.51
CD45RB
Vγ5
D
Vγ5 Cell Number
ns
**
WT
Rank-/-
Immature
Mature
E
Number Of Vγ5+ Thymocytes Per Embryo
ns

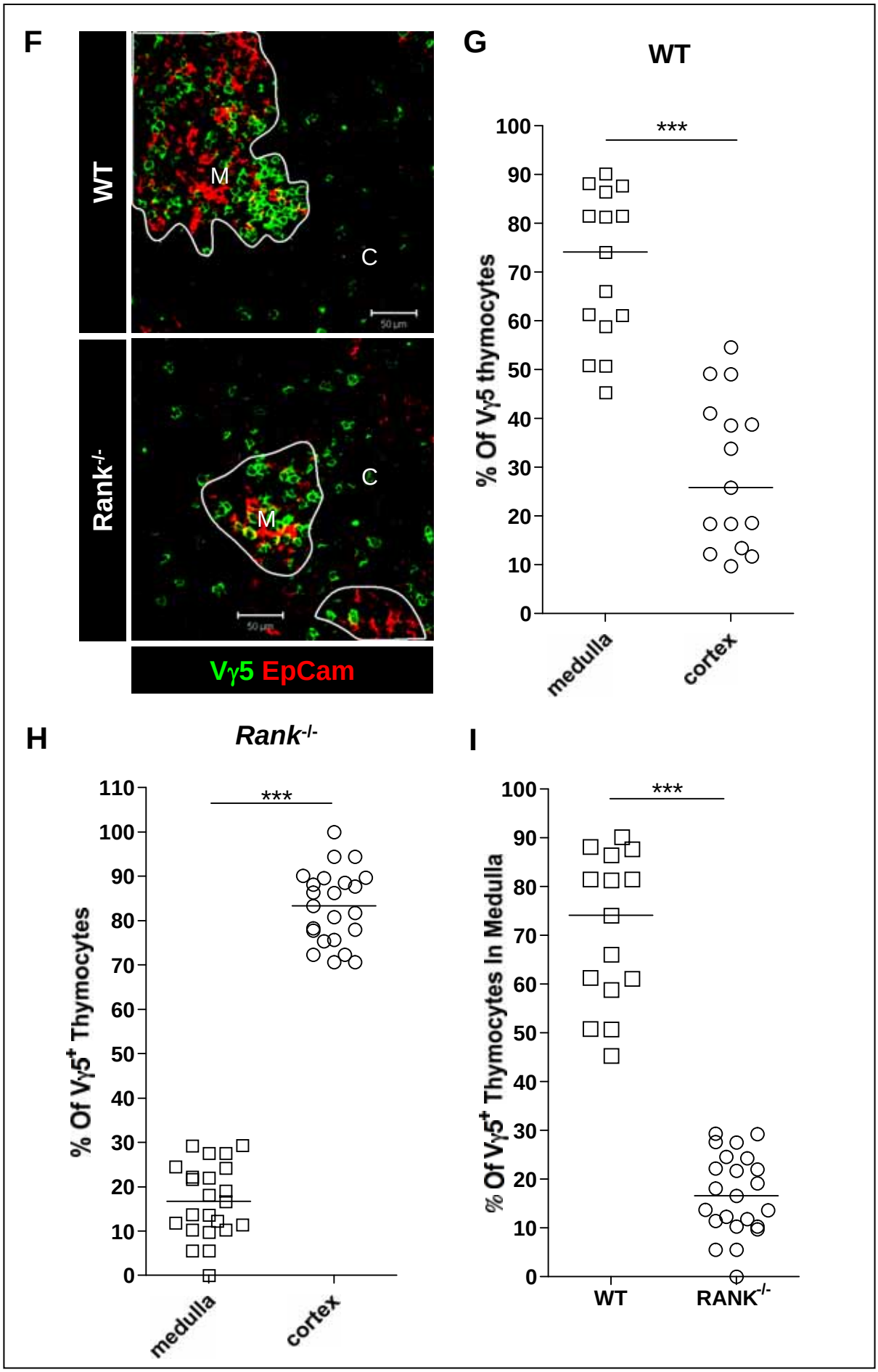
F
WT
M
C
50 µm
Rank-/-
C
M
50 µm
Vγ5 EpCam
G
WT
***
100
90
80
70
60
50
40
30
20
10
0
% Of Vγ5 thymocytes
medulla
cortex
H
Rank-/-
***
110
100
90
80
70
60
50
40
30
20
10
0
% Of Vγ5+ Thymocytes
medulla
cortex
I
***
100
90
80
70
60
50
40
30
20
10
0
% Of Vγ5+ Thymocytes In Medulla
WT
RANK-/-

J

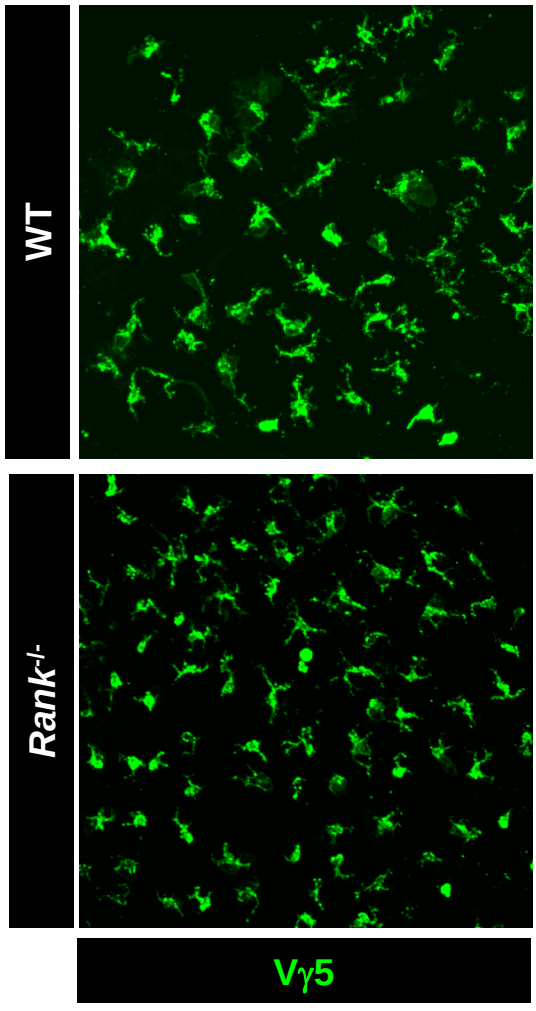

(Figure 3.14C). However, absolute cell numbers revealed a significant reduction in the number of mature Vγ5$^+$ thymocytes in the *Rank*$^{-/-}$ when compared to WT ($p = 0.007$) (3.14D) This indicated that a reduced number of Vγ5$^+$ thymocytes were able to develop when *Skint1* expression was limiting. The total number of Vγ5$^+$ thymocytes revealed a reduction in *Rank*$^{-/-}$ thymus when compared to WT, which was not found to be significant ($p = 0.1608$) (Figure 3.14E).

Additionally, the association of Vγ5$^+$ thymocytes with the thymic medulla was analysed in the *Rank*$^{-/-}$ E17 thymus. In contrast with the observation in E17 WT thymus Vγ5$^+$ thymocytes appeared to be less densely packed within medullary areas of the *Rank*$^{-/-}$ thymus, and more were readily identifiable in the cortex (Figure 3.14F). This observation was confirmed by confocal quantitation, which numerically illustrated the majority of Vγ5$^+$ thymocytes in *Rank*$^{-/-}$ E17 thymus are associated with the cortex (Figure 3.14H), the opposite to what was seen in the WT (Figure 3.14G). Furthermore, the proportion of Vγ5$^+$ thymocytes residing within the medulla of *Rank*$^{-/-}$ E17 thymus was significantly reduced when compared to WT thymus (Figure 3.14I).

To establish whether reduced *Skint1* expression levels and reduced association with the medulla effected the migration of mature Vγ5$^+$ thymocytes to the skin epidermis, epidermal sheets isolated from adult WT and *Rank*$^{-/-}$ skin were stained for Vγ5. Vγ5$^+$ thymocytes were readily identified within the epidermis of both adult WT and *Rank*$^{-/-}$ (Figure 3.14J). Together these data suggest that Vγ5$^+$ thymocytes are able to continue their development despite reduced expression levels of *Skint1* and Rank deficiency does not adversely effect Vγ5$^+$ thymocyte development.

3.4 Discussion

The development of Aire$^+$ mTECs is an essential prerequisite to the establishment of a self-tolerant T cell repertoire. Aire$^+$ mTECs derive from an immature Aire$^-$ mTEC progenitor through a process involving interactions between Rank expressed on the mTEC progenitor and Rankl provided by haematopoietic cells (Hikosaka et al., 2008; Rossi et al., 2007b). Fetal thymic epithelial cell development primarily utilises Rankl provided by lymphoid tissue inducer cells (LTi) (Rossi et al., 2007b). During adult life CD4 SP T cells can additionally provide Rankl (Hikosaka et al., 2008). Nevertheless, the provision of Rankl to enable the development of Aire$^+$ mTECs within the fetal thymus is of greater importance as demonstrated in a recent study. Guerau-de-Arellano *et al* show that Aire expression during the perinatal period is both necessary and sufficient to induce long-lasting tolerance and avoid autoimmunity (Guerau-de-Arellano et al., 2009). However, when LTi are absent from the developing fetal thymus (*Ror*$\gamma^{-/-}$), a population of Aire$^+$ mTECs can still be found, implicating the involvement of an additional cell type (Figure 3.1) (Eberl et al., 2004; White et al., 2008b). Therefore, the aim of this chapter was to identify and characterise an additional cell type that may be involved in the provision of a developmentally stimulating signal required for mTEC maturation and identify the molecular regulators of the mechanism. Based on the data presented in this chapter, a novel role for γδ T cells in medullary thymic epithelial cell development can be proposed.

It was identified that Aire expressing mTECs were first detectable at E16 of gestation, a stage prior to the appearance of mature CD4$^+$TCR^{hi} and CD8$^+$TCR^{hi} thymocytes, even in the absence of LTi (White et al., 2008b). Although, this is the first appearance of Aire$^+$ mTECs the progenitors may have been present before this stage but the signals required for their maturation only appear around E16. Consequently, this narrowed the search for a cell type that might influence embryonic Aire$^+$ mTEC development, to those that develop within the fetal thymus.

The γδ T cell lineage is first detectable at E14 and until E18 is the major TCR^+ population within the thymus (Allison and Havran, 1991; Havran and Allison, 1988). Fetal γδ thymocyte development is unique as defined subsets, characterised by specific Vγ and Vδ gene segment expression, develop in sequential waves throughout ontogeny (Komori et al., 2006). Each subset is of a restricted repertoire due to highly restricted V gene usage, preferential pairing of TCR chains and the lack of junctional diversity due to their development occurring before thymic terminal deoxynucleotidyl transferase (TdT) activation (Havran and Allison, 1988; Hayday, 2000; Houlden et al., 1988; Leclercq and Plum, 1996). In addition there is a tight correlation between TCR V gene segment usage and homing capacity to specific intraepithelial compartments. To gain an understanding as to whether γδ thymocytes were involved two subsets that develop within distinct waves were analysed, the $V\gamma5^+$ thymocytes (Haas et al., 1993) and the $V\gamma4^+$ thymocytes (Figure 3.3B) (Allison and Havran, 1991; Sperling et al., 1992).

$V\gamma5^+$ thymocytes are the first to emerge from the thymus, they predominate in the fetal thymus but are virtually undetectable in the adult (Allison and Havran, 1991). They express a canonical γδ TCR composed of Vγ5-Jγ1Cγ1 and Vδ1-Dδ2-Jδ2Cδ chains that together recognise the epitope 17D1 (Asarnow et al., 1988; Mallick-Wood et al., 1998; Tigelaar and Lewis, 1995; Xiong and Raulet, 2007). Mature $V\gamma5^+$ T cells reside solely within the epidermal epithelium where they have a pronounced dendritic morphology and as a result are known as dendritic epidermal T cells (DETCs); they first appear within the epidermis at days 17–19 of gestation (Havran and Allison, 1988). Within the epidermis they are thought to recognise stress-induced tissue specific antigens in the local environment where they have an important role in the first line of defence and perform innate like functions (Xiong et al., 2004).

$V\gamma4^+$ thymocytes develop during the third wave and begin to appear at around E15. They predominate in the lung and are consequently referred to as Resident Pulmonary Lymphocytes

(Allison and Havran, 1991). Vγ4$^+$ T cells prevail in the adult however their V gene usage differs from that of their fetal counterpart. Another prominent difference between the TCR of fetal and adult γδ T cells is the extensive junctional diversity where large N-nucleotide additions (random nucleotide regions) are observed (Allison and Havran, 1991).

Confocal analysis allowed the localisation of these two cell types within the fetal thymic architecture to be determined and clearly demonstrated that the Vγ5$^+$ γδ T cell subset closely associated with the embryonic thymic medulla (Figure 3.3). Furthermore this visible medullary association was confirmed by a confocal quantitation method, which corroborated earlier studies (Farr et al., 1990). Consequently, this observation lead to the prediction that the interaction between Vγ5$^+$ thymocytes and mTECs was important for mTEC maturation. Thus Vγ5$^+$ thymocyte Rankl expression was determined since Rankl plays a key role in medullary thymic epithelial development (Figure 3.4) (Hikosaka et al., 2008; Rossi et al., 2007b). Together these data validate that Vγ5$^+$ thymocytes residing in medullary islets posses the correct signalling machinery to be involved in mTEC development and are therefore capable of driving mTEC maturation. Interestingly, mature Vγ5$^+$ DETC also express *Rankl* at levels approximately 8 orders of magnitude greater than Vγ5$^+$ thymocytes (Figure 3.4B), however both express *Rankl* at reduced levels when compared to LTi, which express 30 fold more *Rankl* than Vγ5$^+$ thymocytes (Figure 3.4C). Although the PCRs for *Rankl* expression in DETC, LTi and Vγ5$^+$ thymocytes were not within the same reaction, the samples were matched with regard to their *β-actin* levels and were therefore comparable when Vγ5$^+$ thymocytes were used as the calibrator, allowing such conclusions to be drawn.

Two independent assays were performed to test the functional ability of Vγ5$^+$ thymocytes to influence Aire$^+$ mTEC development. *In vivo* analysis of mouse strains containing different combinations of haematopoietic cells were used to assess the affect of both LTi and Vγ5$^+$

thymocytes on the development of Aire^{+} mTECs (Figure 3.6). Rorγ is a regulator of LTi development, thus in its absence LTi do not develop (Eberl et al., 2004; Sun et al., 2000). The reduced frequency of Aire^{+} mTEC within the thymuses of embryonic *Rorγ*$^{-/-}$ and TCRδ$^{-/-}$ mice suggested that they both play a role in mTEC maturation. In support of this the absence of both LTi and Vγ5^{+} thymocytes (CD3ε*tgRorγ*$^{-/-}$ mice) lead to the complete absence of Aire^{+} mTECs. However, previous reports suggesting γδ thymocyte development involves either the expression of, or an interaction with Rorγ raised the issue that Vγ5^{+} thymocyte development maybe defective in these mice (Lochner et al., 2008; Silva-Santos et al., 2005). Therefore their role in the development of Aire^{+} mTECs could not be fully elucidated. To address this Vγ5^{+} thymocyte numbers, maturation and ability to home to the correct peripheral location was evaluated in Rorγ deficient mice. The modulation of cell surface marker and chemokine receptor expression enables the maturation status of γδ thymocytes to be assessed (Leclercq et al., 1993; Tatsumi et al., 1993; Xiong and Raulet, 2007). One characteristic and clear indicator of maturation is the upregulation of CD45RB. CD45RB expression revealed a 16% increase in the ratio of immature (CD45RB^{lo}) to mature (CD45RB^{hi}) Vγ5^{+} thymocytes in the *Rorγ*$^{-/-}$ Vγ5^{+} thymocyte population. The absolute numbers of immature (CD45RB^{lo}) and mature (CD45RB^{hi}) Vγ5^{+} thymocytes substantiated this observation, revealing little difference between the numbers of immature Vγ5^{+} thymocytes in WT or *Rorγ*$^{-/-}$ thymus but a significant reduction in the number of mature Vγ5^{+} thymocytes in *Rorγ*$^{-/-}$ thymus when compared to WT (Figure 3.5D). This may suggest either a lack of survival or reduced proliferation of the mature Vγ5^{+} thymocyte population and may advocate a reciprocal role for Aire^{+} mTECs in Vγ5^{+} thymocyte development. Nevertheless, Vγ5^{+} thymocytes were primarily found associated with the medulla in the *Rorγ*$^{-/-}$ E16 thymus, analogous to the observation in WT E16 thymus (Figure3.5E). DETCs primarily expand in the periphery in response to antigen recognition and keratinocyte derived IL7 and TNFα (Tigelaar &

Lewis 1994; Matsue et al., 1993; Payer et al., 1991). Therefore, despite the reduced Vγ5$^+$ thymocyte output homeostatic proliferation may occur in the epidermis and compensate for the developmental defect. Together these data suggests that a significantly reduced percentage of Vγ5$^+$ thymocytes are able to develop efficiently in the absence of Rorγ therefore, the defect must be a result of a cell extrinsic, environmental mechanism. Consistent with this, RT-PCR analysis showed that Vγ5$^+$ thymocytes do not express *Rorγt* (Figure3.5G). Rorγt is a thymus specific isoform of Rorγ, which has a truncated N terminus (Villey et al., 1999). Further explanation into the regulation of Vγ5$^+$ thymocyte development is discussed in more detail later.

To investigate the role for Vγ5$^+$ thymocytes specifically, in mTEC development the reaggregate thymus organ culture system was employed (White et al., 2008a). Fetal thymic stroma depleted of haematopoietic cells by dGuo treatment of FTOC was used as a starting population. This is an ideal starting population because it contains immature mTEC progenitors primed to respond to Rankl. LTi are a recognised source of Rankl and are known to be functional within this system, consequently they were used as a positive control (Rossi et al., 2007b). dGuo treated stoma was mixed at a ratio of 5:1 with pure Vγ5$^+$ thymocytes, DETC or LTi (Figure 3.7) and analysis illustrated that Vγ5$^+$ thymocytes functionally stimulate the maturation of Aire$^+$ mTECs as efficiently as LTi (Figure 3.7) despite expressing approximately 30 fold less Rankl. Unexpectedly, DETC although they express approximately 8 times more Rankl than Vγ5$^+$ thymocytes were not able to induce the development of Aire$^+$ mTECs. Importantly a CD45$^+$ population was identified in the DETC RTOCs after the 7 days of culture suggesting the DETC had survived (Figure 3.7G), therefore the absence of Aire$^+$ mTECs was not due to the absence of DETC. At present, the significance of this observation and the underlying mechanism are unclear. One reason DETC are unable to induce mTEC maybe that they express the decoy receptor osteoprotegerin (OPG), which can inhibit Rankl functions (Kong et al., 1999; Yasuda et

al., 1998). Creating a mixed RTOC with a 1:1 ratio of Vγ5$^+$ thymocytes and DETC could test this, as OPG is a soluble factor, it would block Rankl provided by the Vγ5$^+$ thymocytes as well as the DETC. In addition, this observation could suggest redundancy with a currently unidentified alternative mechanism; this is supported by the observation in *Rank*$^{-/-}$ mice discussed below. Together these data suggest that Vγ5$^+$ thymocytes, but not mature Vγ5$^+$ DETC, are able to induce the development of *Aire*$^+$ mTECs through the provision of Rankl.

Whether or not γδ thymocytes require or undergo a positive selection event remains controversial, probably due to significant differences between fetal and adult γδ T cell development and differences between the individual γδ T cell subsets making if difficult to draw conclusions. Some reports have suggested that the γδ TCR can mediate a β-selection-like differentiation, a phenomenon associated with reduced receptor expression or strength of signal (Hayes et al., 2005). Evaluation of γδ thymocyte surface marker and chemokine receptor modulation enables their maturation to be assessed and correlates with TCR stimulation (Leclercq et al., 1993; Tatsumi et al., 1993; Xiong and Raulet, 2007). For example, γδ T cell differentiation has been shown to be associated with the upregulation of the γδ TCR and similar to β selection of the αβ T cell lineage, the upregulation of CD5, CD27 and CD45RB and downregulation of CD24 (Leclercq et al., 1996; Prinz et al., 2006; Taghon et al., 2006). Another parallel with β selection in the αβ T cell lineage is that γδ-selection also triggers significant cellular expansion albeit on average two cycles fewer than that observed for αβ T cell differentiation (Prinz et al., 2006; Taghon et al., 2006). However, evidence tends not to suggest a pre-antigen receptor-regulated checkpoint in γδ T cell differentiation and the consensus remains that γδ selection occurs at a single TCR dependent event (Ciofani and Zuniga-Pflucker, 2007; Prinz et al., 2006). A necessary positive selecting thymic stromal determinant was uncovered for Vγ5$^+$ thymocytes nevertheless universal ligand dependence for γδ T cell differentiation remains

unclear (Born et al., 1999; Ciofani and Zuniga-Pflucker, 2007; Prinz et al., 2006). *Skint1* (selection and upkeep of intraepithelial T cells 1) a member of a recently identified gene cluster is thought to be required for positive selection of Vγ5$^+$ thymocytes in the embryonic thymus and for normal numbers and function of DETC in the skin (Boyden et al., 2008). Taken together two independent reports suggest that Skint1 is a thymic stromal determinant (Boyden et al., 2008; Lewis et al., 2006). Intriguingly, the thymic stromal cell compartment expressing Skint1 had not been determined so to gain a better understanding, medullary and cortical thymic epithelial cells were analysed for *Skint1* expression. Careful examination revealed that medullary thymic epithelial cells preferentially expressed *Skint1* and expression involved Rankl signalling (Figure 3.12). However, a marked reduction but not complete absence of *Skint1* expression was observed in *Rank*$^{-/-}$ mice (Figure 3.14B), suggesting redundancy in the regulation of *Skint1* expression. This second unidentified signal may be essential for *Skint1* upregulation and maybe the signal the DETC downregulated during their maturation programme thus explaining their inability to induce Aire$^+$ mTEC development despite their expression of Rankl. This however, is assuming the same cell also provides the second signal.

While it had been reported that Skint1 was the positive selection determinant for Vγ5$^+$ thymocytes, understanding the effect of its reduced availability was investigated. Surprisingly, the reduced expression of Skint1 in the *Rank*$^{-/-}$ thymus did not appear to affect the development of Vγ5$^+$ thymocytes when the percentages of immature (CD45RB^{lo}) and mature (CD45RB^{hi}) cells were analysed (Figure 3.14C). However, cell numbers revealed a significant reduction in the number of mature CD45RB^{hi} cells (Figure 3.14D), which suggests *Skint1* is important for the proliferation and/or survival of Vγ5$^+$ thymocytes, corroborating the observations in the "FVB tac" mouse strain and the notion that *Skint1* is a positive selection determinant (Boyden et al., 2008). This however was not apparent from the total Vγ5$^+$ thymocyte numbers though this may

be due to small group numbers therefore for future experiments greater numbers of mice per group could be used to enable accurate statistical analysis. Vγ5$^+$ DETCs were readily identifiable within the epithelium of *Rank*$^{-/-}$ mice (Figure 3.14H), however, it is important to consider that varying thresholds may be required for the development of different aspects of Vγ5$^+$ T cell function and peripheral expansion may have occurred. In addition, the Vγ5$^+$ DETC found in the *Rank*$^{-/-}$ epidermis may have an idiotypic TCR that is comprised of different γ and δ chain, such as Vγ1-Vδ1 as observed in the "FVB tac" mice (Lewis et al., 2006; Mallick-Wood et al., 1998). Together these data suggest that thymic crosstalk could be occurring between Vγ5$^+$ thymocytes and mTECs; Vγ5$^+$ thymocytes provide Rankl for the maturation of immature mTEC progenitors, in turn Aire$^+$ mTECs upregulate Skint1 and regulate the positive selection and thus development of Vγ5$^+$ thymocytes.

The above data lead to the investigation of whether Skint1 was implicated in the medullary association of Vγ5$^+$ thymocytes. Analysis of E17 thymus from "FVB tac" and *Rank*$^{-/-}$ mice, which have reduced *Skint1* expression, indicated that the medullary association of Vγ5$^+$ thymocytes was reduced. This may suggest ligation of Vγ5$^+$ thymocytes with Skint1 is responsible for a prolonged interaction, which results in the apparent retention of Vγ5$^+$ thymocytes within the medulla. Other process, such as chemokine signalling, discussed below, may also be involved in regulating Vγ5$^+$ thymocyte migration to the medulla, and may still be functional in the absence of Rank and Skint1, aiding the less efficient development of a reduced number of Vγ5$^+$ thymocytes as observed. Therefore the involvement of Skint1 in the localisation of Vγ5$^+$ thymocytes to the medulla remains to be fully elucidated.

Having established that Vγ5$^+$ thymocytes are involved in mTEC development the mechanism regulating their medullary migration and retention was examined. It has been reported that chemokine signalling plays a fundamental role in thymocyte migration throughout

the specialised microenvironments of the thymus (Campbell et al., 1999; Svensson et al., 2008; Ueno et al., 2004). Pertussis toxin established that chemokine signalling was responsible for the association of Vγ5$^+$ thymocytes with the medulla, the development of Aire$^+$ mTECs and the maturation of Vγ5$^+$ thymocytes without having a toxic effect on the number of Vγ5$^+$ thymocytes (Figure 3.8). Consequently, the expression of potential chemokines on thymocyte subsets and chemokine ligands on thymic epithelium were considered. Previous studies have shown Ccl27, a ligand for Ccr10, expression specifically within the skin and the upregulation of Ccr10 in γδ precursors in response to ligand engagement in the fetal thymus was reported (Homey et al., 2000; Jarmin et al., 2000; Payer et al., 1991; Wang et al., 2000; Xiong et al., 2004). In support of this Ccr10 was expressed on Vγ5$^+$ thymocytes (Figure 3.9A and B) and importantly Ccl27 was preferentially expressed in medullary thymic epithelium (Figure 3.9C). However, attempts to block signalling through Ccl27 had little effect on the accumulation of Vγ5$^+$ thymocytes in the medulla and unfortunately attempts to validate the function of the anti Ccl27 blocking antibody proved difficult. In addition, with Ccr7 and Ccl21 previously being implicated in medullary migration of SP αβ thymocytes (Ehrlich et al., 2009; Kurobe et al., 2006; Nitta et al., 2009; Ueno et al., 2004), a fascinating observation was made with the preferential distribution of Ccl21 expression on immature mTECs (Figure 3.10C) and the surface expression of Ccr7 on Vγ5$^+$ thymocytes (Figure 3.10B). These data support the idea that immature Vγ5$^+$ thymocytes interact with immature mTEC to provide Rankl for the development or mTECs, which in turn upregulate *Skint1* expression for the maturation of Vγ5$^+$ thymocytes. Ccr7 expression on the immature (CD45RB^{lo}) and mature (CD45RB^{hi}) Vγ5$^+$ thymocyte subsets would further corroborate this hypothesis. In support of this a significant decrease in the number of Vγ5$^+$ thymocytes associated with the medulla was observed in *Ccr7*$^{-/-}$ E17 thymus (Figure 3.11E), surprisingly this did not effect the frequency of Aire$^+$ mTECs (Figure 3.11H). A recent

report identified that SP thymocyte accumulation within the thymic medulla was the result of two mechanistically distinct G-protein coupled receptor (GPCR) mediated processes where Ccr7 was dispensable for medullary access, implicating other unidentified GPCRs in this process (Ehrlich et al., 2009). Therefore, as a possible explanation, $V\gamma5^+$ thymocytes may enter the thymic medulla transiently using another chemokine receptor and chemokine ligand pair enabling them to provide Rankl to the developing mTEC. However, the duration of the interaction with mTEC may not be sufficient for *Skint1* to be expressed by the mTEC or the positive selection of the $V\gamma5^+$ thymocyte. However, when $V\gamma5^+$ thymocyte maturation in *Ccr7*$^{-/-}$ thymus was investigated, their maturation appeared normal (Figure 3.11J and K). This may suggest that the process of reciprocal signalling does not require a sustained interaction, or may reflect the involvement of other adhesion molecules (Schon et al., 2002). In addition this may imply a defect in the ability of mature $V\gamma5^+$ thymocytes to exit the thymus as Ccr7 has been implicated in this process (Ueno et al., 2002). Thus, any reduction in the number of mature ($CD45RB^+$) cells that may imply a defect, could be masked by their accumulation. The overall greater cell number of $V\gamma5^+$ thymocytes observed in the $Ccr7^{-/-}$ thymus may be due to strain differences (Bergstresser et al., 1983), or could be due to small disparities between the embryonic age of the two strains, as at this time in development a small amount of time can make large differences to the developmental stage. Together these data identify a role for Ccr7 in the retention of $V\gamma5^+$ thymocytes in the fetal thymus medulla, similar to its role in αβ thymocyte migration (Ehrlich et al., 2009). In contrast, a distinct unidentified pertussis toxin sensitive mechanism is involved in $V\gamma5^+$ thymocyte entry to the medulla. It would be interesting to determine which other chemokines are involved and to also ascertain the kinetics of reciprocal signalling within the thymus.

In conclusion, Vγ5$^+$ thymocytes interact with the thymic medulla where they provide Rankl to the immature mTEC progenitors initiating their developmental programme, which results in the expression of Aire on mTECs. Interestingly, this supports previous reports that speculated during initial development of the thymic medulla (E13) Vγ5$^+$ thymocytes were responsible for inducing maturation and the organisation of the medullary epithelium (Shores et al., 1991). In addition, the results presented here suggest that the positive selection determinant for the Vγ5$^+$ thymocyte subset, Skint1, is expressed by mTECs after stimulation predominantly with Rankl, implying the occurrence of reciprocal signalling between Vγ5$^+$ thymocytes and mTECs (Figure 3.15). It is important to note that this study does not rule out the involvement of other fetal γδ thymocyte subsets in the development of Aire$^+$ mTECs. The Vγ5$^+$ subset was chosen as an example because it forms the first cohort of thymocytes to develop within the thymus and must therefore be involved in the initiation of this process. In addition, a specific antibody is commercially available allowing the clear detection and isolation of this population. Future experiments could focus on the involvement of the other fetal γδ T cell subsets, when the reagents become available.

Figure 3.15 A Current Model For The Reciprocal Signalling Between Fetal γδ Thymocytes And Developing mTECs

$V\gamma5^+$ thymocytes interact with the thymic medulla presumably by chemotactic recruitment and through the provision of Rankl initiate the development of $Aire^+$ mTECs. In turn the $Aire^+$ mTECs upregulate expression of Skint1, which is important for the maturation of Vγ5 thymocytes, as indicated by high surface expression of CD45RB. Thus implying the occurrence of reciprocal signalling between $V\gamma5^+$ thymocytes and mTECs.

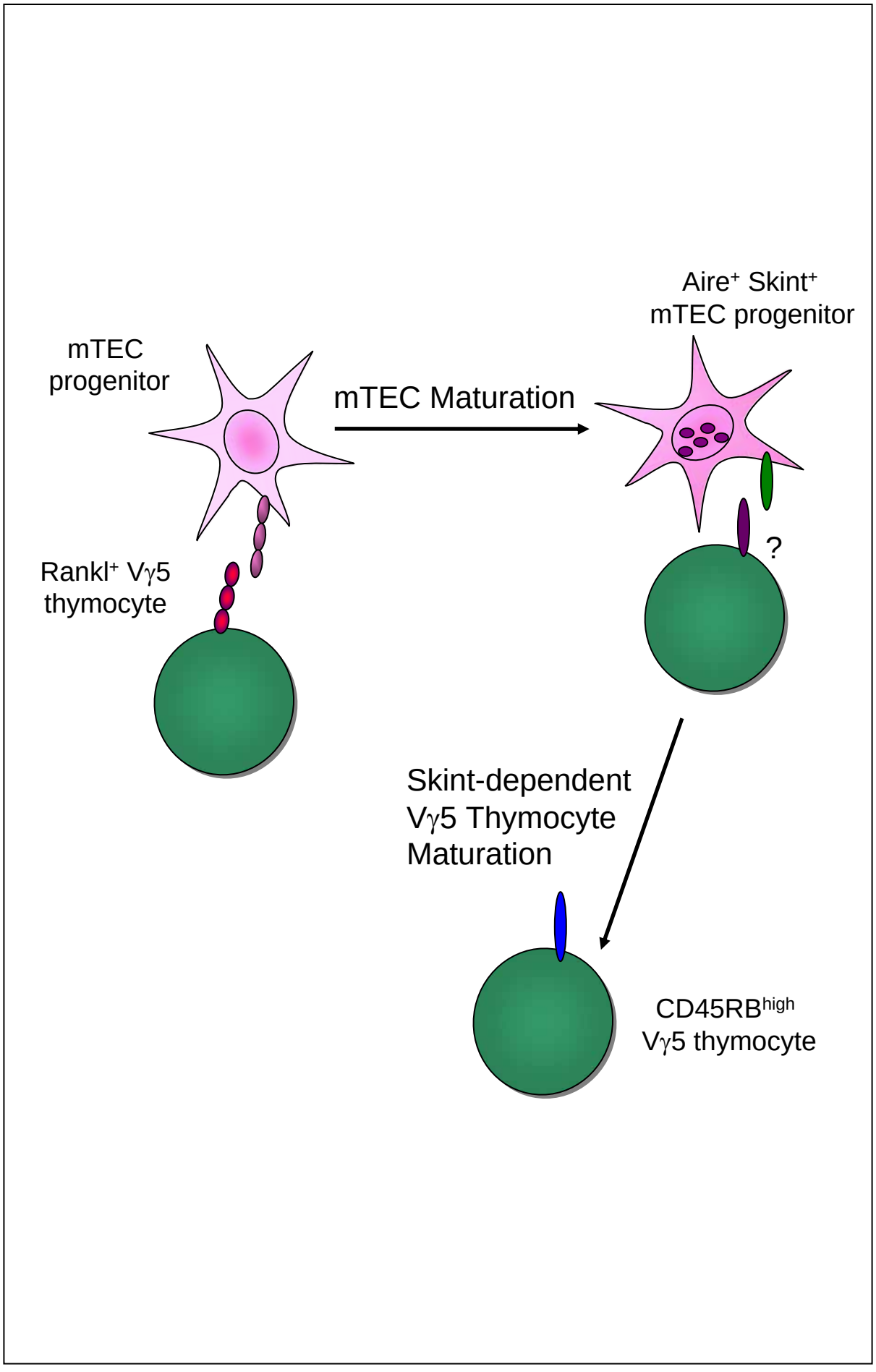
Aire+ Skint+
mTEC progenitor
mTEC
progenitor
mTEC Maturation
Rankl+ Vγ5
thymocyte
?
Skint-dependent
Vγ5 Thymocyte
Maturation
CD45RBhigh
Vγ5 thymocyte

CHAPTER 4: ABSENCE OF THYMUS CROSSTALK IN THE FETUS DOES NOT PRECLUDE HEAMATOPOIETIC INDUCTION OF A FUNCTIONAL THYMUS IN THE ADULT

4.1 Introduction

4.1.1 Thymic Crosstalk

The generation of a diverse non-autoreactive T cell repertoire is dependent on the interaction of thymocytes with thymic epithelial cells. In turn, it is clear that the presence of developing thymocytes simultaneously impacts upon the phenotype, function and the three-dimensional cellular organisation of thymic epithelial cells (TEC). This bidirectional lymphostromal signalling pathway has been entitled 'thymus crosstalk' (Fiorini et al., 2008; van Ewijk et al., 1994). Initial experiments demonstrated that normal thymic medullary epithelial cell organisation in SCID mice could be restored by the introduction of wildtype bone marrow (Shores et al., 1991). Moreover, medullary organisation was shown to be irregular in TCR$\alpha^{-/-}$ mice, suggesting development of medullary thymic epithelial cells depends upon $\alpha\beta$ TCR^{+} thymocyte regulation (Palmer et al., 1993). Thymocyte-TEC interdependence is apparent in mice that display a blockade in T cell development at various immature stages, as this results in the absence of thymic stromal organisation to different extents. Thus blocks at specific stages of thymocyte development differentially impact the development of TEC subsets (Klug et al., 1998). The above studies most notably demonstrated deficiencies in mTEC formation, and have revealed the function of lympho-stromal interactions in the provision of maturation and survival signals necessary for the generation of the mature thymic architecture (Hollander et al., 1995b; Palmer et al., 1993; Shores et al., 1991). Two distinct crosstalk control points have been identified. CD44^{-}CD25^{+} DN3 thymocytes have been shown to induce three-dimensional arrangement of cTECs, and SP thymocytes induce development of and maintain the medullary thymic epithelium (Shores et al., 1991; van Ewijk et al., 2000).

Although these studies reveal a link between T cell development and normal thymic architecture, how T cell precursors influence, and the factors that govern TEC development are

unclear, particularly in comparison to the well-characterised T cell developmental process.

While thymocyte-TEC crosstalk influences some aspects of TEC development, the initial specification of bipotent thymic epithelial cell progenitors (bTECp) in to the cTEC and mTEC lineages can occur independently of thymocytes (Jenkinson et al., 2005; Klug et al., 2002). TEC-thymocyte interactions seem to be required at later stages of fetal thymus development, more specifically from around E15.5 and in the postnatal thymus to extend this initial patterning and to sustain a normal organisation of the TEC compartments (Blackburn and Manley, 2004).

Medullary epithelial cell development is thought to be a relatively plastic process, as reconstitution has been reported at adult stages (Naquet et al., 1999; Ritter and Boyd, 1993). In addition, *in vivo* administration of an LTβR-blocking reagent resulted in the rapid regression of the medullary TEC network, suggesting mTEC maintenance to be a dynamic process (Ladi et al., 2006). Recently a molecular basis for thymus crosstalk was identified. The interaction between Rank ligand (Rankl) expressed on thymic haematopoietic cells, such as $CD4^+$ thymocytes and lymphoid tissue inducer cells (LTi) and its receptor, Rank, on immature mTECs regulates mTEC development (Fiorini et al., 2008; Irla et al., 2008; Rossi et al., 2007b). Interestingly, it has also been suggested that γδ TCR^+ thymocytes may be involved in the maturation of mTECs, as some γδ TCR transgenic mice show an enlarged thymic medulla (Ferrick et al., 1989; van Ewijk et al., 1994).

The requirement for crosstalk dependent mechanisms has also been reported for the establishment of the thymic cortex and cTEC development. However the molecular basis of the crosstalk signals influencing cTEC development remain poorly characterised. However recently, the potential involvement of reciprocal Notch–Delta interactions in the development of TEC has been highlighted and thus might represent an example of molecular crosstalk involved in both the development of the cortex and the medulla (Masuda et al., 2009).

Studies on CD3ε*tg26* mice have led to current models of thymus development and crosstalk (Figure 4.1). CD3ε*tg26* mice express a high copy number of the human CD3ε gene and sustain a block at the DN1 stage of T cell development, with only 2-3% of thymocytes progressing to this stage. This results in a severely hypoplastic thymus with low cellularity, that contains large cysts and aberrantly arranged cTEC and mTEC (Hollander et al., 1995b; Klug et al., 1998; van Ewijk et al., 2000). The current models propose that cTEC development is temporally restricted, as successful reconstitution of the CD3ε*tg26* thymus was only observed with fetal thymus (Hollander et al., 1995b; Tokoro et al., 1998). Furthermore, comparisons between the development of thymic epithelium in *Rag*$^{-/-}$ and CD3ε*tg26* mice reveal a well-developed cortex in the presence of DN3 thymocytes. Additionally, the stepwise reconstitution of CD3ε*tg26* mice, first with *Rag*$^{-/-}$ BM and subsequent transplant of WT BM enabled normal thymopoiesis and the development of the correct thymic architecture (van Ewijk et al., 2000). Thus implying the requirement for an interaction between fetal stromal cells with early prothymocytes (DN3) for the induction of a cortical microenvironment. Moreover, attempts to restore thymic function in adult CD3ε*tg26* mice after closure of this window, lead to aberrant thymic reconstitution with inefficient induction of central and peripheral tolerance and mature T cells with severely deficient immune responses (Hollander et al., 1995a; Hollander et al., 1995b; Manley, 2000). Understanding how the thymic cortex develops is critical, as the generation of the cortex is an important prerequisite to the expansion of the medulla (Hollander et al., 1995b; van Ewijk et al., 2000).

The ability to induce normal thymic function has important implications in relation to the development of strategies aimed at rejuvenation of the atrophied adult thymus or after ablative therapy (Gray et al., 2005; Rossi et al., 2006). In view of this, the aims and objectives of this chapter were to analyse the development of the adult thymus following the prolonged absence of

thymocyte crosstalk. This initially required a model of thymus reconstitution to be established that would allow the specific assessment of:

- the potential plasticity of hypoplastic adult thymic epithelium following lineage negative fetal liver reconstitution.
- the extent of thymic reconstitution by evaluating the thymic epithelial architecture, T cell development as defined by CD4 and CD8 expression and the induction of self tolerance mechanisms.
- whether thymic reconstitution leads to the establishment of the peripheral T cell compartment.

Figure 4.1 The Current Model Of mTEC And cTEC Establishment

Currently it is thought that initial cortical and medullary epithelial cell patterning occurs within the fetus without the requirement for inductive signals from haematopoietic cells. Moreover, the further establishment and expansion of the rudimentary areas requires instructive signals within a developmentally restricted window limited to early life.

mTEC, medullary thymic epithelial cells. cTEC, cortical thymic epithelial cells. Imm, immature, bTECp, bipotent thymic epithelial cell progenitor.

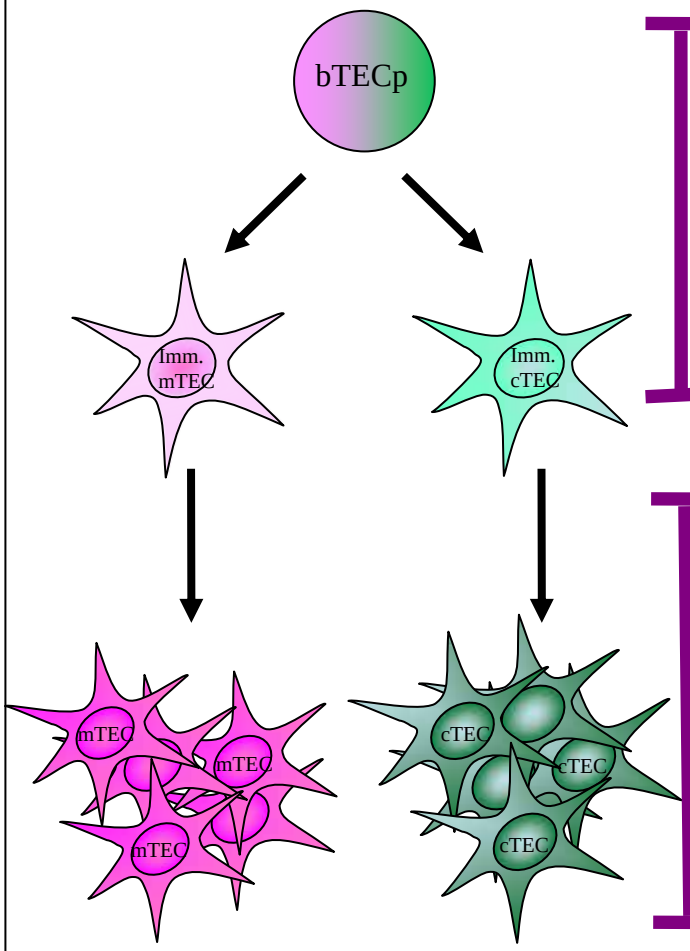

TEC Specification

- **Occurs within the embryo**
- **Does not require inductive signals from haematopoietic cells**

Klug *et al.* JI 2002
Jenkinson *et al.* MOD 2005

cTEC/mTEC Development

- **Occurs within late fetal / neonatal life**
- **Requires inductive signals from T cells**

Hollander *et al.* Immunity 1995
Hollander *et al.* Nature 1995
Van Ewijk *et al.* Development 2000.

4.2 Specialised Materials And Methods

4.2.1 Preparation And Isolation Of Lineage Negative Fetal Liver For Cell Transfer

E15 fetal livers were isolated from WT E15 embryos and fetal liver cell suspensions were obtained by gentle mechanical disaggregation using a P1000 Gilson Pipette. The fetal liver progenitors were antibody stained with a biotinylated lineage panel (see Table 4.1 for details) and streptavidin PE (see section 2.6 for full staining protocol). Single colour staining controls were also prepared to enable compensation of the MoFlo cell sorter. Lineage negative progenitors were subsequently MoFlo sorted (section 2.5.6) into 5ml polypropylene FACS tubes containing 500μl RF10-H. Preparations of a post-sort purity less than 95% were discarded. The total cell number was calculated and the resulting population used for intravenous injection (Section 4.2.3) a minimum of 1.4 $x10^5$cells were introduced per mouse.

Specificity (Clone)	Host/ Isotype
TER-119/Erythroid cells (Ly-76)	Rat IgG_{2b}, κ
Ly-6G and Ly6C (Gr-1) (RB6-8C5)	Rat IgG_{2b}, κ
CD45R/ B220 (RA3-6B2)	Rat IgG_{2b}, κ
CD3ε (145-2C11)	Armenian Hamster IgG1, κ

Table 4.1 Constituents of the Mouse Lineage Panel.

4.2.1 Preparation and Isolation Of Adult $CD4^-CD8^-CD44^-CD25^+$ (TN3) Thymocytes For Cell Transfer

WT Adult thymocyte suspensions were prepared by gentle teasing of whole thymus with glass slides and antibody stained with the fluorochrome-conjugated antibodies CD3ε-PE, CD4-FITC, CD8α-FITC, CD44-PEcy7 and CD25-APC in a PBS, 3% FCS solution (see Table 4.2 for details) (see section 2.6 for full staining protocol). Single colour staining controls were also

prepared to enable compensation of the MoFlo cell sorter. $CD3\varepsilon^{-}CD4^{-}CD8\alpha^{-}CD44^{-}CD25^{+}$ TN3 cells were subsequently MoFlo sorted (section 2.5.6) into 5ml polypropylene FACS tubes containing 800μl PBS, 3% FCS. Preparations of a post-sort purity less than 95% were discarded. As before, the total cell number was calculated and the resulting population used for intravenous injection (Section 4.2.3).

Specificity (Clone)
CD3ε (145-2C11)
CD4 (GK1.5)
CD8α (53-6.7)
CD44 (IM7)
CD25 (7D4)

Table 4.2 Triple Negative Antibody Panel.

4.2.3 Intravenous Cell Transfer

Freshly purified cells were resuspended in sterile PBS (Sigma) at a minimum concentration of 1.4 x 10^5 cells/200μl for the fetal liver progenitors, or a concentration from 2 x 10^4 cells/200μl to 27 x 10^4 cells/200μl for the adult TN3 cells, and allowed to equilibrate to room temperature. The cell suspension was transferred into a 1ml syringe with a 25-gauge needle affixed. Ensuring air bubbles were absent from the cell suspension the cell transfer was completed by intra-venous injection into the tail vein (200μl/mouse).

4.3 Results:

4.3.1 Establishing A Model Of Thymus Reconstitution In Adult *Rag*$^{-/-}$γc$^{-/-}$ Mice

The aim of this study was to reinvestigate the initial requirement for thymus crosstalk to occur during the fetal period. In order to investigate this, an experimental model was generated to enable examination of the ability of exogenous thymocyte progenitor cells to restore both T cell development and the thymus architecture. To characterise restoration, the non-manipulated system required abnormal T cell development and thymic architecture, therefore the *Rag*$^{-/-}$γc$^{-/-}$ mouse was chosen. The common gamma chain (γc) is a growth factor receptor expressed on early thymocytes, and forms complexes with receptors for interleukins (IL). Interleukin signalling, particularly through IL-7 is important for thymocyte growth and differentiation, consequently an absence of γc reduces thymic cellularity (Klug et al., 2002; Rodewald et al., 1997). In addition, the absence of *Rag*2, one of two lymphoid specific components of the V(D)J recombinase, involved in the rearrangement of both the immunoglobulin and the T-cell receptor genes, prevents TCR gene rearrangement (Klug et al., 2002; Takahama, 2006). Thus, there is a profound block in early T cell development and thymocyte cellularity is drastically reduced (Klug et al., 2002). Furthermore, there is a severe block in B and NK cell development (Klug et al., 1998). In addition, a TEC phenotype similar to that of the severely hypoplastic thymus in CD3ε*tg26* mice, is observed in adult *Rag*$^{-/-}$γc$^{-/-}$ thymuses, a disorganised TEC compartment consisting almost entirely of K8^{+}K5^{+} TECs (Klug et al., 2002). However, despite the early block in T cell development and in contrast to the CD3ε*tg26* thymus, the *Rag*$^{-/-}$γc$^{-/-}$ epithelial compartment organises into a three-dimensional structure (Klug et al., 2002). This subtle difference in thymic epithelial cell architecture and the presence of DN1 thymocytes lead to the prediction that the *Rag*$^{-/-}$γc$^{-/-}$ thymus could be restored, thus allowing validation of FL transfer for thymus reconstitution.

Lineage negative (Lin^-) embryonic day 15 (E15) fetal liver (FL) progenitors were intravenously injected into non-irradiated $Rag^{-/-}\gamma c^{-/-}$ (detailed in section 4.2.3) (Figure 4.2) and thymus reconstitution measured using a number of different approaches. After a minimum of 4 weeks, mice were sacrificed and lymphoid tissues harvested. In contrast to uninjected mice, an increase in size and cellularity was observed in the $Rag^{-/-}\gamma c^{-/-}$ injected mice (Figure 4.3A and C). However, in some experiments, individual thymus lobes appeared to be differentially reconstituted (Figure 4.3A). Successful reconstitution was seen in all of the $Rag^{-/-}\gamma c^{-/-}$ mice injected with fetal liver progenitors (Figure 4.3B). Figure 4.3C shows a significant increase ($p = 0.0043$) in cellularity after fetal liver transfer within the $Rag^{-/-}\gamma c^{-/-}$ mice, nevertheless the restored cell number is still significantly ($p = 0.0079$) reduced as compared to WT. Together these data suggest that the host thymus has been colonised with donor derived cells.

The ability of the fetal liver derived progenitors to restore thymocyte development in the $Rag^{-/-}\gamma c^{-/-}$ mice was assessed by flow cytometric analyses of CD4 and CD8 coreceptor expression. While uninjected mice exhibited a complete block in thymocyte development at the $CD4^-CD8^-$ DN stage, adult $Rag^{-/-}\gamma c^{-/-}$ mice that received FL showed a pattern of CD4 and CD8 expression similar to that of WT thymocytes (Figure 4.4). This included the generation of the major $CD4^+CD8^+$ DP compartment and mature $CD4^+CD8^-$ and $CD4^-CD8^+$ single positive (SP) subsets expressing high levels of αβTCR (Figure 4.4B). These data illustrate that the adult thymic epithelium of $Rag^{-/-}\gamma c^{-/-}$ mice retains the ability to recruit fetal liver derived thymocyte progenitors and support a programme of T cell development as identified by the differential expression of CD4 and CD8.

Having established that normal T cell development and maturation was occurring within an adult microenvironment previously deprived of complete thymic crosstalk, it was of interest to identify whether restoration of the thymic microenvironment had occurred. 5μm frozen

Figure 4.2 Experimental Design

Initially an experimental model was generated to enable the ability of exogenous thymocyte progenitor cells to restore both T cell development and the thymus architecture to be examined. E15 Lineage negaive (Lin^-) fetal liver (FL) intravenously transferred into $Rag^{-/-}\gamma c^{-/-}$ adult mice allowed validation of FL transfer for thymus reconstitution. $Rag^{-/-}\gamma c^{-/-}$ adult mice contain DN1 thymocytes, which may enable the thymic epithelium to respond to further developmental signals after a prolonged lack of complete crosstalk.

The plasticity and receptivity of the adult thymic epithelium was investigated in the more robust CD3ε*tg26* system, which lack T cell progenitors. CD3ε*tg26* mice represent a valuable mouse model to study thymic epithelial cell development and the role of thymic crosstalk after the prolonged absence of T cell development.

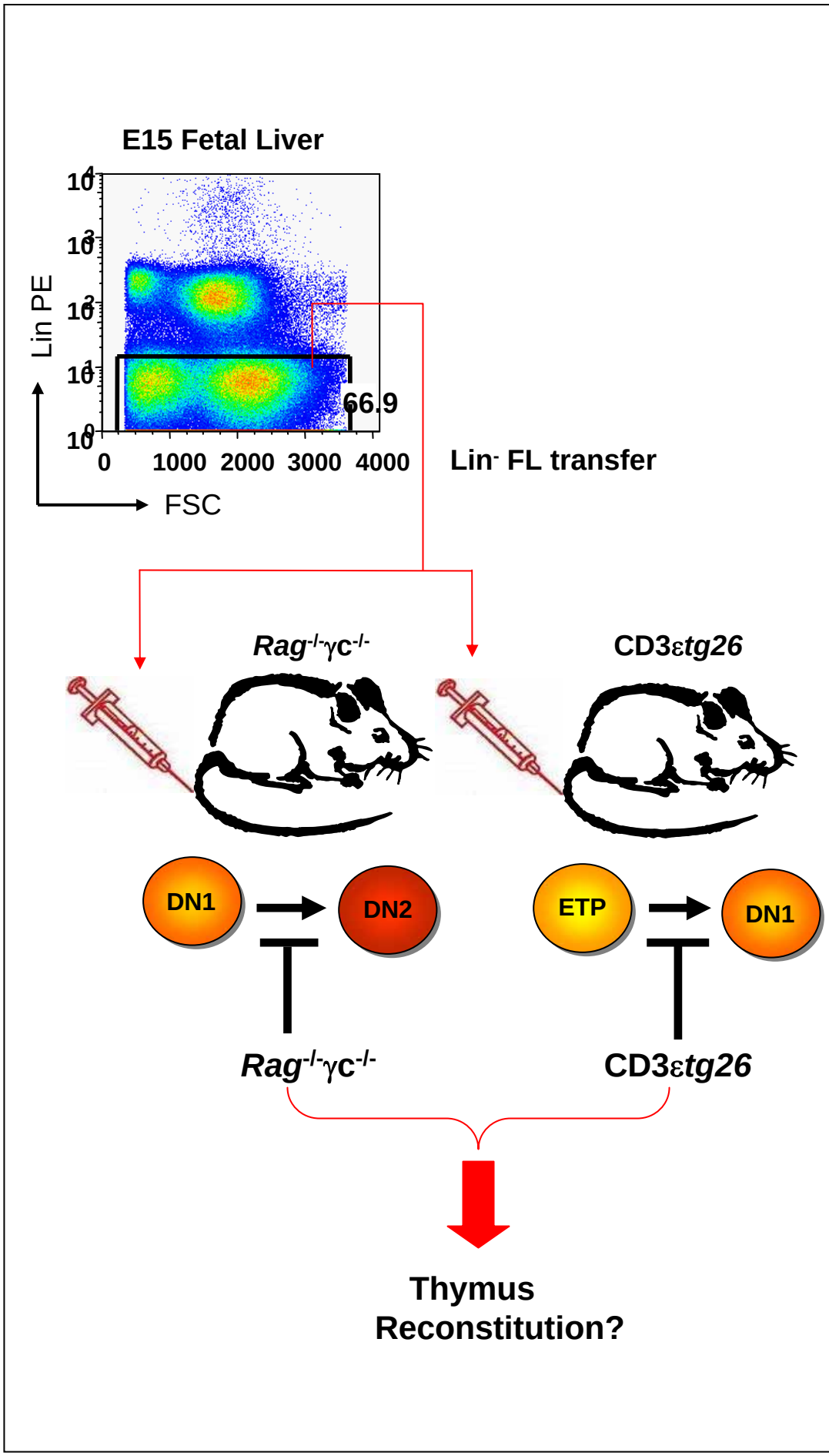
E15 Fetal Liver
Lin PE
FSC
66.9
0
1000
2000
3000
4000
Lin- FL transfer
Rag-/-γc-/-
CD3εtg26
DN1
DN2
ETP
DN1
Rag-/-γc-/-
CD3εtg26
Thymus
Reconstitution?

Figure 4.3 Successful Thymic Reconstitution Of *Rag*$^{-/-}\gamma c^{-/-}$ Adult Mice

Rag$^{-/-}\gamma c^{-/-}$ mice were harvested at ≥4 weeks after intravenous injection with lineage negative (Lin$^-$) (CD3ε$^-$, B220$^-$, TER119$^-$, Gr1$^-$) E15 WT fetal liver (FL). Thymuses from unreconstituted and FL reconstituted mice were analysed visually (4.3A). The proportion of successful thymic reconstitutions is shown (4.3B). Thymic cellularity in WT, *Rag*$^{-/-}\gamma c^{-/-}$ control and *Rag*$^{-/-}\gamma c^{-/-}$ after Lin$^-$ FL transfer (4.3C) illustrates the significant increase in cellularity of *Rag*$^{-/-}\gamma c^{-/-}$ thymus after fetal liver transfer (**p = 0.0043). The increase in cell number is significantly less than WT total cell number (**p = 0.0079). Each point represents the thymus from an individual mouse. The bar indicates the median.

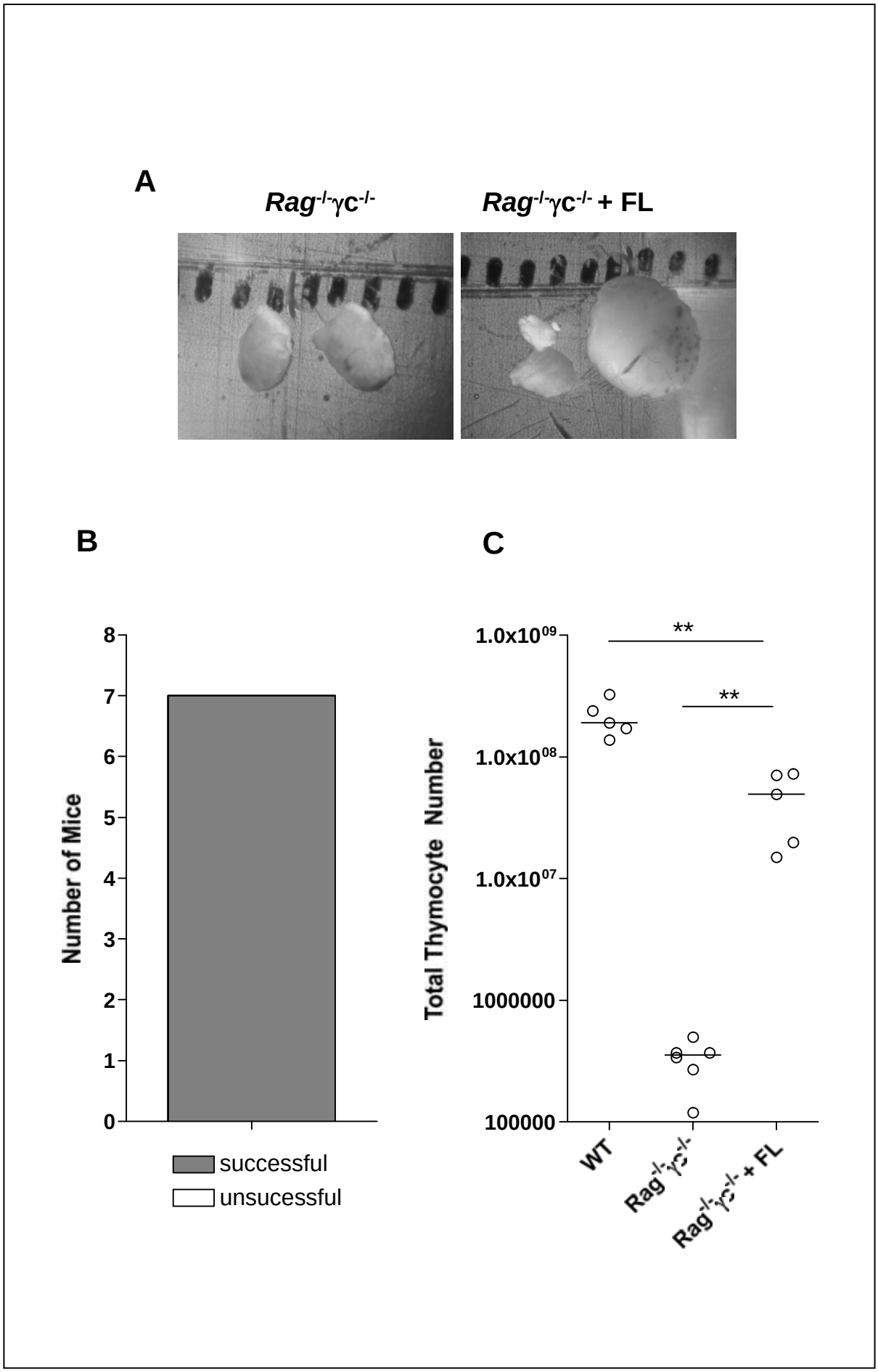
A
Rag-/-γc-/-
Rag-/-γc-/- + FL
B
Number of Mice
8
7
6
5
4
3
2
1
0
successful
unsucessful
C
Total Thymocyte Number
1.0x10^09
1.0x10^08
1.0x10^07
1000000
100000
**
**
WT
Rag-/-γc-/-
Rag-/-γc-/- + FL

Figure 4.4 Normal T Cell Development Occurs In Reconstituted *Rag*$^{-/-}$γc$^{-/-}$ Thymus

Rag$^{-/-}$γc$^{-/-}$ mice were intravenously injected within Lin^{-} (CD3ε, B220, TER119, Gr1) E15 WT fetal liver. The thymus was harvested ≥5 weeks following injection, teased and analysed by flow cytometry for expression of CD4, CD8 and TCRβ. Representative FACS plots illustrate the CD4 and CD8 profile for WT, *Rag*$^{-/-}$γc$^{-/-}$ control and reconstituted *Rag*$^{-/-}$γc$^{-/-}$ (4.4A). Development of CD4^{+}CD8^{-} and CD4^{-}CD8^{+} TCR^{hi} populations was observed (4.4B) Percentages of cells within gated areas are indicated. Data is representative of at least three experiments.

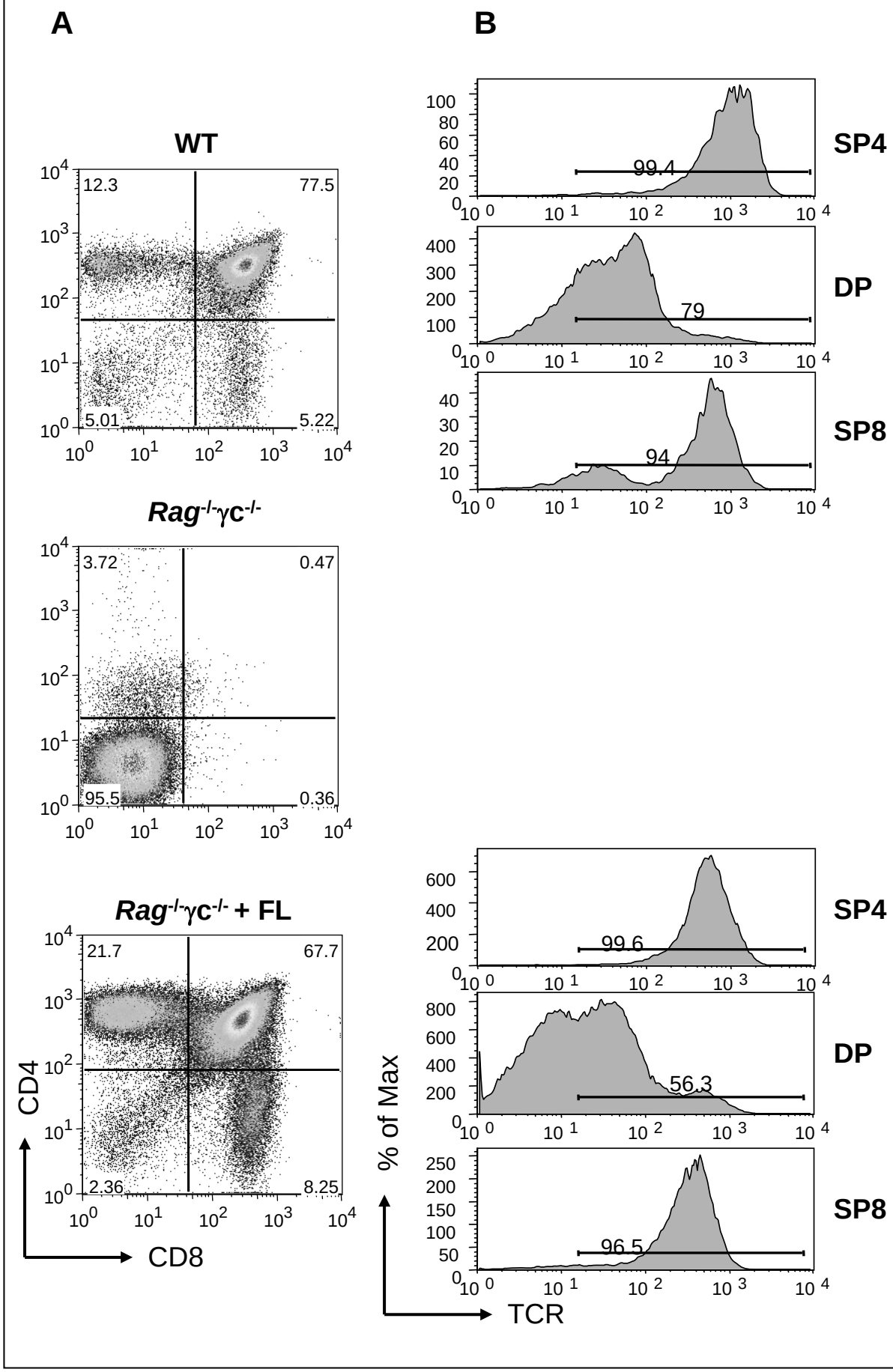
A
B
WT
12.3
77.5
5.01
5.22
Rag-/-γc-/-
3.72
0.47
95.5
0.36
Rag-/-γc-/- + FL
21.7
67.7
2.36
8.25
CD4
CD8
SP4
99.4
DP
79
SP8
94
SP4
99.6
DP
56.3
SP8
96.5
% of Max
TCR

sections were prepared from the thymuses of *Rag*$^{-/-}\gamma c^{-/-}$ mice that received E15 Lin^{-} FL and analysed by confocal microscopy. CD4 and CD8 antibody staining revealed DP and SP thymocyte segregation to the cortex and medullary areas respectively (Figure 4.5A) within the reconstituted *Rag*$^{-/-}\gamma c^{-/-}$ (bottom panel) thymus comparable to observations in WT thymus (top panel), suggesting the presence of normal cortical and medullary architecture.

To examine whether thymic epithelial cell development and compartmentalisation could be restored by FL transfer confocal analysis was completed. Frozen sections were stained with the cortical and medullary markers, CD205 and CD40 respectively (Figure 4.5B) (Shakib et al., 2009), which revealed defined microenvironments within the reconstituted *Rag*$^{-/-}\gamma c^{-/-}$ thymus (bottom panel), equivalent to those in WT thymus (top panel). It is important to note that although CD40 is expressed on both cortical and meduallry epithelium, due to varying expression levels it is only detectible on medullary epithelium by confocal microscopy. Another parameter to measure the restoration of the thymic architecture includes identifying the subcapsular region by confocal analysis of the CD25^{+} DN3 thymocyte population which predominately localise to this region (Lind et al., 2001; Penit, 1988). The presence of a dense population of CD25^{+} cells at the subcapsular region is clearly shown in the new born (NB) thymus (Figure 4.5C), however this restriction is less prominent within adult thymus for reasons yet to be determined. Interestingly, within the reconstituted *Rag*$^{-/-}\gamma c^{-/-}$ thymus, CD25^{+} thymocytes were identified within the subcapsular region, suggesting that the specialised types of microenvironments in the supcapsular cortex have also been formed (van Ewijk, 1991). Together these data imply that the adult thymic epithelium of the *Rag*$^{-/-}\gamma c^{-/-}$ mouse remains receptive to thymic crosstalk from fetal liver derived thymocyte precursors and is able to form the required three-dimensional functional microenvironments characteristic of WT thymus.

Another readout of successful thymic reconstitution is the development of cellular self

Figure 4.5 Restoration Of Normal Thymic Architecture In Reconstituted *Rag*$^{-/-}$γc$^{-/-}$ mice

Thymus sections from WT and reconstituted *Rag*$^{-/-}$γc$^{-/-}$ mice were analysed by confocal microscopy for cTEC and mTEC development and organisation using the markers CD205 and CD40 (4.5A). Thymocyte organisation was also analysed using CD4 and CD8 (4.5B). Note the architecture is comparable to WT in the reconstituted thymus. Scale bars represent 100μm.

Another organisational parameter is the localisation of CD25^{+} DN3 thymocytes at the subcapsular zone, which was clearly observed in new born (NB) thymus and was less obvious in the adult. The subcapsular region can be identified in the reconstituted *Rag*$^{-/-}$γc$^{-/-}$ mice (4.5C). Scale bars represent 50μm. Solid line: thymus capsule, Dotted line: subcapsular region boundary. Data is representative of at least three experiments.

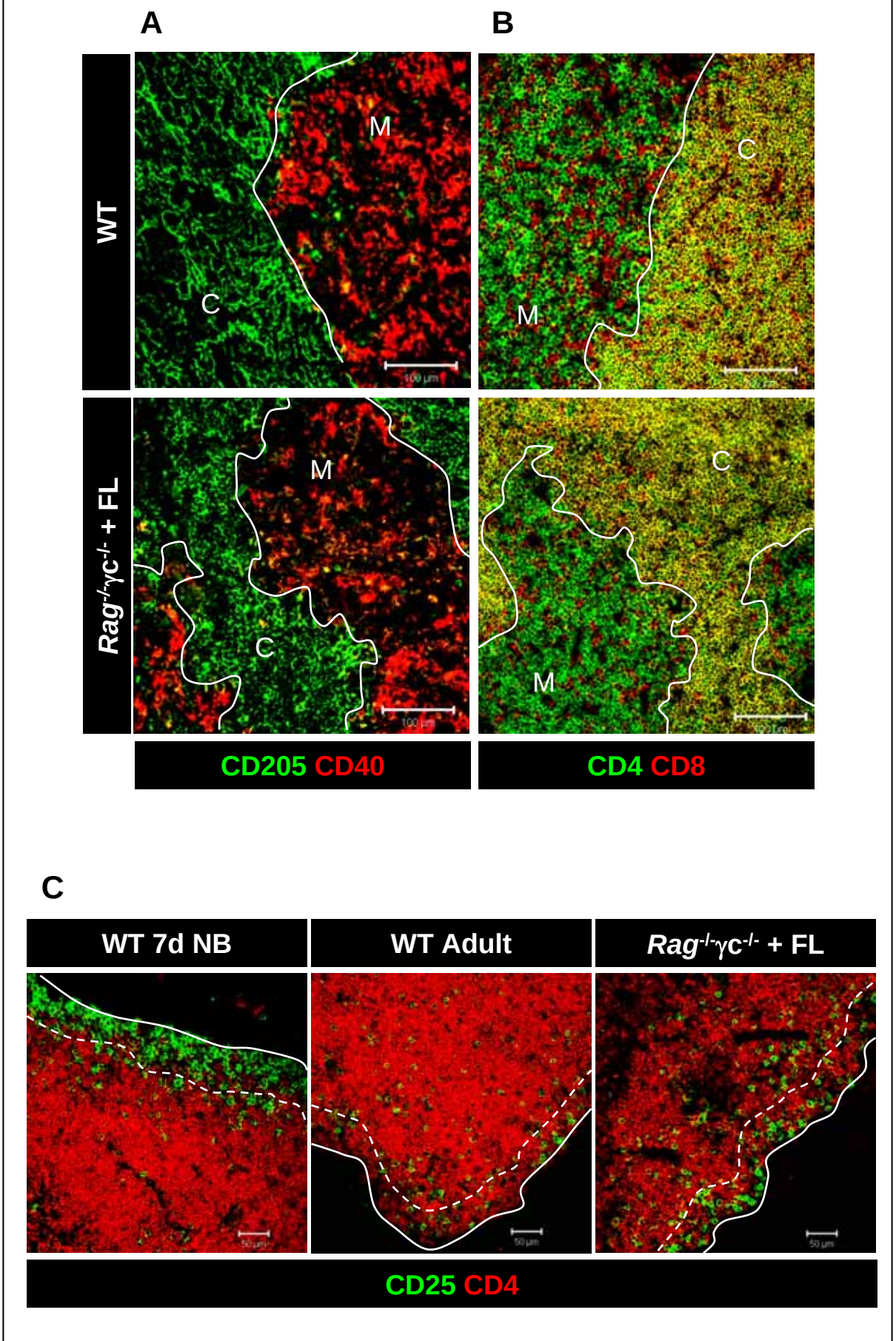
A
B
WT
Rag-/-γc-/- + FL
M
C
CD205 CD40
CD4 CD8
C
WT 7d NB
WT Adult
Rag-/-γc-/- + FL
CD25 CD4

tolerance mediators, including Aire positive mTECs and FoxP3 positive Tregs (Akiyama et al., 2008; Derbinski et al., 2005; Kyewski and Derbinski, 2004; Kyewski and Klein, 2006; Rossi et al., 2007b; Yano et al., 2008). Confocal analysis of frozen sections prepared from WT and reconstituted *Rag*$^{-/-}$γc$^{-/-}$ mice revealed the presence CD4^{+}FoxP3^{+} Tregs (Figure 4.6A) and K5^{+}Aire^{+} mTECs (Figure 4.6B) within the thymic medulla. Presented here are confocal images from one mouse representative of seven successfully reconstituted *Rag*$^{-/-}$γc$^{-/-}$ mice that suggests the establishment of these two fundamental tolerance mechanisms are not impaired after the prolonged absence of complete developmental signals.

Together these data suggest that intravenous introduction of FL progenitors into adult immuno-deficient mice is a good model to investigate thymus reconstitution since the progenitors were able to migrate to the correct location and initiate thymocyte and thymic epithelial cell development. However, *Rag*$^{-/-}$γc$^{-/-}$ mice are not completely devoid of immature thymocytes and our current understanding of the timing and requirement of thymus crosstalk signals is relatively incomplete. Consequently, it can not be ruled out that Rag$^{-/-}$γc$^{-/-}$ mice have already received sufficient thymocyte crosstalk signals from the presence of DN1 thymocytes to enable the thymic epithelium to respond to further developmental signals, after a prolonged lack of complete crosstalk. Therefore, the plasticity and receptivity of the adult thymic epithelium was investigated in the more robust CD3ε*tg26* system, which lack T cell progenitors presumably as a consequence of random transgene integration. Thus CD3ε*tg26* mice represent a valuable mouse model to study thymic epithelial cell development and the role of thymic crosstalk after the prolonged absence of T cell development.

Figure 4.6 Re-establishment Of Cellular Mediators Of T Cell Tolerance After Thymic Reconstitution

Thymus sections from WT and reconstituted *Rag*$^{-/-}\gamma c^{-/-}$ mice were analysed by confocal microscopy for the presence of Keratin 5^{+} Aire^{+} mTEC (4.6A) and CD4^{+}FoxP3^{+} regulatory T cells (4.6B). Note the presence of both in reconstituted *Rag*$^{-/-}\gamma c^{-/-}$ mice. Scale bars represent 10μm. Data is representative of at least three experiments.

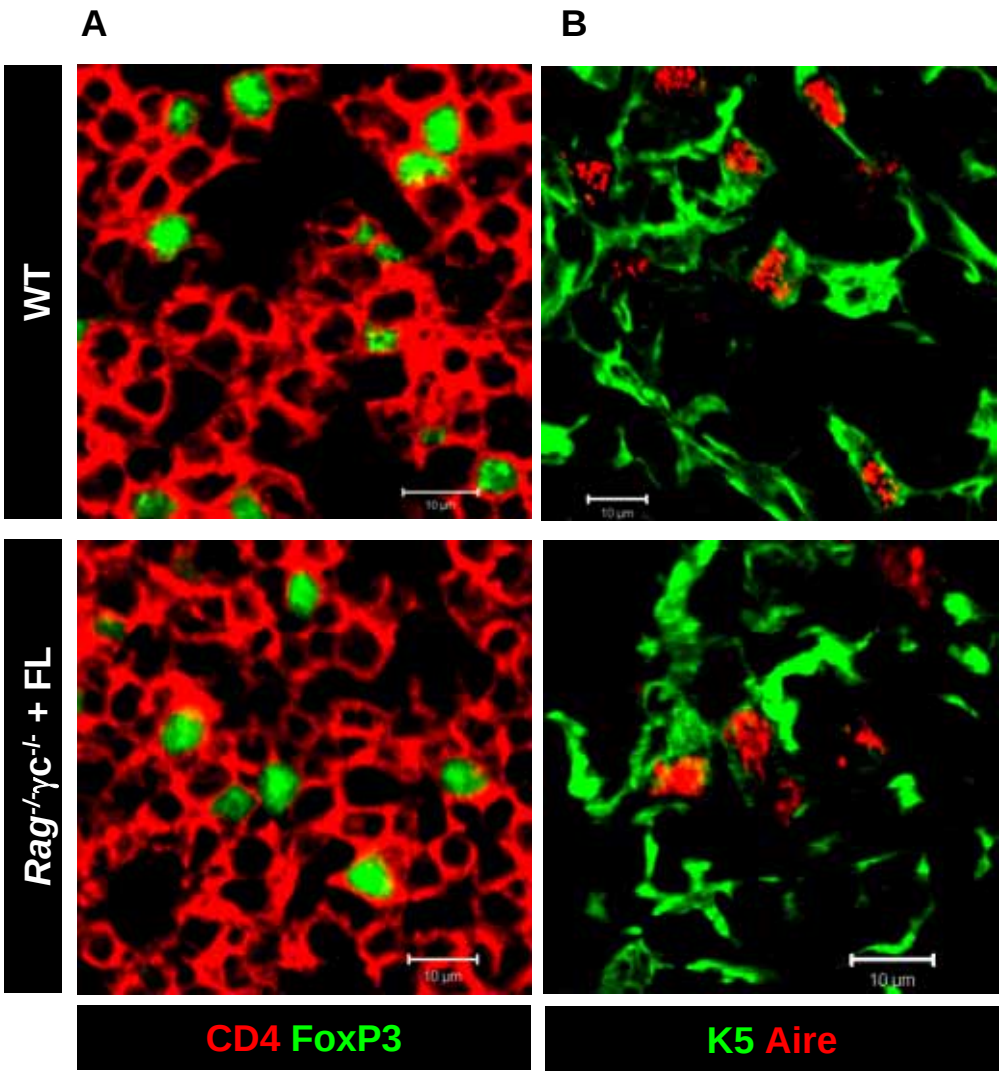
A
B
WT
Rag-/-γc-/- + FL
10 µm
CD4 FoxP3
K5 Aire

4.3.2 Successful Reconstitution Of Adult Thymic Epithelium Previously Lacking Thymus Crosstalk

Previous studies by Hollander and colleagues have shown a temporal regulation of thymic crosstalk, where successful reconstitution of the CD3ε*tg26* thymus was only observed when haematopoietic progenitors were transplanted *in utero* for example (Hollander et al., 1995b). Therefore the initiation of thymic cortex development was thought to take place within a defined, developmentally restricted window, ranging from E14 to the first days after birth (Hollander et al., 1995b; van Ewijk et al., 2000). The previous studies presented here have established an *in vivo* model in which the ability of FL progenitors to restore thymus structure and function could be tested. However, as previously mentioned although a profound block in T cell development is observed in *Rag*$^{-/-}$γc$^{-/-}$ mice, they contain small numbers of DN1 thymocytes (Klug et al., 2002), therefore examination of thymus reconstitution in the complete absence of thymocytes was required. CD3ε*tg26* mice express a high copy number of the human CD3ε gene and sustain an early block in T cell development, resulting in the complete absence of a normal architecture.

To investigate whether thymus crosstalk was dependent on signals received during the fetal/neonatal period, syngeneic Lin^{-} FL progenitors from WT E15 mouse embryos, were transferred, as previously established in *Rag*$^{-/-}$γc$^{-/-}$ mice, into non-irradiated adult CD3ε*tg26* mice. In contrast to un-injected age-matched control thymuses that remained small, cystic and hypotrophic, the CD3ε*tg26* thymus after receiving thymocyte progenitors expanded in size and no longer contained cysts (Figure 4.7A). Furthermore in line with observations made in the *Rag*$^{-/-}$γc$^{-/-}$ reconstitution system, a significant increase in thymus cellularity ($p = 0.0007$) was observed. T cell development as determined by a pattern of CD4 and CD8 coreceptor expression (Figure 4.8A) and the upregulation of αβTCR (Figure 4.8B) appeared comparable to WT.

Figure 4.7 Thymocyte Crosstalk During The Fetal Period Is Not Required For Successful Thymic Reconstitution Of CD3ε*tg26* Adult Mice

CD3ε*tg26* mice were harvested at ≥5 weeks after intravenous injection with lineage negative (Lin^-) ($CD3\varepsilon^-$, $B220^-$, $TER119^-$, $Gr1^-$) E15 WT fetal liver (FL). Thymuses from unreconstituted and FL reconstituted mice were analysed visually; arrow illustrates cystic structure of unreconstituted thymus, scale bars indicate 1mm (4.7A). The proportion of successful thymic reconstitutions is shown (4.7B). Thymic cellularity in WT, CD3ε*tg26* control and CD3ε*tg26* after Lin^- FL transfer (4.7C) illustrates the significant increase in cellularity (***$p = 0.0007$). The increase in cell number is significantly less than WT cell number (**$p = 0.0043$). Each point represents the thymus from an individual mouse. The bar shows the median.

A

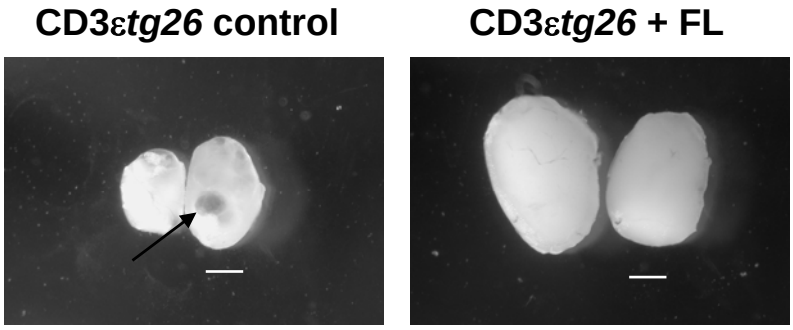
CD3εtg26 control
CD3εtg26 + FL

B

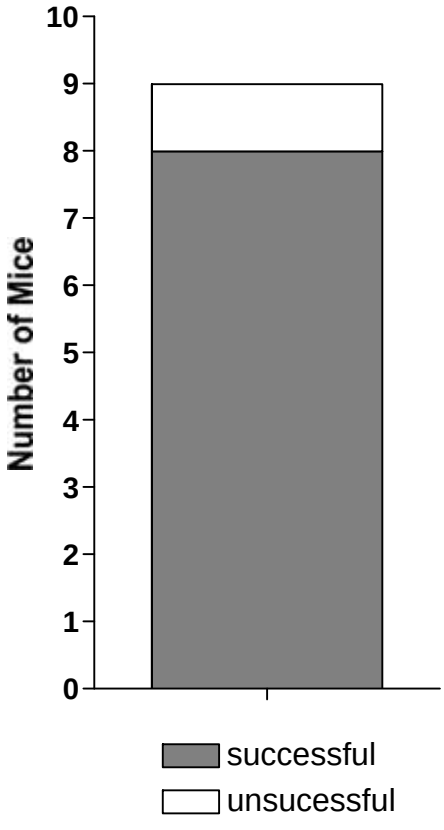
Number of Mice
10
9
8
7
6
5
4
3
2
1
0
successful
unsucessful

C

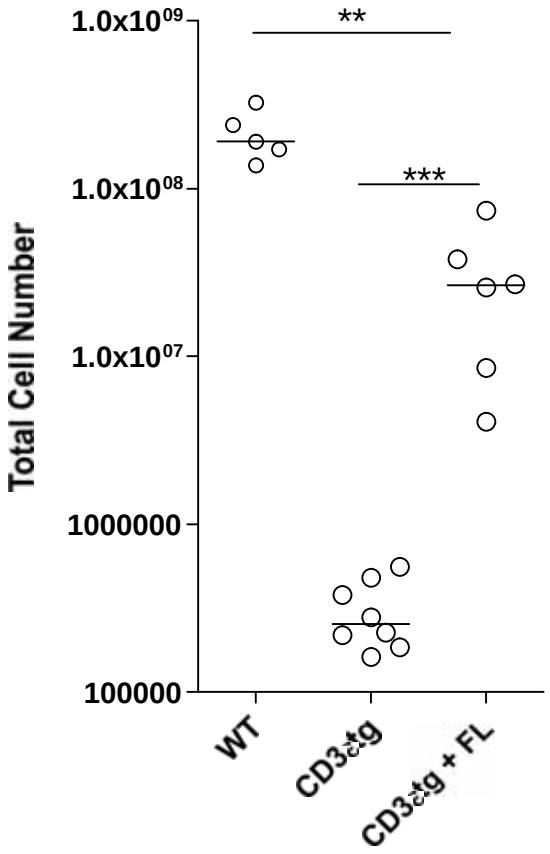
Total Cell Number
1.0x10^09
1.0x10^08
1.0x10^07
1000000
100000
**
***
WT
CD3εtg
CD3εtg + FL

Figure 4.8 Normal T Cell Development Occurs In The Reconstituted CD3ε*tg26* Thymus

CD3ε*tg26* mice were intravenously injected within Lin^- (CD3ε, B220, TER119, Gr1) E15 WT fetal liver. The thymus was harvested ≥5 weeks following injection, teased and analysed by flow cytometry for expression of CD4, CD8 and TCRβ. Representative FACS plots illustrate the CD4 and CD8 profile for WT, CD3ε*tg26* control and reconstituted CD3ε*tg26* (4.8A). Development of $CD4^+CD8^-$ TCR^{hi} and $CD4^-CD8^+$ TCR^{hi} populations were also observed (4.8B). Percentages of cells within gated areas are indicated. Data is representative of at least three experiments.

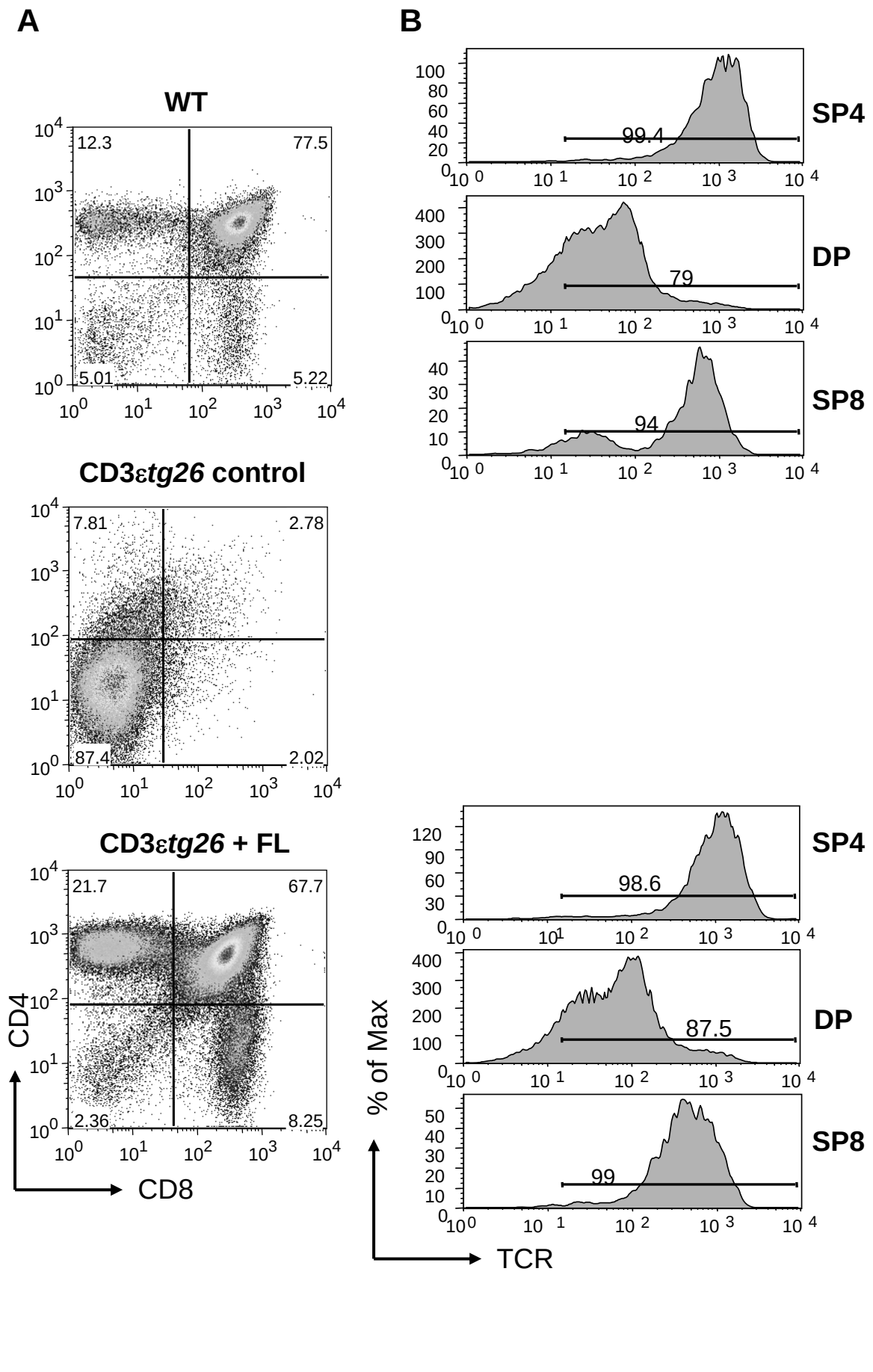
A
WT
12.3
77.5
5.01
5.22
CD3εtg26 control
7.81
2.78
87.4
2.02
CD3εtg26 + FL
21.7
67.7
2.36
8.25
CD4
CD8
B
SP4
99.4
DP
79
SP8
94
SP4
98.6
DP
87.5
SP8
99
% of Max
TCR

Interestingly, the CD3ε*tg* thymus instead of harbouring thymocytes contains B cells (Figure 4.9A) (Tokoro et al., 1998). However, the absolute number of B cells in CD3ε*tg26* control thymuses were reduced as compared to WT. Furthermore, after thymus reconstitution the total B cell number does not appear to alter, suggesting that the number of thymic B cells does not change dramatically in the presence or absence of developing thymocytes or a normal thymic architecture (Figure 4.9B). Unfortunately within this model, it was not possible to determine the origin of the thymic B cells.

To investigate whether a normal thymic microenvironment developed alongside the new programme of T cell development, the thymic architecture of uninjected and FL injected CD3ε*tg26* mice was analysed. As reported previously (Hollander et al., 1995b), thymic epithelial cells were disorganised in control CD3ε*tg26* thymus, and attempts to identify cTEC and mTEC compartments revealed little separation using markers such as Keratin 8 and Keratin 5 for cortical and medullary areas respectively (Figure 4.10A). In contrast clearly defined keratin 8^+ cortical and keratin 5^+ medullary compartments were observed by confocal analysis of CD3ε*tg26* thymus up to 9 weeks after Lin^- FL injection. Moreover, segregation of $CD4^+$ $CD8^+$ double positive and $CD4^+$ and $CD8^+$ single positive thymocytes within the cortical and medullary areas respectively was observed in reconstituted mice (Figure 4.10B). Interestingly, when the thymic microenvironments of control and reconstituted mice were analysed with the markers CD205 and CD40 for cTEC and mTEC (Shakib et al., 2009), a different staining pattern was observed when compared to the keratin 8 and keratin 5, cTEC and mTEC identification. Discrete $CD205^+CD40^-$ and $CD205^-CD40^+$ regions were identified in unreconstituted mice (Figure 4.10C) supporting reports that initial thymus patterning occurs independently of lymphostromal interactions (Jenkinson et al., 2005). Importantly, $CD25^+$ thymocytes were found to reside within the subcapsular region of the reconstituted thymus as observed in WT thymus

Figure 4.9 B Cell Number In Reconstituted CD3ε*tg26* Thymus Do Not Change

CD3ε*tg26* mice predominantly harbour B cells (Tokoro et al., 1998) when percentages are compared to WT (4.9A). Note the depletion of thymic B cell proportions after Lin^- (CD3ε, B220, TER119, Gr1) E15 WT fetal liver reconstitution. Total thymic B cell numbers are indicated (4.9B). Each point represents the thymus form an individual mouse. The bar indicates the median. ns = not significant ($p = 0.3833$). Data is representative of at least three experiments.

A

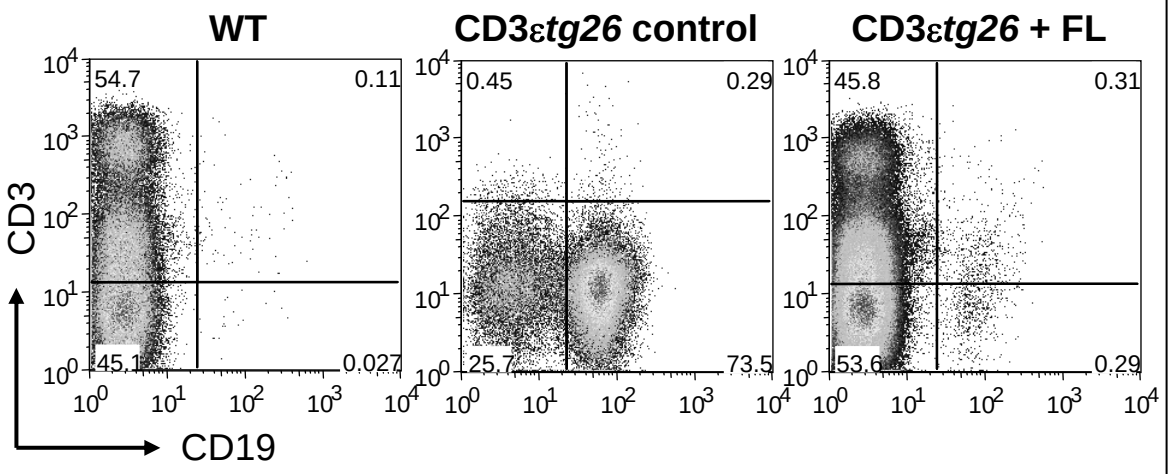
WT
CD3εtg26 control
CD3εtg26 + FL
CD3
CD19
54.7
0.11
45.1
0.027
0.45
0.29
25.7
73.5
45.8
0.31
53.6
0.29

B

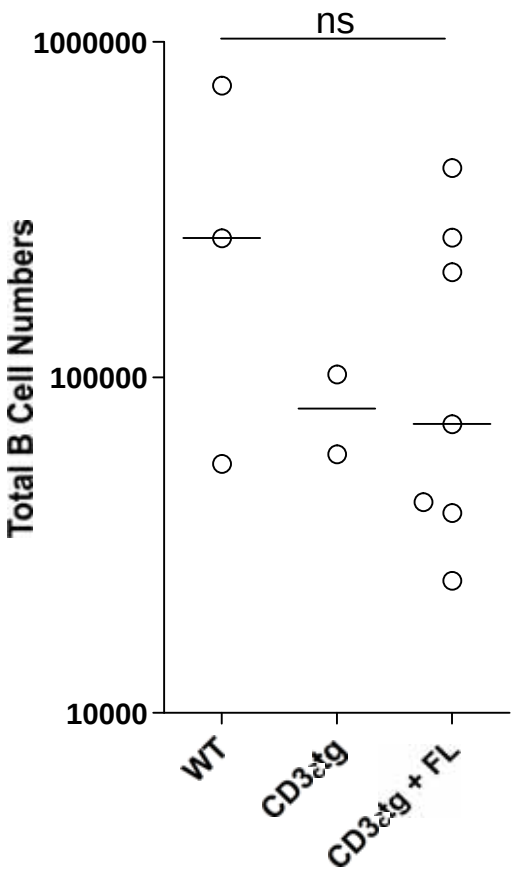
ns
1000000
100000
10000
Total B Cell Numbers
WT
CD3εtg
CD3εtg + FL

Figure 4.10 Restoration Of Normal Thymic Architecture In Reconstituted CD3ε*tg26* Mice

Thymus sections from WT, CD3ε*tg26* unreconstituted and reconstituted mice were analysed by confocal microscopy for cTEC and mTEC development and organisation using the markers Keratin 5 and Keratin 8 (4.10A) and CD205 and CD40 (4.10C). Thymocyte organisation was also analysed using CD4 and CD8 (4.10B). Note the architecture is comparable to WT in the reconstituted thymus. Scale bars represent 100μm. C: cortex, M: medulla

Another organisational parameter analysed was localisation of $CD25^+$ double negative 3 (DN3) thymocytes in the subcapsular zone, which can be clearly observed in new born (NB) thymus and is less obvious in the adult. The subcapsular region can be identified in the reconstituted CD3ε*tg26* mice (4.10D). Scale bars represent 50μm. Solid line: thymus capsule, Dotted line: subcapsular region boundary. Data is representative of at least three experiments.

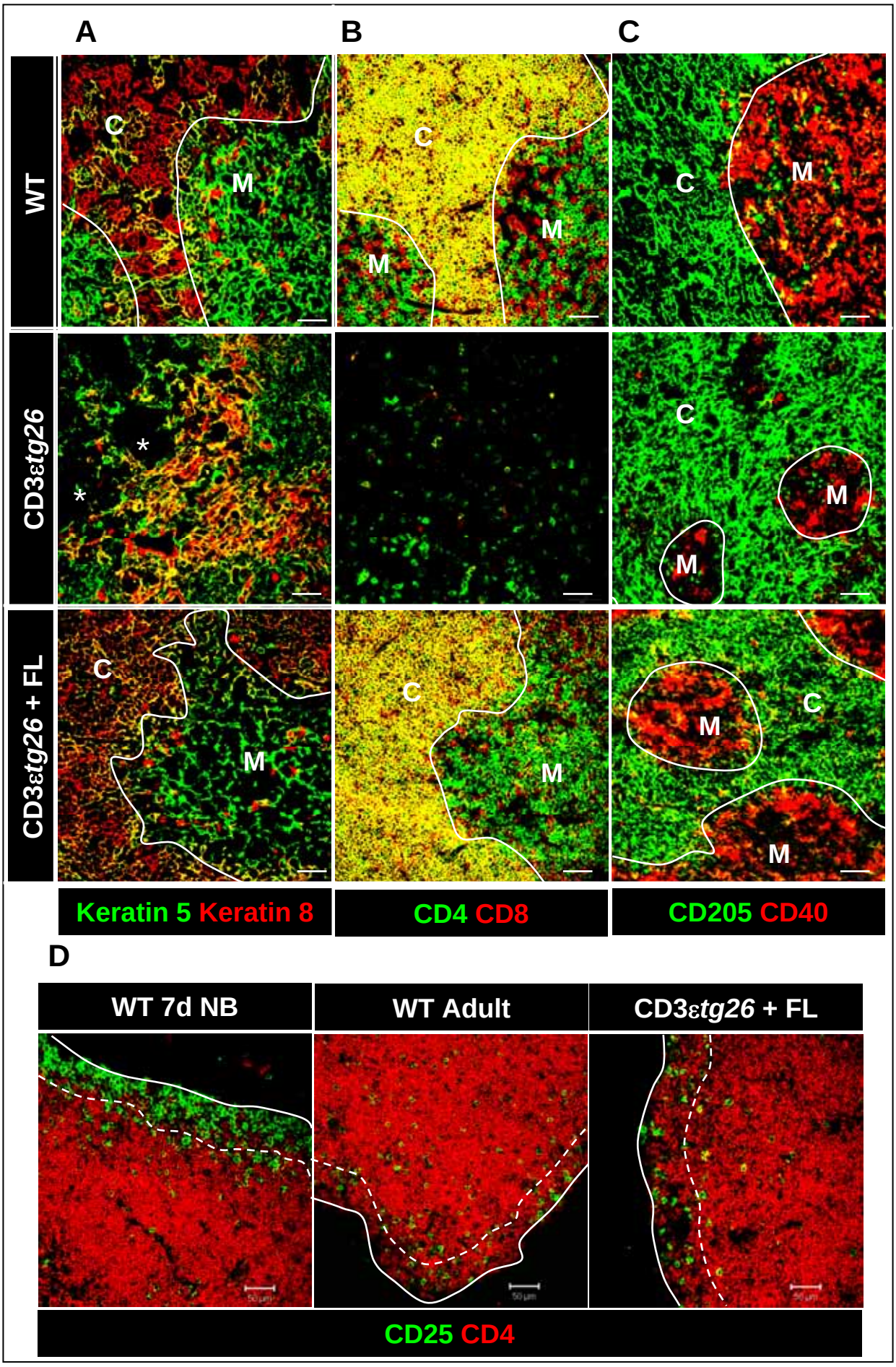
A
B
C
WT
CD3εtg26
CD3εtg26 + FL
C
M
*
Keratin 5 Keratin 8
CD4 CD8
CD205 CD40
D
WT 7d NB
WT Adult
CD3εtg26 + FL
CD25 CD4

(Figure 4.10D). These data suggest that the adult CD3ε*tg26* thymus remains receptive to thymus crosstalk despite the prolonged absence of such signals and can develop into the separate cortex, medulla and subcapsular microenvironments required to support a normal programme of T cell development.

Previous studies implied normal thymic reconstitution of adult CD3ε*tg26* mice with adult T depleted BM failed to occur, and described the occurrence of an inflammatory wasting colitis like disease 5-8 weeks after receiving the transplant (Hollander et al., 1995a). These data suggested a developmental failure of T cell tolerance mechanisms, perhaps due to defective intrathymic microenvironment initiation or maturation. Consequently analysis of two mechanisms important for T cell tolerance, namely Aire expressing mTEC and $FoxP3^+$ Treg generation were investigated as features of thymus reconstitution. Importantly, these tolerance mechanisms were established in the reconstituted CD3ε*tg26* thymus, as $Aire^+$ $K5^+$ mTECs (Figure 4.11), and $CD4^+$ $FoxP3^+$ regulatory T cells were identified within the thymus (Figure 4.12). Moreover $FoxP3^+$ Tregs were successfully exported to the periphery as they were identified in the spleen (Figure 4.13). In addition, reconstituted mice were healthy, and did not exhibit any signs of disease or weight loss at any time up to 9 weeks after receiving Lin^- FL. These data suggests that the absence of thymocyte crosstalk during fetal/neonatal periods does not preclude the establishment of cellular mechanisms of T cell tolerance, after reconstitution of the CD3ε*tg26* thymus with explanted FL cells.

4.3.3 Adult T Lineage Committed Precursors Provide The Necessary Thymus Crosstalk Signals To Establish A Functional Thymus Microenvironment

The above data has shown by restoration of T cell development within the thymus and renewing the thymus microenvironments that it is possible to successfully reconstitute the adult CD3ε*tg26* thymus. However, this is in contrast to studies by Hollander *et al,* which show that

Figure 4.11 Re-establishment Of Thymic T Cell Tolerance Mechanisms After Thymic Reconstitution

Thymus sections from WT and reconstituted CD3ε*tg26* mice were analysed by confocal microscopy for the presence of Keratin 5^+ $Aire^+$ mTECs. Note their presence in both WT and reconstituted CD3ε*tg26* mice. Scale bars represent 10μm. Data is representative of at least four experiments.

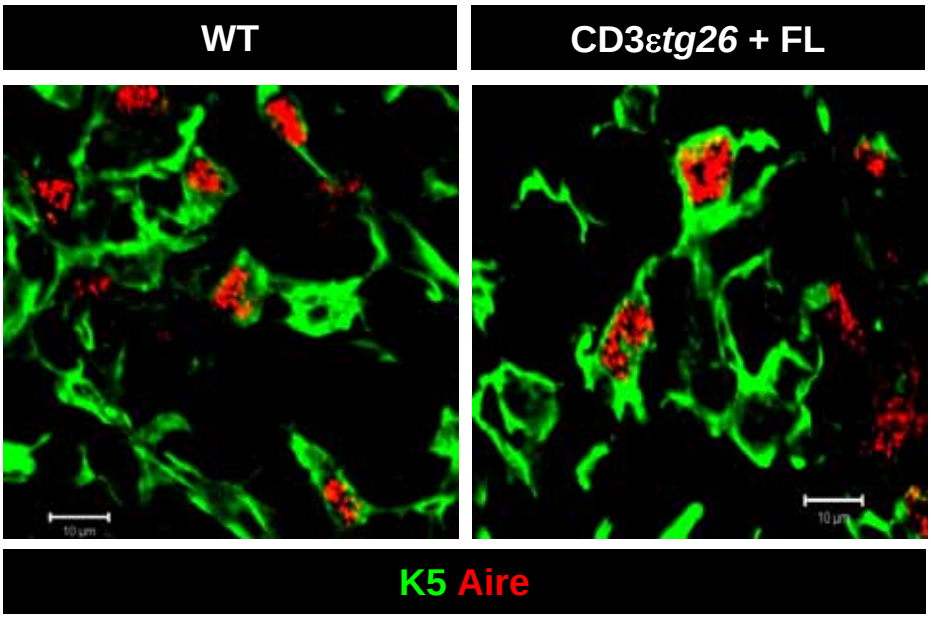
WT
CD3εtg26 + FL
10 µm
10 µm
K5 Aire

Figure 4.12 Re-establishment Of Thymic T Cell Tolerance Mechanisms After Thymic Reconstitution

Flow cytometric analysis of thymocytes isolated from WT, and reconstituted CD3ε*tg26* mice for CD4 and FoxP3 expression (4.12A). Percentages of cells within gated areas are indicated. Frozen thymus sections from WT and reconstituted CD3ε*tg26* mice were analysed by confocal microscopy for the presence of $CD4^{+}FoxP3^{+}$ regulatory T cells (4.12B). Scale bars represent 10μm. Note the presence of $FoxP3^{+}$ Treg in both WT and reconstituted CD3ε*tg26* mice. Data is representative of at least four experiments.

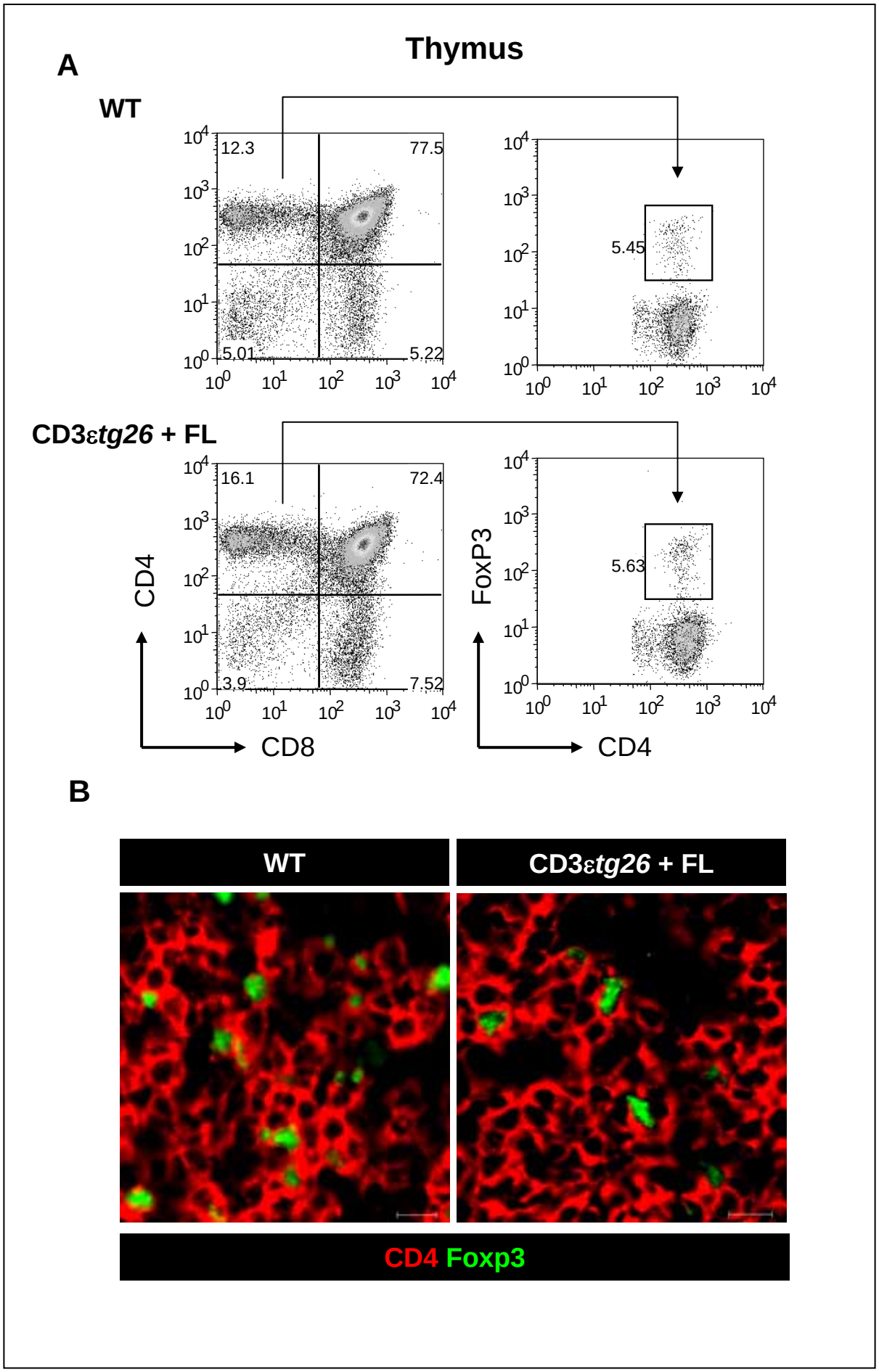
A
Thymus
WT
12.3
77.5
5.01
5.22
5.45
CD3εtg26 + FL
16.1
72.4
3.9
7.52
5.63
CD4
CD8
FoxP3
CD4
B
WT
CD3εtg26 + FL
CD4 Foxp3

Figure 4.13 Re-establishment Of Peripheral T Cell Tolerance Mechanisms After Thymic Reconstitution

Flow cytometric analysis of Splenocytes isolated from WT, and reconstituted CD3ε*tg26* mice for CD4 and FoxP3 expression (4.13A). Percentages of cells within gated areas are indicated. Spleen sections from WT and reconstituted CD3ε*tg26* mice were analysed by confocal microscopy for the presence of $CD4^{+}FoxP3^{+}$ regulatory T cells (4.13B). Scale bars represent 10μm. Note the presence of $FoxP3^{+}$ Treg in WT and reconstituted CD3ε*tg26* mice. Data is representative of at least four experiments.

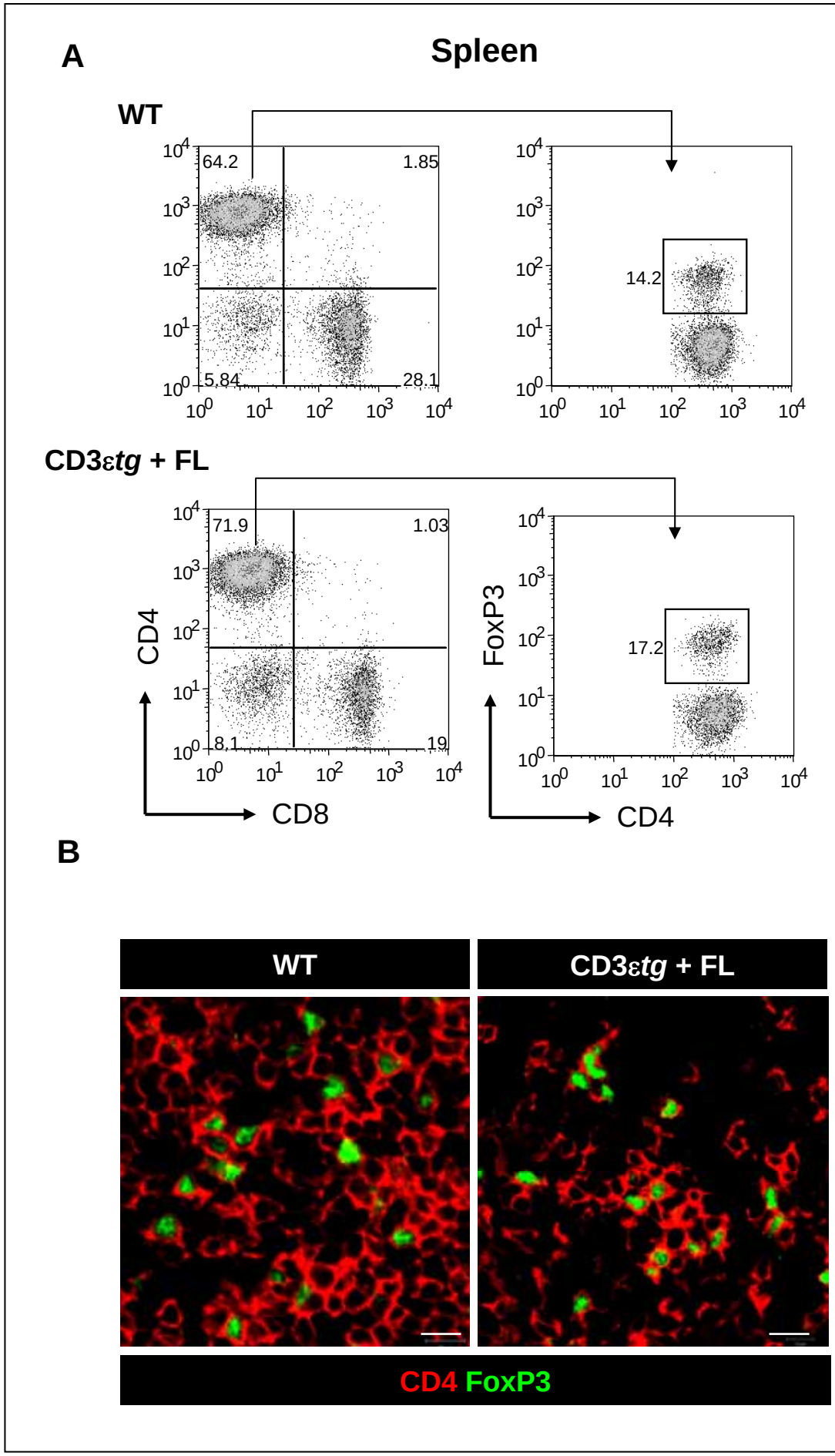
A
Spleen
WT
64.2
1.85
5.84
28.1
14.2
CD3εtg + FL
71.9
1.03
8.1
19
17.2
CD4
CD8
FoxP3
CD4
B
WT
CD3εtg + FL
CD4 FoxP3

bone marrow transplantation did not reconstitute a functional T cell compartment in adult CD3ε*tg26* mice (Hollander et al., 1995b). A possible explanation for the discrepancies between the data presented here and that of earlier studies is the differences between the sources of the progenitor populations used. Fetal liver progenitors may be more efficient at reconstituting the adult CD3ε*tg26* thymus as a result of their ability to generate fetal specific cell types such as γδ T cells (Havran and Allison, 1988) and lymphoid tissue inducer cells (Mebius and Akashi, 2000) that are able to promote successful thymus crosstalk. To investigate the possibility that adult thymocyte progenitors were less efficient than fetal progenitors at thymic reconstitution, $CD3e^-$ $CD4^-$ $CD8^-$ $CD25^+$ $CD44^-$ triple negative (TN3) progenitors that represent T lineage restricted cells (Ceredig and Rolink, 2002), were isolated from adult WT thymus and intravenously transferred into adult CD3ε*tg26* mice. This work was carried out in collaboration with G. Desanti, University of Birmingham.

The data shows that while TN3 cells can restore thymic development and significantly ($p = 010121$) increase cellularity, it is far less than the observed WT thymus cell number (Figure 4.14A). This could be due to the finite number of injected cells whereas the adult WT thymus is continually seeded with new progenitors (Foss et al., 2001). In addition, the generation of $CD4^+$ $CD8^+$ DP thymocytes and mature $CD4^+$ $CD8^-$ TCR^{hi} and $CD4^-$ $CD8^+$ TCR^{hi} SP T cells when compared to CD3ε*tg26* control mice was re-established (Figure 4.14B and C). However, the proportions of these populations were dissimilar to WT, which maybe due to the supply of T cell progenitors being exhausted, resulting in a reduced DP population and increase $CD4^+$ and $CD8^+$ populations. The mature $CD4^+$ and $CD8^+$ T cells were also able to home efficiently to peripheral locations such as splenic T zone (data not shown) as described later for fetal liver derived T cells exported from reconstituted adult CD3ε*tg26* thymus. In addition, a normal thymic architecture was suggested by the separation of DP and SP thymocytes comparable to WT

Figure 4.14 Specific Signals From Fetal Progenitors Are Not Required For Successful Thymic Reconstitution Of CD3ε*tg26* Adult Mice

CD3ε*tg26* mice were harvested at ≥5 weeks after intravenous injection with triple negative 3 (TN3) ($CD3\varepsilon^-$, $CD4^-$, $CD8^-$, $CD25^+$, $CD44^-$) adult WT thymocytes. Thymic cellularity in WT, CD3ε*tg26* control and CD3ε*tg* after TN3 transfer (4.14A) illustrates the significant increase in cellularity (*p = 0.0121). The increase in cell number is significantly less than WT cell number (*p = 0.0357). Each point represents the thymus from an individual mouse. The bar shows the median.

Thymuses were teased and analysed by flow cytometry for expression of CD4 and CD8. Representative FACS plots illustrate the CD4 and CD8 profile for WT, CD3ε*tg26* control and TN3 reconstituted CD3ε*t26g* (4.14B). Development of $CD4^+CD8^-$ TCR^{hi} and $CD4^-CD8^+$ TCR^{hi} populations were also observed (4.14C). Percentages of cells within gated areas are indicated. Data is representative of at least three experiments.

A

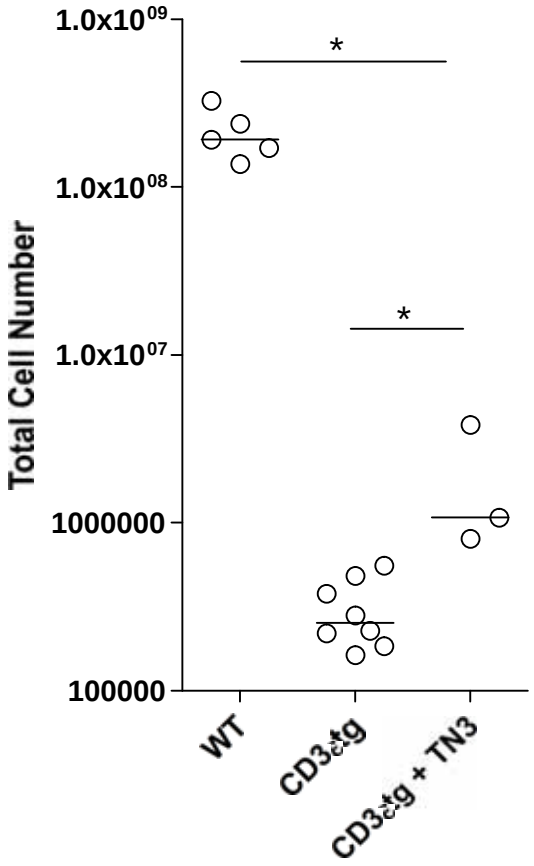
1.0x10^09
1.0x10^08
1.0x10^07
1000000
100000
Total Cell Number
*
*
WT
CD3εtg
CD3εtg + TN3

B

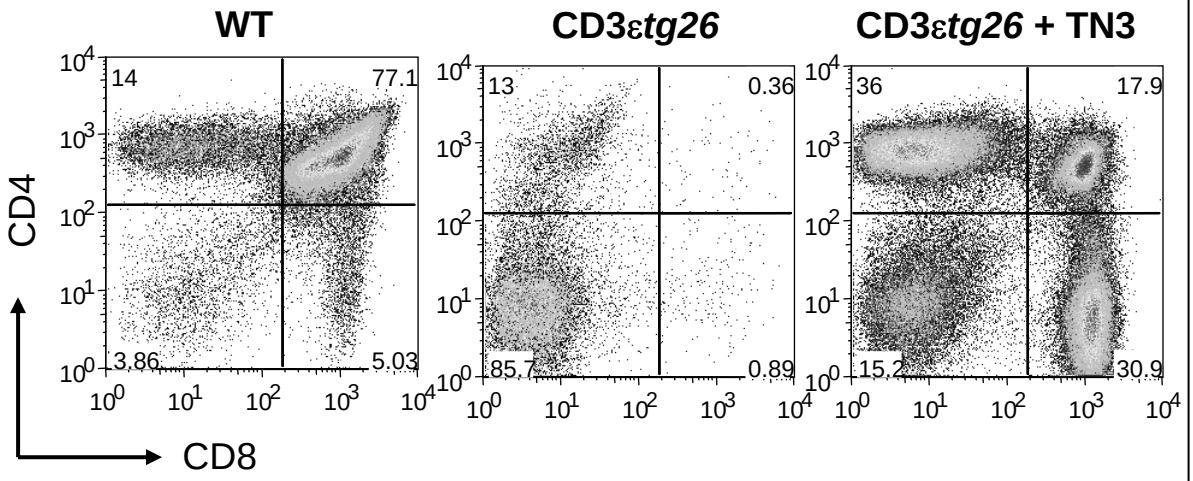
WT
CD3εtg26
CD3εtg26 + TN3
CD4
CD8
14
77.1
3.86
5.03
13
0.36
85.7
0.89
36
17.9
15.2
30.9

C

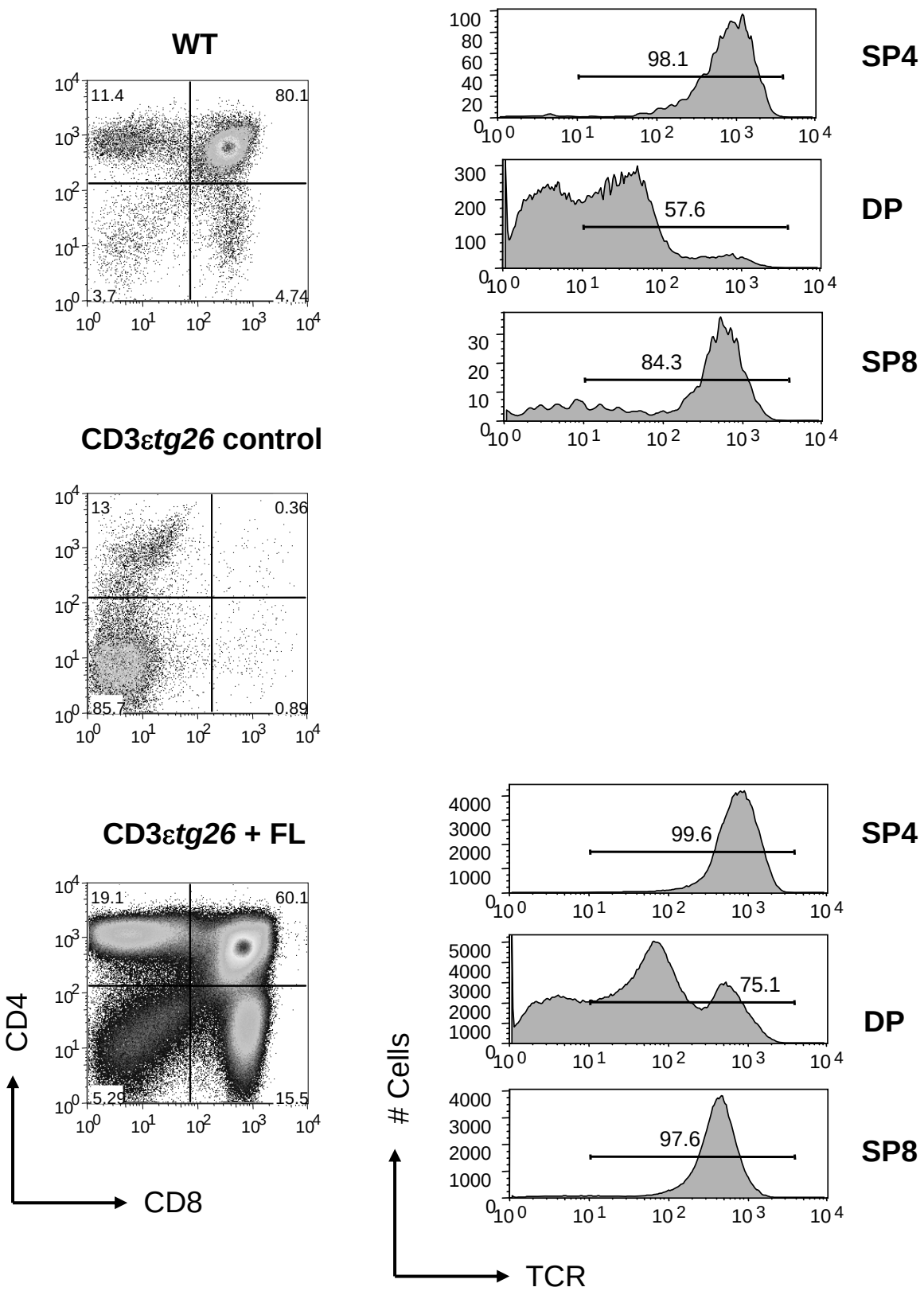
WT
11.4
80.1
3.7
4.74
CD3εtg26 control
13
0.36
85.7
0.89
CD3εtg26 + FL
19.1
60.1
5.29
15.5
CD4
CD8
98.1
SP4
57.6
DP
84.3
SP8
99.6
SP4
75.1
DP
97.6
SP8
Cells
TCR

(Figure 4.15A). Furthermore the distinct staining of the cortical and medullary markers CD205 and CD40 respectively, suggested the thymic epithelial microenvironments had been established (Figure 4.15B). Thus TN3, T lineage committed cells have the capacity to successfully reconstitute adult CD3ε*tg26* thymus arguing that fetal progenitor specific signals are not required to rescue thymic function following a prolonged absence of thymus crosstalk.

4.3.4 Successful Thymus Export And Homing To Secondary Lymphoid Tissue

Mature thymocyte export to the periphery is a prerequisite to a functional immune system. Therefore, to assess whether the newly generated T cells from the reconstituted thymus were being successfully exported to the periphery, the composition of the secondary lymphoid component was examined. In *Rag*$^{-/-}$γc$^{-/-}$ mice both T and B cells are absent due to the absence of recombinase activating gene (*Rag*) 2, which results in the rearrangement of both the immunoglobulin and the T cell receptor genes being abolished (Klug et al., 2002; Takahama, 2006). Consequently this enables the presence of recently exported thymocytes to be identified easily. Flow cytometric analysis of secondary lymphoid components from control *Rag*$^{-/-}$γc$^{-/-}$ and FL injected *Rag*$^{-/-}$γc$^{-/-}$ mice revealed interesting differences. While E15 Lin^{-} FL could restore the CD19^{+} and CD3^{+} compartments, the proportion of CD3^{+} cells were reduced when compared to WT (Figure 4.16). However, when the proportions of CD4^{+} and CD8^{+} T cells were analysed within the CD3^{+} population, the proportions were comparable to WT (Figure 4.16). Together these data suggest that the T cells developing within the restored thymus microenvironment are being efficiently exported to the peripheral lymphoid organs.

In addition, it was of interest to assess the peripheral arrangement of the FL derived T and B cells as their segregation and organisation within secondary lymphoid organs is required to raise efficient immune responses to T-dependent antigen (Glanville et al., 2009). Immunohistochemical analysis of splenic white pulp revealed the absence of site specific

Figure 4.15 Restoration Of Normal Thymic Architecture In TN3 Reconstituted CD3ε*tg26* mice

Thymus sections from WT, CD3ε*tg26* unreconstituted and reconstituted mice were analysed by confocal microscopy for cTEC and mTEC development and organisation using the markers CD4 and CD8 (4.15A). Thymocyte organisation was also analysed using CD205 and CD40 (4.15B). Note the architecture is comparable to WT in the reconstituted thymus. Scale bars represent 100μm. C: cortex, M: medulla.

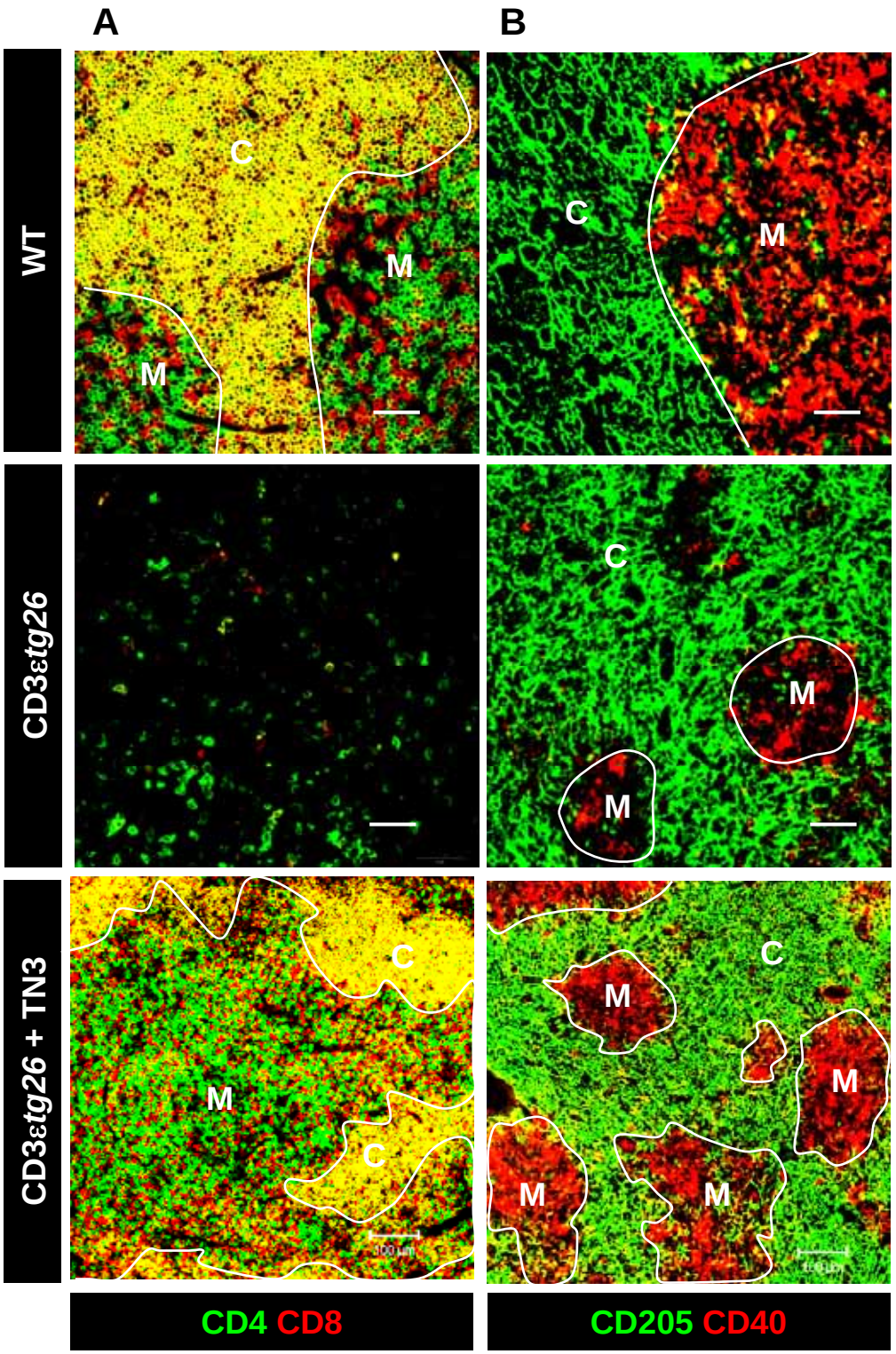
A
B
WT
CD3εtg26
CD3εtg26 + TN3
C
M
CD4 CD8
CD205 CD40

Figure 4.16 T Cell Development In The Reconstituted Thymus Includes Thymic Emigration To The Periphery

Splenic tissue from reconstituted *Rag*$^{-/-}$γc$^{-/-}$ mice was analysed by flow cytometry for expression of CD3, CD19, CD4 and CD8. Note the presence of CD3^{+}CD4^{+} and CD3^{+}CD8^{+} T cells in the reconstituted but not the *Rag*$^{-/-}$γc$^{-/-}$ control spleen Percentages of cells within gated areas are indicated. Data is representative of at least three experiments.

Host Spleen

WT

Total

CD3 Gated

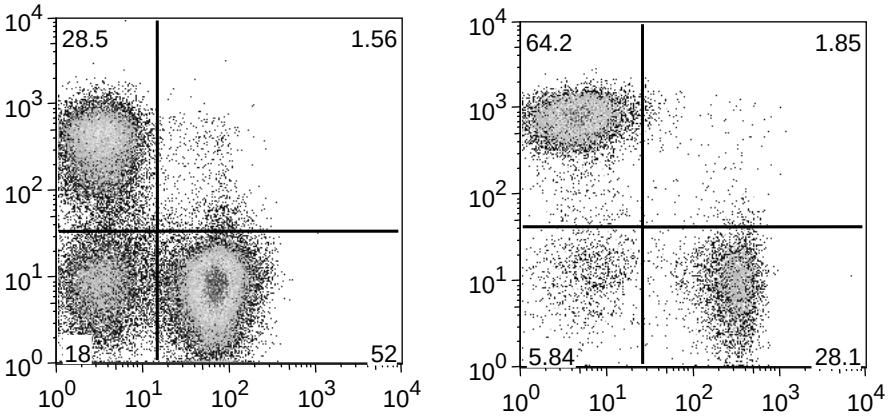

***Rag*$^{-/-}$γc$^{-/-}$**

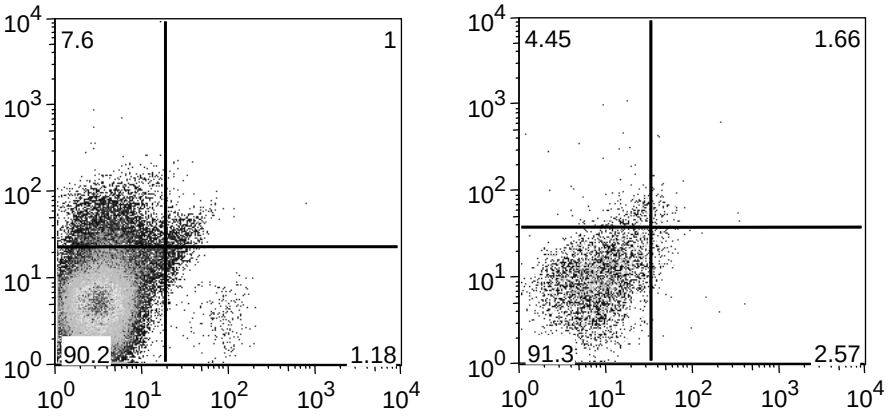

***Rag*$^{-/-}$γc$^{-/-}$ + FL**

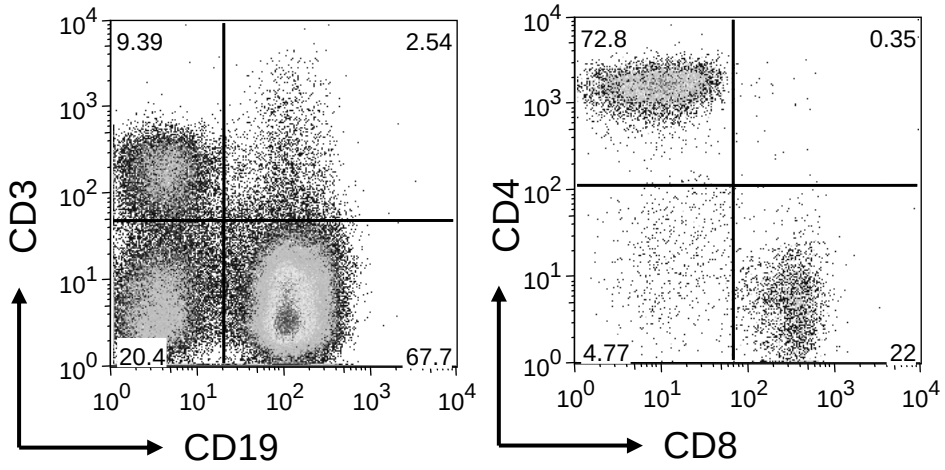

expression of the T zone stromal marker gp38 (Withers et al., 2007) (Figure 4.17A), $CD3^+$ T cells (Figure 4.17B) and the homeostatic chemokine Ccl21 (Ngo et al., 1999) (Figure 4.17C) within unreconstituted *Rag*$^{-/-}\gamma c^{-/-}$ splenic T zone however, these compartments were restored in *Rag*$^{-/-}\gamma c^{-/-}$ mice receiving Lin^- FL when compared to the T zone of WT spleen. Importantly, recruitment of T cells to the newly established $Ccl21^+$ T zone areas was observed in injected *Rag*$^{-/-}\gamma c^{-/-}$ mice suggesting that the presence of T cells is necessary for the expression of gp38 and Ccl21. In addition, the spatial localisation of B cells in white pulp areas was determined using anti B220 or IgM antibody staining, which enabled the clear visualisation of white pulp B cell compartments that are absent from control *Rag*$^{-/-}\gamma c^{-/-}$ mice. This analysis also showed successful establishment and organisation of the B cell areas in reconstituted *Rag*$^{-/-}\gamma c^{-/-}$ mice, similar to those observed in WT mice (Figure 4.17). As previously mentioned *Rag*$^{-/-}\gamma c^{-/-}$ control mice do not possess any such defining features due to the inability to generate mature T and B cells, however interestingly, small numbers of $CD3^-CD4^+$ lymphoid tissue inducer cells were identified in the rudimentary white pulp areas (Figure 4.17B) (Withers et al., 2007). Together these data are suggestive of successful thymic emigration of mature T cells and their efficient homing to the correct peripheral locations after thymus reconstruction in *Rag*$^{-/-}\gamma c^{-/-}$ mice after receiving Lin^- FL.

In addition, reconstitution of the peripheral T cell compartment was also assessed by flow cytometric analysis of secondary lymphoid tissue from reconstituted CD3ε*tg26* mice. Due to an unknown mechanism, presumably due to random incorporation of multiple copies of the human CD3ε gene, CD3ε*tg26* mice lack T cells (Wang et al., 1995). Consequently $CD3^+$ cells are absent in CD3ε*tg26* control mice, conversely CD3ε*tg26* mice that received Lin^- FL contained a $CD3^+$ population albeit a smaller proportion compared to WT. Importantly both $CD3^+CD4^+$ and $CD3^+CD8^+$ T cell compartments were observed in reconstituted CD3ε*tg26* mice although in

Figure 4.17 Establishment Of And T Cell Entry Into The Splenic T-Zone Occurs In Reconstituted *Rag*$^{-/-}\gamma c^{-/-}$ Mice

Frozen serial sections of splenic tissue from reconstituted *Rag*$^{-/-}\gamma c^{-/-}$ mice was analysed by confocal microscopy. The presence of $CD3^+$ T cells within $Ccl21^+$ $Gp38^+$ T zones and IgM^+ and $B220^+$ B cells within the B cell area of the white pulp can be seen. Note the absence of Gp38 (4.17A) and Ccl21 (4.17C) expression in the unreconstituted *Rag*$^{-/-}\gamma c^{-/-}$. In addition the presence of $CD4^+CD3^-$ cells can be identified in unreconstituted *Rag*$^{-/-}\gamma c^{-/-}$ mice, which represent lymphoid tissue inducer cells (Withers et al., 2007). Scale bars represent 100μm. Data is representative of at least three experiments.

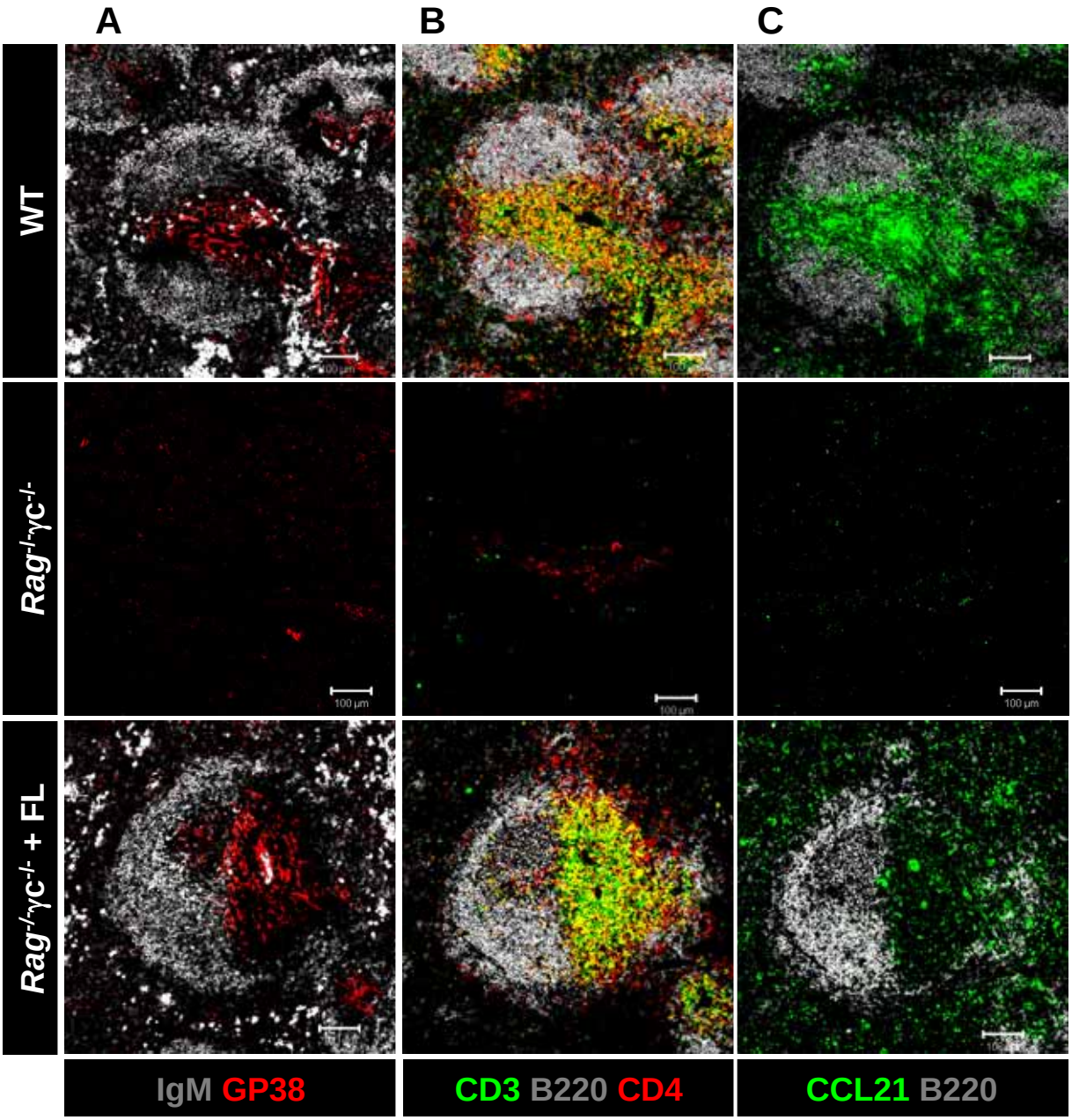
A
B
C
WT
Rag-/-γc-/-
Rag-/-γc-/- + FL
100 µm
IgM GP38
CD3 B220 CD4
CCL21 B220

reduced proportions to WT (Figure 4.18). Furthermore, successful recruitment of $CD3^+$ T cells to the normally T cell deficient but established T zone of the CD3ε*tg26* control spleen was observed (Figure 4.19). Together these data suggest that complete T cell production is occurring within the reconstituted CD3ε*tg26* thymus as identified by successful thymic emigration and effective T cell homing to the correct peripheral locations despite the prolonged absence of thymus crosstalk signals.

Figure 4.18 T Cell Development In The Reconstituted Thymus Includes Thymic Emigration To The Periphery

Splenocytes isolated from reconstituted CD3ε*tg26* mice, ≥5 weeks after receiving the Lin^- FL, were analysed by flow cytometry for expression of CD3, CD19, CD4 and CD8. Note the presence of $CD3^+CD4^+$ and $CD3^+CD8^+$ T cells in WT and reconstituted mice but their absence in CD3ε*tg26* control mice. Percentages of cells within gated areas are indicated. Data is representative of at least three experiments.

Host Spleen

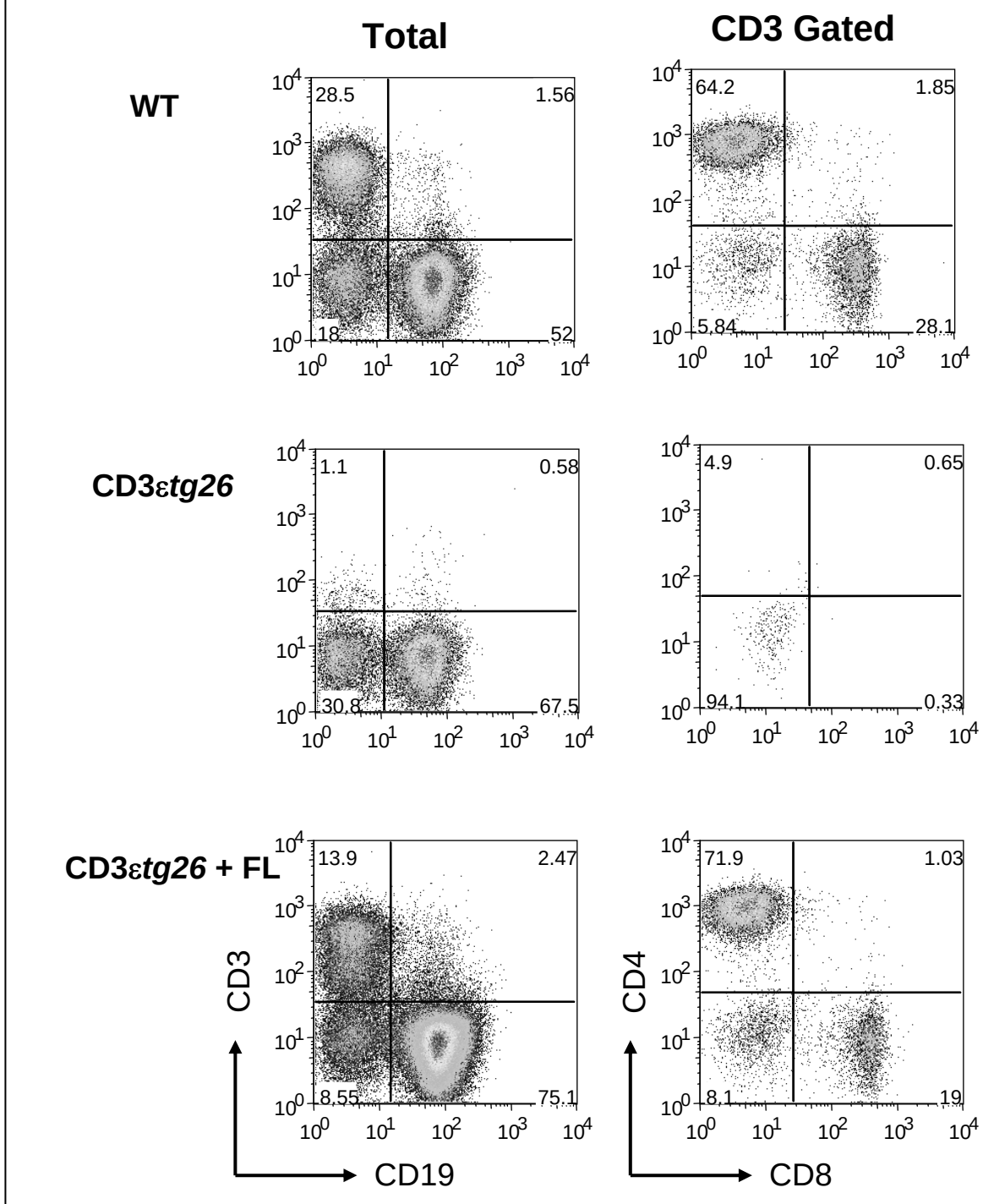
Total
CD3 Gated
WT
28.5
1.56
18
52
64.2
1.85
5.84
28.1
CD3εtg26
1.1
0.58
30.8
67.5
4.9
0.65
94.1
0.33
CD3εtg26 + FL
13.9
2.47
8.55
75.1
71.9
1.03
8.1
19
CD3
CD19
CD4
CD8

Figure 4.19 T Cell Migration To The Splenic T-Zone Occurs In Reconstituted CD3ε*tg26* Mice

Frozen serial sections of splenic tissue from reconstituted CD3ε*tg26* mice were analysed by confocal microscopy. The presence of $CD3^+$ T cells within the $Ccl21^+$ $Gp38^+$ T zone of the white pulp areas can be seen in WT and reconstituted mice. Note the presence of $CD4^+CD3^-$ cells (4.19B) and the expression of Ccl21 (4.19C) in the unreconstituted CD3ε*tg* mice, the latter representing lymphoid tissue inducer cells (Withers et al., 2007). Scale bars represent 100μm. Data is representative of at least four experiments.

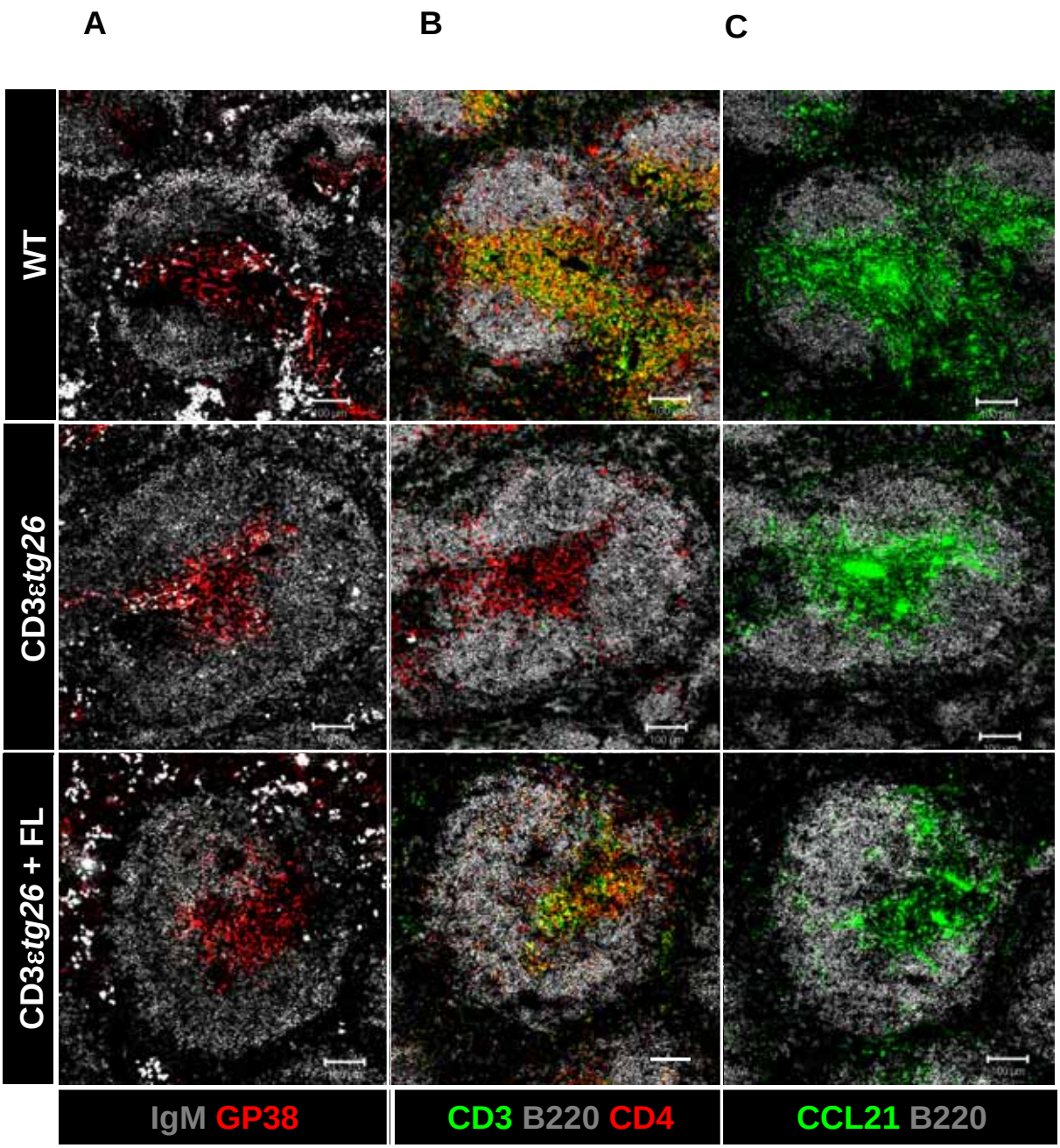
A
B
C
WT
CD3εtg26
CD3εtg26 + FL
IgM GP38
CD3 B220 CD4
CCL21 B220

4.4 Discussion

4.4.1 Successful Thymic Reconstitution

The establishment of differentiated epithelial microenvironments in the thymus is indispensable for development of a self-tolerant T cell repertoire (Rossi et al., 2007a). In turn the integrity of thymic microenvironments is thought to depend on the physical presence of developing thymocytes and the instructive signals they provide (Boehm et al., 2003; van Ewijk et al., 2000). This is clearly indicated by the compromised thymic architecture in mice where T cell development is blocked at distinct developmental stages such as *Rag*$^{-/-}$, *Rag*$^{-/-}$γc$^{-/-}$ and CD3ε*tg26* mice (Figure 4.2) and this process of reciprocal signalling has been termed "thymus crosstalk". While thymic epithelial cell subsets are beginning to be defined, relatively little is understood about the mechanisms and regulation of their development. However, it is currently understood that the development of cortical thymic epithelium is a prerequisite to medullary epithelial cell development and that initiation of successful cTEC development requires interactions between DN3 thymocytes and bipotent epithelial progenitors within a distinct developmental window (Figure 4.1) (Hollander et al., 1995b; van Ewijk et al., 2000). Furthermore, failure of crosstalk to occur during this stage is thought to render the thymus refractory to subsequent crosstalk signals and incapable of supporting effective T cell development and selection; illustrated by BM reconstitution of CD3ε*tg26* mice resulting in the aberrant production of T cells that displayed an autoimmune phenotype leading to the induction of an inflammatory colitis-like disease (Hollander et al., 1995a). These data suggested a failure of the thymic microenvironment to support T cell selection and/or failure of peripheral tolerance mechanisms after prolonged absence of thymus crosstalk signals (Hollander et al., 1995a). Understanding and characterising the process involved in the generation of T cell and thymus epithelial cell development is central to establishing new approaches for the correction of T cell

lymphopenia (Hakim and Gress, 2005). Therefore, the aim of this chapter was to reinvestigate the requirement for thymus crosstalk to occur during embryonic development. Based on the data presented in this chapter, the absence of thymus crosstalk in the fetus does not preclude haematopoietic induction of a functional thymus in the adult (Roberts et al., 2009).

To begin this investigation, a model system was required to test the ability of FL derived T cell precursors to restore T cell development and the thymus architecture. To enable restoration to be characterised the non-manipulated model had to have atypical T cell development and thymic architecture. The *Rag*$^{-/-}$γc$^{-/-}$ mouse was chosen because the absence of the common gamma chain (γc) results in the lack of intact intracellular signalling required for thymocyte growth and differentiation, which consequently reduces thymic cellularity (Klug et al., 2002; Rodewald et al., 1997). In addition, the null mutation in the *Rag* locus prevents the rearrangement of the T-cell receptor genes, resulting in a profound block at the DN3 stage of early T cell development (Klug et al., 2002; Takahama, 2006). Despite *Rag*2$^{-/-}$γc$^{-/-}$ thymuses having a TEC phenotype similar to that of the severely hypoplastic thymus in CD3ε*tg26* mice, which has a disorganised TEC predominantly composed of K8^{+}K5^{+} TECs (Klug et al., 2002), in contrast to CD3ε*tg26* thymus the *Rag*2$^{-/-}$γc$^{-/-}$ thymic epithelial compartment is organised into a three-dimensional structure (Klug et al., 2002). This difference in thymic epithelial cell structure and the presence of DN1 thymocytes suggested that the *Rag*$^{-/-}$γc$^{-/-}$ thymus could be restored, allowing validation of FL transfer for thymus reconstitution. This prediction was supported by previous studies in *Rag*$^{-/-}$ mice, which display a block at the DN3 stage of T cell development, reporting restoration of thymic architecture and TEC development (van Ewijk et al., 2000).

As anticipated the introduction of thymocyte precursors into *Rag*$^{-/-}$γc$^{-/-}$ resulted in successful thymus reconstitution, illustrated by a normal CD4 and CD8 coreceptor profile on thymocytes suggesting normal intrathymic T cell development. In addition, CD4^{+}CD8^{+} DP

thymocytes and $CD4^+CD8^-$, $CD4^-CD8^+$ SP thymocytes were segregated, suggesting the presence of cortical and medullary thymic epithelium respectively. The restoration of the cortical and medullary epithelium was confirmed by distinct staining patterns of epithelial markers. The presence and correct localisation of $CD4^+TCR^{hi}$ and $CD8^+TCR^{hi}$ T cells in secondary lymphoid organs illustrated that mature T cells were developing within the reconstituted thymus and were being efficiently exported to the periphery. Having established the intravenous transfer of fetal liver derived precursors into non-irradiated adult hosts, migrate to and successfully reconstitute the $Rag^{-/-}\gamma c^{-/-}$ thymus, their ability to restore thymic function after a prolonged and complete absence of thymus crosstalk was investigated using CD3ε*tg26* mice.

CD3ε*tg26* mice express a high copy number of the human CD3ε gene and sustain an early block in T cell development. The observed block in T cell development is dependent upon the over expression of the transgenic protein early in fetal development. Over expression (40-60 copies) of the human derived CD3ε transgene begins at or prior to E13 (Tokoro et al., 1998; Wang et al., 1997) and copy numbers of the transgene correlate with the expression levels of the CD3ε transgenic proteins (Wang et al., 1995). The effect of abrogated T cell ontogeny is possibly the result of aberrant signal transduction in pre-thymocytes preventing intracellular TCRβ expression and thus leading to a strong apoptotic signal (Wang et al., 1995; Wang et al., 1997). The apoptotic state of CD3ε*tg26* thymocytes was illustrated by typical apoptotic features such as, small size, electron dense nucleus and the presence of vacuoles the cytoplasm (Wang et al., 1995). Consequently CD3ε*tg26* mice display the earliest block in T cell development and thymus crosstalk signals ordinarily provided by immature thymocytes are absent, which is the reason CD3ε*tg26* mice were chosen.

Our data has shown that it is possible to establish new T cell development within a thymus that has not previously been populated by even the most immature thymocytes. This was

illustrated by an increase in thymus size and cellularity and the production of mature TCR^{hi}, single positive CD4 and CD8 thymocytes via the conventional DN→DP→SP developmental pathway in CD3ε*tg26* mice injected with Lin^- FL. Interestingly, the mechanism involved in the aberrant TEC development in CD3ε*tg26* mice, although currently unclear, has been reported to be most likely due to a defect in the lymphoid precursors rather than the thymic epithelium (Tokoro et al., 1998; Wang et al., 1995). Therefore providing WT precursors to an adult CD3ε*tg26* mouse should restore thymus function. In our study the proportions of $CD4^+CD8^+$ DP and $CD4^+CD8^-$, $CD4^-CD8^+$ SP thymocytes were relatively normal as compared to CD3ε*tg26* control mice. In support of this, an earlier study by Rodewald and colleagues, did not report a requirement for fetal thymus crosstalk in c-$kit^{-/-}\gamma c^{-/-}$ mice where thymocytes and T cell development are virtually absent (Rodewald and Fehling, 1998; Rodewald et al., 1997). However previously Hollander *et al* reported reduced proportions of $CD4^+CD8^+$ DP and the respective increase in $CD4^+CD8^-$, $CD4^-CD8^+$ SP thymocyte proportions (Hollander et al., 1995b). This discrepancy could be explained by the different number of precursor cells being introduced into host CD3ε*tg26* mice and that these eventually become exhausted at different times as they mature into T cells. This is supported by studies where intravenous transfer of BM established that a cohort of haematopoietic progenitors the thymus receives from the blood, maintains thymocyte production for a 6-7 week period (Donskoy and Goldschneider, 1992). Hollander *et al* found that donor derived peripheral T cells displayed an activated phenotype ($CD69^+CD62L^-$) and that they were severely deficient at responding to allogeneic splenocytes (Hollander et al., 1995b). Therefore, it would be interesting to investigate the activation status of the newly generated T cells from FL derived progenitors in the system presented here and their ability to raise an immune response in future studies.

In addition, Hollander *et al* reported only partial regrouping of cortical and medullary epithelial cells and a continuous lack of discrete areas in reconstituted CD3ε*tg26* mice (Hollander et al., 1995b). Furthermore it has been shown *in vitro* that normal T cell development can occur in the absence of a normal thymic architecture (Hare et al., 1999b) therefore, although normal T cell development in FL reconstituted CD3ε*tg26* mice was apparent, it was of interest to investigate whether the normal thymus microenvironment had been restored. The typical structure of the CD3ε*tg26* thymus is cystic due to the abnormal two-dimensional (2D) structure of the epithelium and the presence of at least three types of 'classical' epithelial cells, usually found in other tissues for example cells with microvilli (as in the gastrointestinal tract) (van Ewijk et al., 2000). Importantly in contrast to studies performed by Hollander *et al* this cystic structure was absent from the FL reconstituted CD3ε*tg26* thymus and immunohistochemical analysis revealed the DP and SP thymocytes were residing in separate thymic compartments suggestive of the presence of medullary and cortical epithelial cells. In addition, the expression of epithelial cell markers revealed an independent staining pattern, confirming the presence of descrete groups of cortical and medullary thymic epithelium.

Interestingly, when the microenvironments of control uninjected, CD3ε*tg26* mice were analysed with CD205 and CD40 for cortical and medullary separation respectively, a distinct staining pattern was observed to that seen using K8 and K5. Keratin staining in CD3ε*tg26* mice illustrates the disorganised nature of the thymic epithelium (Hollander et al., 1995b), however, $CD205^{+}CD40^{-}$ and $CD205^{-}CD40^{+}$ staining revealed discrete areas, which may represent rudimentary, cortical and medullary microenvironments that are devoid of developing thymocytes. This difference may suggest that patterns of keratin expression in TEC subsets represent their physical organisation rather than their lineage commitment. Especially as previous studies in $Rag^{-/-}$ mice, which display a block at the DN3 stage of T cell development,

have revealed evidence for the occurrence of initial thymic epithelium patterning, in the absence of mature thymocyte crosstalk (Gray et al., 2006; Shakib et al., 2009).

It is important to note that the previous CD3ε*tg26* reconstitution studies that failed to establish T cell development or a normal thymic architecture, utilised an allogeneic donor-host combination, where T cell depleted bone marrow (BM) from C57Bl/6xCBA/J (H-$2^b x^k$) filial 1 (F1) adult mice was used as a source of thymocyte progenitors (Hollander et al., 1995a; Hollander et al., 1995b). Consequently, residual T cells in the F1 inoculum could be responsible for the experimental outcome. Alternatively this may indicate a fundamental difference between fetal and adult thymic progenitors and the crosstalk signals they are able to provide, rather than a difference in the plasticity of the fetal or adult thymic epithelium. The differences in crosstalk signals may be explained by the ability of fetal liver progenitors to generate fetal specific and unique cell types such as fetal γδ T cells (Hayday, 2000) that play important roles in conditioning the thymus to support efficient T cell development, the molecular players of which are yet to be determined (Bhandoola et al., 2007). To investigate this, adult triple negative 3 (TN3) cells were transferred into adult CD3ε*tg26* mice and successful thymus reconstitution with adult T lineage committed cells was also achieved, arguing against the need for specific fetal progenitor derived signals for the restoration of thymic function.

As Hollander *et al* reported the development of a severe wasting disease after 5 weeks, in BM reconstituted CD3ε*tg26* mice, it was concluded that self tolerance mechanisms were unable to develop and was another example of failed thymus reconstitution in these mice (Hollander et al., 1995a). However, out of the nine CD3ε*tg26* mice that received fetal liver transfers presented here, only one began to show signs of illness, namely weight loss and had to be sacrificed. Upon post-mortem a shortening and thickening of the large bowl was observed suggestive of a colitis like disease however, this may not have been the cause of the complaint. Therefore, these data

argue against the aberrant development of cellular tolerance mechanisms. Furthermore, two different cellular tolerance mechanisms, specifically FoxP3$^+$ Tregs and Aire$^+$ mTECs, were identifiable within the host mice at least 5 weeks after fetal liver transfer. The differences observed between this study and the previous studies with CD3ε*tg26* thymus reconstitution may be explained by the treatment of the host mice with either 5-flurouracil or sublethal irradiation before transplantation. Questions have been raised as to the certainty of the long held assumption that TECs are relatively radioresistent, due to the finding that medullary TECs are highly proliferative (Gray et al., 2007; Rossi et al., 2007b). Therefore it is possible that preconditioning could damage the thymic microenvironment as previously reported and perturb thymus reconstitution, instead promoting inflammation (Adkins et al., 1988; Chung et al., 2001). This is also supported by the previous reports of successful reconstitution of fetal CD3ε*tg26* thymus, where thymocyte progenitors were transferred *in utero* or intravenously transferred into adult CD3ε*tg26* that had previously received a fetal CD3ε*tg26* thymus graft under their kidney capsule. The embryonic thymuses were not subjected to any preconditioning and developed into normal mature thymuses, displaying normal T cell development and a normal thymus architecture (Hollander et al., 1995b). The data presented in this study supports the idea that TECs are sensitive to radiation, resulting in their loss and therefore the subsequent defects in thymocyte differentiation and tolerance (Gray et al., 2007). Therefore it would be of interest to re-evaluate the reconstitution potential of adult BM derived thymocyte precursors to reconstitute adult CD3ε*tg26* thymus without pre-treatment with either 5-flurouracil or sublethal irradiation. Together the data presented in this study suggest that there is no requirement for thymic crosstalk signals to be restricted to a developmental window, and leads to the proposal of a new model for mTEC and cTEC formation where thymic epithelial cells remain receptive to thymocyte crosstalk signals up until adulthood (Figure 4.20).

Figure 4.20 Proposed Model For mTEC And cTEC Establishment

Currently it is thought that initial cortical and medullary epithelial cell patterning occurs within the fetus without the requirement for inductive signals from haematopoietic cells. The further development of the rudimentary medullary and cortical areas requires instructive signals that are not restricted to an early developmental window.

mTEC, medullary thymic epithelial cells. cTEC, cortical thymic epithelial cells. Imm, immature, pTECp, bipotent thymic epithelial cell progentior.

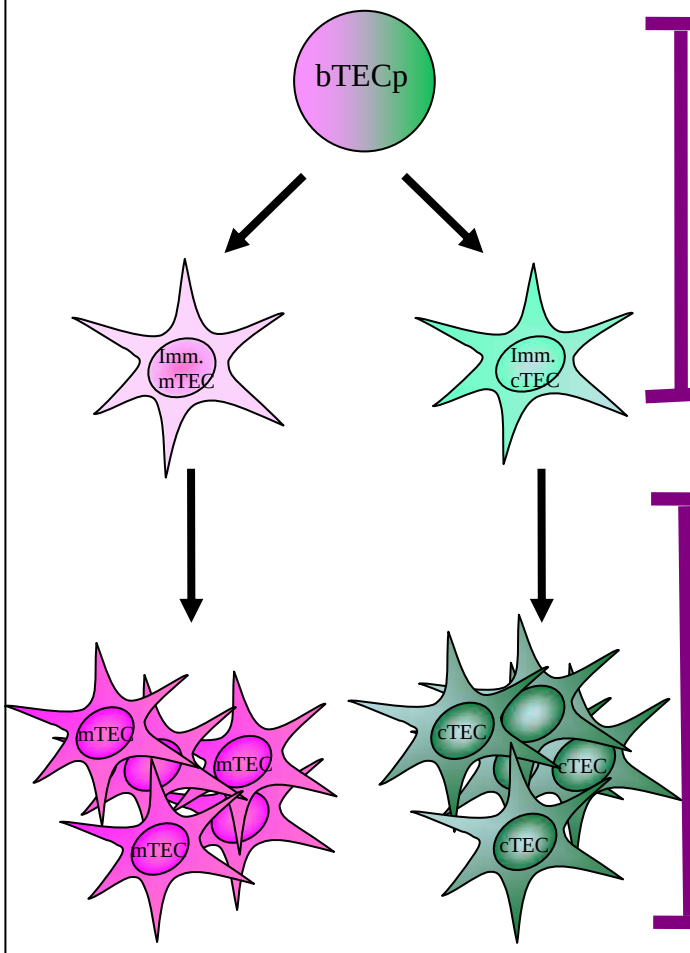

TEC specification

- **Occurs within the embryo**
- **Does not require inductive signals from haematopoietic cells**

Klug *et al.* JI 2002
Jenkinson *et al.* MOD 2005

cTEC/mTEC Development

- **Can occur throughout life**
- **Requires inductive signals from T cells**

Roberts *et al* EJI 2009

CHAPTER 5: ANALYSIS OF A SINGLE COHORT OF LYMPHOID PROGENITORS REVEALS NICHE REGULATION OF EARLY T CELL DEVELOPMENT

5.1 Introduction

Long-term self-renewing potential is not a property of intrathymic progenitors (Goldschneider et al., 1986; Wallis et al., 1975). Consequently, the recruitment of haematopoietic progenitors is required to continuously colonise the thymic microenvironment for efficient T cell generatation (Anderson et al., 2006; Petrie, 2003). Seeding of the thymus with lymphoid progenitor cells occurs as early as embryonic day 11.5 (E11.5) in mice, the eighth week of gestation in humans, and is mediated by at least two different pathways: the vasculature-independent pathway, and the vasculature-dependent pathway (Hollander et al., 2006; Liu et al., 2006; Takahama, 2006). Interestingly, thymus seeding is not a continuous event, but a periodic and gated event that occurs in waves (Foss et al., 2001; Guidos, 2006). This is thought to be because the thymus is only periodically receptive to seeding from the circulation, suggesting limiting numbers of niches, the repletion of which prevents further colonisation until niche vacancy (Bhandoola et al., 2003; Lind et al., 2001).

Since it was realised the thymus did not have self-renewing capacity, the nature of the cells that seed the thymus has been questioned and has long been disputed (Adkins et al., 1987; Shortman and Wu, 1996). If they are T cell committed the question remains as to when the commitment occurred, prethymically or intrathymically? Importantly, an understanding of the developmental steps linking HSCs to T cells is crucial for understanding the T cell defects in aging, the progression of malignant transformation in T lineage cells and improving T cell reconstitution after immunotherapy or BM transplantation for example (Bhandoola et al., 2003). In addition, it is interesting to establish whether the thymic environment has a dual role that concerns the commitment of multipotent progenitors to the T cell lineage and their differentiation into T cells or whether its major task is to support the growth and differentiation of T committed precursors (Kawamoto et al., 1998).

One of the best ways to resolve the nature versus nurture question is to ascertain the lineage potential of thymus seeding cells before thymus entry, that is while still in the bone marrow and/or blood (Petrie and Kincade, 2005). However, characterisation of the progenitors migrating into the thymus to produce T cells has been one of the most basic problems (Kawamoto et al., 1998). Identification of true T cell progenitors is made difficult by the lack of uniform definitions generated by various research groups (Petrie and Kincade, 2005). In addition their frequency in circulation is very low and consequently only a small number can be isolated (Donskoy et al., 2003; Wright et al., 2001), which has necessitated the use of immunodeficient or irradiated recipient mice for *in vivo* experiments. However, the use of such conditioned recipient mice, can lead to inaccurate conclusions due to the creation of artificial conditions by radiation damage, generating structural changes and thus creating new progenitor niches or the loss of competition for existing niches within the host thymus (Bhandoola et al., 2007). Furthermore there is little evidence to suggest that such cells identified in the bone marrow/blood actually home to the thymus or efficiently make T cells under normal circumstances (Petrie and Kincade, 2005). Therefore it is important to assess migration to the thymus as it separates physiological T cell precursors from other progenitors with T lineage potential (Bhandoola et al., 2007). These findings highlight the difficulties in using direct approaches to identify and characterise thymus-settling progenitors (Bhandoola et al., 2003).

Further complications arise as the site of production of T cell precursors changes during ontogeny, such that the early fetal thymus is colonised by fetal liver derived precursors, and the postnatal thymus is colonised by bone marrow derived precursors (Anderson et al., 2006; Kikuchi and Kondo, 2006). Importantly this could indicate that T lymphoid progenitor cells that colonise the fetal thymus differ in developmental potential from those that enter the postnatal thymus (Takahama, 2006).

As the identity of bone-marrow progenitors for T cells remained controversial, studies began to describe the properties of the most primitive T cell progenitors in the thymus because these are recently derived from, and probably similar to, the rare thymus settling progenitors (Bhandoola and Sambandam, 2006). The most immature subset of thymocytes resides within the $CD4^-$ $CD8^-$ $CD25^-$ $CD44^+$ DN1 cell subset. This DN1 subset has been shown to have multilineage potential including B cell, T cell, myeloid cell, natural killer (NK) cell and dendritic cell (DC) potential (Balciunaite et al., 2005; Benlagha et al., 2002; Hashimoto et al., 2002; Porritt et al., 2004). However, it is becoming increasingly clear that this is most likely a result of heterogeneity, consisting of different lineage restricted progenitors and not to the presence of multilineage progenitors (Kawamoto et al., 1998). The possibility of several precursors entering the thymus simultaneously, the uncertainty concerning the relative contribution to differentiating thymocytes, and the functional role of these precursors have hampered progress in understanding the cells to first enter the thymus and their lineage potential (Benz et al., 2008).

In vitro studies have led to the general understanding that fetal thymocytes, fetal blood, and/or fetal liver cells exhibit the capacity to generate T cells, natural killer cells (NK) cells and/or dendritic cells (DCs), but tend not to contain a precursor cell that has both T and B cell capacity (Douagi et al., 2002; Ikawa et al., 2004; Michie et al., 2000; Rodewald et al., 1994). However, again, artificial (*in vitro*) conditions raise the problem of distinguishing between what cells can do when placed in "ideal" conditions from what the same cells do when placed under biological conditions (Petrie and Kincade, 2005). Especially since the thymic environment has been shown to influence cell fate via Notch signalling for example, as disruption to this signalling pathway leads to the generation of B cells (Anderson et al., 2000a; Ciofani and Zuniga-Pflucker, 2007)

Therefore the aim of this study was to try to overcome a number of the difficulties explained above and devise a system, which would allow the identification and isolation of the first wave of early thymic migrants without complication from mature lymphoid stages. Furthermore, the model had to enable physiological development of the earliest thymic migrants to permit investigation of their lineage potential under normal conditions.

5.2 Specialised Materials And Methods

5.2.1 Kidney Capsule Transfer Of Thymic Tissue

The kidney is highly vascularised consequently aiding the import and export of cells and nutrients required for successful engraftment.

Mice undergoing surgery, typically 4-6 weeks old, were first weighed in order to calculate the dose of analgesia to administer. Mice were anaesthetised in a chamber containing 4% isofluorane (May & Baker, Dagenham, UK) carried in oxygen, and monitored until they lost consciousness and their breathing became slower and deeper. At this point they were transferred onto a heat pad to maintain body temperature and anaesthesia was administered at 2% isofluorane in air through a facemask placed over the nose and mouth. Subcutaneously, 2mg/kg pre-operative Buprenorphine (Temgesic, AnimalCare, York, UK) was administered using a syringe fitted with 25-gauge needle. The pedal withdrawal reflex was used as a measure of depth of anaesthesia, surgery commenced once this reflex was lost.

Using electric clippers, fur was removed from the left lumbar region and the area was cleaned with 70% ethanol before an initial incision was made. A small cut was made using surgical blunt ended scissors (F.S.T/interfocus, Heidelberg, Germany), in the region of the left kidney. The incision was increased to approximately 0.5-1cm in length depending on the size of the mouse and space was made between the skin and peritoneum before making a similar size cut, by blunt dissection, in the peritoneum. The kidney was gently drawn out of the body cavity using blunt ended forceps and using the fat attached to the lower end. Once externalised the kidney was held in position by the skin, and kept moist by PBS soaked gauze, which helped to keep the kidney capsule pliable and prevent dehydration of the mouse.

With use of a dissecting microscope a small perforation was made into the fibrous kidney capsule with fine forceps (No.5) (F.S.T), taking care not to damage the kidney parenchyma. The

tissue to be engrafted was loaded onto one edge of the forceps and placed under the kidney capsule. Up to four E15 or six E12 thymus lobes were grafted under the capsule of one kidney. Taking hold of the edge of the peritoneum and elevating, the kidney was gently manoeuvred back into the body cavity. The peritoneum was closed using two sutures (Vicryl, 4-0 16mm roundbodied sutures (Ethicon, Livingston, UK)), and the edges of the skin brought together by a clip after cleaning with a cotton bud dipped in PBS.

The mouse was removed from the anaesthesia, kept warm until consciousness was regained. The mouse was relocated to clean conditions within the BMSU, and its recovery monitored at regular intervals and subsequently weighed daily for the next week and then intermittently until sacrificed (~4/8 weeks).

5.2.2 BrdU Intra-Peritoneal Injection

A sterile 1mg/200μl solution of Bromodeoxyuridine (5-bromo-2-deoxyuridine, BrdU) (10mg/ml stock) (BD Pharmingen) was freshly prepared and allowed to equilibrate to room temperature before transfer into a 1ml syringe with a 25-gauge needle affixed. After ensuring no air bubbles were present in the suspension the transfer was completed by intra-peritoneal injection into the lower left abdominal region, 200μl (1mg) per mouse, 20 minutes before harvesting.

5.3 Results:

5.3.1 E12 Thymus Grafts Develop Normally Exhibiting Standard T cell Development And Typical Thymus Architecture

The aim of this study was to investigate the lineage potential of the earliest thymic migrants, freshly isolated E12 thymus lobes were dissected from CD45.1 WT mice and grafted under the kidney capsule of *Rag*$^{-/-}$γc$^{-/-}$ (CD45.2) mice, allowing them to continue to develop under relatively normal biological conditions. The *Rag*$^{-/-}$γc$^{-/-}$ mouse was chosen because the absence of the common gamma chain (γc) results in the lack of intact intracellular signalling required for thymocyte and NK cell growth and differentiation (Colucci et al., 1999; Klug et al., 2002; Rodewald et al., 1997). In addition, the null mutation in the *Rag* locus prevents the rearrangement of the T-cell receptor and B-cell receptor genes, resulting in a profound block at the DN3 stage of early T cell development and an absence of mature B cells (Klug et al., 2002; Mombaerts et al., 1992; Takahama, 2006). Therefore the mature lymphoid compartment is vacant, aiding the identification of the small number of graft derived progenitors. In addition *Rag*$^{-/-}$γc$^{-/-}$ T cell precursors are blocked between the DN1 and DN2 stage (Klug et al., 2002), therefore subsequent waves of T cell development cannot occur, even if the host progenitors repopulate the graft, enabling the development of the single E12 cohort of T cells to be followed (Figure 5.1).

Before being able to use this *in vivo* system to establish the lineage potential of the earliest thymic progenitors, it was important to establish whether the graft could develop normally and was therefore providing a physiological environment able to support normal T cell development. After 1, 2 and 7 weeks the grafts were harvested and assessed by flow cytometry for CD4 and CD8 coreceptor expression (Figure 5.2). At 1 week post transplant the early thymic precursors had developed into a predominant CD4^{+} CD8^{+} DP population, and a small

Figure 5.1 Experimental Design

An experimental model was generated to investigate the lineage potential of the earliest thymic migrants. Congenically marked freshly isolated E12 thymus lobes were dissected from WT mice and grafted under the kidney capsule of *Rag*$^{-/-}$γc$^{-/-}$ mice. Kidney capsule grafting allows the continued development of the first wave of T cell precurosors under relatively normal biological conditions. *Rag*$^{-/-}$γc$^{-/-}$ mice are T, B and NK cell deficient, making the identification of the small number of graft derived progenitors more straightforward. In addition *Rag*$^{-/-}$γc$^{-/-}$ T cell precursors are blocked between the DN1 and DN2 stage, therefore subsequent waves of T cell development cannot occur, even if the host progenitors repopulate the graft. This enables the development of the single E12 cohort of T cells to be followed. After 1, 2 or 7 weeks the graft and host spleens were harvested and analysed. Scale bar indicate 1mm.

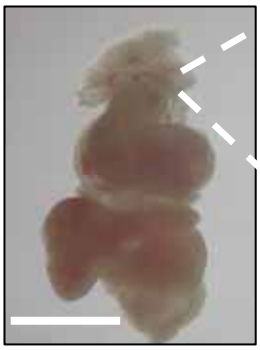

E12 Thoracic tree

Congenically marked

E12 thymus lobe

Kidney capsule transfer

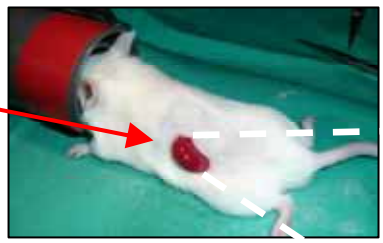

Rag$^{-/-}\gamma c^{-/-}$

NK, T and B cell Deficient

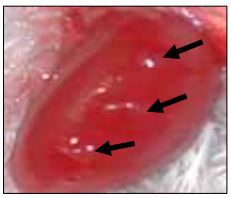

1, 2 or 7 weeks

Host Spleen

Graft

Figure 5.2 Normal αβ T Cell Development Occurs In The E12 Grafted Thymus

E12 fetal thymus lobes were grafted under the kidney capsule of *Rag*$^{-/-}$γc$^{-/-}$ mice. The thymus grafts were harvested at 1, 2 and 7 weeks post grafting, teased and analysed by flow cytometry for expression of CD4, CD8 and TCRβ. Representative FACS plots illustrate the CD4 and CD8 profile for the grafts at the stated time point (5.2A). Development of CD4^{+}CD8^{-} and CD4^{-}CD8^{+} TCR^{hi} populations was observed (5.2B) Percentages of cells within gated areas are indicated. Data is representative of at least three experiments.

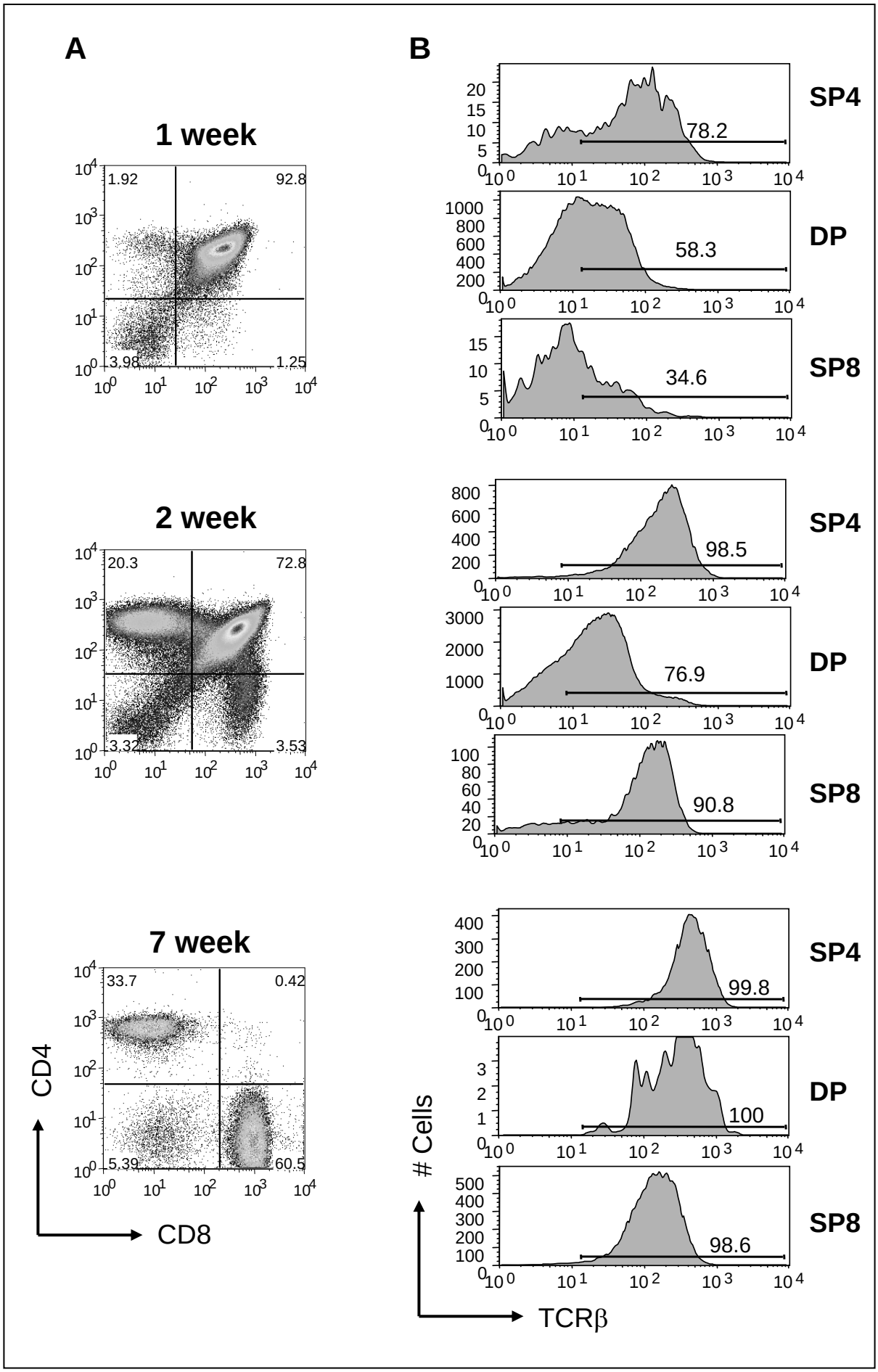
A
1 week
1.92
92.8
3.98
1.25
2 week
20.3
72.8
3.32
3.53
7 week
33.7
0.42
5.39
60.5
CD4
CD8
B
SP4
78.2
DP
58.3
SP8
34.6
SP4
98.5
DP
76.9
SP8
90.8
SP4
99.8
DP
100
SP8
98.6
Cells
TCRβ

number of mature (TCR^{hi}) single positive CD4 thymocytes were beginning to appear. At 2 weeks a typical CD4 and CD8 coreceptor profile, similar to WT can be seen and the occurrence of further T cell development was indicated by the appearance of mature $CD4^+$ $CD8^-$ TCR^{hi} and $CD4^-$ $CD8^+$ TCR^{hi} SP T cells. 7 weeks post engraftment the single cohort of graft derived cells appeared to have pushed through development, suggested by the absence of the double positive population, leaving just the mature CD4 and CD8 single positive thymocytes yet to exit the thymus graft. This was probably due to the absence of continual replenishment of the progenitor pool from the BM.

It is understood that initial thymic epithelium and thymocyte development occur simultaneously via a process that requires bidirectional lymphostromal signalling termed 'thymus crosstalk' (Fiorini et al., 2008; van Ewijk et al., 1994). Therefore to investigate whether a normal thymic microenvironment had developed alongside the early programme of T cell development in the E12 thymus grafts, the thymic architecture of 1, 2 and 7 week grafts was analysed by confocal microscopy (Figure 5.3). An indication that T cell development was occurring in different intrathymic regions was established by antibody staining for CD4 and CD8 (Figure 5.3A). In a normal thymus $CD4^+$ $CD8^+$ DP thymocytes can be found residing within the cortex whilst $CD4^+$ $CD8^-$ and $CD4^-$ $CD8^+$ SP thymocytes reside within the medulla. At week 1 numerous $CD4^+$ $CD8^+$ DP thymocytes were identified within the thymic rudiment suggesting development of the cortical thymic epithelium, also areas devoid of SP thymocytes were identified suggesting the development of small rudimentary medullary areas (Figure 5.3A). This further corroborated previous FACS data of the CD4 and CD8 profile, where at one week, very small numbers of SP thymocytes were present. At week two the thymus epithelium had expanded and contained two distinct compartments colonised by $CD4^+$ $CD8^+$ DP and $CD4^+$ CD8 and $CD4^-$ $CD8^+$ SP thymocytes respectively, again further supporting the flow cytometry data

Figure 5.3 Development And Regression Of The Thymic Architecture In E12 Thymus Grafts

Thymus sections from adult WT thymus and grafts harvested at 1, 2 and 7 weeks were analysed by confocal microscopy for thymocyte organisation with antibodies against the coreceptors CD4 and CD8 (5.3A). $CD4^+CD8^+$ double positive thymocytes can be found in the cortex and $CD4^+CD8^-$, $CD4^-CD8^+$ single postive thymocytes in the medulla. cTEC and mTEC development and organisation was analysed using the markers keratin 5 and keratin 8 (5.3B). Note the emergence of rudimentary medullary areas in the 1 week grafts and the similar architecture of WT and the 2 week graft. asterisk highlights cystic structures. Scale bars represent 100μm. Solid line: subcapsular region boundary. C: cortex, M: medulla

Another indication of normal epithelial cell development is the presence of Aire expressing $K5^+$ mTECs, which were clearly observed in all the grafted thymuses harvested at the indicated time points (5.3C). Scale bars represent 20μm. Data is representative of at least three experiments.

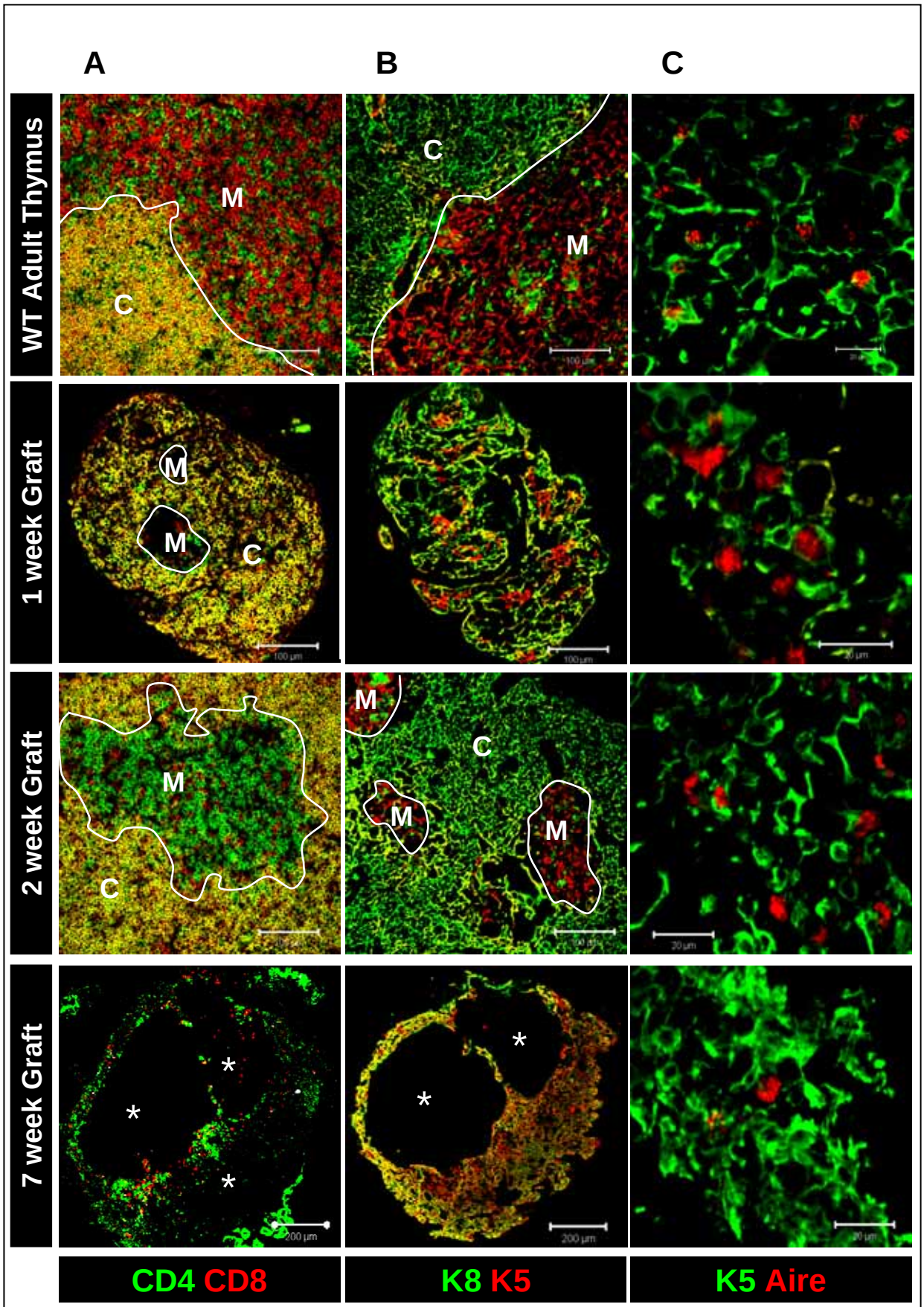
A
B
C
WT Adult Thymus
1 week Graft
2 week Graft
7 week Graft
M
C
CD4 CD8
K8 K5
K5 Aire

and suggesting the development of the cortical and medullary epithelium. Interestingly by 7 weeks the thymic structure had begun to diminish in size, very few SP thymocytes remained within the structure and large cystic structures were identified, which suggested the emigration of the majority of the T lymphocytes from the remaining structure (Figure 5.3A). However, the majority of the staining was of background level as determined by the negative control (not shown).

To ensure the E12 thymic rudiment contained the capacity to develop into a mature, compartmentalised, three dimensional epithelial structure and to examine whether thymic epithelial cell development concomitantly occurred with T cell development, confocal analysis was completed. Frozen tissue sections were stained with the cortical and medullary markers, keratin 8 (K8) and K5 respectively (Figure 5.3B), which established the presence of differentiated epithelial areas. Rudimentary medullary $K5^+$ $K8^-$ areas can be seen at week 1 whereas the $K5^-$ $K8^+$ cortical epithelium appears more substantial. By week 2 both the $K5^+$ $K8^-$ medullary and $K5^-$ $K8^+$ cortical areas were more established and resemble that of WT epithelium. In addition the thymus had expanded in size. However, at week 7 the thymic epithelium had regressed to a more immature state illustrated by substantial $K5^+K8^+$ double positive areas, in addition large cysts were present (Figure 5.3B).

Another parameter to identify normal development and maturation of the thymic epithelial cell compartment is the presence of $Aire^+$ mTECs. $Aire^+$ mTECs are important for central tolerance; their occurrence therefore suggests that normal thymocyte selection was proceeding. $Aire^+$ mTECs were identified as early as 1 week of engraftment, their continued existence was apparent at 2 weeks and at 7 weeks a few still persisted (Figure 5.3C).

Having established that normal T cell development was occurring within the E12 graft within typical thymic microenvironments it was important to examine the export of mature T

cells from the grafted thymus and recruitment of mature T cells to secondary lymphoid organs such as the spleen. The presence of $CD3^+$ $CD4^+$ and $CD3^+$ $CD8^+$ T cells within the host spleen was evaluated by flow cytometric analysis (Figure 5.4). At 1 week as expected $CD3^+$ T cells were not identifiable within the host spleen, this was because within the graft only $CD4^+$ $CD8^+$ DP thymocytes were present as further T cell maturation was yet to occur. Graft derived $CD3^+$ $CD4^+$ and $CD3^+$ $CD8^+$ T cells were identified within the host spleen at 2 and 7 weeks post transplantation. Together these results suggest that the E12 thymus anlage had developed into a functioning thymus lobe that could support a full programme of T cell development, establishment of discrete cortical and medullary epithelial cell microenvironments and the export of mature T cells into the periphery.

5.3.2 E12 Thymocyte Progenitors Give Rise To Multiple Lineages

Existing studies have reported conflicting evidence for the developmental potential of the cells seeding the thymus, most probably as a result of inconsistent definitions of thymic migrants, the difficulties isolating such small numbers of cells and problems utilising *in vitro* experiments for distinguishing between what cells can do when placed under ideal (artificial) conditions from what the same cells normally do under biological conditions (Petrie and Kincade, 2005). The data presented here have established an *in vivo* model in which the lineage potential of the earliest thymic progenitors can be tested without ambiguity as to whether the cells are destined to migrate to the thymus or not and allowing development within physiological conditions. In initial experiments we wanted to investigate the developmental potential of the earliest thymic migrants as a population without taking into account the frequency of precursor potential.

Figure 5.4 T Cell Development In The E12 Grafts Includes Thymic Emigration To The Periphery

Splenic tissue from host *Rag*$^{-/-}\gamma c^{-/-}$ mice was analysed by flow cytometry for expression of CD3, CD19, CD4 and CD8. Note the absence of $CD3^+CD4^+$ and $CD3^+CD8^+$ T cells in the 1 week spleen and their presence at 2 and 7 weeks post grafting. Percentages of cells within gated areas are indicated. Data is representative of at least three experiments.

Adult WT Spleen

CD3 Gated

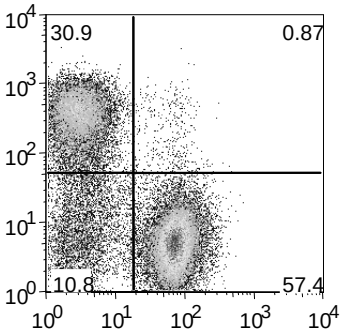

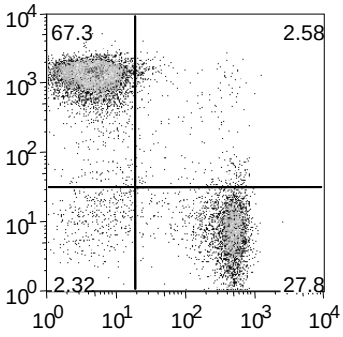

Host Spleen

1 week

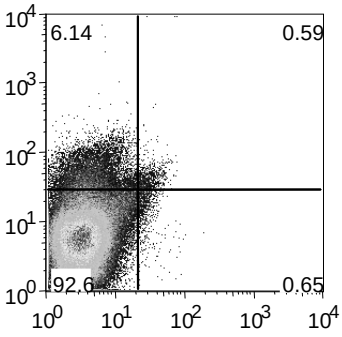

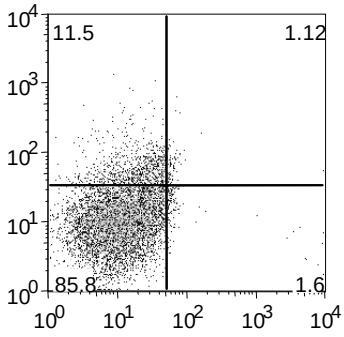

2 week

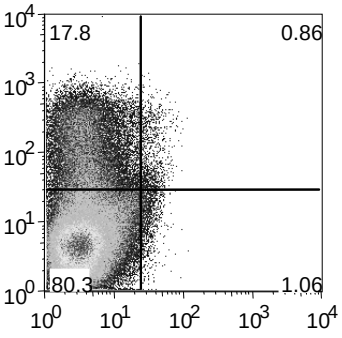

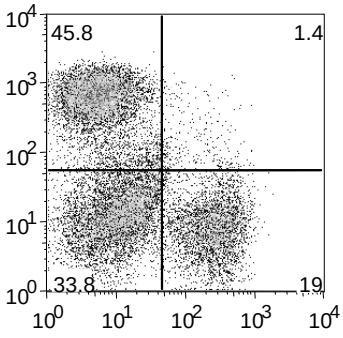

7 week

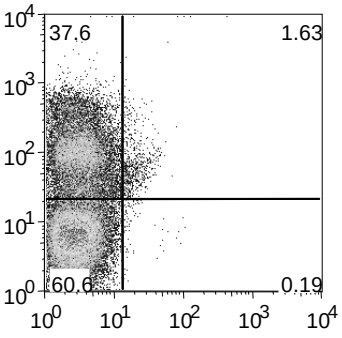

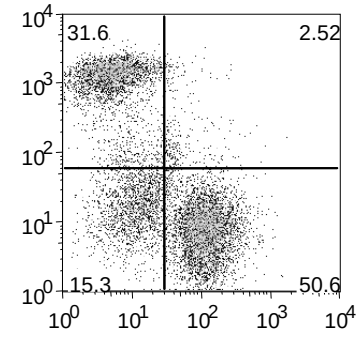

Although the data above has shown that the E12 fetal thymus anlage contains precursors capable of producing αβ T cells it was important to clarify that E12 progenitors were able to generate a broad spectrum of T cells, including those thought to predominantly develop within the fetal thymus, the γδ T cells (Havran and Allison, 1988; Masuda et al., 2005). To address this E12 fetal thymus lobes were grafted under the kidney capsule of *Rag*$^{-/-}$γc$^{-/-}$ mice. After 1 week, thymus grafts were analysed by flow cytometry for the universal (pan) γδ T cell marker, which identified a population within the CD4^{-} CD8^{-} DN fraction of thymocytes (Figure 5.5A). Therefore, early thymic precursors do have the capacity to generate γδ T cells, having recognised this, it was of interest to investigate the presence and location of a specific subset of γδ T cells, the Vγ5^{+} thymocytes. Based on our previous work Vγ5^{+} thymocytes would be expected to be predominantly located within the medulla (Chapter 3). Frozen sections of 1 week grafted tissues were analysed by confocal microscopy for Vγ5, CD4 and ERTR7. As expected Vγ5^{+} thymocytes were identified within rudimentary medullary areas (Figure 5.5B) as identified by the absence of CD4^{+} cells because it was previously shown in this study that at 1 week, only CD4^{+} CD8^{+} DP αβ thymocytes are present (Figure 5.2).

To further assess the spectrum of T cell populations generated by the E12 thymocyte precursors the generation of regulatory T cells (Tregs) was investigated. Tregs are a T cell subset that express an αβ TCR, their selection and generation occurs intrathymically and they are identified by their expression of CD4, CD25 and FoxP3 (Aschenbrenner et al., 2007; Jordan et al., 2001; Sakaguchi, 2004). E12 thymus grafts were harvested after 2 weeks and analysed by confocal microscopy for CD4 and FoxP3. CD4^{+} FoxP3^{+} Tregs were readily found within 2 week grafts (Figure 5.5C and D). Importantly, Tregs were predominantly located within the thymic medulla as comparable to WT adult thymus (Figure 5.5C), which is the reported site for their generation (Aschenbrenner et al., 2007). Collectively these data suggest that E12 thymocyte

Figure 5.5 The Earliest Wave Of Thymocyte Progenitors Have γδ T cell And Treg Potential

Flow cytometric analysis of thymocytes isolated from 1 week grafts for surface expression of pan γδ TCR (5.5A). Percentage of cells within gated area is indicated. Frozen sections of 1 week grafts were analysed by confocal microscopy for expression of CD4, Vγ5 and ERTR7 (5.5B). Note the localisation of $V\gamma5^+$ thymocytes within the $CD4^-$ rudimentary medullary areas. Scale bar: 100μm

Confocal analysis of frozen sections from WT adult thymus and 2 week grafts for CD4 and FoxP3 expression (5.5C). Note the presence of $CD4^+FoxP3^+$ Treg within the medulla of both WT and 2 week grafts. 5.5D is a greater magnification picture. Scale bars represent 50μm. Data is representative of at least four experiments.

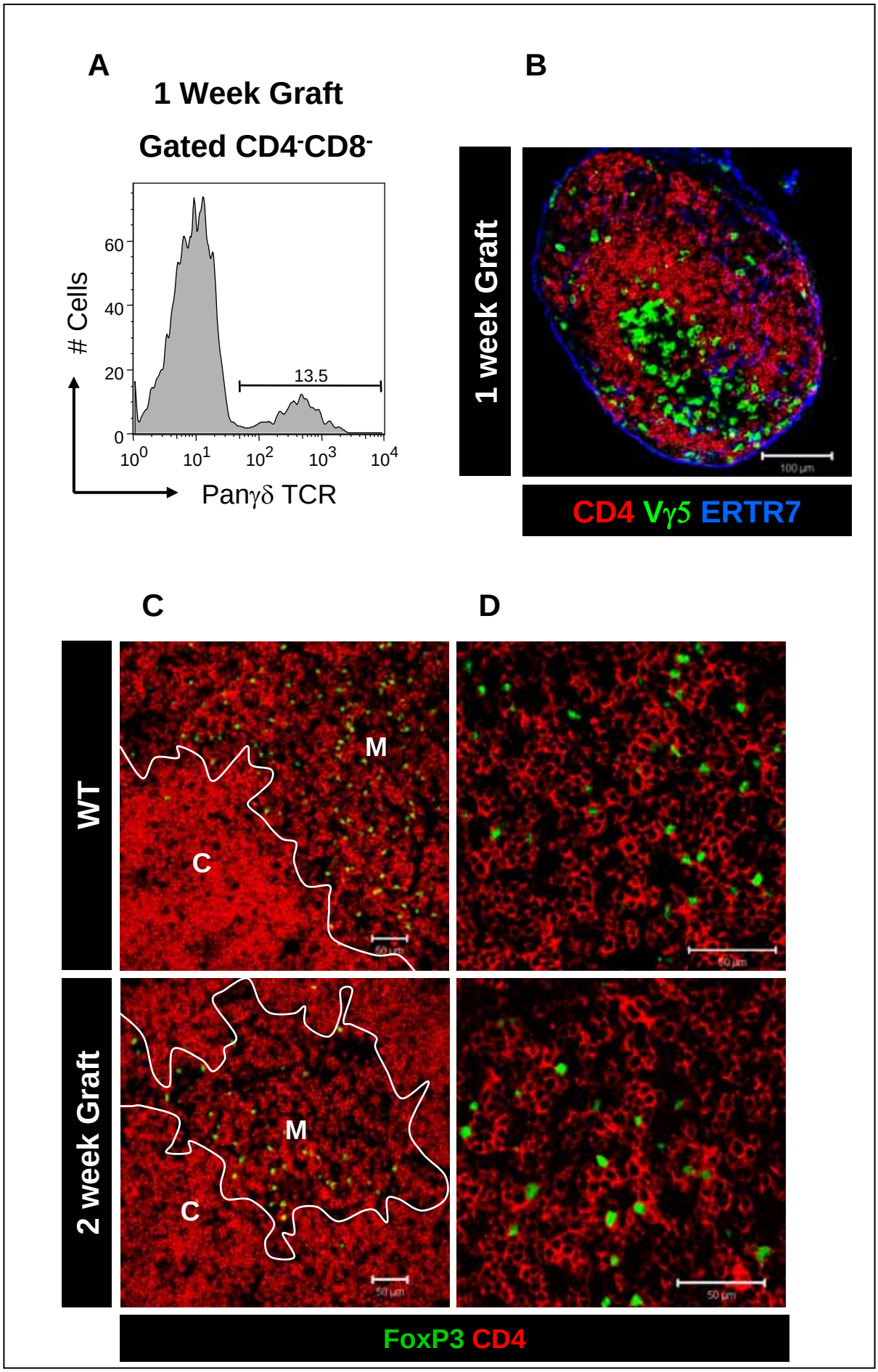
A
1 Week Graft
Gated CD4-CD8-
Cells
60
40
20
0
13.5
10^0
10^1
10^2
10^3
10^4
Panγδ TCR
B
1 week Graft
100 µm
CD4 Vγ5 ERTR7
C
D
WT
M
C
50 µm
2 week Graft
M
C
50 µm
FoxP3 CD4

precursors have the capacity to generate a variety of T cell populations including the αβ T cell, the γδ T cell and regulatory T cell lineages.

Other lineages investigated in this study were those whose generation from E12 thymocytes and progenitors in the fetal blood and fetal liver were previously reported. Ikawa *et al* and Shen *et al* had revealed DC and NK cell potential of the earliest thymic migrants (Ikawa et al., 1999; Shen et al., 2003). Therefore, whether these cell lineages could be identified within the E12 grafting system established in this study was of interest. Confocal analysis of frozen sections prepared from 1 week grafts stained with the congenic marker CD45.1 and the DC specific antigen CD11c, identified E12 precursor derived dendritic cells (Figure 5.6A). The fluorescence profile indicates the overlapping membrane expression of CD45.1 and CD11c suggesting this cell is a graft derived DC rather than an infiltrating host derived DC. The NK cell activating receptor NKp46 (Walzer et al., 2007), identified graft derived ($CD45.1^+$) NK cells within the host spleen 1 week after grafting; the overlapping membrane expression was confirmed by the fluorescence profile (Figure 5.6B). Whether the first wave of thymic precursors possess potential for myeloid cells such as monocytes/macrophages and granulocytes, as distinct from their well-studied DC potential, is less clear. However, it has been shown that the ETP population possesses some degree of myeloid potential in bulk assays (Balciunaite et al., 2005; Matsuzaki et al., 1993; Wu et al., 1991). CD11b is a protein subunit of the myeloid lineage marker macrophage-1 antigen (Mac-1) and was therefore used to investigate the myeloid potential of E12 precursors. Frozen sections of 1 week E12 grafts were analysed by confocal for CD45.1 and CD11b. Graft derived $CD11b^+$ cells were detected and confirmed by the overlapping membrane expression of both CD45.1 and CD11b (Figure 5.6C). Therefore suggesting that E12 progenitors have the capacity to generate myeloid lineages however, further characterisation of these cells would be required to determine which myeloid lineages. Together

Figure 5.6 The Earliest Wave Of Thymocyte Progenitors Have NK And Myeloid Including DC Potential

Confocal analysis of frozen tissue sections from 1 week grafts identified graft derived dendritic cells (DC) (5.6A), note the overlapping surface expression of CD45.1 and CD11c. Frozen sections of 1 week host spleens were analysed by confocal microscopy for expression of NKp46, CD45.1 and DAPI (5.6B). Note the overlapping surface expression of CD45.1 and NKp46, identifying a graft derived natural killer (NK) cell. Confocal analysis of frozen sections from 1 week grafts for CD11b and CD45.1 expression (5.6C). Note the idenification of a potential graft derived $CD11b^{+}CD45.1^{+}$ myeloid cell. Data is representative of at least four experiments.

A

DC

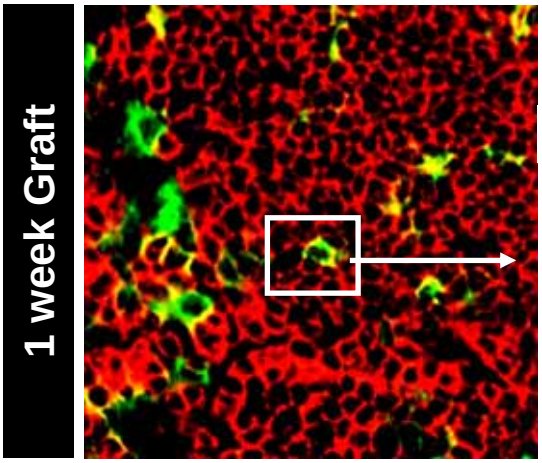

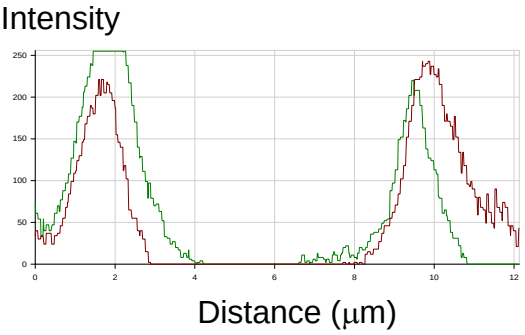

B

NK

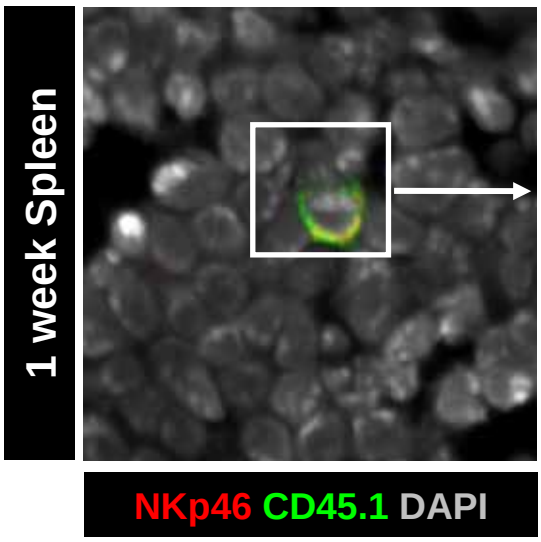

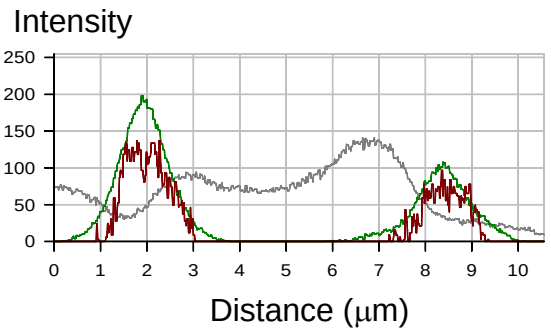

C

Macrophage

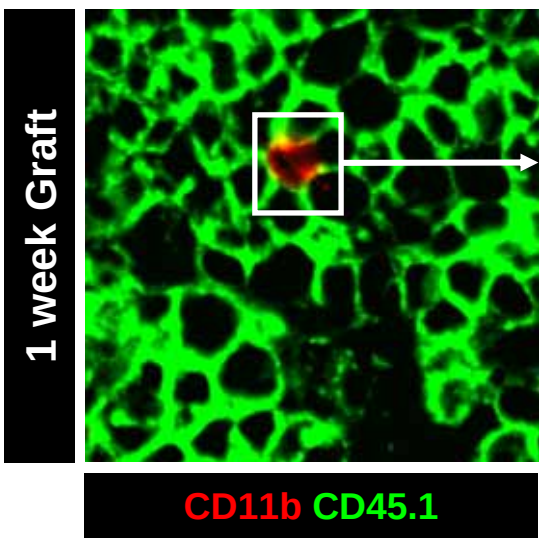

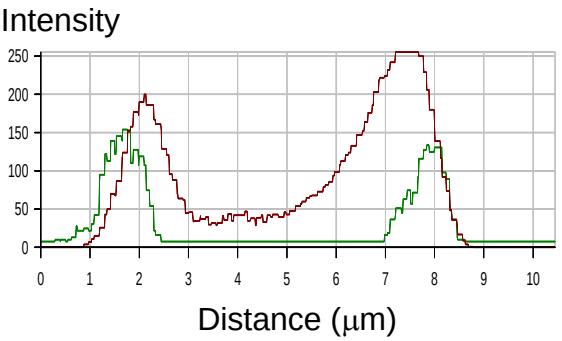

these data suggest the earliest thymic migrants have the potential to produce natural killer cells and myeloid cells including DCs.

The classical model of haematopoiesis postulates that multipotent progenitors (MPPs) subsequently give rise to two lineages that are dissimilar in their potential, dividing the lymphoid and myelo-erythroid lineages. Common lymphoid progenitors (CLPs) possess the potential to produce T, B and NK cells (Akashi et al., 2000; Kondo et al., 1997). Consequently, when the decision to become either a T cell or a B cell occurs has been a long standing question. In an attempt to decipher whether the choice occurs prethymically or intrathymically and to either confirm or contest previous reports that thymic progenitors have B cell potential, the development of graft derived B cells was investigated (Bell and Bhandoola, 2008; Kawamoto et al., 1998). Frozen sections prepared from host spleens harvested 7 weeks after grafting were analysed by confocal microscopy for the presence of B cells. While in a wild type spleen white pulp areas comprised of a central T ($CD3e^+$) zone surrounded by B ($B220^+$) cell areas can be seen (Figure 5.7), the host spleen white pulp areas are only comprised of T cell zones, as identified by a central $VCAM^+$ blood vessel surrounded by $CD3^+$ T cells, however $B220^+$ B cells were absent. In conclusion, B cells cannot be found within this system suggesting that either the earliest thymic migrants do not have the potential to produce B cells when developing within the thymic microenvironment or B cell potential was lost before entering the thymus rudiment. However, it would be interesting to investigate whether these E12 haematopoietic precursors have B cell potential within a B cell permitting environment.

Lymphoid tissue inducer cells (LTi) have important roles in the development of lymphoid tissues. In the thymus they are known to provide Rankl to developing mTECs, which initiates mTEC maturation leading to the appearance of Aire expressing mTECs. The presence of LTi at early stages of development is important to prepare the medullary epithelium for its role

Figure 5.7 The Earliest Wave Of Thymocyte Progenitors Developing *In Situ* Do Not Produce B cells

Frozen sections of WT and host spleens after harbouring an E12 thymus graft for 7 weeks were analysed by confocal microscopy for expression of VCAM, CD3 and B220 (5.7). Note the presence of $CD3^+$ T cells in the T zone of the WT spleen surrounded by $B220^+$ B cell area. Graft derived $CD3^+$ T cells have populated the T zone area of the host spleen. $B220^+$ B cells cannot be seen. Scale bars: 50μm. Data is representative of at least four experiments.

B Cells

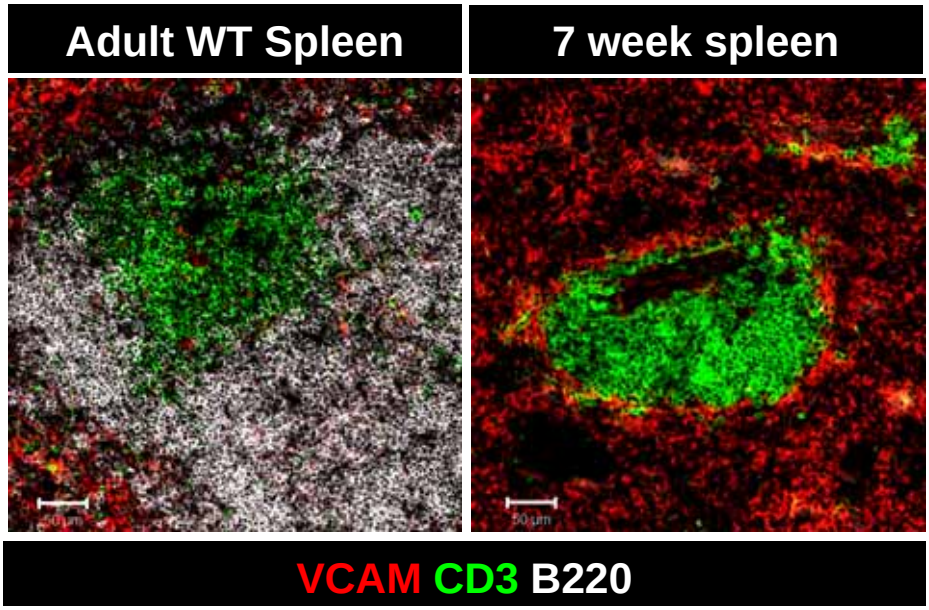

supporting negative selection of the αβ T cell repertoire (Rossi et al., 2007b). However, it is not yet known whether LTi are recruited to the embryonic thymus or whether they develop within the thymic rudiment from an immature precursor that has migrated to the thymus anlage. To decipher whether LTi were generated from the first wave of thymocyte precursors, congenically marked (CD45.1), E12 fetal thymus lobes were transplanted under the kidney capsule of CD3ε*tg*26 mice. CD3ε*tg*26 mice were used because *Rag*$^{-/-}$γc$^{-/-}$ mice contain only 10% of normal numbers of LTi and endogenous, host derived LTi are required to enable comparison of graft and host LTi. Adult LTi differ from embryonic LTi by expressing an additional group of tumor necrosis factor (TNF) family members comprised of OX40 and CD30 ligands (Kim, 2008), consequently host derived LTi will have an OX40L^{+} adult phenotype. To identify if LTi arise from E12 thymic precursors CD3ε*tg*26 host splenocytes were analysed by flow cytometry. Host (CD45.1^{-}) derived B220^{-} CD11c^{-} CD3^{-} CD4^{+} IL-7Rα^{+} LTi were readily identified (Figure 5.8A) and were also expressing CD25 and OX40L, verifying them as adult LTi. Interestingly, a B220^{-} CD11c^{-} CD3^{-} CD4^{+} IL-7Rα^{+} LTi population was also present in the CD45.1^{+} graft derived cell fraction (Figure 5.8B), however, this cell population appeared to have an embryonic LTi phenotype as they did not express CD25 or OX40L. Their embryonic phenotype could be due to their recent development meaning they are yet to upregulated CD25 or OX40L expression. To further confirm this cell population to be E12 derived fetal LTi and to remove the argument that they may be T cells, the B220^{-} CD11c^{-} CD3^{+} T cell populations from both host and graft are shown (Figure 5.8C). Collectively these data suggest that E12 thymocyte progenitors are able to give rise to αβ T cells, γδ T cells, specifically Vγ5^{+} γδ T cells, FoxP3^{+} Tregs, NK cells, DCs, possibly other myeloid lineages and fetal LTi as a population. However, it was decided at this point to postpone the lineage potential experiments and pursue investigation of another interesting observation that had arisen from the grafting experiments.

Figure 5.8 The Earliest Thymic Progenitors Have Lymphoid Tissue Inducer Cell Potential

E12 thymus lobes were grafted under the kidney capsule of CD3ε*tg26* mice. CD3ε*tg26* host spleens were harvested 4 weeks after grafting and the isolated splenocytes analysed by flow cytometry. Host derived ($CD45.1^-$) $B220^-CD11c^-CD3^-$IL-$7R\alpha^{hi}CD4^{hi}$ LTi were identified (5.8A). A population of splenocytes were cultured over night in standard culture conditions (DMEM, 37°C, 10% CO_2), to promote upregulation of OX40L and CD25 expression and identify adult LTi. The host derived LTi population were $OX40L^+CD25^+$ adult LTi. Graft derived ($CD45.1^+$) $B220^-CD11c^-CD3^-$IL-$7R\alpha^{hi}CD4^{hi}OX40L^-CD25^-$ embryonic LTi were identified (5.8B). Note the distinction between graft and host derived IL-$7R\alpha^+CD4^+$ T cells and LTi (5.8C). Percentages of cells within gated areas are indicated. Data is representative of at least two experiments.

A

Host derived

B220^{-}CD11c^{-}CD3^{-}

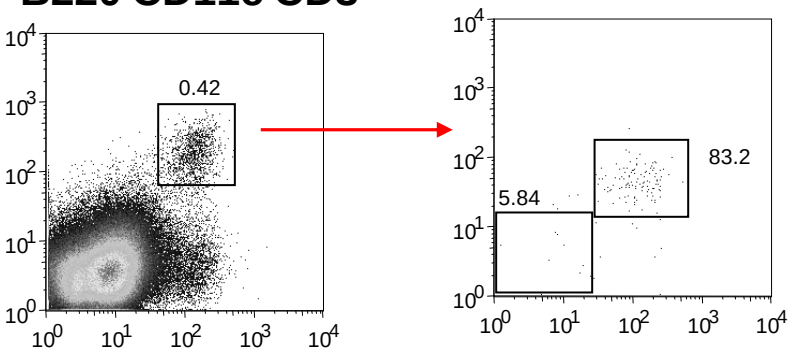

B

Graft derived

B220^{-}CD11c^{-}CD3^{-}

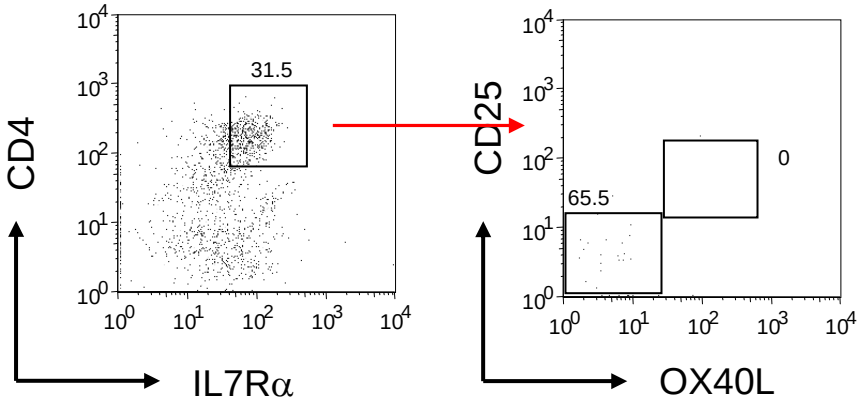

C

B220^{-}CD11c^{-}CD3^{+} Gated

Graft derived

Host derived

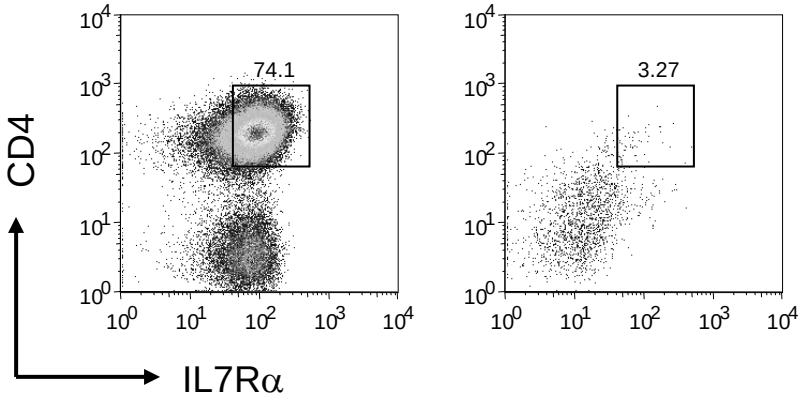

5.3.3 An Absence Of Thymocyte Niche Competition Results In Persisting DP Thymocyte Residency

Whilst investigating the lineage potential of the first wave of T cell precursors it was observed that a number of 7 week grafts remained large and lymphoid (Figure 5.9A). Furthermore these grafts contained a persisting population of double positive thymocytes (Figure 5.9B). This was unexpected as generally the single cohort of E12 T cell precursors would be exhausted by 7 weeks, as indicated by an absence of $CD4^+$ $CD8^+$ DP thymocytes. Therefore investigations into what may be causing this began. Lymphoid 7 week grafts were harvested and analysed by flow cytometry for CD4, CD8 and TCRβ. Two examples of E12 persisting grafts are given (Figure 5.9B) and interestingly E15 grafts were also found to contain a prolonged population of persisting $CD4^+$ $CD8^+$ DP thymocytes (Figure 5.9C), however a large variation in the CD4 and CD8 profiles was observed and many were atypical when compared to adult WT thymus (Figure 5.9D). Furthermore E15 grafts persisted at a greater frequency (Figure 5.9E) than observed for E12 grafts, where a persisting graft was defined as a graft containing ≥10000 cells and a DP thymocyte population when harvested at ≥7 weeks. Overall, 44% (55/125) of grafts apparently maintained T cell development without precursor replenishment (Figure 5.9F), hence this was not an infrequent event and warranted further investigation.

It was important to eliminate the possibility that the prolonged T cell development was a result of thymocyte conversion to a growth factor independent state. Thymocytes were isolated from persisting grafts and cultured for a minimum of 4 days in standard culture conditions (DMEM, 37^oC, 10% CO_2) to assess their ability to survive indefinitely. Following the time in culture the cells were harvested and antibody stained for CD4 and CD8. The forward side scatter clearly illustrated that the cultured cells had not survived (Figure 5.10A and B), suggesting that a malignant transformation had not occurred.

Figure 5.9 Persistence Of A Lymphoid Graft Containing The Four Stages Of T cell Development

E12 thymus lobes were grafted under the kidney capsule of *Rag*$^{-/-}\gamma c^{-/-}$ mice. After 7 weeks the grafts were harvested and were analysed visually (5.9A). 7 week thymus grafts was harvested, teased and analysed by flow cytometry for expression of CD4, CD8 and TCRβ. Representative FACS plots illustrate the CD4 and CD8 profile for E12 7 week persisting grafts (5.9B) and E15 7 week persisting grafts (5.9C). Adult WT thymocyte CD4 and CD8 profile with TCRβ expression (5.9D). The presence of $CD4^+CD8^-$ and $CD4^-CD8^+$ TCR^{hi} populations was observed. Percentages of cells within gated areas are indicated. Data is representative of at least three experiments.

The numbers of grafts that continued to contain lymphocytes compared to those that exhausted the graft derived precursors are illustrated (5.9E), Note that E15 thymus grafts persisted more frequently than E12 thymus grafts (5.9F). A persisting graft was defined as a graft containing ≥10000 cells and a DP thymocyte population that was harvested at ≥7 weeks.

A

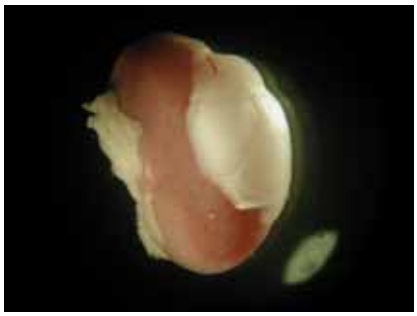

B

E12 Persisting grafts

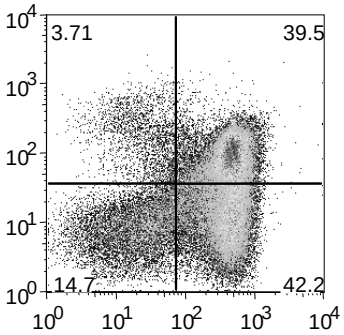

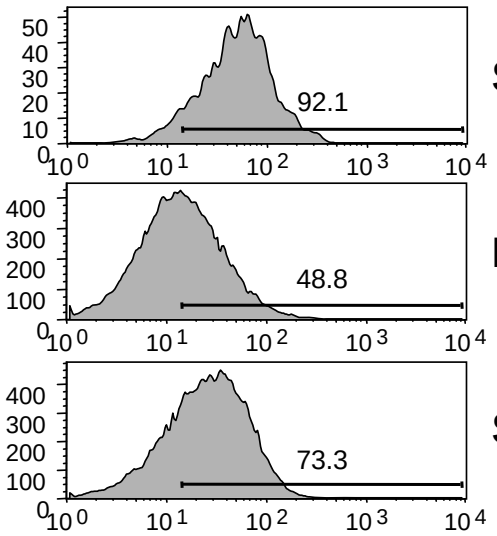

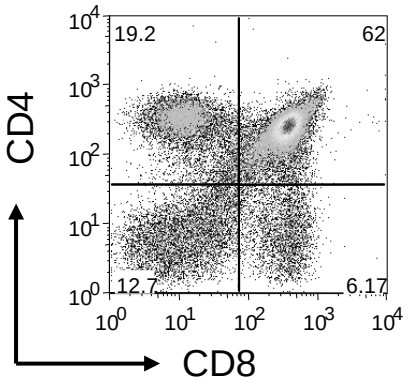

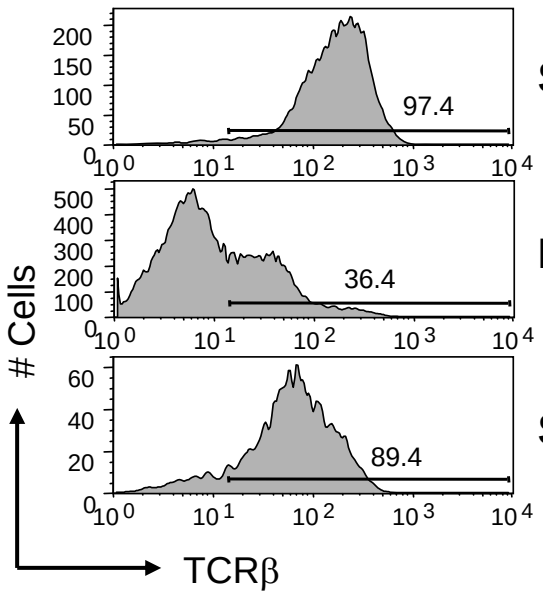

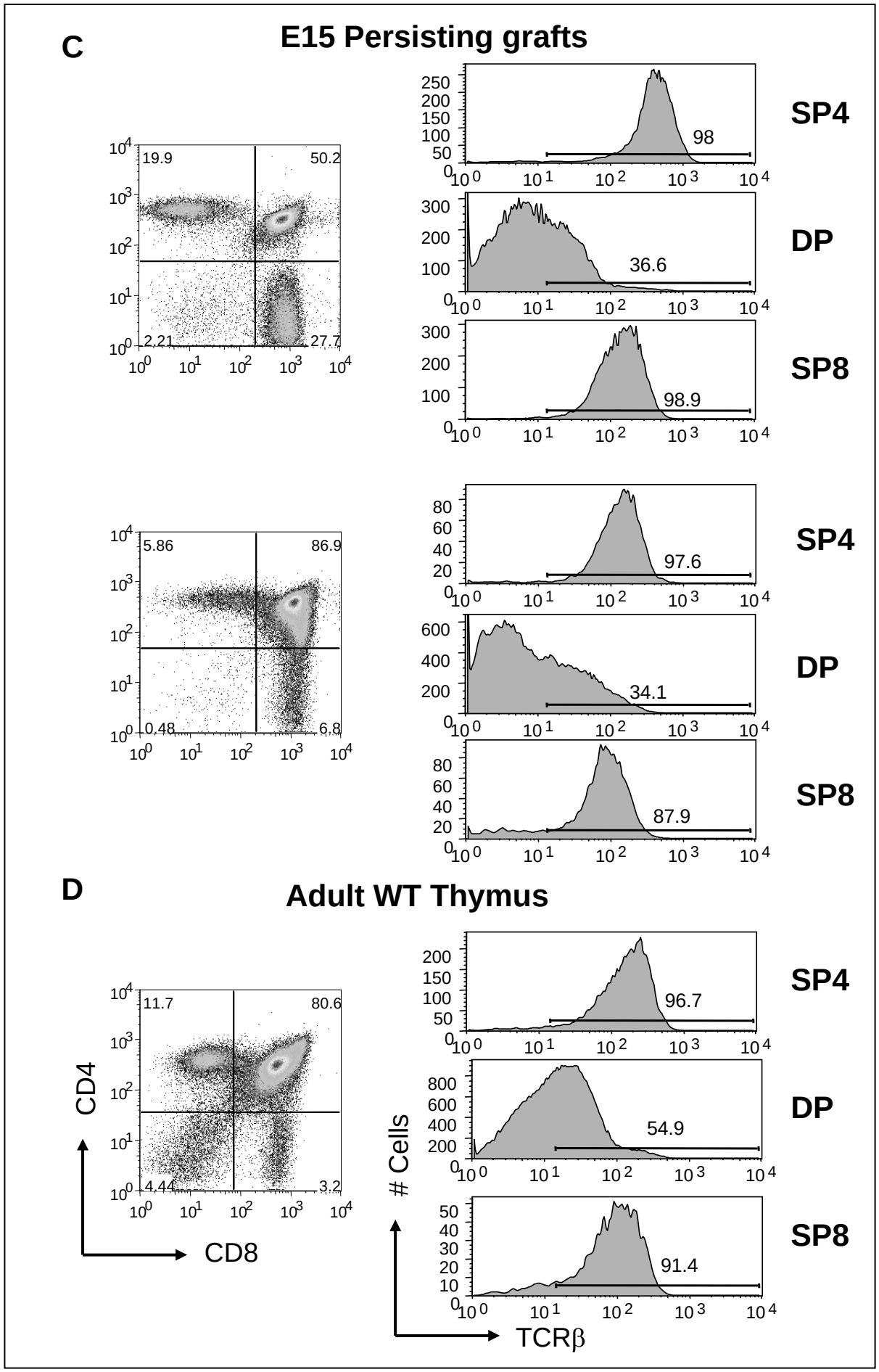
C
E15 Persisting grafts
19.9
50.2
2.21
27.7
SP4
98
DP
36.6
SP8
98.9
5.86
86.9
0.48
6.8
SP4
97.6
DP
34.1
SP8
87.9
D
Adult WT Thymus
11.7
80.6
4.44
3.2
CD4
CD8
SP4
96.7
DP
54.9
SP8
91.4
Cells
TCRβ

Persisting Grafts

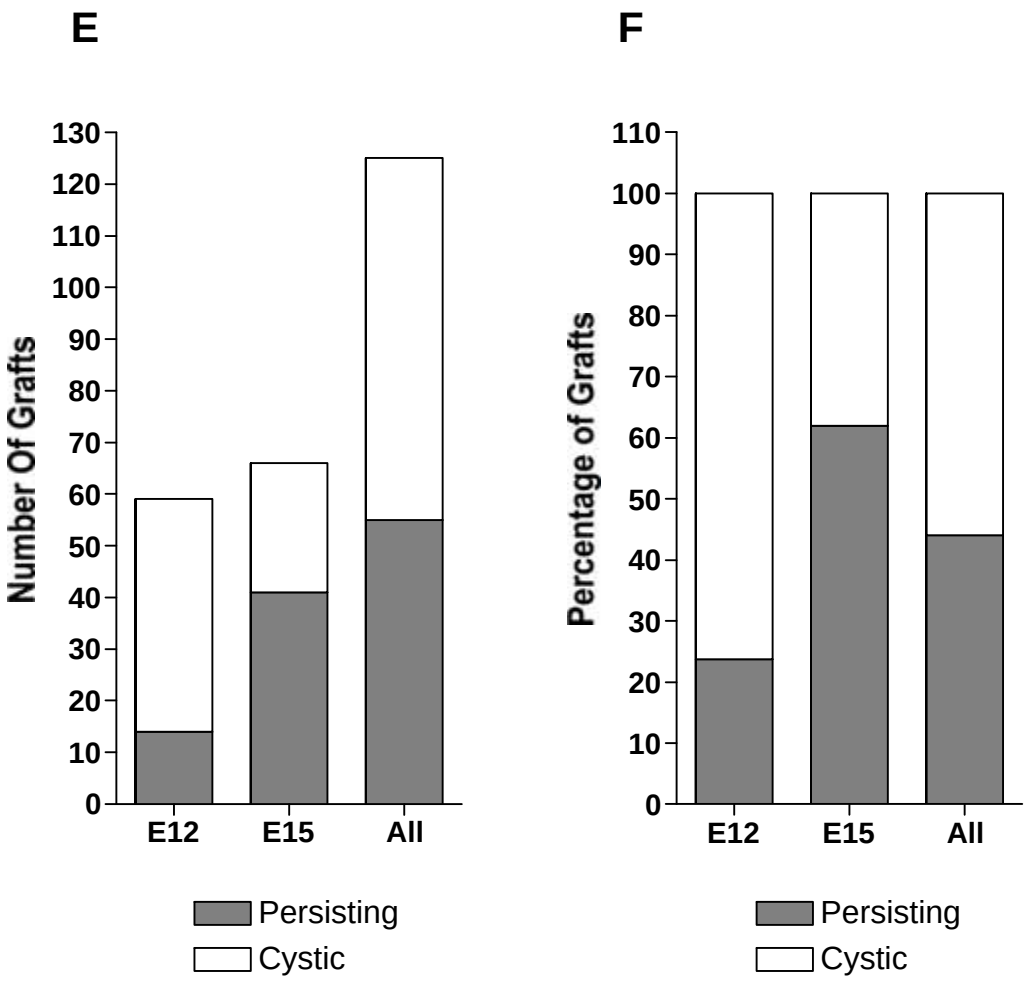

Figure 5.10 Prolonged T Cell Development Is Not Due To Thymocytes Transformation

Adult WT and persisting thymocytes were cultured for a minimum of four days in standard culture conditions (DMEM, 37^{o}C, 10% CO_2). After culture the thymocytes were analysed by flow cytometry for their FSC SSC profile, example FACS plots are shown. Note the small percentages of viable cells after cell culture (5.10A). Percentages of cells within gated areas are indicated. Data is representative of at least three experiments. The percentage survival is plotted against time (5.10B). Note the dramatic decline in survival.

A

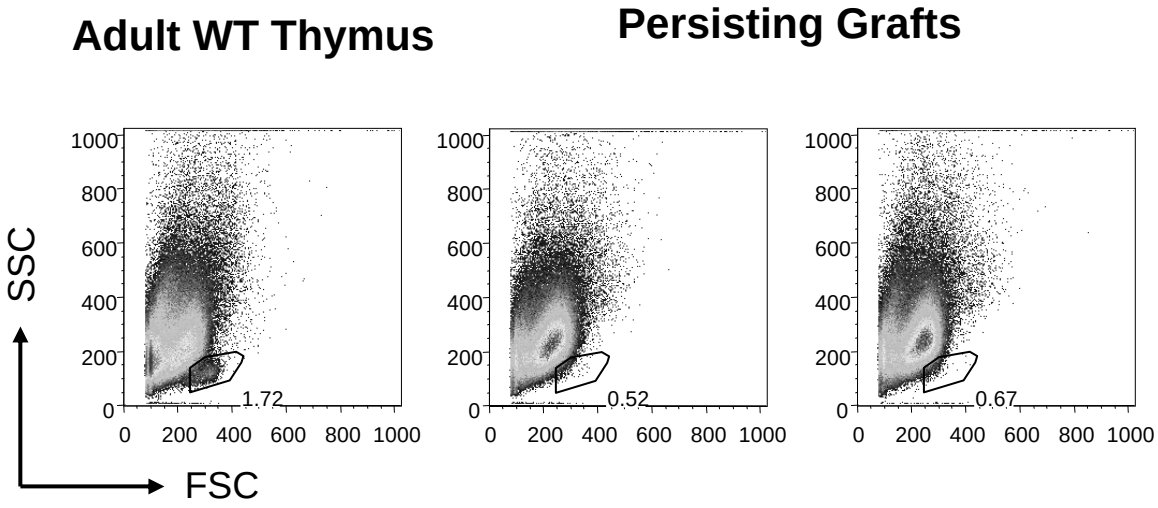
Adult WT Thymus
Persisting Grafts
SSC
FSC
1000
800
600
400
200
0
0 200 400 600 800 1000
1.72
0.52
0.67

B

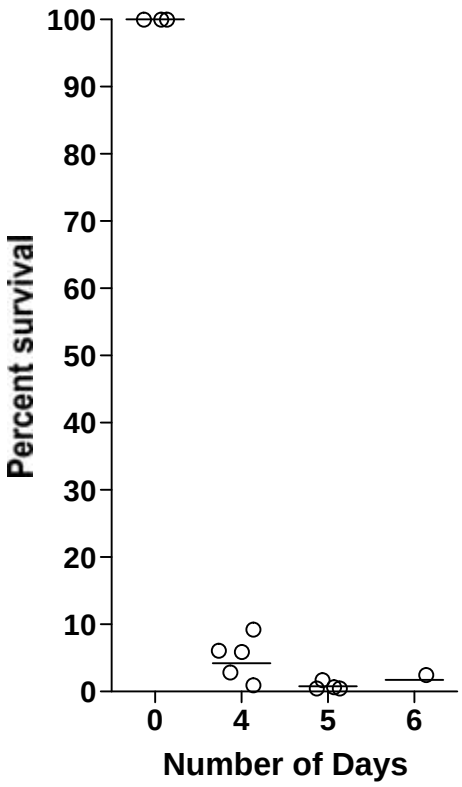
Percent survival
100
90
80
70
60
50
40
30
20
10
0
0 4 5 6
Number of Days

Having established that the persistence was not a result of transformation, another possibility to exclude was whether the persisting DP thymocyte population was a non-cycling population residing within the graft because the internal regulation of their predetermined lifespan of 3-4 days had been disrupted (Ioannidis et al., 2001; Starr et al., 2003; Sun et al., 2000). One way to analyse this was to establish whether the cells were proliferating by assessing the incorporation of Bromodeoxyuridine (5-bromo-2-deoxyuridine, BrdU). BrdU is a synthetic nucleoside analogous to thymidine and is incorporated into the newly synthesized DNA of replicating cells, substituting for thymidine. BrdU specific antibodies can then be used to detect its incorporation, thus enabling detection of actively dividing cells by flow cytometry. E12 thymus lobes were grafted under the kidney capsule of *Rag*$^{-/-}$γc$^{-/-}$ mice and after 7 weeks BrdU was injected into the host via the peritoneum 20 minutes prior to harvesting. The grafts were harvested, the thymocytes isolated and analysed by flow cytometry. During WT T cell development proliferation mainly occurs during the transition from the DN to DP developmental stage, as illustrated by the greatest incorporation of BrdU within the DP thymocytes (Figure 5.11A). A similar BrdU incorporation profile was observed within persisting grafts albeit with varying percentages (Figure 5.11B). These data suggest that the persistence of grafts was probably the result of continual thymocyte development from an early progenitor rather than an inactive DP thymocyte population staying resident within the graft.

The realisation that graft persistence was most likely due to continued thymocyte development, from an immature progenitor that has maintained its location within the grafted thymus, lead to investigation into what regulates precursor residency within the thymus. It was hypothesised that perhaps competition for intrathymic niches would influence the duration of immature thymocyte residency within the thymus because subsequent waves of T cell development did not occur in the *Rag*$^{-/-}$γc$^{-/-}$ host. To test this prediction grafts were placed under

Figure 5.11 Graft Survival Is Not A Result Of Thymocyte Inactivity

E12 thymus lobes were grafted under the kidney capsule of *Rag*$^{-/-}\gamma c^{-/-}$ mice. After 7 weeks the grafts were harvested, teased and analysed by flow cytometry for BrdU incorporation and CD4 and CD8 expression. Representative FACS plots illustrate an adult WT thymus CD4 and CD8 profile and the proliferation of each thymocyte subset (5.11A). Note the similar profile for a persisting 7 week graft (5.11B). Percentages of cells within gated areas are indicated. Data is representative of at least three experiments.

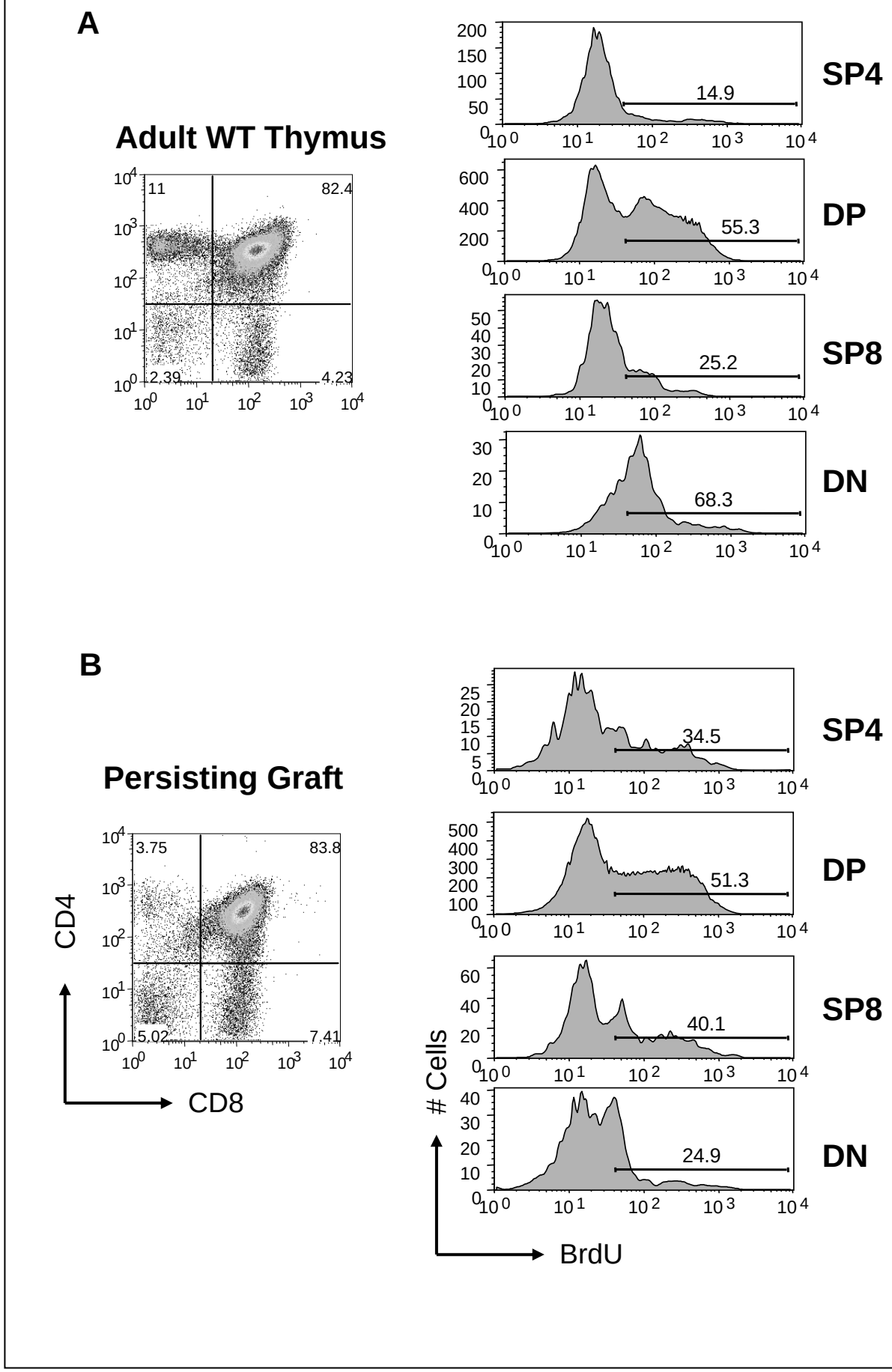
A
Adult WT Thymus
11
82.4
2.39
4.23
SP4
14.9
DP
55.3
SP8
25.2
DN
68.3
B
Persisting Graft
3.75
83.8
5.02
7.41
CD4
CD8
SP4
34.5
DP
51.3
SP8
40.1
DN
24.9
Cells
BrdU

the kidney capsule of Nude hosts (Figure 5.12). Due to a mutation in the *forkhead/winged-helix n1* (FoxN1) gene, Nude mice are unable to generate normal thymic epithelium resulting in a primitive thymic anlage unable to sustain T cell development (Nehls et al., 1994). As their T cell deficiency is the result of a stromal cell defect the thymocyte precursors are capable of populating a functional stromal compartment and completing a normal programme of T cell development. Therefore Nude mice permit further waves of T cell development to occur within the graft and host T cell precursors compete for the intrathymic niches. 7 week grafts were harvested and the developing thymocytes analysed by flow cytometry for CD45.1, CD4 and CD8. Figure 5.13A illustrates that grafts in the $Rag^{-/-}\gamma c^{-/-}$ hosts do not get repopulated with host thymocyte precursors, as very few host ($CD45.1^{-}$) thymocytes are present. 96% of the thymocytes in a graft from a $Rag^{-/-}\gamma c^{-/-}$ host are persisting donor ($CD45.1^{+}$) derived thymocytes that are undergoing development as illustrated by a $CD4^{+}$ $CD8^{+}$ DP. In contrast grafts from Nude hosts are comprised of a majority (98%) of host ($CD45.1^{-}$) derived thymocytes that have repopulated the graft and competed out the $CD45.1^{+}$ graft derived thymocytes. Furthermore the host derived thymocytes are undergoing thymocyte development as indicated by a normal CD4 and CD8 profile (Figure 5.13B). 100% (26/26) of grafts transplanted into Nude hosts did not contain donor derived thymocytes at 7 weeks post engraftment whereas 44% of grafts within $Rag^{-/-}\gamma c^{-/-}$ hosts did contain graft derived thymocytes (Figure 5.13C). Together these data suggest that competition for intrathymic niches influences the amount of time T cells occupy the niche.

To confirm that graft derived ($CD45.1^{+}$) thymocytes had once populated the graft in the Nude system the existence of mature T cells in the periphery of the Nude host was examined. Host splenocytes were analysed by flow cytometry for CD45.1, CD4 and CD8. Graft derived ($CD45.1^{+}$) $CD3^{+}$ $CD4^{+}$ and $CD3^{+}$ $CD8^{+}$ mature T cells were identified (Figure 5.13D),

Figure 5.12 Change Of Experimental Design To Allow Subsequent T cell Development

The experimental model was altered to investigate whether the lack of competition for intrathymic niches was influencing the time immature thymocytes were residing within the graft. Congenically marked E12 thymus lobes were grafted under the kidney capsule of both *Rag*$^{-/-}\gamma c^{-/-}$ and Nude mice. Subsequent waves of T cell development do not occur in *Rag*$^{-/-}\gamma c^{-/-}$ mice due to an early block in T cell development. T cell precursors of Nude mice are not blocked in their development and can therefore repopulate the graft and compete for intrathymic niches.

Embryonic thymus containing single wave of congenically marked (CD45.1) T-cell precursors

$Rag^{-/-}\gamma c^{-/-}$ host:

No host T-cell Precursors:

No subsequent waves of T-cell development

Nude host:

Host T-cell precursors available:

Enables further waves of T-cell development

Figure 5.13 Competition For Intrathymic Niches Prevents Graft Persistence

E12 thymus lobes were grafted under the kidney capsule of *Rag*$^{-/-}$γc$^{-/-}$ and Nude mice. After 7 weeks the grafts were harvested, teased and analysed by flow cytometry for CD45.1, CD4 and CD8 expression. Representative FACS plots illustrate that ~96% of the thymocytes in grafts harvested from *Rag*$^{-/-}$γc$^{-/-}$ hosts are CD45.1^{+} donor derived, and comprise CD4^{+}CD8^{+} DP and CD4^{+}CD8^{-}, CD4^{-}CD8^{+} SP thymocytes (5.13A). Grafts harvested from Nude hosts contain predominantly CD45.1^{-} host derived thymocytes, which display a normal CD4 and CD8 profile (5.13B). Percentages of cells within gated areas are indicated. Data is representative of at least three experiments.

44% of grafts from *Rag*$^{-/-}$γc$^{-/-}$ hosts continued to contain graft derived thymocytes from all four developmental stages. 100% of grafts from Nude hosts did not contain graft derived thymocytes (5.13C). A persisting graft was defined as a graft containing ≥10000 cells and a DP thymocyte population that was harvested at ≥7 weeks.

Nude host spleens were harvested 7 weeks after grafting, teased and analysed by flow cytometry for CD45.1, CD4 and CD8. CD45.1^{+} graft derived thymocytes were identified within the Nude host spleen (5.13D). Percentages of cells within gated areas are indicated. Data is representative of at least three experiments.

A

Rag$^{-/-}\gamma c^{-/-}$ host:

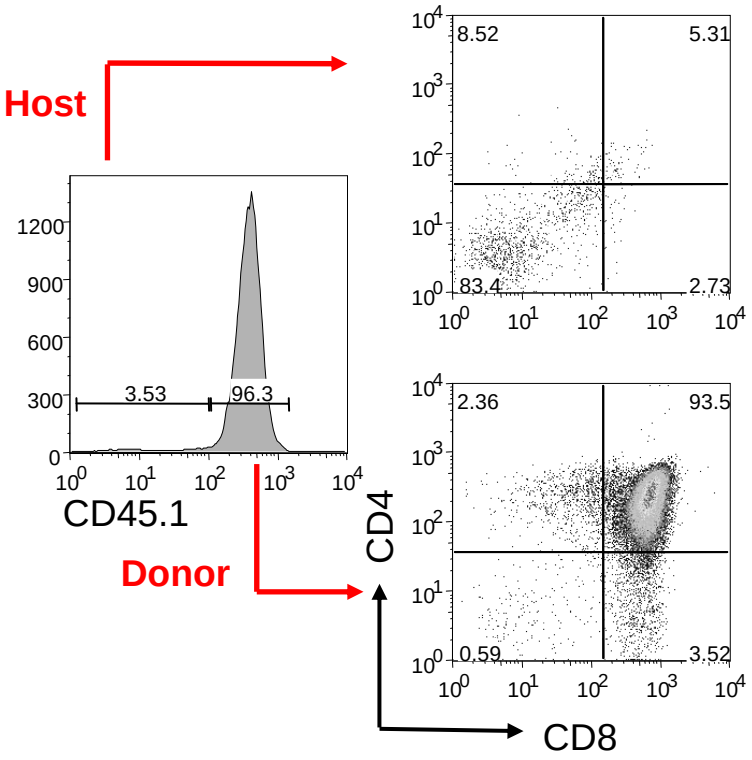

B

Nude host:

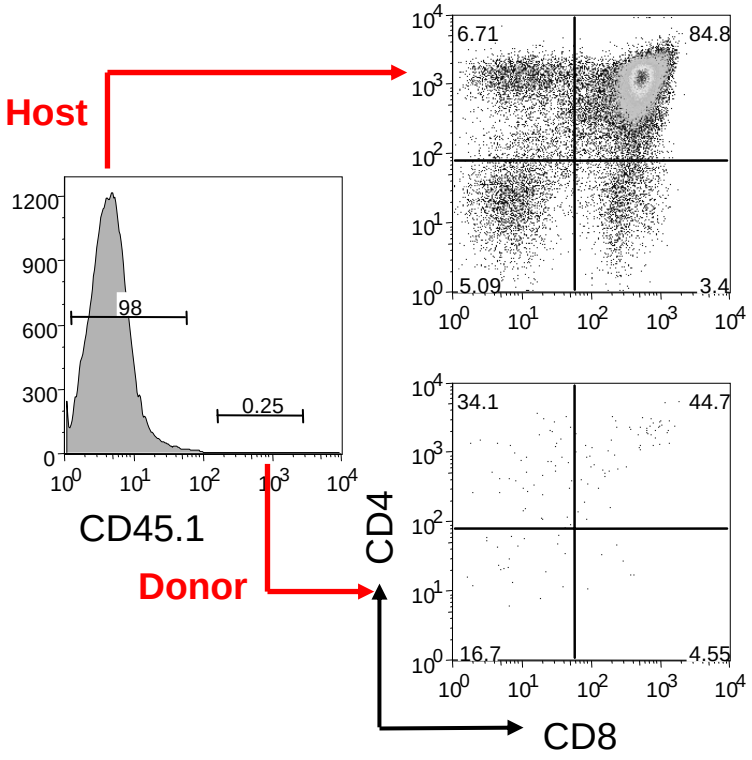

C

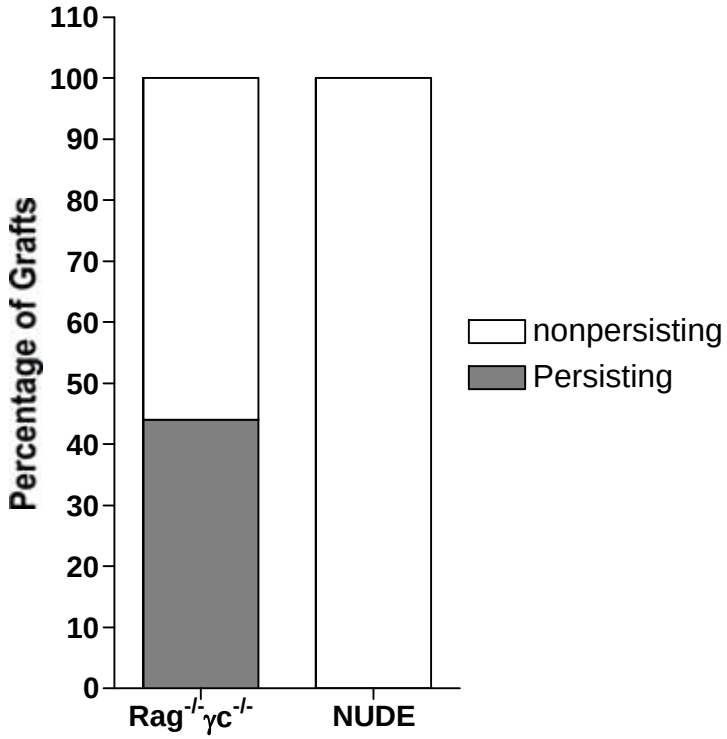
Percentage of Grafts
110
100
90
80
70
60
50
40
30
20
10
0
Rag-/-γc-/-
NUDE
nonpersisting
Persisting

D

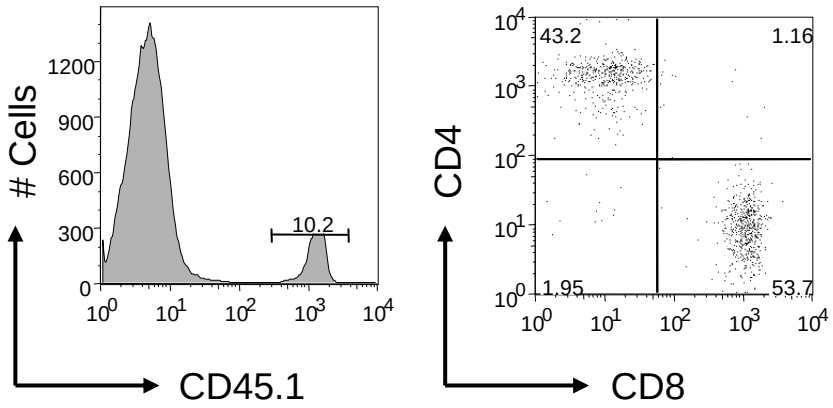
Cells
1200
900
600
300
0
10.2
CD45.1
CD4
CD8
43.2
1.16
1.95
53.7

confirming that in a competitive environment graft derived thymocytes did not remain in the graft.

Grafting into Nude hosts illustrated that a lack of competition for intrathymic niches was likely to be the cause of the continuous presence of developing thymocytes in the grafts. However Nude precursors are able to undergo T cell development until completion and therefore, it was not possible to determine if graft persistence was due to the residence of a single T cell subset, at a specific stage of development. The incorporation of BrdU had previously (Figure 5.11) suggested that the persistence was due to the prolonged residency of a Pre-DP population, as the DP thymocytes had incorporated BrdU. With this in mind and to begin to investigate which thymocyte developmental stage could be responsible, *Rag*$^{-/-}$ hosts were used as T cell development is blocked at the CD4^{-} CD8^{-} CD44^{-} CD25^{+} DN3 stage. In addition, despite the block, T cell development until the DN3 stage is thought to be normal in *Rag*$^{-/-}$ mice (Diamond et al., 1997). Consequently, the graft would be populated by host derived thymocytes at the ETP, DN1 (CD4^{-} CD8^{-} CD44^{+} CD25^{-}), DN2 (CD4^{-} CD8^{-} CD44^{+} CD25^{+}) and DN3 stages of development. Although *Rag*$^{-/-}$γc$^{-/-}$ mice contain thymocytes up to the DN1 stage (Klug et al., 1998) it is unlikely there are sufficient numbers to efficiently compete for the intrathymic niches as supported by our previous findings that 7 week grafts from *Rag*$^{-/-}$γc$^{-/-}$ host mice are able to continue to house developing T cells. 7 week grafts were harvested from *Rag*$^{-/-}$ hosts and analysed by flow cytometry, interestingly 96% of CD45^{+} cells within the graft were host derived. Furthermore, the small proportion of graft derived cells remaining had a mature CD4^{+} CD8^{-} and CD4^{-} CD8^{+} SP phenotype (Figure 5.14A), suggesting host derived double negative thymocytes have competed out graft derived thymocytes. Importantly this was observed in 100% (12/12) the grafts transferred into *Rag*$^{-/-}$ hosts, therefore graft persistence was not observed in *Rag*$^{-/-}$ hosts (Figure 5.14B). The absence of a persisting graft derived thymocyte

Figure 5.14 Competition For Intrathymic Niches Between The ETP And DN3 Developmental Stages Prevents Graft Persistence

E12 thymus lobes were grafted under the kidney capsule of *Rag*$^{-/-}$ mice. After 7 weeks the grafts were harvested and the thymocytes analysed by flow cytometry for CD45.1, CD4 and CD8 expression. Representative FACS plots illustrate that ~96% of the thymocytes in grafts are CD45.1^{-} host derived, and comprise CD4^{-}CD8^{-} DN thymocytes (5.14A). Note the absence of CD45.1^{+} graft derived CD4^{+}CD8^{+} DPs. Percentages of cells within gated areas are indicated. Data is representative of at least three experiments. 100% of grafts from *Rag*$^{-/-}$ mice did not contain a persisting population of graft derived thymocytes (5.14B). A persisting graft was defined as a graft containing ≥10000 cells and a DP thymocyte population that was harvested at ≥7 weeks.

A

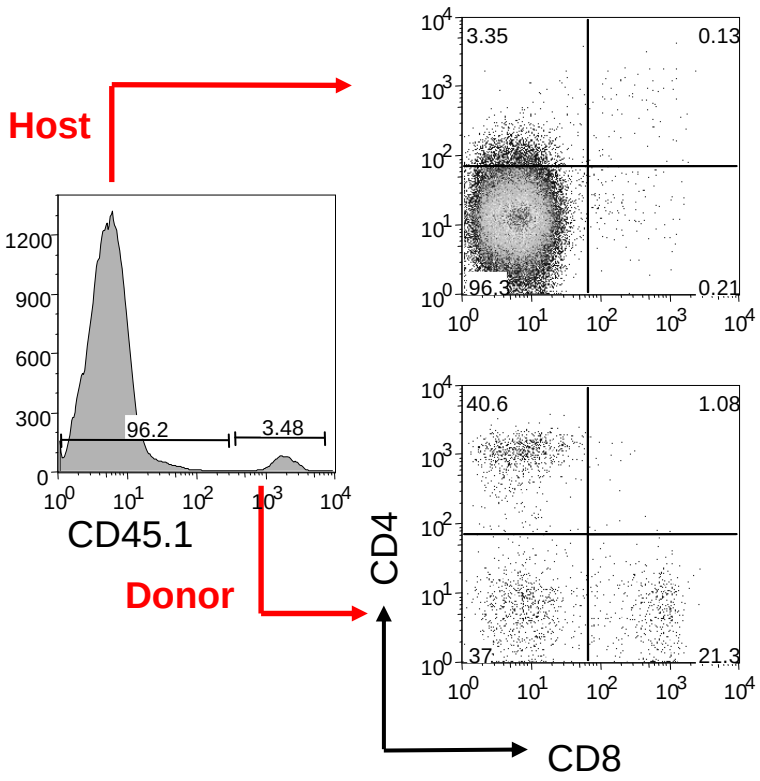
Rag-/- host:
Host
1200
900
600
300
0
96.2
3.48
CD45.1
Donor
3.35
0.13
96.3
0.21
40.6
1.08
37.
21.3
CD4
CD8

B

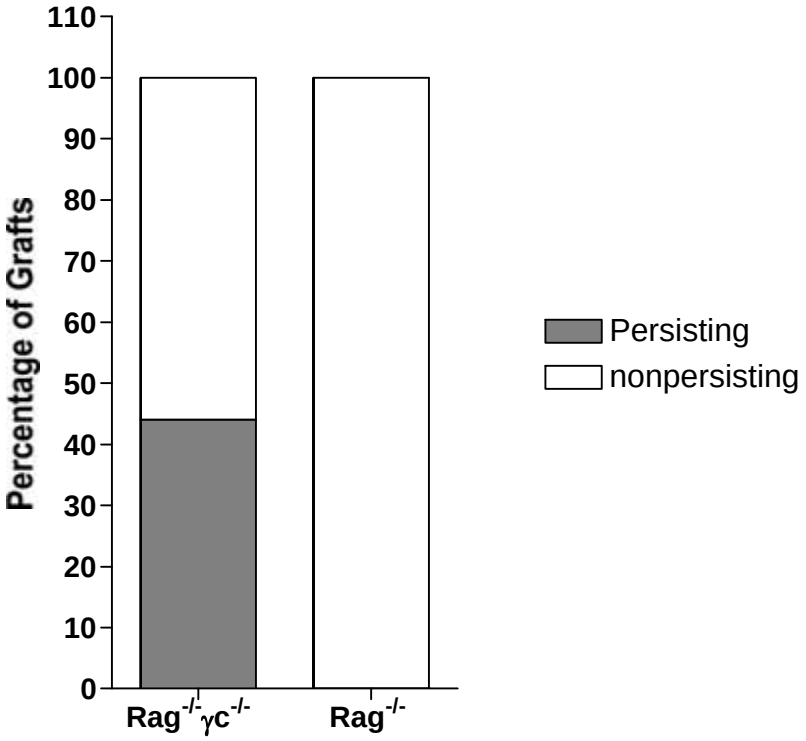
Percentage of Grafts
110
100
90
80
70
60
50
40
30
20
10
0
Rag-/-γc-/-
Rag-/-
Persisting
nonpersisting

population suggests that the thymocyte population that can continue to reside in the thymus is within the $CD4^-CD8^-CD44^+CD25^-$ DN1 to $CD4^-CD8^-CD44^-CD25^+$ DN3 populations.

Understanding that the observed persistence was due to a residing population within the early stages of T cell development, we next sought to identify the resident population. It was also understood that the persisting T cell development was relatively normal and was therefore commencing from an early stage in T cell development. Hence, early thymic progenitors (ETPs) were considered to be the persisting thymocyte population. Thymocytes were isolated from 7 week persisting grafts and analysed by flow cytometry for a lineage panel including CD8, TCRβ, TCRγδ, CD11b, Gr1 and B220 and CD45.1, CD44, and cKit. $CD45.1^+Lin^-CD44^{hi}cKit^{hi}$ ETPs were readily identified by flow cytometry within adult WT thymus (Figure 5.15A) in contrast, an ETP population could not be found within the persisting grafts (Figure 5.15B), suggesting that the continued T cell development was not the result of a surviving ETP population.

As ETPs could not be identified, the next populations to investigate were the $CD4^-CD8^-$ double negative thymocytes. Double negative thymocytes can be subdivided into four stages that are designated, DN1- DN4, and are defined by their differential expression of CD44 (phagocytic glycoprotein 1) and CD25 (IL-2 receptor α) (Ciofani and Zuniga-Pflucker, 2007; Godfrey et al., 1993; Porritt et al., 2004). However, the DN1 ($CD44^+CD25^-$) phenotype is virtually consistent with the definitions for all non T cells (Ponta et al., 2003; Porritt et al., 2004), consequently a comprehensive staining protocol was used, to eliminated numerous lineage committed cells and therefore refine the DN1 subset. A lineage panel consisting of CD11b, Gr1, B220, NK1.1, CD3 and CD11c was used along with CD45.1, CD4 and CD8 to identify the graft derived DN thymocytes and CD44 and CD25 to identify the DN stages. Thymocytes were isolated from WT thymus and grafts harvested 7 weeks post grafting and

Figure 5.15 Graft Persistence Is Not A Result Of Prolonged ETP Residency

E12 thymus lobes were grafted under the kidney capsule of *Rag*$^{-/-}\gamma c^{-/-}$ mice. After 7 weeks the grafts were harvested, teased and analysed by flow cytometry for CD45.1, Lineage, cKit CD25 and CD44 expression. Representative FACS plots illustrate that ETPs can be identified within adult WT thymus (5.15A). Note the absence of graft derived ETP in persisting grafts (5.15B). Percentages of cells within gated areas are indicated. Data is representative of at least three experiments.

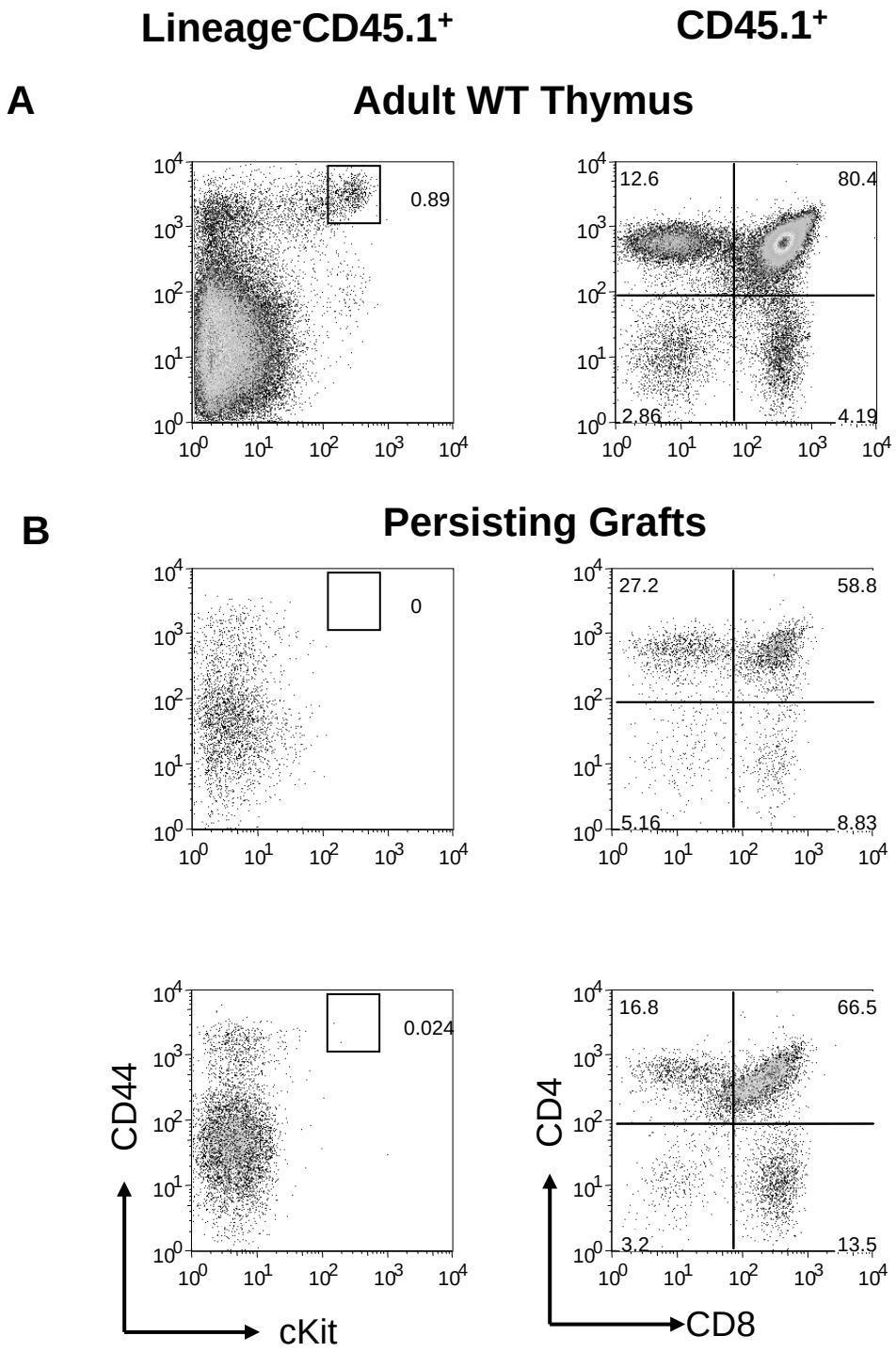
Lineage-CD45.1+
CD45.1+
A
Adult WT Thymus
0.89
12.6
80.4
2.86
4.19
B
Persisting Grafts
0
27.2
58.8
5.16
8.83
0.024
16.8
66.5
3.2
13.5
CD44
cKit
CD4
CD8

analysed by flow cytometry. As expected the DN1 population was virtually absent from the DN profile of WT thymocytes after gating on the lineage negative population, however the DN2 ($CD44^+$ $CD25^+$), DN3 ($CD44^-$ $CD25^+$) and DN4 ($CD44^-CD25^-$) (Godfrey et al., 1993) populations were readily identified (Figure 5.16A). Interestingly, the DN profile of the 7 week grafts appeared abnormal containing the DN3 and DN4 populations only (Figure 5.16B). The absence of the DN1 and DN2 populations would suggest that graft persistence was due to a surviving DN3 thymocyte population, however, these experiments are only preliminary and more repeats are required to draw firm conclusions.

Together these data suggest that during normal thymus homeostasis, a dynamic equilibrium is formed by the entry of new thymocyte progenitors, and the removal of double negative thymocytes through the competition for intrathymic niches.

Figure 5.16 Graft Persistence Is Possibly Due To Prolonged DN3-DN4 Survival

E12 thymus lobes were grafted under the kidney capsule of *Rag*$^{-/-}\gamma c^{-/-}$. After 7 weeks the grafts were harvested, and the thymocytes analysed by flow cytometry for CD45.1, CD11b, Gr1, B220, NK1.1, CD3, CD11c, CD44 and CD25 expression. Representative FACS plots show adult WT control staining where very few lineage negative DN1 can be identified in WT thymocytes yet DN2, DN3 and DN4 populations are still present (5.16A). Note the absence of DN2 population and the presence of dominant DN3 and DN3 populations in persisting grafts. Percentages of cells within gated areas are indicated. Data is representative of at least three experiments.

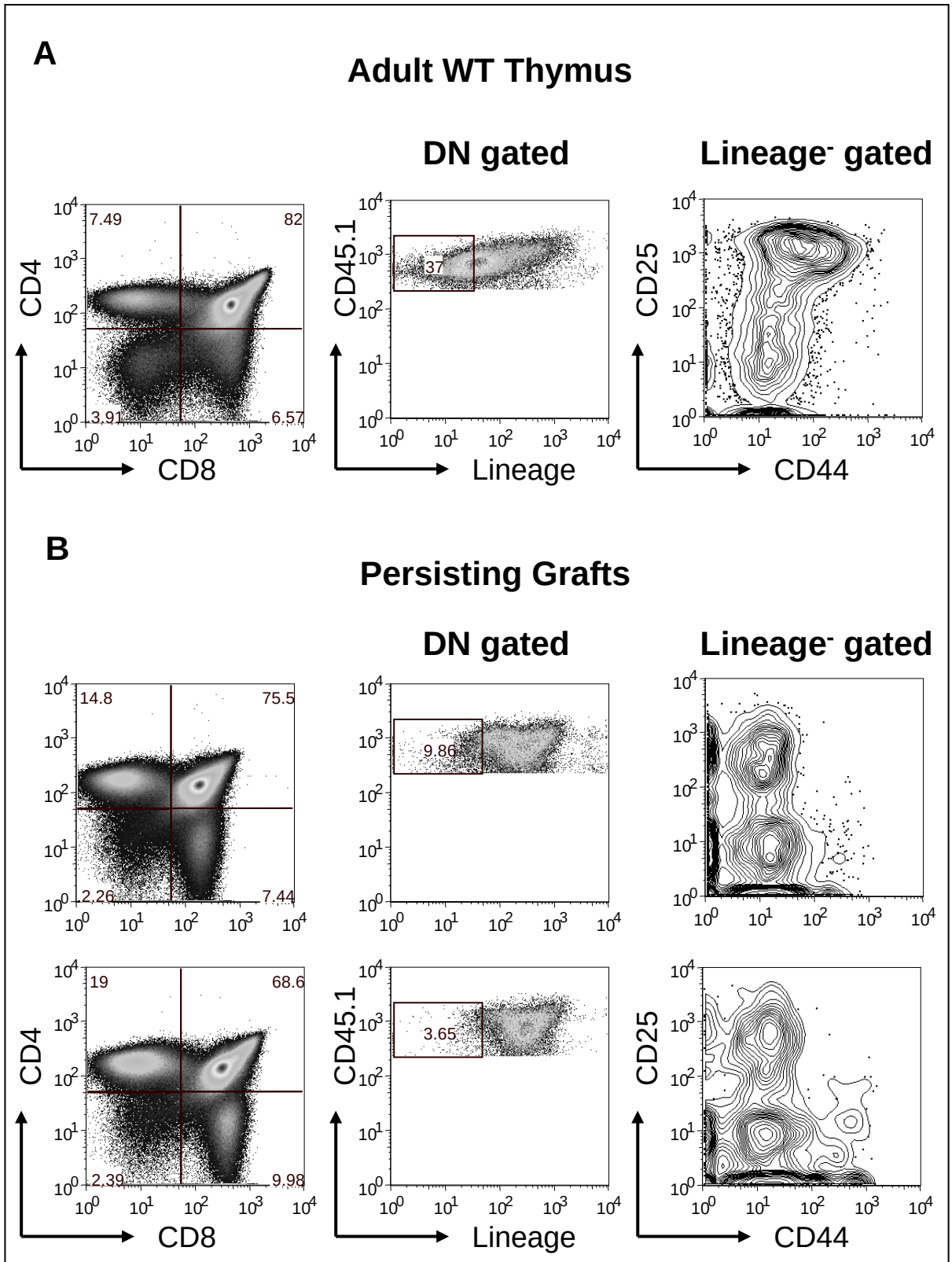
A
Adult WT Thymus
DN gated
Lineage- gated
7.49
82
3.91
6.57
CD4
CD8
37
CD45.1
Lineage
CD25
CD44
B
Persisting Grafts
DN gated
Lineage- gated
14.8
75.5
2.26
7.44
9.86
19
68.6
2.39
9.98
3.65

5.4 Discussion

5.4.1 Lineage Potential Of The Earliest Thymic Migrants

New haematopoietic lineages must be produced throughout life, however, contrary to other blood cell lineages developing from bone marrow derived HSCs, T lymphocytes are produced in the thymus (Porritt et al., 2003). However, the thymus does not contain cells with self-renewing capacity (Goldschneider et al., 1986) and instead depends on the semicontinuous recruitment of bone marrow derived progenitors that circulate in the blood (Foss et al., 2001), for continuous function (Petrie, 2007). Furthermore it has been suggested that the release of precursors into the circulation is coordinated with the requirements of the thymus (Donskoy et al., 2003). This phenomenon has led to a long debate as to whether T specific progenitors, as a result of their lineage commitment home to the thymus, or whether uncommitted precursors are restricted to the T lineage as a consequence of exposure to the thymic stromal microenvironment (Petrie, 2007). Despite intense research into thymic precursor biology, the phenotype and characteristics of the progenitors that enter the thymus remain controversial (Bhandoola and Sambandam, 2006; Petrie and Kincade, 2005).

The controversy is likely the result of many experimental differences and limitations including the absence of consistent definitions used by all research groups (Petrie and Kincade, 2005) and the incredibly low frequency of such precursors in circulation and consequently the small number isolated allowing limited experiments to be performed (Donskoy et al., 2003; Wright et al., 2001). Limiting numbers necessitated the use of immunodeficient or irradiated recipient mice for *in vivo* experiments which lead to inaccurate conclusions due to the creation of artificial conditions by radiation damage, generating structural changes and thus creating new progenitor niches or the loss of competition for existing niches within the host thymus (Bhandoola et al., 2007). In addition the use of artificial (*in vitro*) conditions raised problems

distinguishing between what cells can do when placed in "ideal" conditions from what the same cells do when placed under biological conditions (Petrie and Kincade, 2005), specifically whether cells identified in the bone marrow/blood with T lineage potential actually homed to the thymus or efficiently made T cells under normal circumstances. Therefore the aim of this chapter was to establish a model that would allow isolation and development of a single cohort of thymus colonising cells within a thymic environment that would enable investigation of their lineage potential.

To begin this investigation, a model system was required, for which it was necessary to isolate a single cohort of early thymic migrants. Since isolating thymus precursors from the circulation was complicated by their very small numbers, undefined phenotype and uncertain thymus homing ability, in addition to the understanding that the thymus stromal microenvironment influences the development of the newly recruited precursors, it was decided to investigate the lineage potential of the progenitors that had entered the thymus. As thymus seeding is a continuous event occurring in waves, it would be difficult to determine the lineage potential of a single cohort in the adult thymus because it contains more than one cohort (Foss et al., 2001). Therefore, it was decided to study fetal thymus precursor potential, specifically within the E12 thymus rudiment as thymus seeding by haematopoietic cells begins from E11.5, thus the E12 anlage contains a single wave of thymocyte precursors (Ikawa et al., 2004; Kawamoto et al., 2000; Kawamoto et al., 1998). Moreover, isolation of the whole thymus rudiment removed the need for numerous phenotypic markers, for example Lin, CD44, CD25, c-kit (CD117), CD24 (HSA), Sca-1, Flt3 and CD62L, to identify the first precursors to enter the thymus (Benz et al., 2008) and importantly these cells have migrated to the thymus under physiological conditions.

Grafting of E12 thymus lobes under the kidney capsule of *Rag*$^{-/-}$γc$^{-/-}$ mice resulted in the development of the thymic rudiment into an established thymus lobe, illustrated in part by the

development of distinct cortical and medullary microenvironments, supporting previous reports by Rossi *et al* and Bennett *et al* (Bennett et al., 2002; Rossi et al., 2006). This suggested that the E12 epithelium had undergone the initial specification into either the cortical or medullary lineage and had received the necessary crosstalk signals to allow maturation of these epithelial compartments. Together these observations proposed that T cell development was occurring concurrently and that cell lineages responsible for providing key maturational signals, such as LTi, were also present (Rossi et al., 2007b). Interestingly, 7 weeks after grafting, the thymic epithelium of the grafts that harboured transient T cell development, consisted primarily of a substantial $K5^+K8^+$ double positive area, reminiscent of the unmanipulated *Rag*$^{-/-}$ $\gamma c^{-/-}$ thymus, which possibly represents the de-differentiation of redundant cortical thymic epithelium back to the $K5^+K8^+$ epithelial progenitor phenotype (Anderson et al., 2006). The de-differentiation process has been suggested to occur after a prolonged absence of thymocytes or alternatively, that the continued survival of $K5^+K8^-$ and $K5^-K8^+$ cells may require the presence of thymocytes (Anderson et al., 2006), such as positively selected $CD4^+$ thymocytes providing Rankl to maintain a functional medullary environment (Hikosaka et al., 2008). Therefore as thymocyte numbers diminish, $K5^+K8^+$ cells preferentially accumulate. Furthermore, the appearance of cysts may suggest that the thymic epithelium has lost its three-dimensional integrity and become unusually two dimensional as observed in CD3ε*tg26* mice and reminiscent of a 'classical' type epithelial organisation (van Ewijk et al., 1999). It would be interesting to investigate whether like the CD3ε*tg26* thymus these thymic cysts contain 'classical' epithelial cells, such as absorptive cells, ciliated cells and goblet cells, all placed on a basement membrane (van Ewijk et al., 1999).

Development of the E12 thymus anlage into a functional thymus lobe was further supported by the ability of the grafts to support normal αβ thymocyte development as identified

by a typical CD4 and CD8 co-receptor profile. Since the double negative ($CD4^-CD8^-$) stages of thymocyte development spans a period of approximately 14 days (Shortman et al., 1990) the E12 grafts displayed normal kinetics of thymocyte development, where at 1 week the grafts were comprised solely of DN and DP thymocytes and by two weeks the CD4 and CD8 co-receptor profile resembled that of adult WT thymocyte development. Interestingly the duration of each sequential wave of thymopoiesis is thought to be approximately 6 weeks (Foss et al., 2001). Consistent with this and with the end of a nonself renewing wave of precursors, at 7 weeks the relative proportion of DP cells had diminished and the ratio of SP cells had increased disproportionately (Porritt et al., 2003).

In contrast to previous studies by Douagi *et al*, which suggested that E12 progenitor activity was too low to contribute to the first generation of thymopoiesis, the data presented in this study demonstrated that the E12 thymic immigrants are quite competent at generating a large number of thymocytes *in vivo* (approximately 2×10^5 cells 2 weeks post grafting) (Douagi et al., 2000). Furthermore, the mature thymocytes generated within the E12 thymus graft were able to populate the hosts peripheral T cell compartment quite substantially, which together suggests the E12 thymic immigrants do contribute to the first generation of T cells as recently proposed by Masuda *et al* (Masuda et al., 2005). It would be of interest to further investigate the functional ability of these early T cells to further corroborate their contribution to the peripheral T cell pool. However, this may be difficult to interpret as these naïve T cells are entering a chronic lymphopenic environment due to the *Rag* deficiency of the host. Therefore, it is likely that these cells are undergoing chronic lymphopenia induced proliferation (cLIP) (Surh and Sprent, 2008). Unlike typical slow homeostatic proliferation, cLIP is rapid, requires costimulatory signals through CD28, and the expanding cells display many characteristics of T cells responding to foreign Ags, including rapid upregulation of acute activation markers and the acquisition of

effector function (Surh and Sprent, 2008).

In addition to αβ thymocytes and in support of work from Masuda and colleagues the E12 precursors were found to produce γδ T cells including Vγ5 thymocytes (Masuda et al., 2005). Moreover, E12 progenitors were found to give rise to myeloid cells including DC, NK and LTi. Another T cell lineage to investigate in the future would be the ability of E12 precursors to generate NK-T cells because while NK cell potential was identified by expression of the activation receptor NKp46, which detects all NK cells from the immature $CD122^{+}$ $NK1.1^{+}$ $DX5^{-}$ stage and on a minute fraction of NK-like T cells, it is not expressed on CD1d-restricted NKT cells (Walzer et al., 2007).

Although the data presented here has shown the potential of the first cohort of precursors to enter the thymus have the potential to produce T cells, NK cells and myeloid cells including DCs supporting previous studies (Lu et al., 2005; Masuda et al., 2005; Shen et al., 2003), it is still unclear as to whether these alternative lineages arise from a single multipotent progenitor or from a heterogeneous population of thymic migrants. In support of the former, findings made by disrupting or compromising Notch signalling pathways, such as enforced expression of Deltex or Lunatic fringe (Izon et al., 2002; Koch et al., 2001; Radtke et al., 1999) proposed that Notch signals control the cell fate decision of a multipotent progenitor such as a CLP in the thymus. However, heterogeneity of the earliest thymic migrants has also been identified by differential expression of chemokine receptors on T cell progenitors present within the perithymic mesenchyme and one explanation for the variety of chemokine receptor expression is that they represent a mixture of cell lineages (Jenkinson et al., 2007; Kawamoto et al., 1998). An added complication however, is all $CD45^{+}$ cells attracted to the thymus were found to express paired immunoglobulin receptor (PIR), indicating that chemokine receptor heterogeneity reflects heterogeneity in the early thymic migrants committed towards the T cell lineage (Jenkinson et

al., 2007). Therefore, whether this heterogeneity also reflects heterogeneity in lineage potential is unclear, but it is tempting to believe the possibility that each may be more or less biased toward specific sublineages of T cells, for example CD4, CD8, NK-T, regulatory T, TCRγδ, etc (Jenkinson et al., 2007).

5.4.2 Regulation Of Early T Cell Development By Intrathymic Niches

Since 40% of the grafts harvested at 7 weeks did not demonstrate depletion of the single cohort of thymocyte precursors and instead contained a persisting population of DP thymocytes, it was hypothesised that regulation of DP thymocyte lifespan (typically 3-4 days) had been disrupted (Ioannidis et al., 2001; Starr et al., 2003; Sun et al., 2000). To investigate this a pulse chase analysis with a short 20 minute pulse of BrdU was completed, which indicated that the DP population had incorporated BrdU and had therefore been generated during the 20 minute BrdU availability. This removed the possibility that the DP thymocytes were inactive and continuing to reside within the graft and instead suggested the presence of a pre-DP population continuing to generate new DP thymocytes. Interestingly previous reports have shown that competition for intrathymic stromal niches regulates intrathymic expansion of the DN stages (Prockop and Petrie, 2004). Therefore the observed persistence of a Pre DP subset might be the result of continued intrathymic expansion of a particular subset in the absence of competition. Therefore it was hypothesised that competition for intrathymic niches would influence the duration of immature thymocyte residency.

To establish whether competition for intrathymic niches influenced double positive thymocyte survival, grafts were placed under the kidney capsule of Nude hosts. When provided with a functional stromal compartment, Nude thymocyte precursors are capable of completing a normal programme of T cell development. Therefore, Nude precursors repopulate the graft and compete for the intrathymic niches. Detailed analysis revealed that in a competitive environment

graft derived thymopoeisis did not persist within 7 week grafts. It would be interesting to analyse the kinetics in this system and establish how quickly graft derived thymocytes are competed out. Studies completed by Foss *et al* have revealed the cyclical pattern of progenitor recruitment occurs every 3 weeks, which may suggest graft derived precursors would have exited the graft within 3 weeks of grafting (Foss et al., 2001). In addition it would be interesting to analyse how long continued thymocyte development can occur in the absence of precursor replenishment.

Having established that the persistence of thymocytes within 7 week grafts was at the level of the DN subsets we wanted to begin to narrow down the possible populations responsible. Therefore embryonic thymus anlage were grafted into *Rag*$^{-/-}$ mice, which proposed that the developmental stage responsible for prolonged thymocyte development was between the ETP and DN3 stages, as graft persistence was prevented. Subsequent flow cytometric analysis of the DN stages present within the persisting grafts suggested that the ($CD4^-$ $CD8^-$ $CD44^-$ $CD25^+$) DN3 population was able to maintain itself within the graft. Interestingly the DN3 population has been shown to be accountable for the receptivity of the thymus to progenitor entry, regulating gate opening in a manner consistent with feedback inhibition resulting from competition for occupancy of limited intrathymic niches. Although it is not fully understood, receptivity is thought to occur as each wave of precursors is exhausted, the periodic reduction in cellularity then initiates active regulation (Prockop and Petrie, 2004). Many aspects of the active regulation of precursor entry remain undefined however, it has been reported that seeding of the adult thymus is regulated by the adhesive interaction between P-selectin (CD62P), a carbohydrate binding protein, expressed by thymic endothelium and P-selectin glycoprotein ligand 1 (PSGL1) expressed on circulating lymphoid progenitor cells (Gossens et al., 2009; Scimone et al., 2006). Therefore, in the absence of competition, although the DN3 population may not ordinarily persist, it is able to remain within its intrathymic niche. This idea is supported by the notion that

intrathymic expansion of the DN stages is limited by competition for intrathymic niches therefore the absence of competition allows this population to continue to expand (Prockop and Petrie, 2004). Little is known about what constitutes an intrathymic niche but it is likely that the DN3 population resides within a stromal cell niche as precursor entry appears to be influenced mainly by radiation sensitive lymphoid cells (Prockop and Petrie, 2004). Furthermore previous studies have shown that DN cells must remain in constant contact with the $VCAM^{+}$ stromal matrix that permeates the cortex for their development (Prockop et al., 2002). However it has been suggested that their presence within the niche requires survival signals that are absent in IL-7Rα deficient mice, which may advocate a role for survival signals in regulating the duration of intrathymic niche residency (Prockop and Petrie, 2004) and therefore increased availability of survival signals due to the absence of competition may enable the DN3 population to remain in the thymus graft.

The outer half of the cortex defines the inductive microenvironment for DN3 differentiation (Porritt et al., 2003) and interestingly, some similarities can be drawn between this intrathymic region and the stem cell niche, namely the expression of Cxcl12 (Petrie and Zuniga-Pflucker, 2007) which has been identified as a crucial factor involved in retention and maintenance of adult HSCs (Wilson and Trumpp, 2006). In addition adhesion to the stromal matrix via VCAM-1 expression has been implicated in DN development (Petrie and Zuniga-Pflucker, 2007; Prockop et al., 2002) and in the HSC niche VCAM-1 has an important role in HSC engraftment (Wilson and Trumpp, 2006). Furthermore, signalling through Notch receptors is thought to have a role in the maintenance of stem cells in a variety of tissues (Wilson and Trumpp, 2006) and at the DN3 stage of thymocyte development Notch signalling is heavily involved. Together these similarities may suggest the presence of a niche within the thymus capable of supporting thymocyte survival for long periods of time. This maybe the result of the

limitless supply of growth factors as other developing thymocytes are not competing for and depleting them. Perhaps in the absence of competition the DN3 thymocytes are able to reveal their long lived T cell committed potential to continually generate DP thymocytes as they are not being forced to leave this permissive environment that enables them to survive. In order to test this hypothesis it would be interesting to observe the maximum length of time a graft is able to persist for. Maybe the model presented here could be used to characterise the elusive nature of intrathymic stromal niches and the signals they deliver to developing lymphocytes. Furthermore it is attractive to speculate that this could lead to the identification of a T lineage restricted self renewing population within the thymus.

CHAPTER 6: GENERAL DISCUSSION

The thymus is a primary lymphoid organ responsible for the generation of a diverse, self-tolerant T cell repertoire. This unique function of the thymus is attributable to the specialised thymic microenvironment, in particular the thymic epithelium, which is organised into two distinct microenvironments that play essential, yet unique roles in educating the developing thymocyte population. Epithelial cells of the cortical lineage via positive selection impose self-MHC restriction on the nascent thymocytes and medullary epithelial cells are responsible for the deletion of autoreactive thymocytes via negative selection (Anderson et al., 2009). The highly organised migration of the developing thymocytes between these specific microenvironments ensures ordered provision of essential maturational signals through a combination of direct cell-cell contact and the production of soluble factors (Aw et al., 2009). In contrast to the relatively well-defined stages of T cell development, the developmental progression and molecular signals that govern the establishment of the thymic microenvironments remain largely undefined. Therefore, the aim of this thesis was to further investigate the cellular and molecular mechanisms involved in thymic epithelial cell development.

One of the striking paradoxical characteristics of the thymus is that it undergoes age-associated atrophy, a process that becomes apparent as early as the first year of life in humans (Chidgey et al., 2008; Lynch et al., 2009). The functional thymic epithelium is replaced over time by peri-vascular spaces and fibrofatty tissue, which disrupts the normal architecture (Chidgey et al., 2008). In addition, age related changes to the remaining epithelium include a decline in cortical and medullary markers, morphological alterations and disorganisation, which have been implicated in the modified expression of important signals such as Notch (Aw et al., 2009). Involution of the thymic epithelium results in a decline in naïve T cell output to the periphery due to the reduced efficiency of thymopoiesis (Berzins et al., 2002). Homeostatic mechanisms counteract this loss by expanding the existing T cell pool, which detrimentally

reduces the peripheral T cell repertoire which is the major contributor to the age-associated deterioration of the immune systems ability to respond to infection and vaccination (Aw et al., 2009). However, under most circumstances, thymus regression is of minimal consequence to a healthy individual, but the reduced efficacy of the immune system with age is linked to increased morbidity and mortality in a wide rage of clinical settings (Lynch et al., 2009). Furthermore, high dose conditioning regimes, such as chemotherapy and radiation, result in the severe depletion of the immune system through the targeting of highly proliferating cells such as developing and naïve T cells (Chidgey et al., 2008). In addition, these damaging treatments also affect the overall cellularity and architectural organisation of the thymic stromal cell population. Consequently, the inability to proficiently restore a heterogeneous T cell population and re-establish immune function further increases morbidity and mortality in the aged. Whether epithelial tissue degeneration is causative for or a response to reduction in developing thymocytes is still under debate, but given the complexity and interdependent processes of thymic crosstalk, it is likely to involve both.

The functional rejuvenation of the thymus, with renewed naïve T cell output and replenishment of the peripheral T cell pool, remains one of the biggest challenges of clinical immunology despite its therapeutic potential (Gray et al., 2005). Therefore, the data presented in this thesis have important implications for strategies aimed at the functional rejuvenation of the atrophied thymus or after insult induced by chemotherapy, ionizing radiation exposure and infections (e.g. HIV-1) (Gray et al., 2005; Lynch et al., 2009).

The data presented within this study supports the notion that the reciprocal signalling termed “thymus crosstalk” is necessary for the development of a functional thymic epithelial structure. Interestingly however, it was previously thought that thymus crosstalk was temporally restricted to the fetal period, where failure of crosstalk to occur during this developmental

window rendered the thymus refractory to subsequent signals and resulted in aberrant T cell selection (Hollander et al., 1995a; Hollander et al., 1995b). In support of a requirement for crosstalk during the fetal period, this study has identified a novel role for the γδ T cell subset Vγ5, which are thought to develop solely from fetal progenitors that require a fetal environment, in the initiation of development of the thymic medulla, thus extending the current understanding of Aire$^+$ mTEC development and the involvement of LTi and SP4 thymocytes (Ikuta et al., 1990; Rossi et al., 2007b; White et al., 2008b). Together these data propose a new model of Rank-mediated mTEC maturation, where fetal Vγ5$^+$ thymocytes and thymic LTi comprise the fetal programme, involved in the initiation and both thymic LTi and SP4 cells constitute the post-natal and adult programme (Figure 6.1) (Akiyama et al., 2008; Rossi et al., 2007b; White et al., 2008b). The functional consequences of the observed role of Vγ5$^+$ thymocytes in Aire$^+$ mTEC development may be that Vγ5$^+$ thymocytes induce the maturation of the medullary thymic microenvironment, to establish a tolerising environment in preparation for the subsequent αβ thymocyte development.

In contrast to crosstalk being required during fetal development we have shown that adult thymic epithelium remains responsive to crosstalk signals despite the prolonged absence of crosstalk signalling, which has important implications for strategies aimed at reviving thymus function and T cell production after extended periods of thymic inactivity (Roberts et al., 2009). In addition, supporting the occurrence of crosstalk at later time points, cell types that appear in the post natal thymus such as CD4$^+$ SP thymocytes briefly mentioned above, have been implicated in the provision of crosstalk signals possibly concerned with the maintenance of the medulla (Akiyama et al., 2008; White et al., 2008b). Together, these data highlight the importance of crosstalk but emphasize the requirement for further analysis into the timing of crosstalk signals and the differences between initiation of developmental processes and the

Figure 6.1 A New Model For Rank-Mediated mTEC Maturation

Fetal $V\gamma5^+$ thymocytes and thymic LTi comprise the fetal programme during the initial stages of mTEC development. Later in ontogeny thymic LTi and SP4 thymocytes constitute the post-natal and adult programme of mTEC maturation.

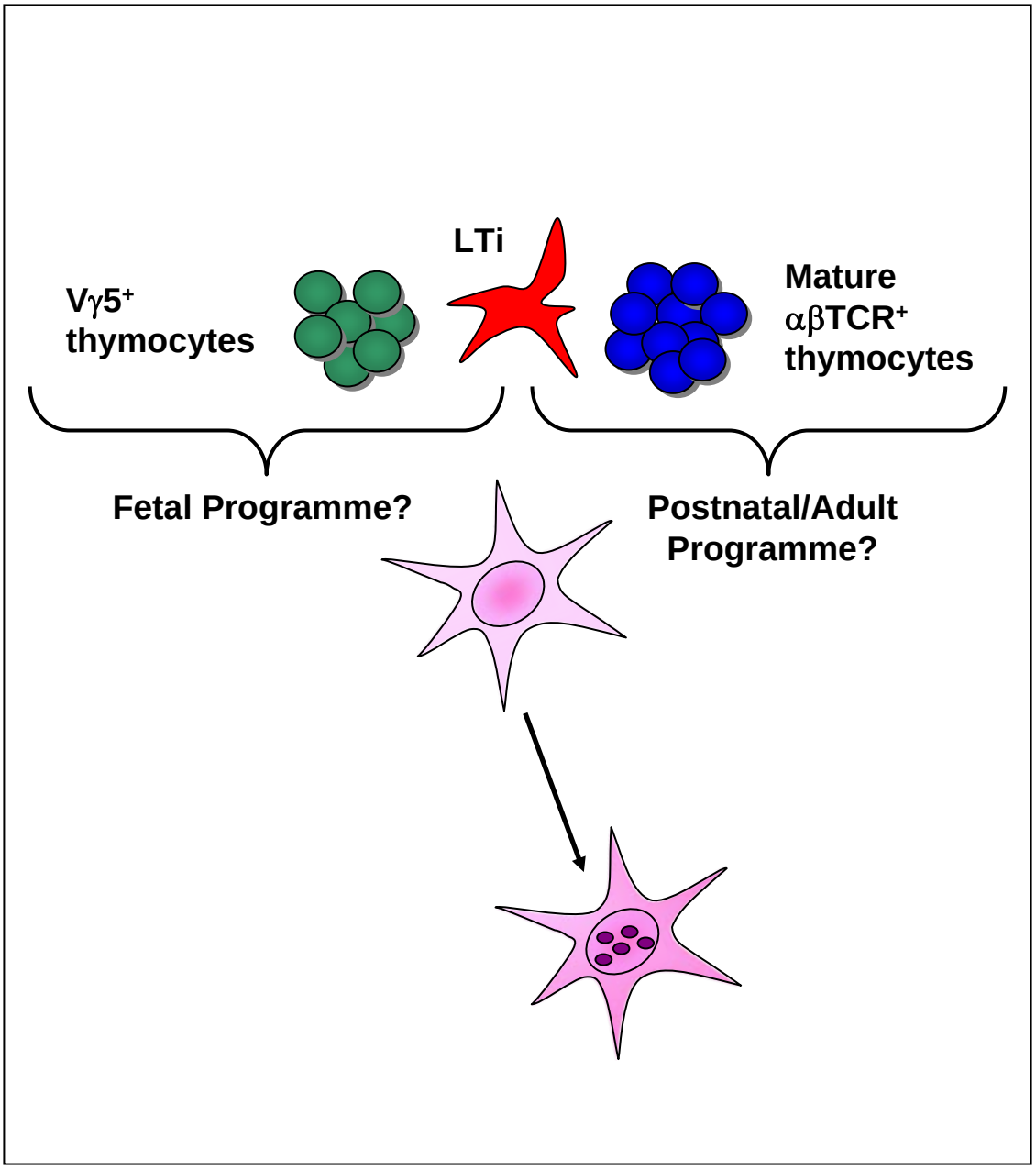
LTi
Vγ5+
thymocytes
Mature
αβTCR+
thymocytes
Fetal Programme?
Postnatal/Adult
Programme?

maintenance of mature epithelial compartments.

The importance of timing and order of signals is beginning to emerge. In addition to identifying the role of positively selected SP $CD4^+$ thymocytes in the provision of Rankl to developing medullary epithelium, it has recently been shown that activation of the LTα-LTβR axis by mature thymocytes is required for the terminal differentiation of $Aire^+$ mTECs only after they have fulfilled their role negatively selecting the nascent T cell repertoire (White *et al* JI in press)(Akiyama et al., 2008). Additionally, data presented in this thesis has suggested that the first wave of precursors to enter the thymic rudiment includes cells either committed to or with the development potential to become LTi and Vγ5, both of which are important for the development of mature $Aire^+$ mTECs. Furthermore, new production of DCs at the beginning of each progressive wave of thymocyte development, which are thought to enhance the intact medullary tolerising microenvironment in preparation for the ensuing thymocyte development has been reported (Porritt et al., 2003).

It is interesting to speculate why there are two different cell types involved in the maturation of the medullary epithelium in the fetal thymic rudiment. γδ T cells probably developed evolutionarily before LTi and were initially involved in the development of $Aire^+$ mTECs for their own benefit as $Aire^+$ mTECs provide Skint1, a molecule implicated in the positive selection of $Vγ5^+$ T cells in the embryonic thymus and normal numbers in the skin (Boyden et al., 2008). It is likely the $Aire^+$ mTEC compartment then became important as a negatively selecting environment for the development of αβ T cells, resulting in selective pressure to ensure this process occurred properly. LTi and Vγ5 T cells are not that dissimilar, they are both an innate cell type, so perhaps a gene duplication event was beneficial by providing a second cell type able to prime the mTECs. Immunological crosstalk between the innate and adaptive immune system is frequently observed at the cellular level (for instance priming of αβ

T cells by DCs) (Basset et al., 2003; Medzhitov and Janeway, 1997). The observation that LTi and γδ thymocytes are required to set up central tolerance by priming the adaptive immune environment is analogous to crosstalk at the cellular level. It would be interesting to speculate that any cell expressing Rankl would be able to influence the development of the thymic medulla however, data presented within this study may imply that other signals are involved in this process as DETC that express high levels of Rankl do not appear to possess the ability to induce mTEC development. Whether a second agonistic signal or if an inhibitory signal such as the expression of the decoy receptor OPG is involved or even a combination of the two is yet to be determined (Yasuda et al., 1998).

Although an understanding of the crosstalk signals involved in the development of the thymic cortex are yet to be fully elucidated, these advances in understanding the cellular mechanisms implicated in mTEC development are particularly relevant for thymus reconstitution after ablative therapy because the medullary epithelium has been shown to be more susceptible to radiation damage (Adkins et al., 1988; Chung et al., 2001).

The elucidation of the signals involved in the development of the thymic cortex is required to further understand the importance of the timing of thymus crosstalk as it has previously been proposed that establishing a thymic cortex is an important prerequisite to the expansion of the medulla (Hollander et al., 1995b; van Ewijk et al., 2000). Moreover, the importance of thymic crosstalk during cTEC development has been shown by its necessity for cTEC differentiation and acquisition of markers associated with functional maturation (i.e. MHC II and CD40 expression) (Shakib et al., 2009). Early stages of thymocyte development, the maturation of which occurs within the cortex are likely to provide specific crosstalk signals. This is illustrated by the subtle differences between mouse models blocked at different double negative stages of development. The *Rag*$^{-/-}$γc$^{-/-}$ thymus contains thymocytes at the (CD44^{+}CD25^{-}

) DN1 stage and TEC have a 3D structure whereas, the CD3ε*tg26* thymus is completely devoid of thymocytes and TEC have a 2D structure (Klug et al., 2002). These observations suggest that DN1 thymocytes are involved in promoting the characteristic 3D architecture of the thymic epithelium. As the DN1 compartment is comprised of multiple cell types, it would be interesting to investigate the involvement of each and elucidate their role in initiating cTEC development and the 3D architecture (Ponta et al., 2003; Porritt et al., 2004).

The cortex is further subdivided into inner, outer and subcapsular regions and it would be interesting to dissect the differences in the signals required to establish and constitute these unique regions. It is interesting to speculate that these probably occur as a result of signalling from the progressive development of each double negative stage of thymocyte development, as these stages require each microenvironment. To address this, future experiments could involve purifying CD3ε*tg26* embryonic epithelial cells, reaggregating them with each of the four DN thymocyte subsets and following culture analyse the subtle differences in the development of the three dimensional epithelial structure. This would be particularly interesting with regard to the subcapsular region, which has been implicated in the development of the DN3 stage of thymocyte maturation and the receptivity of the thymus to progressive rounds of precursor entry (Prockop and Petrie, 2004). The importance of intrathymic niches in regulating early T cell progenitor development has been recognised in this study, where the abnormal opportunity to reside within the subcapsular zone, the DN3 intrathymic niche, resulted in the prolonged life span of the DN3 population and continued thymocyte development. Therefore development of this niche could have the potential to promote more permanent thymocyte development, the length of which is yet to be revealed but is longer than a single wave of thymocyte development (Foss et al., 2001). Whether the prolonged survival of the DN3 thymocytes is the result of prolonged availability of growth factors or survival signals or whether the DN3 population itself

represents a long lived T cell committed progenitor remains to be elucidated. Interestingly, in support of the presence of a niche able to support a long lived T cell precursor, a recent study demonstrated, that under conditions in which recipients were not conditioned, in situ early T cell progenitors could sustain long-term thymopoiesis, provided they are injected directly into the thymus (Vicente et al., 2010).

Due to the role of DN thymocytes in regulating the availability of intrathymic niches, understanding the signals involved in the development of the thymic cortex may have important implications in understanding precursor entry into the thymus. Precursor entry is important because it is generally accepted that intrathymic progenitors do not contain long-term self-renewing potential (Goldschneider et al., 1986; Wallis et al., 1975). Therefore, the continuous colonisation of the thymus is required for efficient T cell generation (Anderson et al., 2006; Petrie, 2003). This is of significance because if the order of cells entering the thymus is important for the provision of specific crosstalk signals and thus the subsequent development of certain epithelial cell types, understanding the heterogeneity of the input population and the particular signals they provide at a certain time, will help to ensure that the thymic microenvironment can be rejuvenated after atrophy and/or ensure the proper maintenance of the existing thymus.

Although we have established that thymic crosstalk is not restricted to the fetal period, these studies were completed in adult mice whose thymus has never previously undergone complete development or produced a cohort of T cells. It would be interesting to investigate whether the thymus has the capacity to repeat the developmental process after undergoing regression. A possible way to investigate this would be to employ the grafting system established in this study where thymus lobes are under the kidney capsule of *Rag*$^{-/-}$γc$^{-/-}$ hosts. T cell progenitor development is blocked at an early stage in these mice and therefore host progenitors

are not able to provide subsequent waves of T cell development. This allows the graft to support the development of the single cohort of T cells and after their depletion the epithelial structure begins to regress, becoming composed of $K5^{+}K8^{+}$ predominantly and cystic structures start to appear as the 3D epithelial structure collapses and becomes 2D. Once this has occurred it would be possible to investigate reconstitution of the graft by intravenous transfer of FL derived thymocyte precursors, as data presented in this thesis established this as a successful model to investigate reconstitution of the orthotopic thymus. This could assist the identification of a bipotent or lineage restricted TEC progenitor stem cell pool with self-renewal capacity. In support of the existence of a thymic epithelial stem cell, studies have revealed the reversal of the degenerative state of the aged thymus, for example after sex steroid ablation therapy (Greenstein et al., 1987).

Additionally, the data presented here has illustrated the success of renewed thymic function in reconstituting the peripheral T cell compartment. Efficient immune responses to T-dependent antigen require the presence of mature naive T cells in the periphery and the segregation and organisation of the T and B cell populations within secondary lymphoid organs (Glanville et al., 2009). This study established that mature T cells were efficiently exported from the Lin^{-} FL reconstituted CD3ε*tg26* and *Rag*$^{-/-}$γc$^{-/-}$ thymuses and have the capacity to home efficiently to the normally T cell deficient T zones of the hosts spleens.

Interestingly the transfer of fetal liver cells into *Rag*$^{-/-}$γc$^{-/-}$ mice had a more profound effect on the splenic white pulp stroma as a result of reconstituting both the T and B cell compartments of the host. The spleen within a *Rag*$^{-/-}$γc$^{-/-}$ normally contains only rudimentary white pulp areas that are identified by the presence of a small number of $CD4^{+}CD3^{-}$ lymphoid tissue inducer (LTi) (Withers et al., 2007). Here it has been shown that organised white pulp areas develop after fetal liver reconstitution including the upregulation of the T zone markers

Ccl21 (Ngo et al., 1999) and Gp38 (Withers et al., 2007), which demonstrate site-specific expression. Moreover, the presence of B cells within B cell areas is also observed, therefore the white pulp areas in the Lin^- FL reconstituted *Rag*$^{-/-}\gamma c^{-/-}$ mice were completely restored. Thus fetal liver reconstitution has the potential to introduce a peripheral immune system within patients with severe combined immunodeficiency for example.

However, the functional ability of the T cells generated within reconstituted thymic epithelium has not yet been analysed and may be difficult to interpret as these naïve T cells are entering a chronic lymphopenic environment due to the Rag deficiency of the host. As a result it is likely that these cells will have undergone chronic lymphopenia induced proliferation (cLIP) upon entry to the periphery (Surh and Sprent, 2008). Unlike typical slow homeostatic proliferation, cLIP is rapid and the expanding cells display many characteristics of T cells responding to foreign antigens (Surh and Sprent, 2008). Unfortunately, this process has been linked to a reduction in the peripheral repertoire and abridged efficiency of the T cell response to foreign antigen. Therefore, it is important to consider the peripheral immune system and its potential effect on the nascent T cells during immune reconstitution. Furthermore, as 'space' within the haematopoietic bone marrow niche has not been created by ablative therapy, stem cells within the inoculum have not reconstituted the bone marrow and hence the renewed thymic function is transient, illustrated by exhaustion of haematopoietic precursors resulting in the cessation of new T cell development. Interestingly, it has been reported that repetitive transplantation can lead to high levels of bone marrow engraftment (Blomberg et al., 1998) therefore, it may be possible to sufficiently reconstitute the host bone marrow of immunocompromised patients with haematopoietic precursors, which will subsequently replenish thymocyte precursors, maintain thymocyte development and output, resulting in the establishment or maintenance of a peripheral immune system.

Papers arising from this thesis

Roberts NA, Desanti GE, Withers DR, Scott HR, Jenkinson WE, Lane PJ, Jenkinson EJ, Anderson G, (2009), *Absence of thymus crosstalk in the fetus does not preclude hematopoietic induction of a functional thymus in the adult,* Eur J Immunol, 39;2395.

CHAPTER 7: LIST OF REFERENCES

Adkins, B., Gandour, D., Strober, S., and Weissman, I. (1988). Total lymphoid irradiation leads to transient depletion of the mouse thymic medulla and persistent abnormalities among medullary stromal cells. J Immunol *140*, 3373-3379.

Adkins, B., Mueller, C., Okada, C.Y., Reichert, R.A., Weissman, I.L., and Spangrude, G.J. (1987). Early events in T-cell maturation. Annu Rev Immunol *5*, 325-365.

Ajitkumar, P., Geier, S.S., Kesari, K.V., Borriello, F., Nakagawa, M., Bluestone, J.A., Saper, M.A., Wiley, D.C., and Nathenson, S.G. (1988). Evidence that multiple residues on both the alpha-helices of the class I MHC molecule are simultaneously recognized by the T cell receptor. Cell *54*, 47-56.

Akashi, K., Traver, D., Miyamoto, T., and Weissman, I.L. (2000). A clonogenic common myeloid progenitor that gives rise to all myeloid lineages. Nature *404*, 193-197.

Akira, S. (2009). Pathogen recognition by innate immunity and its signaling. Proc Jpn Acad Ser B Phys Biol Sci *85*, 143-156.

Akiyama, T., Maeda, S., Yamane, S., Ogino, K., Kasai, M., Kajiura, F., Matsumoto, M., and Inoue, J. (2005). Dependence of self-tolerance on TRAF6-directed development of thymic stroma. Science *308*, 248-251.

Akiyama, T., Shimo, Y., Yanai, H., Qin, J., Ohshima, D., Maruyama, Y., Asaumi, Y., Kitazawa, J., Takayanagi, H., Penninger, J.M.*, et al.* (2008). The tumor necrosis factor family receptors RANK and CD40 cooperatively establish the thymic medullary microenvironment and self-tolerance. Immunity *29*, 423-437.

Allison, J.P., and Havran, W.L. (1991). The immunobiology of T cells with invariant gamma delta antigen receptors. Annu Rev Immunol *9*, 679-705.

Allman, D., Sambandam, A., Kim, S., Miller, J.P., Pagan, A., Well, D., Meraz, A., and Bhandoola, A. (2003). Thymopoiesis independent of common lymphoid progenitors. Nat Immunol *4*, 168-174.

Alt, F.W., Oltz, E.M., Young, F., Gorman, J., Taccioli, G., and Chen, J. (1992). VDJ recombination. Immunol Today *13*, 306-314.

Alves, N.L., Huntington, N.D., Rodewald, H.R., and Di Santo, J.P. (2009). Thymic epithelial cells: the multi-tasking framework of the T cell "cradle". Trends Immunol *30*, 468-474.

Anderson, G., Harman, B.C., Hare, K.J., and Jenkinson, E.J. (2000a). Microenvironmental regulation of T cell development in the thymus. Semin Immunol *12*, 457-464.

Anderson, G., and Jenkinson, E.J. (2001). Lymphostromal interactions in thymic development and function. Nat Rev Immunol *1*, 31-40.

Anderson, G., Jenkinson, E.J., and Rodewald, H.R. (2009). A roadmap for thymic epithelial cell development. Eur J Immunol *39*, 1694-1699.

Anderson, G., Jenkinson, W.E., Jones, T., Parnell, S.M., Kinsella, F.A., White, A.J., Pongrac'z, J.E., Rossi, S.W., and Jenkinson, E.J. (2006). Establishment and functioning of intrathymic microenvironments. Immunol Rev *209*, 10-27.

Anderson, G., Lane, P.J., and Jenkinson, E.J. (2007). Generating intrathymic microenvironments to establish T-cell tolerance. Nat Rev Immunol *7*, 954-963.

Anderson, G., Owen, J.J., Moore, N.C., and Jenkinson, E.J. (1994). Thymic epithelial cells provide unique signals for positive selection of CD4+CD8+ thymocytes in vitro. J Exp Med *179*, 2027-2031.

Anderson, M., Anderson, S.K., and Farr, A.G. (2000b). Thymic vasculature: organizer of the medullary epithelial compartment? Int Immunol *12*, 1105-1110.

Anderson, M.S., Venanzi, E.S., Klein, L., Chen, Z., Berzins, S.P., Turley, S.J., von Boehmer, H., Bronson, R., Dierich, A., Benoist, C., and Mathis, D. (2002). Projection of an immunological self shadow within the thymus by the aire protein. Science *298*, 1395-1401.

Ardouin, L., Bracke, M., Mathiot, A., Pagakis, S.N., Norton, T., Hogg, N., and Tybulewicz, V.L. (2003). Vav1 transduces TCR signals required for LFA-1 function and cell polarization at the immunological synapse. Eur J Immunol *33*, 790-797.

Asarnow, D.M., Kuziel, W.A., Bonyhadi, M., Tigelaar, R.E., Tucker, P.W., and Allison, J.P. (1988). Limited diversity of gamma delta antigen receptor genes of Thy-1+ dendritic epidermal cells. Cell *55*, 837-847.

Aschenbrenner, K., D'Cruz, L.M., Vollmann, E.H., Hinterberger, M., Emmerich, J., Swee, L.K., Rolink, A., and Klein, L. (2007). Selection of Foxp3+ regulatory T cells specific for self antigen expressed and presented by Aire+ medullary thymic epithelial cells. Nat Immunol *8*, 351-358.

Ashwell, J.D., and Klusner, R.D. (1990). Genetic and mutational analysis of the T-cell antigen receptor. Annu Rev Immunol *8*, 139-167.

Aw, D., Taylor-Brown, F., Cooper, K., and Palmer, D.B. (2009). Phenotypical and morphological changes in the thymic microenvironment from ageing mice. Biogerontology *10*, 311-322.

Azzam, H.S., Grinberg, A., Lui, K., Shen, H., Shores, E.W., and Love, P.E. (1998). CD5 expression is developmentally regulated by T cell receptor (TCR) signals and TCR avidity. J Exp Med *188*, 2301-2311.

Balciunaite, G., Ceredig, R., and Rolink, A.G. (2005). The earliest subpopulation of mouse thymocytes contains potent T, significant macrophage, and natural killer cell but no B-lymphocyte potential. Blood *105*, 1930-1936.

Baldwin, T.A., Sandau, M.M., Jameson, S.C., and Hogquist, K.A. (2005). The timing of TCR alpha expression critically influences T cell development and selection. J Exp Med *202*, 111-121.

Banchereau, J., Briere, F., Caux, C., Davoust, J., Lebecque, S., Liu, Y.J., Pulendran, B., and Palucka, K. (2000). Immunobiology of dendritic cells. Annu Rev Immunol *18*, 767-811.

Basset, C., Holton, J., O'Mahony, R., and Roitt, I. (2003). Innate immunity and pathogen-host interaction. Vaccine *21 Suppl 2*, S12-23.

Bell, J.J., and Bhandoola, A. (2008). The earliest thymic progenitors for T cells possess myeloid lineage potential. Nature *452*, 764-767.

Bellantuono, I. (2004). Haemopoietic stem cells. Int J Biochem Cell Biol *36*, 607-620.

Bendelac, A., Matzinger, P., Seder, R.A., Paul, W.E., and Schwartz, R.H. (1992). Activation events during thymic selection. J Exp Med *175*, 731-742.

Benlagha, K., Kyin, T., Beavis, A., Teyton, L., and Bendelac, A. (2002). A thymic precursor to the NK T cell lineage. Science *296*, 553-555.

Bennett, A.R., Farley, A., Blair, N.F., Gordon, J., Sharp, L., and Blackburn, C.C. (2002). Identification and characterization of thymic epithelial progenitor cells. Immunity *16*, 803-814.

Benz, C., Heinzel, K., and Bleul, C.C. (2004). Homing of immature thymocytes to the subcapsular microenvironment within the thymus is not an absolute requirement for T cell development. Eur J Immunol *34*, 3652-3663.

Benz, C., Martins, V.C., Radtke, F., and Bleul, C.C. (2008). The stream of precursors that colonizes the thymus proceeds selectively through the early T lineage precursor stage of T cell development. J Exp Med *205*, 1187-1199.

Bergstresser, P.R., and Juarez, D.V. (1984). Detection by immunochemical techniques of cell surface markers on epidermal Langerhans cells. Methods Enzymol *108*, 683-691.

Bergstresser, P.R., Tigelaar, R.E., Dees, J.H., and Streilein, J.W. (1983). Thy-1 antigen-bearing dendritic cells populate murine epidermis. J Invest Dermatol *81*, 286-288.

Berzins, S.P., Uldrich, A.P., Sutherland, J.S., Gill, J., Miller, J.F., Godfrey, D.I., and Boyd, R.L. (2002). Thymic regeneration: teaching an old immune system new tricks. Trends Mol Med *8*, 469-476.

Bhandoola, A., and Sambandam, A. (2006). From stem cell to T cell: one route or many? Nat Rev Immunol *6*, 117-126.

Bhandoola, A., Sambandam, A., Allman, D., Meraz, A., and Schwarz, B. (2003). Early T lineage progenitors: new insights, but old questions remain. J Immunol *171*, 5653-5658.

Bhandoola, A., von Boehmer, H., Petrie, H.T., and Zuniga-Pflucker, J.C. (2007). Commitment and developmental potential of extrathymic and intrathymic T cell precursors: plenty to choose from. Immunity *26*, 678-689.

Blackburn, C.C., and Manley, N.R. (2004). Developing a new paradigm for thymus organogenesis. Nat Rev Immunol *4*, 278-289.

Bleul, C.C., Corbeaux, T., Reuter, A., Fisch, P., Monting, J.S., and Boehm, T. (2006). Formation of a functional thymus initiated by a postnatal epithelial progenitor cell. Nature *441*, 992-996.

Blomberg, M., Rao, S., Reilly, J., Tiarks, C., Peters, S., Kittler, E., and Quesenberry, P. (1998). Repetitive bone marrow transplantation in nonmyeloablated recipients. Exp Hematol *26*, 320-324.

Blumberg, R.S., Ley, S., Sancho, J., Lonberg, N., Lacy, E., McDermott, F., Schad, V., Greenstein, J.L., and Terhorst, C. (1990). Structure of the T-cell antigen receptor: evidence for two CD3 epsilon subunits in the T-cell receptor-CD3 complex. Proc Natl Acad Sci U S A *87*, 7220-7224.

Boehm, T. (2008). Thymus development and function. Curr Opin Immunol.

Boehm, T., Scheu, S., Pfeffer, K., and Bleul, C.C. (2003). Thymic medullary epithelial cell differentiation, thymocyte emigration, and the control of autoimmunity require lympho-epithelial cross talk via LTbetaR. J Exp Med *198*, 757-769.

Bommhardt, U., Beyer, M., Hunig, T., and Reichardt, H.M. (2004). Molecular and cellular mechanisms of T cell development. Cell Mol Life Sci *61*, 263-280.

Born, W., Cady, C., Jones-Carson, J., Mukasa, A., Lahn, M., and O'Brien, R. (1999). Immunoregulatory functions of gamma delta T cells. Adv Immunol *71*, 77-144.

Boursalian, T.E., Golob, J., Soper, D.M., Cooper, C.J., and Fink, P.J. (2004). Continued maturation of thymic emigrants in the periphery. Nat Immunol *5*, 418-425.

Boyd, R.L., Tucek, C.L., Godfrey, D.I., Izon, D.J., Wilson, T.J., Davidson, N.J., Bean, A.G., Ladyman, H.M., Ritter, M.A., and Hugo, P. (1993). The thymic microenvironment. Immunol Today *14*, 445-459.

Boyden, L.M., Lewis, J.M., Barbee, S.D., Bas, A., Girardi, M., Hayday, A.C., Tigelaar, R.E., and Lifton, R.P. (2008). Skint1, the prototype of a newly identified immunoglobulin superfamily gene cluster, positively selects epidermal gammadelta T cells. Nat Genet *40*, 656-662.

Brent, L. (1997). The discovery of immunologic tolerance. Hum Immunol *52*, 75-81.

Brugnera, E., Bhandoola, A., Cibotti, R., Yu, Q., Guinter, T.I., Yamashita, Y., Sharrow, S.O., and Singer, A. (2000). Coreceptor reversal in the thymus: signaled CD4+8+ thymocytes initially terminate CD8 transcription even when differentiating into CD8+ T cells. Immunity *13*, 59-71.

Bryant, P., and Ploegh, H. (2004). Class II MHC peptide loading by the professionals. Curr Opin Immunol *16*, 96-102.

Bryant, P.W., Lennon-Dumenil, A.M., Fiebiger, E., Lagaudriere-Gesbert, C., and Ploegh, H.L. (2002). Proteolysis and antigen presentation by MHC class II molecules. Adv Immunol *80*, 71-114.

Bubeck Wardenburg, J., Fu, C., Jackman, J.K., Flotow, H., Wilkinson, S.E., Williams, D.H., Johnson, R., Kong, G., Chan, A.C., and Findell, P.R. (1996). Phosphorylation of SLP-76 by the ZAP-70 protein-tyrosine kinase is required for T-cell receptor function. J Biol Chem *271*, 19641-19644.

Burns, D.L. (1988). Subunit structure and enzymic activity of pertussis toxin. Microbiol Sci *5*, 285-287.

Cabarrocas, J., Cassan, C., Magnusson, F., Piaggio, E., Mars, L., Derbinski, J., Kyewski, B., Gross, D.A., Salomon, B.L., Khazaie, K.*, et al.* (2006). Foxp3+ CD25+ regulatory T cells specific for a neo-self-antigen develop at the double-positive thymic stage. Proc Natl Acad Sci U S A *103*, 8453-8458.

Call, M.E., and Wucherpfennig, K.W. (2005). The T cell receptor: critical role of the membrane environment in receptor assembly and function. Annu Rev Immunol *23*, 101-125.

Cambier, J.C. (1995). New nomenclature for the Reth motif (or ARH1/TAM/ARAM/YXXL). Immunol Today *16*, 110.

Campbell, J.J., Pan, J., and Butcher, E.C. (1999). Cutting edge: developmental switches in chemokine responses during T cell maturation. J Immunol *163*, 2353-2357.

Carroll, M.C. (2004). The complement system in regulation of adaptive immunity. Nat Immunol *5*, 981-986.

Ceredig, R., and Rolink, T. (2002). A positive look at double-negative thymocytes. Nat Rev Immunol *2*, 888-897.

Cheng, A.M., Rowley, B., Pao, W., Hayday, A., Bolen, J.B., and Pawson, T. (1995). Syk tyrosine kinase required for mouse viability and B-cell development. Nature *378*, 303-306.

Chidgey, A.P., Seach, N., Dudakov, J., Hammett, M.V., and Boyd, R.L. (2008). Strategies for reconstituting and boosting T cell-based immunity following haematopoietic stem cell transplantation: pre-clinical and clinical approaches. Semin Immunopathol *30*, 457-477.

Chien, Y.H., and Konigshofer, Y. (2007). Antigen recognition by gammadelta T cells. Immunol Rev *215*, 46-58.

Chin, R.K., Lo, J.C., Kim, O., Blink, S.E., Christiansen, P.A., Peterson, P., Wang, Y., Ware, C., and Fu, Y.X. (2003). Lymphotoxin pathway directs thymic Aire expression. Nat Immunol *4*, 1121-1127.

Chung, B., Barbara-Burnham, L., Barsky, L., and Weinberg, K. (2001). Radiosensitivity of thymic interleukin-7 production and thymopoiesis after bone marrow transplantation. Blood *98*, 1601-1606.

Ciofani, M., Knowles, G.C., Wiest, D.L., von Boehmer, H., and Zuniga-Pflucker, J.C. (2006). Stage-specific and differential notch dependency at the alphabeta and gammadelta T lineage bifurcation. Immunity *25*, 105-116.

Ciofani, M., and Zuniga-Pflucker, J.C. (2007). The thymus as an inductive site for T lymphopoiesis. Annu Rev Cell Dev Biol *23*, 463-493.

Colucci, F., Soudais, C., Rosmaraki, E., Vanes, L., Tybulewicz, V.L., and Di Santo, J.P. (1999). Dissecting NK cell development using a novel alymphoid mouse model: investigating the role of the c-abl proto-oncogene in murine NK cell differentiation. J Immunol *162*, 2761-2765.

Crump, A.L., Grusby, M.J., Glimcher, L.H., and Cantor, H. (1993). Thymocyte development in major histocompatibility complex-deficient mice: evidence for stochastic commitment to the CD4 and CD8 lineages. Proc Natl Acad Sci U S A *90*, 10739-10743.

Davis, M.M., Boniface, J.J., Reich, Z., Lyons, D., Hampl, J., Arden, B., and Chien, Y. (1998). Ligand recognition by alpha beta T cell receptors. Annu Rev Immunol *16*, 523-544.

Delves, P.J., and Roitt, I.M. (2000a). The immune system. First of two parts. N Engl J Med *343*, 37-49.

Delves, P.J., and Roitt, I.M. (2000b). The immune system. Second of two parts. N Engl J Med *343*, 108-117.

Depreter, M.G., Blair, N.F., Gaskell, T.L., Nowell, C.S., Davern, K., Pagliocca, A., Stenhouse, F.H., Farley, A.M., Fraser, A., Vrana, J.*, et al.* (2008). Identification of Plet-1 as a specific marker of early thymic epithelial progenitor cells. Proc Natl Acad Sci U S A *105*, 961-966.

Derbinski, J., Gabler, J., Brors, B., Tierling, S., Jonnakuty, S., Hergenhahn, M., Peltonen, L., Walter, J., and Kyewski, B. (2005). Promiscuous gene expression in thymic epithelial cells is regulated at multiple levels. J Exp Med *202*, 33-45.

Derbinski, J., and Kyewski, B. (2005). Linking signalling pathways, thymic stroma integrity and autoimmunity. Trends Immunol *26*, 503-506.

DeVoss, J., Hou, Y., Johannes, K., Lu, W., Liou, G.I., Rinn, J., Chang, H., Caspi, R.R., Fong, L., and Anderson, M.S. (2006). Spontaneous autoimmunity prevented by thymic expression of a single self-antigen. J Exp Med *203*, 2727-2735.

Diamond, R.A., Ward, S.B., Owada-Makabe, K., Wang, H., and Rothenberg, E.V. (1997). Different developmental arrest points in RAG-2 -/- and SCID thymocytes on two genetic backgrounds: developmental choices and cell death mechanisms before TCR gene rearrangement. J Immunol *158*, 4052-4064.

Dong, Y., Du, X., Ye, J., Han, M., Xu, T., Zhuang, Y., and Tao, W. (2009). A cell-intrinsic role for Mst1 in regulating thymocyte egress. J Immunol *183*, 3865-3872.

Donskoy, E., Foss, D., and Goldschneider, I. (2003). Gated importation of prothymocytes by adult mouse thymus is coordinated with their periodic mobilization from bone marrow. J Immunol *171*, 3568-3575.

Donskoy, E., and Goldschneider, I. (1992). Thymocytopoiesis is maintained by blood-borne precursors throughout postnatal life. A study in parabiotic mice. J Immunol *148*, 1604-1612.

Dooley, J., Erickson, M., and Farr, A.G. (2008). Alterations of the medullary epithelial compartment in the Aire-deficient thymus: implications for programs of thymic epithelial differentiation. J Immunol *181*, 5225-5232.

Douagi, I., Andre, I., Ferraz, J.C., and Cumano, A. (2000). Characterization of T cell precursor activity in the murine fetal thymus: evidence for an input of T cell precursors between days 12 and 14 of gestation. Eur J Immunol *30*, 2201-2210.

Douagi, I., Colucci, F., Di Santo, J.P., and Cumano, A. (2002). Identification of the earliest prethymic bipotent T/NK progenitor in murine fetal liver. Blood *99*, 463-471.

Dunn, R.J., Luedecker, C.J., Haugen, H.S., Clegg, C.H., and Farr, A.G. (1997). Thymic overexpression of CD40 ligand disrupts normal thymic epithelial organization. J Histochem Cytochem *45*, 129-141.

Eberl, G., Marmon, S., Sunshine, M.J., Rennert, P.D., Choi, Y., and Littman, D.R. (2004). An essential function for the nuclear receptor RORgamma(t) in the generation of fetal lymphoid tissue inducer cells. Nat Immunol *5*, 64-73.

Egerton, M., Scollay, R., and Shortman, K. (1990). Kinetics of mature T-cell development in the thymus. Proc Natl Acad Sci U S A *87*, 2579-2582.

Ehrlich, L.I., Oh, D.Y., Weissman, I.L., and Lewis, R.S. (2009). Differential contribution of chemotaxis and substrate restriction to segregation of immature and mature thymocytes. Immunity *31*, 986-998.

Farr, A., Hosier, S., Nelson, A., Itohara, S., and Tonegawa, S. (1990). Distribution of thymocytes expressing gamma delta receptors in the murine thymus during development. J Immunol *144*, 492-498.

Ferrero, I., Wilson, A., Beermann, F., Held, W., and MacDonald, H.R. (2001). T cell receptor specificity is critical for the development of epidermal gammadelta T cells. J Exp Med *194*, 1473-1483.

Ferrick, D.A., Sambhara, S.R., Ballhausen, W., Iwamoto, A., Pircher, H., Walker, C.L., Yokoyama, W.M., Miller, R.G., and Mak, T.W. (1989). T cell function and expression are dramatically altered in T cell receptor V gamma 1.1J gamma 4C gamma 4 transgenic mice. Cell *57*, 483-492.

Fiorini, E., Ferrero, I., Merck, E., Favre, S., Pierres, M., Luther, S.A., and MacDonald, H.R. (2008). Cutting edge: thymic crosstalk regulates delta-like 4 expression on cortical epithelial cells. J Immunol *181*, 8199-8203.

Flutter, B., and Gao, B. (2004). MHC class I antigen presentation--recently trimmed and well presented. Cell Mol Immunol *1*, 22-30.

Fontenot, J.D., Dooley, J.L., Farr, A.G., and Rudensky, A.Y. (2005). Developmental regulation of Foxp3 expression during ontogeny. J Exp Med *202*, 901-906.

Foss, D.L., Donskoy, E., and Goldschneider, I. (2001). The importation of hematogenous precursors by the thymus is a gated phenomenon in normal adult mice. J Exp Med *193*, 365-374.

Foster, K., Sheridan, J., Veiga-Fernandes, H., Roderick, K., Pachnis, V., Adams, R., Blackburn, C., Kioussis, D., and Coles, M. (2008). Contribution of neural crest-derived cells in the embryonic and adult thymus. J Immunol *180*, 3183-3189.

Fugmann, S.D., Lee, A.I., Shockett, P.E., Villey, I.J., and Schatz, D.G. (2000). The RAG proteins and V(D)J recombination: complexes, ends, and transposition. Annu Rev Immunol *18*, 495-527.

Fujimoto, Y., Tu, L., Miller, A.S., Bock, C., Fujimoto, M., Doyle, C., Steeber, D.A., and Tedder, T.F. (2002). CD83 expression influences CD4+ T cell development in the thymus. Cell *108*, 755-767.

Garcia, K.C., Teyton, L., and Wilson, I.A. (1999). Structural basis of T cell recognition. Annu Rev Immunol *17*, 369-397.

Germain, R.N. (2002). T-cell development and the CD4-CD8 lineage decision. Nat Rev Immunol *2*, 309-322.

Gill, J., Malin, M., Hollander, G.A., and Boyd, R. (2002). Generation of a complete thymic microenvironment by MTS24(+) thymic epithelial cells. Nat Immunol *3*, 635-642.

Glanville, S.H., Bekiaris, V., Jenkinson, E.J., Lane, P.J., Anderson, G., and Withers, D.R. (2009). Transplantation of embryonic spleen tissue reveals a role for adult non-lymphoid cells in initiating lymphoid tissue organization. Eur J Immunol *39*, 280-289.

Godfrey, D.I., Kennedy, J., Mombaerts, P., Tonegawa, S., and Zlotnik, A. (1994). Onset of TCR-beta gene rearrangement and role of TCR-beta expression during CD3-CD4-CD8- thymocyte differentiation. J Immunol *152*, 4783-4792.

Godfrey, D.I., Kennedy, J., Suda, T., and Zlotnik, A. (1993). A developmental pathway involving four phenotypically and functionally distinct subsets of CD3-CD4-CD8- triple-negative adult mouse thymocytes defined by CD44 and CD25 expression. J Immunol *150*, 4244-4252.

Godfrey, D.I., Stankovic, S., and Baxter, A.G. (2009). Developing NKT cells need their calcium. Nat Immunol *10*, 231-233.

Godfrey, D.I., and Zlotnik, A. (1993). Control points in early T-cell development. Immunol Today *14*, 547-553.

Goldman, K.P., Park, C.S., Kim, M., Matzinger, P., and Anderson, C.C. (2005). Thymic cortical epithelium induces self tolerance. Eur J Immunol *35*, 709-717.

Goldrath, A.W., and Bevan, M.J. (1999). Selecting and maintaining a diverse T-cell repertoire. Nature *402*, 255-262.

Goldschneider, I., Komschlies, K.L., and Greiner, D.L. (1986). Studies of thymocytopoiesis in rats and mice. I. Kinetics of appearance of thymocytes using a direct intrathymic adoptive transfer assay for thymocyte precursors. J Exp Med *163*, 1-17.

Gommeaux, J., Gregoire, C., Nguessan, P., Richelme, M., Malissen, M., Guerder, S., Malissen, B., and Carrier, A. (2009). Thymus-specific serine protease regulates positive selection of a subset of CD4+ thymocytes. Eur J Immunol *39*, 956-964.

Gossens, K., Naus, S., Corbel, S.Y., Lin, S., Rossi, F.M., Kast, J., and Ziltener, H.J. (2009). Thymic progenitor homing and lymphocyte homeostasis are linked via S1P-controlled expression of thymic P-selectin/CCL25. J Exp Med *206*, 761-778.

Gray, D., Abramson, J., Benoist, C., and Mathis, D. (2007). Proliferative arrest and rapid turnover of thymic epithelial cells expressing Aire. J Exp Med *204*, 2521-2528.

Gray, D.H., Seach, N., Ueno, T., Milton, M.K., Liston, A., Lew, A.M., Goodnow, C.C., and Boyd, R.L. (2006). Developmental kinetics, turnover, and stimulatory capacity of thymic epithelial cells. Blood *108*, 3777-3785.

Gray, D.H., Ueno, T., Chidgey, A.P., Malin, M., Goldberg, G.L., Takahama, Y., and Boyd, R.L. (2005). Controlling the thymic microenvironment. Curr Opin Immunol *17*, 137-143.

Greenstein, B.D., Fitzpatrick, F.T., Kendall, M.D., and Wheeler, M.J. (1987). Regeneration of the thymus in old male rats treated with a stable analogue of LHRH. J Endocrinol *112*, 345-350.

Guerau-de-Arellano, M., Martinic, M., Benoist, C., and Mathis, D. (2009). Neonatal tolerance revisited: a perinatal window for Aire control of autoimmunity. J Exp Med *206*, 1245-1252.

Guermonprez, P., Valladeau, J., Zitvogel, L., Thery, C., and Amigorena, S. (2002). Antigen presentation and T cell stimulation by dendritic cells. Annu Rev Immunol *20*, 621-667.

Guidos, C. (2006). Thymus and T-lymphocyte development: what is new in the 21st century? Immunol Rev *209*, 5-9.

Gunther, T., Chen, Z.F., Kim, J., Priemel, M., Rueger, J.M., Amling, M., Moseley, J.M., Martin, T.J., Anderson, D.J., and Karsenty, G. (2000). Genetic ablation of parathyroid glands reveals another source of parathyroid hormone. Nature *406*, 199-203.

Haas, W., Pereira, P., and Tonegawa, S. (1993). Gamma/delta cells. Annu Rev Immunol *11*, 637-685.

Hakim, F.T., and Gress, R.E. (2005). Reconstitution of the lymphocyte compartment after lymphocyte depletion: a key issue in clinical immunology. Eur J Immunol *35*, 3099-3102.

Hamazaki, Y., Fujita, H., Kobayashi, T., Choi, Y., Scott, H.S., Matsumoto, M., and Minato, N. (2007). Medullary thymic epithelial cells expressing Aire represent a unique lineage derived from cells expressing claudin. Nat Immunol *8*, 304-311.

Hamrouni, A., Olsson, A., Wiegers, G.J., and Villunger, A. (2007). Impact of cellular lifespan on the T cell receptor repertoire. Eur J Immunol *37*, 1978-1985.

Harding, C.V., Ramachandra, L., and Wick, M.J. (2003). Interaction of bacteria with antigen presenting cells: influences on antigen presentation and antibacterial immunity. Curr Opin Immunol *15*, 112-119.

Hare, K.J., Jenkinson, E.J., and Anderson, G. (1999a). CD69 expression discriminates MHC-dependent and -independent stages of thymocyte positive selection. J Immunol *162*, 3978-3983.

Hare, K.J., Jenkinson, E.J., and Anderson, G. (1999b). In vitro models of T cell development. Semin Immunol *11*, 3-12.

Hare, K.J., Wilkinson, R.W., Jenkinson, E.J., and Anderson, G. (1998). Identification of a developmentally regulated phase of postselection expansion driven by thymic epithelium. J Immunol *160*, 3666-3672.

Hashimoto, Y., Montecino-Rodriguez, E., Leathers, H., Stephan, R.P., and Dorshkind, K. (2002). B-cell development in the thymus is limited by inhibitory signals from the thymic microenvironment. Blood *100*, 3504-3511.

Havran, W.L., and Allison, J.P. (1988). Developmentally ordered appearance of thymocytes expressing different T-cell antigen receptors. Nature *335*, 443-445.

Havran, W.L., Chien, Y.H., and Allison, J.P. (1991). Recognition of self antigens by skin-derived T cells with invariant gamma delta antigen receptors. Science *252*, 1430-1432.

Hayday, A.C. (2000). [gamma][delta] cells: a right time and a right place for a conserved third way of protection. Annu Rev Immunol *18*, 975-1026.

Hayday A & Pao W. T cell receptor, γδ. In: Delves PJ, Roitt IM, eds*Encyclopedia of Immunology* (1998) San Diego:Academic Press pp 2268–2278.

Hayes, S.M., Li, L., and Love, P.E. (2005). TCR signal strength influences alphabeta/gammadelta lineage fate. Immunity *22*, 583-593.

Hayes, S.M., Shores, E.W., and Love, P.E. (2003). An architectural perspective on signaling by the pre-, alphabeta and gammadelta T cell receptors. Immunol Rev *191*, 28-37.

He, X., Dave, V.P., Zhang, Y., Hua, X., Nicolas, E., Xu, W., Roe, B.A., and Kappes, D.J. (2005). The zinc finger transcription factor Th-POK regulates CD4 versus CD8 T-cell lineage commitment. Nature *433*, 826-833.

Hedrick, S.M., Nielsen, E.A., Kavaler, J., Cohen, D.I., and Davis, M.M. (1984). Sequence relationships between putative T-cell receptor polypeptides and immunoglobulins. Nature *308*, 153-158.

Hikosaka, Y., Nitta, T., Ohigashi, I., Yano, K., Ishimaru, N., Hayashi, Y., Matsumoto, M., Matsuo, K., Penninger, J.M., Takayanagi, H.*, et al.* (2008). The cytokine RANKL produced by positively selected thymocytes fosters medullary thymic epithelial cells that express autoimmune regulator. Immunity *29*, 438-450.

Hollander, G., Gill, J., Zuklys, S., Iwanami, N., Liu, C., and Takahama, Y. (2006). Cellular and molecular events during early thymus development. Immunol Rev *209*, 28-46.

Hollander, G.A., Simpson, S.J., Mizoguchi, E., Nichogiannopoulou, A., She, J., Gutierrez-Ramos, J.C., Bhan, A.K., Burakoff, S.J., Wang, B., and Terhorst, C. (1995a). Severe colitis in mice with aberrant thymic selection. Immunity *3*, 27-38.

Hollander, G.A., Wang, B., Nichogiannopoulou, A., Platenburg, P.P., van Ewijk, W., Burakoff, S.J., Gutierrez-Ramos, J.C., and Terhorst, C. (1995b). Developmental control point in induction of thymic cortex regulated by a subpopulation of prothymocytes. Nature *373*, 350-353.

Homey, B., Wang, W., Soto, H., Buchanan, M.E., Wiesenborn, A., Catron, D., Muller, A., McClanahan, T.K., Dieu-Nosjean, M.C., Orozco, R.*, et al.* (2000). Cutting edge: the orphan chemokine receptor G protein-coupled receptor-2 (GPR-2, CCR10) binds the skin-associated chemokine CCL27 (CTACK/ALP/ILC). J Immunol *164*, 3465-3470.

Honey, K., and Rudensky, A.Y. (2003). Lysosomal cysteine proteases regulate antigen presentation. Nat Rev Immunol *3*, 472-482.

Houlden, B.A., Cron, R.Q., Coligan, J.E., and Bluestone, J.A. (1988). Systematic development of distinct T cell receptor-gamma delta T cell subsets during fetal ontogeny. J Immunol *141*, 3753-3759.

Huang, E.Y., Gallegos, A.M., Richards, S.M., Lehar, S.M., and Bevan, M.J. (2003). Surface expression of Notch1 on thymocytes: correlation with the double-negative to double-positive transition. J Immunol *171*, 2296-2304.

Hugo, P., Waanders, G.A., Scollay, R., Shortman, K., and Boyd, R.L. (1990). Ontogeny of a novel CD4+CD8-CD3- thymocyte subpopulation: a comparison with CD4- CD8+ CD3- thymocytes. Int Immunol *2*, 209-218.

Ikawa, T., Kawamoto, H., Fujimoto, S., and Katsura, Y. (1999). Commitment of common T/Natural killer (NK) progenitors to unipotent T and NK progenitors in the murine fetal thymus revealed by a single progenitor assay. J Exp Med *190*, 1617-1626.

Ikawa, T., Masuda, K., Lu, M., Minato, N., Katsura, Y., and Kawamoto, H. (2004). Identification of the earliest prethymic T-cell progenitors in murine fetal blood. Blood *103*, 530-537.

Ikuta, K., Kina, T., MacNeil, I., Uchida, N., Peault, B., Chien, Y.H., and Weissman, I.L. (1990). A developmental switch in thymic lymphocyte maturation potential occurs at the level of hematopoietic stem cells. Cell *62*, 863-874.

Ioannidis, V., Beermann, F., Clevers, H., and Held, W. (2001). The beta-catenin--TCF-1 pathway ensures CD4(+)CD8(+) thymocyte survival. Nat Immunol *2*, 691-697.

Irla, M., Hugues, S., Gill, J., Nitta, T., Hikosaka, Y., Williams, I.R., Hubert, F.X., Scott, H.S., Takahama, Y., Hollander, G.A., and Reith, W. (2008). Autoantigen-specific interactions with CD4+ thymocytes control mature medullary thymic epithelial cell cellularity. Immunity *29*, 451-463.

Izon, D.J., Aster, J.C., He, Y., Weng, A., Karnell, F.G., Patriub, V., Xu, L., Bakkour, S., Rodriguez, C., Allman, D., and Pear, W.S. (2002). Deltex1 redirects lymphoid progenitors to the B cell lineage by antagonizing Notch1. Immunity *16*, 231-243.

Jarmin, D.I., Rits, M., Bota, D., Gerard, N.P., Graham, G.J., Clark-Lewis, I., and Gerard, C. (2000). Cutting edge: identification of the orphan receptor G-protein-coupled receptor 2 as CCR10, a specific receptor for the chemokine ESkine. J Immunol *164*, 3460-3464.

Jenkins, M.K., Chu, H.H., McLachlan, J.B., and Moon, J.J. (2010). On the composition of the preimmune repertoire of T cells specific for Peptide-major histocompatibility complex ligands. Annu Rev Immunol *28*, 275-294.

Jenkinson, E.J., and Anderson, G. (1994). Fetal thymic organ cultures. Curr Opin Immunol *6*, 293-297.

Jenkinson, E.J., Franchi, L.L., Kingston, R., and Owen, J.J. (1982). Effect of deoxyguanosine on lymphopoiesis in the developing thymus rudiment in vitro: application in the production of chimeric thymus rudiments. Eur J Immunol *12*, 583-587.

Jenkinson, W., Jenkinson, E., and Anderson, G. (2008). Preparation of 2-dGuo-treated thymus organ cultures. J Vis Exp.

Jenkinson, W.E., Jenkinson, E.J., and Anderson, G. (2003). Differential requirement for mesenchyme in the proliferation and maturation of thymic epithelial progenitors. J Exp Med *198*, 325-332.

Jenkinson, W.E., Rossi, S.W., Jenkinson, E.J., and Anderson, G. (2005). Development of functional thymic epithelial cells occurs independently of lymphostromal interactions. Mech Dev *122*, 1294-1299.

Jenkinson, W.E., Rossi, S.W., Parnell, S.M., Agace, W.W., Takahama, Y., Jenkinson, E.J., and Anderson, G. (2007). Chemokine receptor expression defines heterogeneity in the earliest thymic migrants. Eur J Immunol *37*, 2090-2096.

Jiang, W., Swiggard, W.J., Heufler, C., Peng, M., Mirza, A., Steinman, R.M., and Nussenzweig, M.C. (1995). The receptor DEC-205 expressed by dendritic cells and thymic epithelial cells is involved in antigen processing. Nature *375*, 151-155.

Jin, R., Wang, W., Yao, J.Y., Zhou, Y.B., Qian, X.P., Zhang, J., Zhang, Y., and Chen, W.F. (2008). Characterization of the in vivo dynamics of medullary CD4+CD8- thymocyte development. J Immunol *180*, 2256-2263.

Jordan, M.S., Boesteanu, A., Reed, A.J., Petrone, A.L., Holenbeck, A.E., Lerman, M.A., Naji, A., and Caton, A.J. (2001). Thymic selection of CD4+CD25+ regulatory T cells induced by an agonist self-peptide. Nat Immunol *2*, 301-306.

Jotereau, F., Heuze, F., Salomon-Vie, V., and Gascan, H. (1987). Cell kinetics in the fetal mouse thymus: precursor cell input, proliferation, and emigration. J Immunol *138*, 1026-1030.

Kane, L.P., Lin, J., and Weiss, A. (2000). Signal transduction by the TCR for antigen. Curr Opin Immunol *12*, 242-249.

Kappes, D.J., and He, X. (2006). Role of the transcription factor Th-POK in CD4:CD8 lineage commitment. Immunol Rev *209*, 237-252.

Kawamoto, H., Ikawa, T., Ohmura, K., Fujimoto, S., and Katsura, Y. (2000). T cell progenitors emerge earlier than B cell progenitors in the murine fetal liver. Immunity *12*, 441-450.

Kawamoto, H., Ohmura, K., and Katsura, Y. (1998). Presence of progenitors restricted to T, B, or myeloid lineage, but absence of multipotent stem cells, in the murine fetal thymus. J Immunol *161*, 3799-3802.

Kieusseian, A., Chagraoui, J., Kerdudo, C., Mangeot, P.E., Gage, P.J., Navarro, N., Izac, B., Uzan, G., Forget, B.G., and Dubart-Kupperschmitt, A. (2006). Expression of Pitx2 in stromal cells is required for normal hematopoiesis. Blood *107*, 492-500.

Kikuchi, K., and Kondo, M. (2006). Developmental switch of mouse hematopoietic stem cells from fetal to adult type occurs in bone marrow after birth. Proc Natl Acad Sci U S A *103*, 17852-17857.

Kim, M.Y. (2008). Roles of embryonic and adult lymphoid tissue inducer cells in primary and secondary lymphoid tissues. Yonsei Med J *49*, 352-356.

Kim, M.Y., Rossi, S., Withers, D., McConnell, F., Toellner, K.M., Gaspal, F., Jenkinson, E., Anderson, G., and Lane, P.J. (2008). Heterogeneity of lymphoid tissue inducer cell populations present in embryonic and adult mouse lymphoid tissues. Immunology *124*, 166-174.

Klug, D.B., Carter, C., Crouch, E., Roop, D., Conti, C.J., and Richie, E.R. (1998). Interdependence of cortical thymic epithelial cell differentiation and T-lineage commitment. Proc Natl Acad Sci U S A *95*, 11822-11827.

Klug, D.B., Carter, C., Gimenez-Conti, I.B., and Richie, E.R. (2002). Cutting edge: thymocyte-independent and thymocyte-dependent phases of epithelial patterning in the fetal thymus. J Immunol *169*, 2842-2845.

Knittler, M.R., Alberts, P., Deverson, E.V., and Howard, J.C. (1999). Nucleotide binding by TAP mediates association with peptide and release of assembled MHC class I molecules. Curr Biol *9*, 999-1008.

Koble, C., and Kyewski, B. (2009). The thymic medulla: a unique microenvironment for intercellular self-antigen transfer. J Exp Med *206*, 1505-1513.

Koch, U., Lacombe, T.A., Holland, D., Bowman, J.L., Cohen, B.L., Egan, S.E., and Guidos, C.J. (2001). Subversion of the T/B lineage decision in the thymus by lunatic fringe-mediated inhibition of Notch-1. Immunity *15*, 225-236.

Komori, H.K., Meehan, T.F., and Havran, W.L. (2006). Epithelial and mucosal gamma delta T cells. Curr Opin Immunol *18*, 534-538.

Kondo, M., Weissman, I.L., and Akashi, K. (1997). Identification of clonogenic common lymphoid progenitors in mouse bone marrow. Cell *91*, 661-672.

Kong, Y.Y., Yoshida, H., Sarosi, I., Tan, H.L., Timms, E., Capparelli, C., Morony, S., Oliveira-dos-Santos, A.J., Van, G., Itie, A.*, et al.* (1999). OPGL is a key regulator of osteoclastogenesis, lymphocyte development and lymph-node organogenesis. Nature *397*, 315-323.

Krangel, M.S. (2009). Mechanics of T cell receptor gene rearrangement. Curr Opin Immunol *21*, 133-139.

Krueger, M., and Bechmann, I. (2010). CNS pericytes: concepts, misconceptions, and a way out. Glia *58*, 1-10.

Kurobe, H., Liu, C., Ueno, T., Saito, F., Ohigashi, I., Seach, N., Arakaki, R., Hayashi, Y., Kitagawa, T., Lipp, M.*, et al.* (2006). CCR7-dependent cortex-to-medulla migration of positively selected thymocytes is essential for establishing central tolerance. Immunity *24*, 165-177.

Kyewski, B., and Derbinski, J. (2004). Self-representation in the thymus: an extended view. Nat Rev Immunol *4*, 688-698.

Kyewski, B., and Klein, L. (2006). A central role for central tolerance. Annu Rev Immunol *24*, 571-606.

Ladi, E., Yin, X., Chtanova, T., and Robey, E.A. (2006). Thymic microenvironments for T cell differentiation and selection. Nat Immunol *7*, 338-343.

Laky, K., Lewis, J.M., Tigelaar, R.E., and Puddington, L. (2003). Distinct requirements for IL-7 in development of TCR gamma delta cells during fetal and adult life. J Immunol *170*, 4087-4094.

Lane, P.J., and Brocker, T. (1999). Developmental regulation of dendritic cell function. Curr Opin Immunol *11*, 308-313.

Leclercq, G., Debacker, V., de Smedt, M., and Plum, J. (1996). Differential effects of interleukin-15 and interleukin-2 on differentiation of bipotential T/natural killer progenitor cells. J Exp Med *184*, 325-336.

Leclercq, G., and Plum, J. (1996). Thymic development of V gamma 3 cells. Semin Immunol *8*, 315-321.

Leclercq, G., Plum, J., Nandi, D., De Smedt, M., and Allison, J.P. (1993). Intrathymic differentiation of V gamma 3 T cells. J Exp Med *178*, 309-315.

Lederberg, J. (1959). Genes and antibodies. Science *129*, 1649-1653.

Levelt, C.N., Wang, B., Ehrfeld, A., Terhorst, C., and Eichmann, K. (1995). Regulation of T cell receptor (TCR)-beta locus allelic exclusion and initiation of TCR-alpha locus rearrangement in immature thymocytes by signaling through the CD3 complex. Eur J Immunol *25*, 1257-1261.

Lewis, J.M., Girardi, M., Roberts, S.J., Barbee, S.D., Hayday, A.C., and Tigelaar, R.E. (2006). Selection of the cutaneous intraepithelial gammadelta+ T cell repertoire by a thymic stromal determinant. Nat Immunol *7*, 843-850.

Lin, W., Haribhai, D., Relland, L.M., Truong, N., Carlson, M.R., Williams, C.B., and Chatila, T.A. (2007). Regulatory T cell development in the absence of functional Foxp3. Nat Immunol *8*, 359-368.

Lind, E.F., Prockop, S.E., Porritt, H.E., and Petrie, H.T. (2001). Mapping precursor movement through the postnatal thymus reveals specific microenvironments supporting defined stages of early lymphoid development. J Exp Med *194*, 127-134.

Liu, C., Saito, F., Liu, Z., Lei, Y., Uehara, S., Love, P., Lipp, M., Kondo, S., Manley, N., and Takahama, Y. (2006). Coordination between CCR7- and CCR9-mediated chemokine signals in prevascular fetal thymus colonization. Blood *108*, 2531-2539.

Livak, F., Tourigny, M., Schatz, D.G., and Petrie, H.T. (1999). Characterization of TCR gene rearrangements during adult murine T cell development. J Immunol *162*, 2575-2580.

Lochner, M., Peduto, L., Cherrier, M., Sawa, S., Langa, F., Varona, R., Riethmacher, D., Si-Tahar, M., Di Santo, J.P., and Eberl, G. (2008). In vivo equilibrium of proinflammatory IL-17+ and regulatory IL-10+ Foxp3+ RORgamma t+ T cells. J Exp Med *205*, 1381-1393.

Lu, M., Tayu, R., Ikawa, T., Masuda, K., Matsumoto, I., Mugishima, H., Kawamoto, H., and Katsura, Y. (2005). The earliest thymic progenitors in adults are restricted to T, NK, and dendritic cell lineage and have a potential to form more diverse TCRbeta chains than fetal progenitors. J Immunol *175*, 5848-5856.

Lucas, B., and Germain, R.N. (1996). Unexpectedly complex regulation of CD4/CD8 coreceptor expression supports a revised model for CD4+CD8+ thymocyte differentiation. Immunity *5*, 461-477.

Lynch, H.E., Goldberg, G.L., Chidgey, A., Van den Brink, M.R., Boyd, R., and Sempowski, G.D. (2009). Thymic involution and immune reconstitution. Trends Immunol *30*, 366-373.

Mallick-Wood, C.A., Lewis, J.M., Richie, L.I., Owen, M.J., Tigelaar, R.E., and Hayday, A.C. (1998). Conservation of T cell receptor conformation in epidermal gammadelta cells with disrupted primary Vgamma gene usage. Science *279*, 1729-1733.

Manley, N.R. (2000). Thymus organogenesis and molecular mechanisms of thymic epithelial cell differentiation. Semin Immunol *12*, 421-428.

Manley, N.R., and Blackburn, C.C. (2003). A developmental look at thymus organogenesis: where do the non-hematopoietic cells in the thymus come from? Curr Opin Immunol *15*, 225-232.

Masuda, K., Germeraad, W.T., Satoh, R., Itoi, M., Ikawa, T., Minato, N., Katsura, Y., van Ewijk, W., and Kawamoto, H. (2009). Notch activation in thymic epithelial cells induces development of thymic microenvironments. Mol Immunol *46*, 1756-1767.

Masuda, K., Itoi, M., Amagai, T., Minato, N., Katsura, Y., and Kawamoto, H. (2005). Thymic anlage is colonized by progenitors restricted to T, NK, and dendritic cell lineages. J Immunol *174*, 2525-2532.

Matsue, H., Bergstresser, P.R., and Takashima, A. (1993). Reciprocal cytokine-mediated cellular interactions in mouse epidermis: promotion of gamma delta T-cell growth by IL-7 and TNF alpha and inhibition of keratinocyte growth by gamma IFN. J Invest Dermatol *101*, 543-548.

Matsuzaki, Y., Gyotoku, J., Ogawa, M., Nishikawa, S., Katsura, Y., Gachelin, G., and Nakauchi, H. (1993). Characterization of c-kit positive intrathymic stem cells that are restricted to lymphoid differentiation. J Exp Med *178*, 1283-1292.

McCaughtry, T.M., Baldwin, T.A., Wilken, M.S., and Hogquist, K.A. (2008). Clonal deletion of thymocytes can occur in the cortex with no involvement of the medulla. J Exp Med *205*, 2575-2584.

McCaughtry, T.M., Wilken, M.S., and Hogquist, K.A. (2007). Thymic emigration revisited. J Exp Med *204*, 2513-2520.

Mebius, R., and Akashi, K. (2000). Precursors to neonatal lymph nodes: LT beta+CD45+CD4+CD3- cells are found in fetal liver. Curr Top Microbiol Immunol *251*, 197-201.

Medzhitov, R., and Janeway, C., Jr. (2000). Innate immunity. N Engl J Med *343*, 338-344.

Medzhitov, R., and Janeway, C.A., Jr. (1997). Innate immunity: impact on the adaptive immune response. Curr Opin Immunol *9*, 4-9.

Merkenschlager, M., Graf, D., Lovatt, M., Bommhardt, U., Zamoyska, R., and Fisher, A.G. (1997). How many thymocytes audition for selection? J Exp Med *186*, 1149-1158.

Meurens, F., Whale, J., Brownlie, R., Dybvig, T., Thompson, D.R., and Gerdts, V. (2007). Expression of mucosal chemokines TECK/CCL25 and MEC/CCL28 during fetal development of the ovine mucosal immune system. Immunology *120*, 544-555.

Michie, A.M., Carlyle, J.R., Schmitt, T.M., Ljutic, B., Cho, S.K., Fong, Q., and Zuniga-Pflucker, J.C. (2000). Clonal characterization of a bipotent T cell and NK cell progenitor in the mouse fetal thymus. J Immunol *164*, 1730-1733.

Michie, A.M., and Zuniga-Pflucker, J.C. (2002). Regulation of thymocyte differentiation: pre-TCR signals and beta-selection. Semin Immunol *14*, 311-323.

Miller, J.F. (2002). The discovery of thymus function and of thymus-derived lymphocytes. Immunol Rev *185*, 7-14.

Misslitz, A., Pabst, O., Hintzen, G., Ohl, L., Kremmer, E., Petrie, H.T., and Forster, R. (2004). Thymic T cell development and progenitor localization depend on CCR7. J Exp Med *200*, 481-491.

Mombaerts, P., Iacomini, J., Johnson, R.S., Herrup, K., Tonegawa, S., and Papaioannou, V.E. (1992). RAG-1-deficient mice have no mature B and T lymphocytes. Cell *68*, 869-877.

Mosmann, T.R., Cherwinski, H., Bond, M.W., Giedlin, M.A., and Coffman, R.L. (1986). Two types of murine helper T cell clone. I. Definition according to profiles of lymphokine activities and secreted proteins. J Immunol *136*, 2348-2357.

Muller, S.M., Stolt, C.C., Terszowski, G., Blum, C., Amagai, T., Kessaris, N., Iannarelli, P., Richardson, W.D., Wegner, M., and Rodewald, H.R. (2008). Neural crest origin of perivascular mesenchyme in the adult thymus. J Immunol *180*, 5344-5351.

Murata, S., Sasaki, K., Kishimoto, T., Niwa, S., Hayashi, H., Takahama, Y., and Tanaka, K. (2007). Regulation of CD8+ T cell development by thymus-specific proteasomes. Science *316*, 1349-1353.

Nakano, H., and Gunn, M.D. (2001). Gene duplications at the chemokine locus on mouse chromosome 4: multiple strain-specific haplotypes and the deletion of secondary lymphoid-organ chemokine and EBI-1 ligand chemokine genes in the plt mutation. J Immunol *166*, 361-369.

Naquet, P., Naspetti, M., and Boyd, R. (1999). Development, organization and function of the thymic medulla in normal, immunodeficient or autoimmune mice. Semin Immunol *11*, 47-55.

Nasreen, M., Ueno, T., Saito, F., and Takahama, Y. (2003). In vivo treatment of class II MHC-deficient mice with anti-TCR antibody restores the generation of circulating CD4 T cells and optimal architecture of thymic medulla. J Immunol *171*, 3394-3400.

Nehls, M., Kyewski, B., Messerle, M., Waldschutz, R., Schuddekopf, K., Smith, A.J., and Boehm, T. (1996). Two genetically separable steps in the differentiation of thymic epithelium. Science *272*, 886-889.

Nehls, M., Pfeifer, D., Schorpp, M., Hedrich, H., and Boehm, T. (1994). New member of the winged-helix protein family disrupted in mouse and rat nude mutations. Nature *372*, 103-107.

Nelson, A.J., Hosier, S., Brady, W., Linsley, P.S., and Farr, A.G. (1993). Medullary thymic epithelium expresses a ligand for CTLA4 in situ and in vitro. J Immunol *151*, 2453-2461.

Ngo, V.N., Korner, H., Gunn, M.D., Schmidt, K.N., Riminton, D.S., Cooper, M.D., Browning, J.L., Sedgwick, J.D., and Cyster, J.G. (1999). Lymphotoxin alpha/beta and tumor necrosis factor are required for stromal cell expression of homing chemokines in B and T cell areas of the spleen. J Exp Med *189*, 403-412.

Nishikawa, Y., Hirota, F., Yano, M., Kitajima, H., Miyazaki, J., Kawamoto, H., Mouri, Y., and Matsumoto, M. (2010). Biphasic Aire expression in early embryos and in medullary thymic epithelial cells before end-stage terminal differentiation. J Exp Med *207*, 963-971.

Nitta, T., Nitta, S., Lei, Y., Lipp, M., and Takahama, Y. (2009). CCR7-mediated migration of developing thymocytes to the medulla is essential for negative selection to tissue-restricted antigens. Proc Natl Acad Sci U S A *106*, 17129-17133.

Osada, M., Ito, E., Fermin, H.A., Vazquez-Cintron, E., Venkatesh, T., Friedel, R.H., and Pezzano, M. (2006). The Wnt signaling antagonist Kremen1 is required for development of thymic architecture. Clin Dev Immunol *13*, 299-319.

Owen, R.D. (1945). Immunogenetic Consequences of Vascular Anastomoses between Bovine Twins. Science *102*, 400-401.

Palmer, D.B., Viney, J.L., Ritter, M.A., Hayday, A.C., and Owen, M.J. (1993). Expression of the alpha beta T-cell receptor is necessary for the generation of the thymic medulla. Dev Immunol *3*, 175-179.

Pan, J., Kunkel, E.J., Gosslar, U., Lazarus, N., Langdon, P., Broadwell, K., Vierra, M.A., Genovese, M.C., Butcher, E.C., and Soler, D. (2000). A novel chemokine ligand for CCR10 and CCR3 expressed by epithelial cells in mucosal tissues. J Immunol *165*, 2943-2949.

Pappu, R., Schwab, S.R., Cornelissen, I., Pereira, J.P., Regard, J.B., Xu, Y., Camerer, E., Zheng, Y.W., Huang, Y., Cyster, J.G., and Coughlin, S.R. (2007). Promotion of lymphocyte egress into blood and lymph by distinct sources of sphingosine-1-phosphate. Science *316*, 295-298.

Payer, E., Elbe, A., and Stingl, G. (1991). Circulating CD3+/T cell receptor V gamma 3+ fetal murine thymocytes home to the skin and give rise to proliferating dendritic epidermal T cells. J Immunol *146*, 2536-2543.

Penit, C. (1988). Localization and phenotype of cycling and post-cycling murine thymocytes studied by simultaneous detection of bromodeoxyuridine and surface antigens. J Histochem Cytochem *36*, 473-478.

Peterson, P., Org, T., and Rebane, A. (2008). Transcriptional regulation by AIRE: molecular mechanisms of central tolerance. Nat Rev Immunol *8*, 948-957.

Petrie, H.T. (2003). Cell migration and the control of post-natal T-cell lymphopoiesis in the thymus. Nat Rev Immunol *3*, 859-866.

Petrie, H.T. (2007). Early commitment: T cell progenitors in the blood. Immunity *26*, 7-8.

Petrie, H.T., and Kincade, P.W. (2005). Many roads, one destination for T cell progenitors. J Exp Med *202*, 11-13.

Petrie, H.T., Livak, F., Schatz, D.G., Strasser, A., Crispe, I.N., and Shortman, K. (1993). Multiple rearrangements in T cell receptor alpha chain genes maximize the production of useful thymocytes. J Exp Med *178*, 615-622.

Petrie, H.T., and Zuniga-Pflucker, J.C. (2007). Zoned out: functional mapping of stromal signaling microenvironments in the thymus. Annu Rev Immunol *25*, 649-679.

Plotkin, J., Prockop, S.E., Lepique, A., and Petrie, H.T. (2003). Critical role for CXCR4 signaling in progenitor localization and T cell differentiation in the postnatal thymus. J Immunol *171*, 4521-4527.

Pongracz, J., Hare, K., Harman, B., Anderson, G., and Jenkinson, E.J. (2003). Thymic epithelial cells provide WNT signals to developing thymocytes. Eur J Immunol *33*, 1949-1956.

Ponta, H., Sherman, L., and Herrlich, P.A. (2003). CD44: from adhesion molecules to signalling regulators. Nat Rev Mol Cell Biol *4*, 33-45.

Porritt, H.E., Gordon, K., and Petrie, H.T. (2003). Kinetics of steady-state differentiation and mapping of intrathymic-signaling environments by stem cell transplantation in nonirradiated mice. J Exp Med *198*, 957-962.

Porritt, H.E., Rumfelt, L.L., Tabrizifard, S., Schmitt, T.M., Zuniga-Pflucker, J.C., and Petrie, H.T. (2004). Heterogeneity among DN1 prothymocytes reveals multiple progenitors with different capacities to generate T cell and non-T cell lineages. Immunity *20*, 735-745.

Prinz, I., Sansoni, A., Kissenpfennig, A., Ardouin, L., Malissen, M., and Malissen, B. (2006). Visualization of the earliest steps of gammadelta T cell development in the adult thymus. Nat Immunol *7*, 995-1003.

Prockop, S., and Petrie, H.T. (2000). Cell migration and the anatomic control of thymocyte precursor differentiation. Semin Immunol *12*, 435-444.

Prockop, S.E., Palencia, S., Ryan, C.M., Gordon, K., Gray, D., and Petrie, H.T. (2002). Stromal cells provide the matrix for migration of early lymphoid progenitors through the thymic cortex. J Immunol *169*, 4354-4361.

Prockop, S.E., and Petrie, H.T. (2004). Regulation of thymus size by competition for stromal niches among early T cell progenitors. J Immunol *173*, 1604-1611.

Raab, M., da Silva, A.J., Findell, P.R., and Rudd, C.E. (1997). Regulation of Vav-SLP-76 binding by ZAP-70 and its relevance to TCR zeta/CD3 induction of interleukin-2. Immunity *6*, 155-164.

Radtke, F., Wilson, A., Stark, G., Bauer, M., van Meerwijk, J., MacDonald, H.R., and Aguet, M. (1999). Deficient T cell fate specification in mice with an induced inactivation of Notch1. Immunity *10*, 547-558.

Rao, A., Luo, C., and Hogan, P.G. (1997). Transcription factors of the NFAT family: regulation and function. Annu Rev Immunol *15*, 707-747.

Raviola, E., and Karnovsky, M.J. (1972). Evidence for a blood-thymus barrier using electron-opaque tracers. J Exp Med *136*, 466-498.

Reth, M. (1989). Antigen receptor tail clue. Nature *338*, 383-384.

Ritter, M.A., and Boyd, R.L. (1993). Development in the thymus: it takes two to tango. Immunol Today *14*, 462-469.

Roberts, N.A., Desanti, G.E., Withers, D.R., Scott, H.R., Jenkinson, W.E., Lane, P.J., Jenkinson, E.J., and Anderson, G. (2009). Absence of thymus crosstalk in the fetus does not preclude hematopoietic induction of a functional thymus in the adult. Eur J Immunol *39*, 2395-2402.

Rodewald, H.R. (2008). Thymus organogenesis. Annu Rev Immunol *26*, 355-388.

Rodewald, H.R., and Fehling, H.J. (1998). Molecular and cellular events in early thymocyte development. Adv Immunol *69*, 1-112.

Rodewald, H.R., Kretzschmar, K., Takeda, S., Hohl, C., and Dessing, M. (1994). Identification of pro-thymocytes in murine fetal blood: T lineage commitment can precede thymus colonization. EMBO J *13*, 4229-4240.

Rodewald, H.R., Ogawa, M., Haller, C., Waskow, C., and DiSanto, J.P. (1997). Pro-thymocyte expansion by c-kit and the common cytokine receptor gamma chain is essential for repertoire formation. Immunity *6*, 265-272.

Rodewald, H.R., Paul, S., Haller, C., Bluethmann, H., and Blum, C. (2001). Thymus medulla consisting of epithelial islets each derived from a single progenitor. Nature *414*, 763-768.

Ropke, C., Van Soest, P., Platenburg, P.P., and Van Ewijk, W. (1995). A common stem cell for murine cortical and medullary thymic epithelial cells? Dev Immunol *4*, 149-156.

Rossi, D., and Zlotnik, A. (2000). The biology of chemokines and their receptors. Annu Rev Immunol *18*, 217-242.

Rossi, S.W., Chidgey, A.P., Parnell, S.M., Jenkinson, W.E., Scott, H.S., Boyd, R.L., Jenkinson, E.J., and Anderson, G. (2007a). Redefining epithelial progenitor potential in the developing thymus. Eur J Immunol *37*, 2411-2418.

Rossi, S.W., Jenkinson, W.E., Anderson, G., and Jenkinson, E.J. (2006). Clonal analysis reveals a common progenitor for thymic cortical and medullary epithelium. Nature *441*, 988-991.

Rossi, S.W., Kim, M.Y., Leibbrandt, A., Parnell, S.M., Jenkinson, W.E., Glanville, S.H., McConnell, F.M., Scott, H.S., Penninger, J.M., Jenkinson, E.J*., et al.* (2007b). RANK signals from CD4(+)3(-) inducer cells regulate development of Aire-expressing epithelial cells in the thymic medulla. J Exp Med *204*, 1267-1272.

Rudd, C.E. (1990). CD4, CD8 and the TCR-CD3 complex: a novel class of protein-tyrosine kinase receptor. Immunol Today *11*, 400-406.

Sakaguchi, S. (2004). Naturally arising CD4+ regulatory t cells for immunologic self-tolerance and negative control of immune responses. Annu Rev Immunol *22*, 531-562.

Sambandam, A., Maillard, I., Zediak, V.P., Xu, L., Gerstein, R.M., Aster, J.C., Pear, W.S., and Bhandoola, A. (2005). Notch signaling controls the generation and differentiation of early T lineage progenitors. Nat Immunol *6*, 663-670.

Samelson, L.E. (2002). Signal transduction mediated by the T cell antigen receptor: the role of adapter proteins. Annu Rev Immunol *20*, 371-394.

Schmitt, T.M., Ciofani, M., Petrie, H.T., and Zuniga-Pflucker, J.C. (2004). Maintenance of T cell specification and differentiation requires recurrent notch receptor-ligand interactions. J Exp Med *200*, 469-479.

Schon, M.P., Schon, M., Parker, C.M., and Williams, I.R. (2002). Dendritic epidermal T cells (DETC) are diminished in integrin alphaE(CD103)-deficient mice. J Invest Dermatol *119*, 190-193.

Schwab, S.R., Pereira, J.P., Matloubian, M., Xu, Y., Huang, Y., and Cyster, J.G. (2005). Lymphocyte sequestration through S1P lyase inhibition and disruption of S1P gradients. Science *309*, 1735-1739.

Scimone, M.L., Aifantis, I., Apostolou, I., von Boehmer, H., and von Andrian, U.H. (2006). A multistep adhesion cascade for lymphoid progenitor cell homing to the thymus. Proc Natl Acad Sci U S A *103*, 7006-7011.

Shakib, S., Desanti, G.E., Jenkinson, W.E., Parnell, S.M., Jenkinson, E.J., and Anderson, G. (2009). Checkpoints in the development of thymic cortical epithelial cells. J Immunol *182*, 130-137.

Sharpe, A.H., and Freeman, G.J. (2002). The B7-CD28 superfamily. Nat Rev Immunol *2*, 116-126.

Shen, H.Q., Lu, M., Ikawa, T., Masuda, K., Ohmura, K., Minato, N., Katsura, Y., and Kawamoto, H. (2003). T/NK bipotent progenitors in the thymus retain the potential to generate dendritic cells. J Immunol *171*, 3401-3406.

Shevach, E.M. (2006). From vanilla to 28 flavors: multiple varieties of T regulatory cells. Immunity *25*, 195-201.

Shiow, L.R., Rosen, D.B., Brdickova, N., Xu, Y., An, J., Lanier, L.L., Cyster, J.G., and Matloubian, M. (2006). CD69 acts downstream of interferon-alpha/beta to inhibit S1P1 and lymphocyte egress from lymphoid organs. Nature *440*, 540-544.

Shores, E.W., Van Ewijk, W., and Singer, A. (1991). Disorganization and restoration of thymic medullary epithelial cells in T cell receptor-negative scid mice: evidence that receptor-bearing lymphocytes influence maturation of the thymic microenvironment. Eur J Immunol *21*, 1657-1661.

Shortman, K., Egerton, M., Spangrude, G.J., and Scollay, R. (1990). The generation and fate of thymocytes. Semin Immunol *2*, 3-12.

Shortman, K., and Wu, L. (1996). Early T lymphocyte progenitors. Annu Rev Immunol *14*, 29-47.

Silva-Santos, B., Pennington, D.J., and Hayday, A.C. (2005). Lymphotoxin-mediated regulation of gammadelta cell differentiation by alphabeta T cell progenitors. Science *307*, 925-928.

Singer, A., Adoro, S., and Park, J.H. (2008). Lineage fate and intense debate: myths, models and mechanisms of CD4- versus CD8-lineage choice. Nat Rev Immunol *8*, 788-801.

Singer, A., and Bosselut, R. (2004). CD4/CD8 coreceptors in thymocyte development, selection, and lineage commitment: analysis of the CD4/CD8 lineage decision. Adv Immunol *83*, 91-131.

Sperling, A.I., Cron, R.Q., Decker, D.C., Stern, D.A., and Bluestone, J.A. (1992). Peripheral T cell receptor gamma delta variable gene repertoire maps to the T cell receptor loci and is influenced by positive selection. J Immunol *149*, 3200-3207.

Starr, T.K., Jameson, S.C., and Hogquist, K.A. (2003). Positive and negative selection of T cells. Annu Rev Immunol *21*, 139-176.

Sullivan, S., Bergstresser, P.R., Tigelaar, R.E., and Streilein, J.W. (1985). FACS purification of bone marrow-derived epidermal populations in mice: Langerhans cells and Thy-1+ dendritic cells. J Invest Dermatol *84*, 491-495.

Sun, Z., Unutmaz, D., Zou, Y.R., Sunshine, M.J., Pierani, A., Brenner-Morton, S., Mebius, R.E., and Littman, D.R. (2000). Requirement for RORgamma in thymocyte survival and lymphoid organ development. Science *288*, 2369-2373.

Surh, C.D., and Sprent, J. (2008). Homeostasis of naive and memory T cells. Immunity *29*, 848-862.

Svensson, M., Marsal, J., Uronen-Hansson, H., Cheng, M., Jenkinson, W., Cilio, C., Jacobsen, S.E., Sitnicka, E., Anderson, G., and Agace, W.W. (2008). Involvement of CCR9 at multiple stages of adult T lymphopoiesis. J Leukoc Biol *83*, 156-164.

Taghon, T., Yui, M.A., Pant, R., Diamond, R.A., and Rothenberg, E.V. (2006). Developmental and molecular characterization of emerging beta- and gammadelta-selected pre-T cells in the adult mouse thymus. Immunity *24*, 53-64.

Takahama, Y. (2006). Journey through the thymus: stromal guides for T-cell development and selection. Nat Rev Immunol *6*, 127-135.

Takeda, K., Kaisho, T., and Akira, S. (2003). Toll-like receptors. Annu Rev Immunol *21*, 335-376.

Tatsumi, Y., Kumanogoh, A., Saitoh, M., Mizushima, Y., Kimura, K., Suzuki, S., Yagi, H., Horiuchi, A., Ogata, M., Hamaoka, T., and et al. (1990). Differentiation of thymocytes from CD3-CD4-CD8- through CD3-CD4-CD8+ into more mature stages induced by a thymic stromal cell clone. Proc Natl Acad Sci U S A *87*, 2750-2754.

Tatsumi, Y., Pena, J.C., Matis, L., Deluca, D., and Bluestone, J.A. (1993). Development of T cell receptor-gamma delta cells. Phenotypic and functional correlations of T cell receptor-gamma delta thymocyte maturation. J Immunol *151*, 3030-3041.

Teague, T.K., Tan, C., Marino, J.H., Davis, B.K., Taylor, A.A., Huey, R.W., and Van De Wiele, C.J. (2010). CD28 expression redefines thymocyte development during the pre-T to DP transition. Int Immunol *22*, 387-397.

Tigelaar, R.E., and Lewis, J.M. (1995). Immunobiology of mouse dendritic epidermal T cells: a decade later, some answers, but still more questions. J Invest Dermatol *105*, 43S-49S.

Tigelaar R.E, Lewis J.M. Factors involved in the localization and activation of murine gd positive dendritic epidermal T cells. In: Lambert WC, Giannotti B, van Vloten WA, editors. *Basic mechanisms of physiologic and aberrant lymphoproliferation in the skin.* New York: Plenum Press, 1994:39–55.

Tokoro, Y., Sugawara, T., Yaginuma, H., Nakauchi, H., Terhorst, C., Wang, B., and Takahama, Y. (1998). A mouse carrying genetic defect in the choice between T and B lymphocytes. J Immunol *161*, 4591-4598.

Toro, I., and Olah, I. (1967). Penetration of thymocytes into the blood circulation. J Ultrastruct Res *17*, 439-451.

Ueno, T., Hara, K., Willis, M.S., Malin, M.A., Hopken, U.E., Gray, D.H., Matsushima, K., Lipp, M., Springer, T.A., Boyd, R.L.*, et al.* (2002). Role for CCR7 ligands in the emigration of newly generated T lymphocytes from the neonatal thymus. Immunity *16*, 205-218.

Ueno, T., Saito, F., Gray, D.H., Kuse, S., Hieshima, K., Nakano, H., Kakiuchi, T., Lipp, M., Boyd, R.L., and Takahama, Y. (2004). CCR7 signals are essential for cortex-medulla migration of developing thymocytes. J Exp Med *200*, 493-505.

Urban, J.A., and Winandy, S. (2004). Ikaros null mice display defects in T cell selection and CD4 versus CD8 lineage decisions. J Immunol *173*, 4470-4478.

van Ewijk, W. (1991). T-cell differentiation is influenced by thymic microenvironments. Annu Rev Immunol *9*, 591-615.

van Ewijk, W., Hollander, G., Terhorst, C., and Wang, B. (2000). Stepwise development of thymic microenvironments in vivo is regulated by thymocyte subsets. Development *127*, 1583-1591.

van Ewijk, W., Shores, E.W., and Singer, A. (1994). Crosstalk in the mouse thymus. Immunol Today *15*, 214-217.

van Ewijk, W., Wang, B., Hollander, G., Kawamoto, H., Spanopoulou, E., Itoi, M., Amagai, T., Jiang, Y.F., Germeraad, W.T., Chen, W.F., and Katsura, Y. (1999). Thymic microenvironments, 3-D versus 2-D? Semin Immunol *11*, 57-64.

van Leeuwen, J.E., and Samelson, L.E. (1999). T cell antigen-receptor signal transduction. Curr Opin Immunol *11*, 242-248.

Vassileva, G., Soto, H., Zlotnik, A., Nakano, H., Kakiuchi, T., Hedrick, J.A., and Lira, S.A. (1999). The reduced expression of 6Ckine in the plt mouse results from the deletion of one of two 6Ckine genes. J Exp Med *190*, 1183-1188.

Veillette, A., Bookman, M.A., Horak, E.M., Samelson, L.E., and Bolen, J.B. (1989). Signal transduction through the CD4 receptor involves the activation of the internal membrane tyrosine-protein kinase p56lck. Nature *338*, 257-259.

Vicente, R., Adjali, O., Jacquet, C., Zimmermann, V.S., and Taylor, N. (2010). Intrathymic transplantation of bone marrow-derived progenitors provides long-term thymopoiesis. Blood *115*, 1913-1920.

Villey, I., de Chasseval, R., and de Villartay, J.P. (1999). RORgammaT, a thymus-specific isoform of the orphan nuclear receptor RORgamma / TOR, is up-regulated by signaling through the pre-T cell receptor and binds to the TEA promoter. Eur J Immunol *29*, 4072-4080.

von Boehmer, H., Aifantis, I., Feinberg, J., Lechner, O., Saint-Ruf, C., Walter, U., Buer, J., and Azogui, O. (1999). Pleiotropic changes controlled by the pre-T-cell receptor. Curr Opin Immunol *11*, 135-142.

Wallis, V.J., Leuchars, E., Chwalinski, S., and Davies, A.J. (1975). On the sparse seeding of bone marrow and thymus in radiation chimaeras. Transplantation *19*, 2-11.

Walzer, T., Blery, M., Chaix, J., Fuseri, N., Chasson, L., Robbins, S.H., Jaeger, S., Andre, P., Gauthier, L., Daniel, L.*, et al.* (2007). Identification, activation, and selective in vivo ablation of mouse NK cells via NKp46. Proc Natl Acad Sci U S A *104*, 3384-3389.

Wang, B., Levelt, C., Salio, M., Zheng, D., Sancho, J., Liu, C.P., She, J., Huang, M., Higgins, K., Sunshine, M.J., and et al. (1995). Over-expression of CD3 epsilon transgenes blocks T lymphocyte development. Int Immunol *7*, 435-448.

Wang, B., She, J., Salio, M., Allen, D., Lacy, E., Lonberg, N., and Terhorst, C. (1997). CD3-epsilon overexpressed in prothymocytes acts as an oncogene. Mol Med *3*, 72-81.

Wang, W., Soto, H., Oldham, E.R., Buchanan, M.E., Homey, B., Catron, D., Jenkins, N., Copeland, N.G., Gilbert, D.J., Nguyen, N.*, et al.* (2000). Identification of a novel chemokine (CCL28), which binds CCR10 (GPR2). J Biol Chem *275*, 22313-22323.

Wange, R.L., and Samelson, L.E. (1996). Complex complexes: signaling at the TCR. Immunity *5*, 197-205.

Watts, C. (2004). The exogenous pathway for antigen presentation on major histocompatibility complex class II and CD1 molecules. Nat Immunol *5*, 685-692.

Weaver, C.T., Harrington, L.E., Mangan, P.R., Gavrieli, M., and Murphy, K.M. (2006). Th17: an effector CD4 T cell lineage with regulatory T cell ties. Immunity *24*, 677-688.

Weiss, A., and Littman, D.R. (1994). Signal transduction by lymphocyte antigen receptors. Cell *76*, 263-274.

White, A., Jenkinson, E., and Anderson, G. (2008a). Reaggregate thymus cultures. J Vis Exp.

White, A.J., Withers, D.R., Parnell, S.M., Scott, H.S., Finke, D., Lane, P.J., Jenkinson, E.J., and Anderson, G. (2008b). Sequential phases in the development of Aire-expressing medullary thymic epithelial cells involve distinct cellular input. Eur J Immunol *38*, 942-947.

Wilkinson, B., Downey, J.S., and Rudd, C.E. (2005). T-cell signalling and immune system disorders. Expert Rev Mol Med *7*, 1-29.

Williams, J.A., Hathcock, K.S., Klug, D., Harada, Y., Choudhury, B., Allison, J.P., Abe, R., and Hodes, R.J. (2005). Regulated costimulation in the thymus is critical for T cell development: dysregulated CD28 costimulation can bypass the pre-TCR checkpoint. J Immunol *175*, 4199-4207.

Wilson, A., and Trumpp, A. (2006). Bone-marrow haematopoietic-stem-cell niches. Nat Rev Immunol *6*, 93-106.

Withers, D.R., Kim, M.Y., Bekiaris, V., Rossi, S.W., Jenkinson, W.E., Gaspal, F., McConnell, F., Caamano, J.H., Anderson, G., and Lane, P.J. (2007). The role of lymphoid tissue inducer cells in splenic white pulp development. Eur J Immunol *37*, 3240-3245.

Witt, C.M., Raychaudhuri, S., Schaefer, B., Chakraborty, A.K., and Robey, E.A. (2005). Directed migration of positively selected thymocytes visualized in real time. PLoS Biol *3*, e160.

Wright, D.E., Wagers, A.J., Gulati, A.P., Johnson, F.L., and Weissman, I.L. (2001). Physiological migration of hematopoietic stem and progenitor cells. Science *294*, 1933-1936.

Wu, L., Antica, M., Johnson, G.R., Scollay, R., and Shortman, K. (1991). Developmental potential of the earliest precursor cells from the adult mouse thymus. J Exp Med *174*, 1617-1627.

Wurbel, M.A., Malissen, M., Guy-Grand, D., Meffre, E., Nussenzweig, M.C., Richelme, M., Carrier, A., and Malissen, B. (2001). Mice lacking the CCR9 CC-chemokine receptor show a mild impairment of early T- and B-cell development and a reduction in T-cell receptor gammadelta(+) gut intraepithelial lymphocytes. Blood *98*, 2626-2632.

Xiong, N., Kang, C., and Raulet, D.H. (2004). Positive selection of dendritic epidermal gammadelta T cell precursors in the fetal thymus determines expression of skin-homing receptors. Immunity *21*, 121-131.

Xiong, N., and Raulet, D.H. (2007). Development and selection of gammadelta T cells. Immunol Rev *215*, 15-31.

Yamasaki, S., Ishikawa, E., Sakuma, M., Ogata, K., Sakata-Sogawa, K., Hiroshima, M., Wiest, D.L., Tokunaga, M., and Saito, T. (2006). Mechanistic basis of pre-T cell receptor-mediated autonomous signaling critical for thymocyte development. Nat Immunol *7*, 67-75.

Yano, M., Kuroda, N., Han, H., Meguro-Horike, M., Nishikawa, Y., Kiyonari, H., Maemura, K., Yanagawa, Y., Obata, K., Takahashi, S.*, et al.* (2008). Aire controls the differentiation program of thymic epithelial cells in the medulla for the establishment of self-tolerance. J Exp Med.

Yasuda, H., Shima, N., Nakagawa, N., Yamaguchi, K., Kinosaki, M., Mochizuki, S., Tomoyasu, A., Yano, K., Goto, M., Murakami, A.*, et al.* (1998). Osteoclast differentiation factor is a ligand for osteoprotegerin/osteoclastogenesis-inhibitory factor and is identical to TRANCE/RANKL. Proc Natl Acad Sci U S A *95*, 3597-3602.

Yewdell, J.W., and Haeryfar, S.M. (2005). Understanding presentation of viral antigens to CD8+ T cells in vivo: the key to rational vaccine design. Annu Rev Immunol *23*, 651-682.

Yokoyama, W.M., Kim, S., and French, A.R. (2004). The dynamic life of natural killer cells. Annu Rev Immunol *22*, 405-429.

Yu, Q., Erman, B., Bhandoola, A., Sharrow, S.O., and Singer, A. (2003). In vitro evidence that cytokine receptor signals are required for differentiation of double positive thymocytes into functionally mature CD8+ T cells. J Exp Med *197*, 475-487.

Yung Yu, C., Yang, Z., Blanchong, C.A., and Miller, W. (2000). The human and mouse MHC class III region: a parade of 21 genes at the centromeric segment. Immunol Today *21*, 320-328.

Zachariah, M.A., and Cyster, J.G. (2010). Neural crest-derived pericytes promote egress of mature thymocytes at the corticomedullary junction. Science *328*, 1129-1135.

Zamisch, M., Moore-Scott, B., Su, D.M., Lucas, P.J., Manley, N., and Richie, E.R. (2005). Ontogeny and regulation of IL-7-expressing thymic epithelial cells. J Immunol *174*, 60-67.

Zhu, J., and Paul, W.E. (2008). CD4 T cells: fates, functions, and faults. Blood *112*, 1557-1569.